



**HAL**  
open science

# Cosmological Inflation: Theoretical Aspects and Observational Constraints

Vincent Vennin

► **To cite this version:**

Vincent Vennin. Cosmological Inflation: Theoretical Aspects and Observational Constraints. General Relativity and Quantum Cosmology [gr-qc]. Université Pierre et Marie Curie, 2014. English. NNT : . tel-01094199

**HAL Id: tel-01094199**

**<https://theses.hal.science/tel-01094199>**

Submitted on 11 Dec 2014

**HAL** is a multi-disciplinary open access archive for the deposit and dissemination of scientific research documents, whether they are published or not. The documents may come from teaching and research institutions in France or abroad, or from public or private research centers.

L'archive ouverte pluridisciplinaire **HAL**, est destinée au dépôt et à la diffusion de documents scientifiques de niveau recherche, publiés ou non, émanant des établissements d'enseignement et de recherche français ou étrangers, des laboratoires publics ou privés.



THÈSE DE DOCTORAT DE L'UNIVERSITÉ PIERRE ET MARIE CURIE

Spécialité: Cosmologie

Ecole Doctorale 127 "Astronomie et Astrophysique d'Île de France"  
Institut d'Astrophysique de Paris  
GRÉCO

Présentée par

VINCENT VENNIN

Pour obtenir le grade de

DOCTEUR DE L'UNIVERSITÉ PIERRE ET MARIE CURIE

**Sujet de la thèse:**

INFLATION COSMOLOGIQUE:  
ASPECTS THÉORIQUES ET CONTRAINTES OBSERVATIONNELLES

soutenue le 5 septembre 2014 devant le jury composé de

M. Jérôme MARTIN	directeur de thèse
M. Daniel BAUMANN	rapporteur
M. Eiichiro KOMATSU	rapporteur
M. Michael G. F. JOYCE	examineur
M. Alexei A. STAROBINSKY	examineur
M. Paul J. STEINHARDT	examineur



# Acknowledgements

First, I would like to express my deepest gratitude to Jérôme Martin. First as a teacher and then as a Ph.D. director, he introduced me to the beauty of early universe cosmology and he taught me the trade of research with a lot of patience and pedagogy. I learnt a lot from his scientific rigour, his great intellectual honesty and his profound inquisitiveness. With constant support and encouragement, he offered me a very motivating and pleasant environment for doing research.

I want to thank my reporters Daniel Baumann and Eiichiro Komatsu for their patience in light of the size of this manuscript, as well as the members of my thesis jury, Michael Joyce, Aleksei Starobinsky, and Paul Steinhardt. I deeply appreciate their time and effort and I am grateful for their scientific interest in my work.

I am delighted to thank my collaborators, Robert Brandenberger, Laurence Perreault-Levasseur, Patrick Peter, Christophe Ringeval, Roberto Trotta and Jun'ichi Yokoyama with whom I worked closely and from whom I learnt a lot. I thank them for their hospitality and constant advice. Special thanks come to Christophe for having been my “computer hotline” during these three years.

I want to thank the directors of IAP, Laurent Vigroux and Francis Bernardeau, and the director of the  $\mathcal{GR}\varepsilon\mathcal{CO}$  group, Guillaume Faye, for having provided me with ideal conditions for carrying out research, specially in a context of limited funding.

It is a pleasure to thank all those who contributed to make my work environment a very nice one: my office mates Sandrine and Charlotte, and the *Salut Gorêt* championship members Cédric, Jean-Philippe, Jean-Baptiste, Jérôme, Kumiko, Patrick and Stéphane. Above all, my heartfelt gratitude comes to Evaluator-IAP for teaching me interesting english expressions and for his constant encouragement in *getting back to work* (although I never stopped).

Finally, I want to thank my wife Dorothée and my baby daughter Maëlle for their love and support during these years and all the ones to come.



## Résumé

Dans cette thèse sur articles nous nous intéressons aux contraintes observationnelles sur les modèles d'inflation cosmologique et nous étudions certains aspects fondamentaux liés à la nature quantique de la physique inflationnaire. L'inflation est une période d'expansion accélérée intervenant dans l'Univers primordial à très hautes énergies. En plus d'être une solution possible aux problèmes du modèle standard de la cosmologie dit du "big bang chaud", combinée à la mécanique quantique, l'inflation permet la production causale de fluctuations cosmologiques sur les grandes échelles, qui sont à l'origine des structures cosmiques actuelles. Mettant en jeu des énergies colossales au regard de ce qui peut être réalisé dans un accélérateur de particules, l'inflation est devenue un objet d'intérêt majeur en cosmologie pour tester la physique des hautes énergies au delà de son modèle standard.

Nous commençons par analyser de façon systématique tous les modèles inflationnaires à un champ scalaire et avec terme cinétique standard, à la lumière des mesures du fonds diffus cosmologique les plus récentes. Dans l'approximation du roulement lent, et en intégrant les contraintes venant de la phase de réchauffement, nous dérivons les prédictions associées à environ 75 potentiels. Nous utilisons ensuite les techniques d'inférence Bayésienne pour classer près de 200 modèles inflationnaires et contraindre leurs paramètres. Cela permet d'identifier les modèles favorisés par les observations et de quantifier les niveaux de tensions entre les différents jeux de données. L'intérêt d'une telle approche est renforcé par l'étude de méthodes indépendantes du modèle telle que le "flot de Hubble", qui se révèle biaisé. Nous calculons également le spectre de puissance au deuxième ordre pour les modèles d'inflation- $k$ , afin de permettre leur intégration future dans notre analyse numérique.

Dans une deuxième partie, nous décrivons certains aspects liés à la nature quantique de la physique inflationnaire. Le formalisme de l'inflation stochastique, qui incorpore les corrections quantiques aux dynamiques inflationnaires, est notamment utilisé dans le cadre du modèle à deux champs d'inflation hybride. Nous discutons l'impact de ces corrections sur les prédictions de ce modèle, et à l'aide d'un formalisme récursif, nous nous intéressons à la façon dont elles modifient l'amplitude des perturbations. Finalement, la transition quantique-classique, et le problème de la mesure quantique, sont étudiés dans un contexte cosmologique. Un modèle de réduction dynamique du paquet d'onde est appliqué à la description des perturbations inflationnaires.

**Mots Clés:** cosmologie, inflation, fonds diffus cosmologique, inflation stochastique, inférence Bayésienne et comparaison de modèles, perturbations quantiques.



## Abstract

This thesis by publication is devoted to the study of the observational constraints on cosmological inflationary models, and to the investigation of fundamental aspects related to the quantum nature of the inflationary physics. Inflation is an early phase of accelerated expansion taking place at very high energy. On top of being a solution for the hot big bang model problems, combined with quantum mechanics, inflation provides a causal mechanism for the production of cosmological fluctuations on large scales, that later give rise to today's cosmic structures. Given that it takes place at energy scales many orders of magnitude larger than what can be achieved in conventional particle physics experiments, inflation has become of great interest to test beyond standard model physics.

We first present a systematic analysis of all single-scalar-field inflationary models with canonical kinetic terms, in light of the most up-to-date Cosmic Microwave Background (CMB) measurements. Reheating consistent slow-roll predictions are derived for  $\sim 75$  potentials, and Bayesian inference and model comparison techniques are developed to arrange a landscape of  $\sim 200$  inflationary models and associated priors. In this way, we discuss what are the best models of inflation in light of the recent observations, and we properly quantify tension between data sets. Related to this massive sampling, we highlight the shortcomings of model independent approaches such as the one of "horizon-flow". We also pave the way for extending our computational pipeline to k-inflation models by calculating the power spectrum at next-to-next-to leading order for this class of models.

In a second part, we describe some aspects related to the quantum nature of the inflationary setup. In particular, we make use of the stochastic inflation formalism, which incorporates the quantum corrections to the inflationary dynamics, in the two-field model of hybrid inflation. We discuss how the quantum diffusion can affect the observable predictions in such models, and we design a recursive strategy that incorporates its effects on the perturbations amplitude. Finally, we investigate the quantum-to-classical transition and the quantum measurement problem in a cosmological context. We apply a dynamical wavefunction collapse model to the description of inflationary perturbations.

**Keywords:** cosmology, inflation, cosmic microwave background radiation, stochastic inflation, Bayesian inference and model comparison, quantum perturbations.



# Introduction

Inflation is a phase of accelerated expansion that took place in the early Universe at very high energy. Originally intended to dispose of some of the hot big bang shortcomings, it was soon realized that inflation may be responsible for a powerful manifestation of our Universe's quantum nature. Indeed, the deviations from homogeneity and isotropy that give rise to today's cosmic structures (galaxies, clusters, filaments, *etc.*) can be traced back to the quantum fluctuations of gravitational and matter fields during inflation. Stretched by the quasi-exponential expansion of space-time to distances of cosmological interest today, these fluctuations serve as the primordial seeds for inhomogeneities that later grow under the influence of gravitational instability. Inflation has become a very active field of research in the past years, since the energy scales involved during this early epoch are many orders of magnitude greater than those accessible in particle physics experiments. Therefore, the early Universe is certainly one of the most promising probes to test beyond standard model physics.

Another consequence of the fact that inflation takes place at energy scales where particle physics remain unknown, is that the physical nature of the fields driving inflation, and their relation with the standard model of particle physics, is still unclear. There have been a crowd of inflationary candidates proposed so far, and an important task is to discriminate between them. On the other hand, there is now a flow of increasingly accurate astrophysical data which provides us with a unique opportunity to constrain the inflationary landscape. These data mostly consist in measurements of the Cosmic Microwave Background (CMB), but they also concern other astrophysical probes such as supernovae, galaxy surveys, and 21 cm observations. It becomes therefore of paramount importance to be able to process such a huge amount of observational data, comprising measurements that are very different in nature, with hundreds of inflationary scenarios, often equally different. It is the first purpose of this thesis to design scientific and technical tools enabling to carry out such a programme, and to determine which inflationary models the data seem to prefer.

At the fundamental level, inflation is also probably one of the only cases in physics where an effect based on General Relativity and Quantum Mechanics leads to predictions that, given our present day technological capabilities, can be tested experimentally. This makes inflation an ideal playground to discuss deep questions related to its quantum aspects. The other purpose of this thesis is to study some of them, ranging from the quantum-to-classical transition of cosmological perturbations, to the quantum corrections to the inflationary dynamics by means of the stochastic inflation formalism.

The present manuscript is a thesis by publication. It presents the works realized at the Institut d'Astrophysique de Paris between September 2011 and September 2014 under the direction of Jérôme Martin. It first contains a brief presentation of the cosmological groundwork for our analysis, which introduces the main aspects of the cosmological standard model and of inflation. Mainly, this part **I** aims at providing the reader with the conceptual and technical tools that may be helpful to the understanding of the results presented in part **II**. This second part collects the research articles published during this thesis time (except from section **3.4** which, at the

time of drafting this manuscript, is going through the reviewing process).

More precisely, this document is organized as follows. In chapter 1, we review the cornerstones of the standard model of modern cosmology. In the framework of General Relativity, we describe homogeneous and isotropic universes and derive the associated Einstein equations. By an explicit comparison with the corresponding Newtonian physics, we highlight the deeply relativistic nature of the expansion, especially its possible acceleration. We then give a brief description of the main constituents of the Universe, and of the main lines of its history. Finally, we turn to the presentation of the problems of the hot big band model, namely the horizon, flatness and monopole problems. For each of these problems, we give a detailed calculation of its formulation and show how it can be solved with a phase of accelerated expansion. In particular, we characterize the number of  $e$ -folds that is required in each case.

In chapter 2, we review some aspects of cosmological inflation, the physical setups it relies on, the predictions it makes and the fundamental issues it raises. We explain why and under which conditions a single scalar field can support a phase of inflation and we present the “slow-roll” approximation which enables to solve its dynamics perturbatively. It also provides us with a convenient frame of calculation to compare inflationary predictions with observational data, which we make widely use of in chapter 3. We then turn to the description of inflationary perturbations, and show how cosmological fluctuations need to be quantized. For illustrative purpose, we provide a detailed calculation of the power spectrum of scalar perturbations, at first order in slow roll. Finally, we devote a large part of this second chapter to the presentation of the stochastic inflation formalism which is used in chapter 4. We first present a detailed heuristic derivation of the Langevin equation which is at the heart of this formalism, before turning to the question of the time variable that should be used when solving such equations, in order to reproduce results from Quantum Field Theories. Lastly, we address the issue of the calculation of physical observable quantities in stochastic inflation, such as the power spectrum of adiabatic perturbations. We show that the stochastic setup allows to reproduce the standard result, before providing complete solutions which do not rely on an expansion in the noise term. To our knowledge, this is the first time that such a non perturbative calculation of the power spectrum in stochastic inflation is presented. It has not been pre-printed or published yet since it has been derived in the course of drafting this manuscript.

We then turn to part II where the articles published during this thesis are presented and displayed. The first chapter, chapter 3, deals with a systematic analysis of all single-field inflationary models with minimal kinetic terms, in light of the most up-to-date CMB data, especially the ones coming from the Planck experiment and more recently from BICEP2. This somewhat “industrial” project aims at deriving reheating consistent slow-roll predictions for  $\sim 75$  inflationary potentials, and using Bayesian inference and model comparison techniques to arrange a landscape of  $\sim 200$  inflationary models and well studied priors. In this way, one can discuss which are the best models of inflation. This also allows us to assess the compatibility level of the two data sets (Planck and Bicep2) given inflation, or given a specific inflationary model. The relevance of such an approach is further advocated for in an article pointing out the shortcomings of model independent parametrizations of inflation such as the one of “horizon flow”, and another one paves the way for including single field  $k$ -inflation (*i.e.* non minimal kinetic terms) models in our analysis, by calculating the power spectrum at next-to-next-to leading order for this class of models.

In chapter 4, we turn to the description of some aspects related to the quantum nature of the inflationary setup. In particular, the stochastic inflation formalism incorporates the quantum corrections to the inflationary dynamics by means of stochastic Langevin equations. This gives

---

rise to non trivial inflationary trajectories, especially when multiple fields are present. This is why we study stochastic effects in hybrid inflation, a two-field model where inflation ends by tachyonic instability, and we discuss how the quantum diffusion can affect the observable predictions in such models. Making use of a recursive formalism for backreacting effects, we also address the issue of evolving cosmological perturbations on top of stochastically shifted backgrounds, in the same type of models. Finally, we investigate the quantum-to-classical transition and the quantum measurement problem in a cosmological context. More precisely, we apply the continuous spontaneous localization modification of the Schrödinger equation to the case of inflationary perturbations. We establish what an efficient collapse of the wavefunction implies for the inflationary predictions, and which constraints can be derived on the collapse models themselves.

Finally, in a last section, we sum up our results and present some concluding remarks and possible prospects for the present work.



# Contents

<b>Acknowledgements</b>	<b>iii</b>
<b>Résumé</b>	<b>v</b>
<b>Abstract</b>	<b>vii</b>
<b>Introduction</b>	<b>ix</b>
<b>I. Cosmology and Inflation</b>	<b>1</b>
<b>1. The Cosmological Standard Model</b>	<b>3</b>
1.1. The Homogeneous and Isotropic Universe . . . . .	3
1.1.1. The Friedmann-Lemaître-Robertson-Walker Metric . . . . .	4
1.1.1.1. The Hubble Law . . . . .	4
1.1.1.2. Redshift and Comoving Coordinates . . . . .	6
1.1.1.3. Einstein Equations . . . . .	6
1.1.2. An Expanding Universe . . . . .	7
1.1.2.1. Friedmann and Raychaudhuri Equations . . . . .	8
1.1.2.2. The Newtonian Expanding Sphere . . . . .	8
1.1.2.3. Constant Equations of State . . . . .	11
1.2. The Present Composition of the Universe . . . . .	12
1.3. The History of the Universe: the Hot Big Bang Model . . . . .	14
1.3.1. Dominant Constituant . . . . .	14
1.3.2. Age of the Universe . . . . .	16
1.3.3. A Brief Cosmological History . . . . .	18
1.4. The Big Bang Model Problems and Inflation . . . . .	21
1.4.1. The Horizon Problem . . . . .	21
1.4.1.1. Cosmological Horizon . . . . .	22
1.4.1.2. Angular Distance to the Horizon . . . . .	22
1.4.1.3. Formulation of the Problem . . . . .	23
1.4.1.4. Inflation as a Solution to the Horizon Problem . . . . .	24
1.4.1.5. Heuristic Understanding: Conformal Diagrams . . . . .	25
1.4.2. The Flatness Problem . . . . .	27
1.4.2.1. Formulation of the Problem . . . . .	28
1.4.2.2. Inflation as a Solution to the Flatness Problem . . . . .	28
1.4.3. The Monopole Problem . . . . .	29
1.4.3.1. Formulation of the Problem . . . . .	29
1.4.3.2. Inflation as a Solution to the Monopole Problem . . . . .	30

1.A. FLRW Christoffel symbols, Einstein tensor and Geodesics . . . . .	33
1.B. Numerical Values of Cosmological Parameters . . . . .	36
<b>2. Cosmological Inflation</b>	<b>39</b>
2.1. Single-Field Inflation . . . . .	41
2.2. The Slow-Roll Approximation . . . . .	42
2.2.1. The Slow-Roll Parameters . . . . .	43
2.2.2. The Slow-Roll Trajectory . . . . .	44
2.2.3. Next-to-Leading Orders in Slow Roll . . . . .	45
2.3. Inflationary Perturbations . . . . .	48
2.3.1. Basic Formalism . . . . .	48
2.3.1.1. SVT Decomposition . . . . .	48
2.3.1.2. Gauge Invariant Variables . . . . .	49
2.3.1.3. Equation of Motion for the Perturbations . . . . .	49
2.3.2. Quantization in the Schrödinger Picture . . . . .	52
2.3.3. The Power Spectrum . . . . .	55
2.3.4. Power Spectrum at Leading Order in Slow Roll . . . . .	57
2.4. Stochastic Inflation . . . . .	62
2.4.1. Heuristic Derivation of the Langevin Equations . . . . .	63
2.4.1.1. Coarse-Grained Field . . . . .	64
2.4.1.2. Split Klein-Gordon Equation . . . . .	64
2.4.1.3. Stochastic Processes . . . . .	65
2.4.1.4. Noise Moments . . . . .	66
2.4.1.5. Window Function and Coloured Noises . . . . .	67
2.4.1.6. Case of a de Sitter Background . . . . .	68
2.4.1.7. Case of a Light Field . . . . .	69
2.4.1.8. Case of a Slow-Rolling Field . . . . .	69
2.4.2. Why should we use the Number of $e$ -folds as the Time Variable in the Langevin Equations? . . . . .	69
2.4.2.1. Steady-State Distributions . . . . .	70
2.4.2.2. Perturbations Equation derived from the Background Equation . . . . .	71
2.4.2.3. Stochastic Inflation and QFT on Curved Space-Times . . . . .	74
2.4.3. Stochastic Inflation and the Scalar Power Spectrum . . . . .	76
2.4.3.1. The $\delta N$ Formalism . . . . .	78
2.4.3.2. Stochastic Inflation and Number of $e$ -folds . . . . .	81
2.4.3.3. Ending Point Probability . . . . .	82
2.4.3.4. Mean Number of $e$ -folds . . . . .	84
2.4.3.5. Number of $e$ -folds Dispersion . . . . .	88
2.4.3.6. Scalar Power Spectrum . . . . .	90
2.4.3.7. Scalar Spectral Index . . . . .	91
2.4.3.8. A Complete Example: Large Field Inflation . . . . .	91
2.4.3.9. Discussion . . . . .	98
<b>II. Results and Publications</b>	<b>101</b>
<b>3. Inflationary Predictions and Comparison with “Big Data” Observations</b>	<b>103</b>
3.1. “Horizon-Flow off-track for Inflation” (article) . . . . .	106
3.2. “Encyclopædia Inflationaris” (article) . . . . .	108
3.3. “The Best Inflationary Models After Planck” (article) . . . . .	110
3.4. “Compatibility of Planck and BICEP2 in the Light of Inflation” (article) . . . . .	112

3.5. “K-inflationary Power Spectra at Second Order” (article) . . . . .	114
<b>4. Quantum Aspects of Inflation and the Stochastic Formalism</b>	<b>117</b>
4.1. “Stochastic Effects in Hybrid Inflation” (article) . . . . .	120
4.2. “Recursive Stochastic Effects in Valley Hybrid Inflation” (article) . . . . .	122
4.3. “Cosmological Inflation and the Quantum Measurement Problem” (article) . . . . .	124
<b>Conclusion</b>	<b>127</b>
<b>List of figures</b>	<b>133</b>
<b>List of tables</b>	<b>135</b>
<b>Bibliography</b>	<b>137</b>
<b>Compte rendu français</b>	<b>165</b>
5.1. L’inflation et le Modèle Standard de la Cosmologie . . . . .	165
5.1.1. L’Univers Homogène . . . . .	165
5.1.2. Le Modèle du Big Bang Chaud et ses Problèmes . . . . .	166
5.1.3. L’Inflation Cosmologique . . . . .	167
5.2. Prédiction Inflationnaires et Observations en Données Massives . . . . .	168
5.2.1. Roulement Lent et Flot de Hubble . . . . .	168
5.2.2. Modèles à un Champ et <i>Encyclopædia Inflationaris</i> . . . . .	169
5.2.3. Inférence Bayésienne et Meilleurs Modèles Inflationnaires selon Planck . . . . .	171
5.2.4. Inflation et Tension entre Planck et BICEP2 . . . . .	172
5.2.5. Spectres de Puissance au Deuxième Ordre en Inflation-k . . . . .	174
5.3. Aspects Quantiques de l’Inflation et Formalisme Stochastique . . . . .	175
5.3.1. Effets Stochastiques en Inflation Hybride . . . . .	176
5.3.2. Formalisme Stochastique Récursif . . . . .	178
5.3.3. Le Problème de la Mesure Quantique en Cosmologie . . . . .	179
5.4. Conclusion . . . . .	182



**Part I.**

# **Cosmology and Inflation**



# 1. The Cosmological Standard Model

*In this chapter, we review the cornerstones of the standard model of modern cosmology. The Hot Big Bang scenario describes a series of events that occurred since an initial singularity 13.7 billion years ago, and for which we now have accurate observational evidence. Questions left unanswered by this model are discussed, which are solved by the introduction of an era of accelerated expansion in the early Universe. In this section, only a brief and partial overview of the standard cosmological model is given, the various aspects of which are further detailed in a broad range of textbooks [1, 2, 3, 4, 5, 6, 7, 8].*

Considerations about the extent and the structure of the Universe exist in almost every culture and seem to be intrinsic to the development of human awareness. In this sense, Cosmology is a matter of concern which may be considered as old as mankind itself. However, for a very long time, it consisted in a very speculative approach to metaphysical (more than physical) issues in which philosophy or even religion were also at stake. This radically changed only in the first half of the twentieth century with the advent of the theory of general relativity, which provided for the first time a mathematical consistent framework for describing space and time. Cosmological models, in which space is expanding, were derived from this theory and enabled to understand many observations starting with galaxies receding. During these years, Cosmology was mainly about describing and reconstructing *a posteriori* observational effects of this expansion. Then, in the second half of the twentieth century, was formulated the hot big bang model, which includes the description of physical processes occurring in this expanding space-time, and the associated thermal history of the Universe. More recently, Cosmology has entered a precision era with the inflow of high accuracy observational data such as the Cosmic Microwave Background (CMB) measurements, galaxy and supernova surveys, 21 cm astrophysics data, forthcoming cosmic rays and gravitational waves detectors, etc. Together with theoretical developments in high energy and gravitational physics, this enabled to upgrade Cosmology to the status of a genuine Science, *i.e.* a field of research in which falsifiable predictions can be made and tested.

## 1.1. The Homogeneous and Isotropic Universe

The distribution of galaxies and cosmological structures in space around us appears to be isotropic on large scales [ $\sim \mathcal{O}(100)$  Mpc], which implies that space-time possesses a spherical symmetry around us. This observational fact, combined with the Copernican principle<sup>1</sup> which states that we should not live in a central or specially favoured position in the Universe, leads to the conclusion that the Universe must be homogeneous on large scales. This is the

---

<sup>1</sup>The Copernican Principle is to be understood as opposed to the anthropocentrist view that human beings should be at the center of the Universe. For example, the Aristotelian model of the solar system in the Middle Ages placed the Earth at the center of the solar system, a unique place since it “appeared” that everything revolves around the Earth. Nicolaus Copernicus demonstrated that this view was incorrect and that the Sun was at the center of the solar system with the Earth in orbit around the Sun.

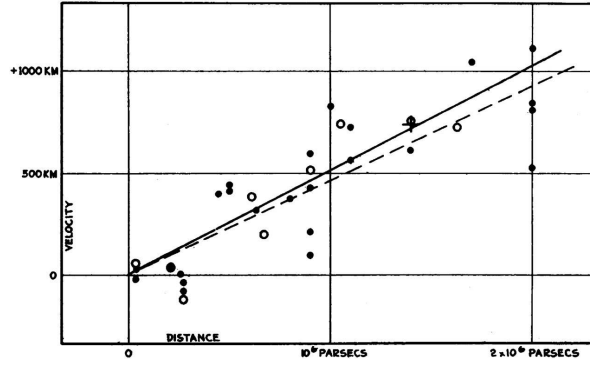


Figure 1.1.: Hubble diagram (*i.e.* velocity against distance) for extra-galactic nebulae, from the 1929 original paper [13] by Edwin Hubble. Such diagrams lead to the hypothesis of an expanding universe with a linear expansion law  $v = Hr$ . The radial velocities are obtained from redshift measurements and are corrected for solar motion, and distances are estimated from involved stars and mean luminosities of nebulae in a cluster. The black discs and full line represent the solution for solar motion using the nebulae individually; the circles and broken line represent the solution combining the nebulae into groups; the cross represents the mean velocity corresponding to the mean distance of 22 nebulae whose distances could not be estimated individually.

so-called cosmological principle.

### 1.1.1. The Friedmann-Lemaître-Robertson-Walker Metric

The cosmological principle is a statement about the amount of symmetry present in the observable Universe. As always in physics, this symmetry constrains and simplifies the mathematical description of the system under consideration. In this manner, under the cosmological principle symmetry, the metric of space-time  $ds^2 = g_{\mu\nu}dx^\mu dx^\nu$  can be shown to be entirely determined up to a free function of time, the scale factor  $a(t)$ , and a discrete parameter  $\mathcal{K} = -1, 0, 1$  which encodes the spatial curvature (open, flat or closed). With the  $(-, +, +, +)$  signature convention, it is of the form [9, 10, 11, 12]

$$ds^2 = -dt^2 + a^2(t) \left[ \frac{dr^2}{1 - \mathcal{K}r^2} + r^2 (d\theta^2 + \sin^2 \theta d\phi^2) \right] \quad (1.1)$$

and is called the Friedmann-Lemaître-Robertson-Walker (FLRW) metric. In this parametrization,  $t$  is the cosmic time,  $r$  is the comoving radial coordinate which is unitless,  $\theta$  and  $\phi$  are the comoving angular coordinates, and  $a(t)$  has units of length.<sup>2</sup>

#### 1.1.1.1. The Hubble Law

From the FLRW metric (1.1), one can see that the physical distance  $L_{\text{phys}}$  between two points measured on a constant  $t$  hypersurface scales as the scale factor  $a$ , that is to say

$$L_{\text{phys}} = a(t)L_{\text{com}}, \quad (1.2)$$

<sup>2</sup>Hereafter and unless stated otherwise, we work in the unit system where  $c = \hbar = k_B = 1$ .

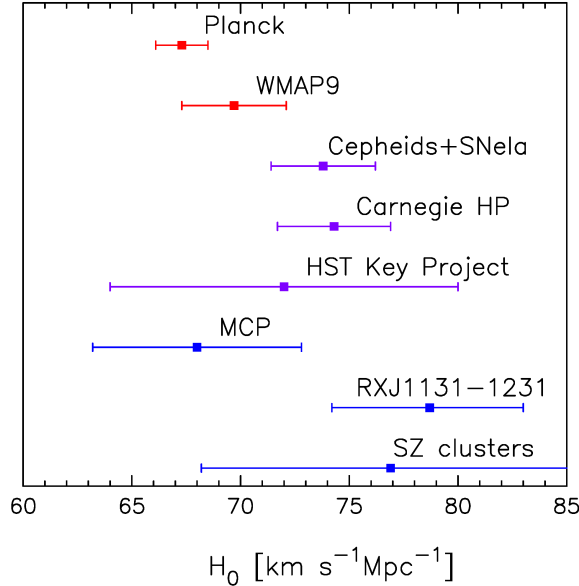


Figure 1.2.: Comparison of  $H_0$  measurements, with estimated of  $\pm 1\sigma$  errors, from a number of different astrophysical techniques, and compared with the spatially-flat  $\Lambda$ CDM model constraints from Planck and WMAP9. Image Credit: Ref. [15].

where  $L_{\text{com}}$  is the so-called comoving distance, which is constant in time for still objects in the FLRW frame. The scale factor  $a$  thus sets the overall expansion (or contraction) level of space hypersurfaces, hence its name. Another consequence of the FLRW metric is a linear relation between distance and velocity. Indeed, from differentiating Eq. (1.2) with respect to cosmic time  $t$ , one obtains

$$v = \frac{dL_{\text{phys}}}{dt} = \frac{\dot{a}}{a} L_{\text{phys}} = H L_{\text{phys}}, \quad (1.3)$$

where we have defined the Hubble parameter  $H \equiv \dot{a}/a$ . This is the so-called Hubble law. It was first observed in 1929, as presented in Fig. 1.1, where the current value of  $H$ , that we denote  $H_0$ , was determined to be of the order of 500 km/sec/Mpc. As we will see below, this value contains valuable information about the content of the Universe and this is why it has been the object of much research effort. The first good estimation was realized in 1958 in Ref. [14], where the value 75 km/sec/Mpc was obtained. Finally, the most up to date measurements provided by the Planck mission [15] gave the value  $67.80 \pm 0.77$  km/sec/Mpc for the value of  $H_0$ . This value is rather low compared with previous measurements, see Fig. 1.2, and the tension between the CMB-based estimates in the  $\Lambda$ CDM model and the astrophysical measurements of  $H_0$  is still intriguing [15, 16, 17, 18, 19, 20, 21].

The reduced Hubble parameter  $h$  is also often used, and is defined as

$$H_0 = 100 h \text{ km/sec/Mpc}. \quad (1.4)$$

The Hubble parameter sets the fundamental physical scale of space-time. It provides a characteristic time scale  $H_0^{-1} \simeq 4.551 \times 10^{17}$  sec called the ‘‘Hubble time’’ and a characteristic length scale  $H_0^{-1} \simeq 1.364 \times 10^{26}$  m called the ‘‘Hubble radius’’. As we will see later, the Hubble time sets the scale for the age of the Universe, and the Hubble length sets the scale for the size of the observable Universe. These values are displayed in table 1.2 where we collect all the numerical values given and used throughout this section 1.

### 1.1.1.2. Redshift and Comoving Coordinates

Another interesting property of FLRW space-times is that light gets redshifted as it travels, due to the time dependence of the scale factor. Let us consider an emitting object at rest in the comoving coordinates system, with radial coordinate  $r_1$ , while an observer is located at  $r_0 = 0$ . Light is emitted from this first object at time  $t_1$  with frequency  $\nu_1$ , and received by the observer at time  $t_0$  with frequency  $\nu_0$ . Let us determine the relation between  $\nu_0$  and  $\nu_1$ . Since light travels along geodesics with  $ds = 0$ , radial light path traveling towards the observer ( $d\theta = d\phi = 0$  and  $dr/dt < 0$ ) follows

$$\frac{dt}{a(t)} = \frac{dr}{\sqrt{1 - \mathcal{K}r^2}}. \quad (1.5)$$

Now consider the emission of two subsequent crests of a light wave. The first one is emitted at  $(t_1, r_1)$  and received at  $(t_0, 0)$  while the second one is emitted at  $(t_1 + \delta t_1, r_1)$  and received at  $(t_0 + \delta t_0, 0)$ . From Eq. (1.5), one has

$$\int_{r_1}^0 \frac{dr}{\sqrt{1 - \mathcal{K}r^2}} = \int_{t_1}^{t_0} \frac{dt}{a(t)} = \int_{t_1 + \delta t_1}^{t_0 + \delta t_0} \frac{dt}{a(t)}. \quad (1.6)$$

Subtracting the third integral from the second, in the limit  $\delta t_0, \delta t_1 \ll a/\dot{a}$ , one obtains

$$\frac{\delta t_0}{a(t_0)} = \frac{\delta t_1}{a(t_1)}. \quad (1.7)$$

Since the time delay  $\delta t$  between two crests is nothing but the inverse frequency, one obtains

$$\frac{\nu_1}{\nu_0} = \frac{a(t_0)}{a(t_1)} = 1 + z, \quad (1.8)$$

where the last equality defines the redshift  $z$ . This quantity only depends on the ratio of the scale factor at reception to the scale factor at emission.

In terms of wavelength  $\lambda$ , Eq. (1.8) gives  $\lambda_0/\lambda_1 = a(t_0)/a(t_1)$ . We see that the wavelength of light just contracts and stretches with the scale factor  $\lambda \propto a$ . Another way to look at this is to say that a photon traveling through an FLRW space-time loses momentum as the Universe expands,

$$p = h\nu \propto a^{-1}(t). \quad (1.9)$$

As shown in appendix 1.A, see Eqs. (1.95) and (1.96), this momentum loss applies to massive particles as well as photons, and any particle moving in an expanding FLRW space-time loses momentum as  $p \propto a^{-1}$ . This means that a massive particle asymptotically comes to rest relative to the comoving coordinates system. Thus, comoving coordinates represent a preferred reference frame which is such that any free body with a peculiar velocity relative to the comoving frame eventually comes to rest in this frame.

### 1.1.1.3. Einstein Equations

The Einstein-Hilbert action [22, 23, 24] describes the dynamics of space-time metrics, and reads

$$\mathcal{S}_{\text{grav}} = \frac{1}{2\kappa} \int d^4x \sqrt{-g} (R - 2\Lambda), \quad (1.10)$$

where  $\kappa \equiv 8\pi G = 8\pi/m_{\text{Pl}}^2 = 1/M_{\text{Pl}}^2$ , where  $G$  is the Newton gravitational constant,  $m_{\text{Pl}}$  is the Planck mass and  $M_{\text{Pl}} \simeq 2.4 \times 10^{18}$  GeV is the reduced Planck mass. In the above expression,

$\Lambda$  is a cosmological constant,  $g$  is the determinant of  $g_{\mu\nu}$  and  $R$  is the Ricci curvature scalar  $R \equiv g^{\mu\nu} R_{\mu\nu}$ . It is constructed from the Ricci tensor  $R_{\mu\nu} = 2\Gamma_{\mu[\nu,\rho]}^\rho + 2\Gamma_{\lambda[\rho}^\rho \Gamma_{\nu]\mu}^\lambda$ , where brackets mean anti-symmetrization over the indices and where the Christoffel symbols are given by  $\Gamma_{\mu\nu}^\rho = \frac{1}{2}g^{\rho\lambda}(\partial_\nu g_{\lambda\mu} + \partial_\mu g_{\lambda\nu} - \partial_\lambda g_{\mu\nu})$ .

To this action should be added a part  $\mathcal{S}_{\text{matter}} = \int \mathcal{L}_{\text{matter}} \sqrt{-g} d^4x$  describing matter in the Universe. When varying these two action terms with respect to  $g_{\mu\nu}$ , one obtains two tensors, namely the Einstein tensor  $G_{\mu\nu}$  defined as

$$G_{\mu\nu} + \Lambda g_{\mu\nu} \equiv \frac{2\kappa}{\sqrt{-g}} \frac{\partial \mathcal{S}_{\text{grav}}}{\partial g_{\mu\nu}} = R_{\mu\nu} - \frac{1}{2} R g_{\mu\nu} + \Lambda g_{\mu\nu} \quad (1.11)$$

for the gravity part, and the energy-momentum tensor

$$T_{\mu\nu} \equiv -\frac{2}{\sqrt{-g}} \frac{\partial \mathcal{S}_{\text{matter}}}{\partial g_{\mu\nu}} = g_{\mu\nu} \mathcal{L}_{\text{matter}} - 2 \frac{\delta \mathcal{L}_{\text{matter}}}{\delta g^{\mu\nu}} \quad (1.12)$$

for the matter part. This leads to the well-known Einstein equations

$$G_{\mu\nu} + g_{\mu\nu} \Lambda = \kappa T_{\mu\nu}. \quad (1.13)$$

Let us now work out the two tensors  $G_{\mu\nu}$  and  $T_{\mu\nu}$  for an FLRW metric. When the metric (1.1) is plugged into the definition (1.11), one obtains (a detailed calculation is provided in appendix 1.A)

$$G_{00} = 3 \left( H^2 + \frac{\mathcal{K}}{a^2} \right), \quad G_{ij} = - \left( H^2 + 2 \frac{\ddot{a}}{a} + \frac{\mathcal{K}}{a^2} \right) g_{ij}, \quad (1.14)$$

where the index 0 is for time  $t$ , and the indexes  $i$  and  $j$  are for space coordinates so that  $g_{ij}$  is just the spatial part of the full metric  $g_{\mu\nu}$ .

Given the symmetries of space-time, one can show that the most generic form of the energy-momentum tensor is given by

$$T_{\mu\nu} = \rho u_\mu u_\nu + \frac{p}{a^2} g_{\mu\nu}, \quad (1.15)$$

where  $g_{\mu\nu} = g_{ij}$  when  $\mu$  and  $\nu$  are space indexes and 0 otherwise. In the above expression,  $\rho$  and  $p$  are two constants depending on time only, and  $u_\mu$  is the four velocity of a comoving observer for whom space is homogeneous and isotropic. One thus has  $u_\mu = \delta_{\mu,0}$ , where  $\delta$  is the Kröneckers symbol. Since  $p$  is associated to the spatial part of the tensor, it can be interpreted as the pressure of matter, while  $\rho = T_{\mu\nu} u^\mu u^\nu$  is the energy density measured by a comoving observer. The above form of  $T_{\mu\nu}$  is entirely fixed by the cosmological principle. Finally, let us mention that the time component of the conservation relation  $\nabla_\mu T^{\mu\nu} = 0$  leads to

$$\dot{\rho} + 3H(\rho + p) = 0. \quad (1.16)$$

Heuristically, this equation can be understood as a translation of the first law of thermodynamics,  $dU = -pdV$ , with  $U = \rho V$  and  $V = a^3$ .

### 1.1.2. An Expanding Universe

Let us now detail how this general relativistic framework allows to relate the dynamics of the expansion of space-time to the matter content properties of the Universe.

### 1.1.2.1. Friedmann and Raychaudhuri Equations

If one plugs the above expressions for  $G_{\mu\nu}$ , Eqs. (1.14), and for  $T_{\mu\nu}$ , Eq. (1.15), in the Einstein equation (1.13), one obtains the two following dynamical equations

$$H^2 = \frac{\kappa}{3}\rho - \frac{\mathcal{K}}{a^2} + \frac{\Lambda}{3}, \quad (1.17)$$

$$\frac{\ddot{a}}{a} = -\frac{\kappa}{6}(\rho + 3p) + \frac{\Lambda}{3}. \quad (1.18)$$

These two equations are known as the Friedmann [25] and the Raychaudhuri [26] equations, respectively. Because of the Bianchi identities, when combined together, one can check that they account for the conservation equation (1.16).

The Friedmann equation relates the change of the scale factor of the Universe to its energy density, spatial curvature and cosmological constant. If the Universe is assumed to be flat ( $\mathcal{K} = 0$ ) and if the cosmological constant vanishes ( $\Lambda = 0$ ), this means that the only presence of energy will cause the Universe to expand ( $H > 0$ ) or to contract ( $H < 0$ ). In the following, we shall mostly consider expanding universes, even if contracting universes are key ingredients of some cosmological models [27, 28, 29, 30, 31, 32, 33, 34].

From the Raychaudhuri equation, one can notice that in absence of a cosmological constant, any form of matter such that  $\rho + 3p < 0$  will cause an acceleration of the scale factor  $\ddot{a} > 0$  if it dominates the energy budget of the Universe. The energy density is always positive, but in some cases the pressure can be negative and the inequality  $\rho + 3p < 0$  may be realized. This simple property is deeply rooted in the inflationary scenario and will be discussed in more details in chapter 2. As we shall now see, it is intimately related to the fundamental principles of general relativity.

### 1.1.2.2. The Newtonian Expanding Sphere

In order to highlight the relativistic effects in the above setup more clearly, let us derive the Newtonian version [35, 36, 37] of the Friedmann and Raychaudhuri equations. In Fig. 1.3, we sketch the case of an expanding sphere of radius  $a$  filled with uniform matter with mass density  $\rho$ . Let us consider a particle of mass  $m$  sitting on the out-shell of this sphere. The Gauss theorem states that the gravitational attractive force seen by such a particle is given by  $GmM/a$ , where  $M = 4/3\pi\rho a^3$  is the integrated mass of the sphere. Its acceleration being simply  $\ddot{a}$ , the second Newton law gives rise to  $m\ddot{a} = -MGm/a$ , *i.e.*

$$\left. \frac{\ddot{a}}{a} \right|_{\text{Newton}} = -\frac{4}{3}\pi\rho G = -\frac{\kappa}{6}\rho. \quad (1.19)$$

This matches the Raychaudhuri equation (1.18) without cosmological constant and without the pressure term. This is why in Newtonian mechanics, one must have  $\ddot{a} < 0$  and the expansion of the sphere can only decelerate. The reason why acceleration is allowed in the general relativistic setup is because all forms of energy gravitate, including pressure.<sup>3</sup> As a consequence, the presence of pressure in the Raychaudhuri equation is a crucial signature of the relativistic nature

<sup>3</sup>Acceleration of FRLW space-times is actually one of the only manifestations of pressure's self-gravity [38], otherwise tested only in the context of big bang nucleosynthesis [39] where it is necessary to account for current light element abundances. For example, even in compact objects such as neutron stars, pressure's self-gravity is immeasurable given uncertainties on the equation of state [40, 41].

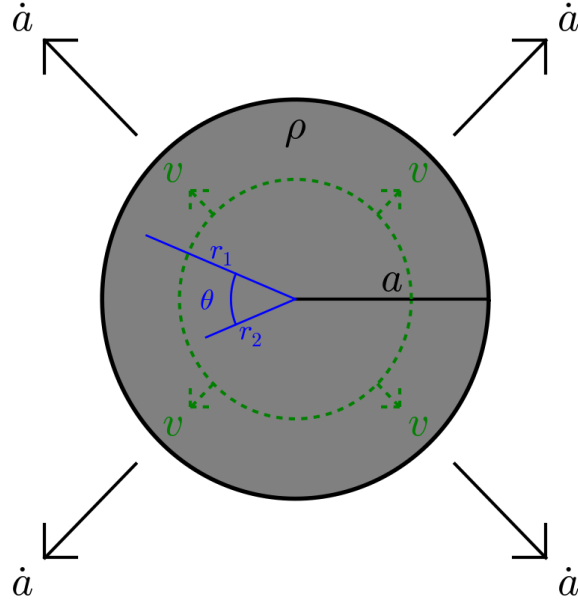


Figure 1.3.: Homogeneous sphere in Newtonian radial expansion.

of the setup. Indeed, in newtonian mechanics, masses source the gravity field, but relativity relates mass to energy. Since energy is not a relativistic invariant but mixes up with momentum when changing frames, momentum, hence pressure, naturally comes into play in a relativistic context.

It is also interesting to calculate the newtonian energy  $E_{\text{Newton}}$  of the sphere of Fig. 1.3. In order to do this, we first need to derive the velocity profile  $v(r)$  of the sphere radial expansion. When diluting, let us assume that the mass density scales as the inverse of the volume to some power  $1 + w$ ,  $\rho \propto V^{-(1+w)}$  (where for ordinary “newtonian” matter,  $w = 0$ ). One can first show<sup>4</sup> that its evolution is given by

$$\dot{\rho} = -(w + 1) \left[ v'(r) + 2\frac{v(r)}{r} \right] \rho. \quad (1.20)$$

In order for the sphere to remain homogeneous (*i.e.* to be such that  $\rho$ , hence  $\dot{\rho}$ , does not depend on  $r$ ), the term factorizing  $\rho$  in the right hand side of the previous relation should not depend on  $r$ , *i.e.* one must have  $v' + 2v/r = \text{constant}$ . This leads to the two-branch solution

$$v(r) = Ar + \frac{B}{r^2} \quad (1.21)$$

for the radial velocity, where  $A$  and  $B$  are two integration constants that can only depend on time. In this manner the sphere is and remains homogeneous. However, there is no reason why it should be isotropic. Indeed, even if the sphere is taken to be infinite, the direction pointing towards its center is a priori a privileged direction. This is not the case only if the velocity law (1.21)  $v(r)$  is valid not only for  $r$  being the distance between the center of the sphere and one of its shells, but for  $r$  being the distance between any two points within the sphere. As we shall now see, this selects out one of the two branches of the solution (1.21). Let us thus consider

<sup>4</sup>Two shells of radius  $r_1$  and  $r_2 = r_1 + dr$  respectively become, after a  $dt$  long expansion, two shells of radius  $r'_1 = r_1 + v(r_1)dt$  and  $r'_2 = r_1 + dr + [v(r_1) + v'(r_1)dr]dt$ . The volume contained between these two shells thus evolves from  $V = 4\pi r_1^2 dr$  to  $V' = 4\pi r_1'^2 (r'_2 - r'_1) \simeq V [1 + 2v(r_1)/r_1 dt + v'(r_1)dt]$ . From here one gets  $dV/dt = V (v' + 2v/r)$ , and with  $\rho V^{w+1} = \text{constant}$ , Eq. (1.20).

two points of radial distances  $r_1$  and  $r_2$  respectively, and with angular separation  $\theta$  as in Fig. 1.3. The distance between these two points is simply given by  $d_{12} = \sqrt{r_1^2 + r_2^2 - 2r_1r_2 \cos \theta}$ . Since  $\theta$  is conserved through the radial expansion, its time variation is

$$\dot{d}_{12} = \frac{r_1 v(r_1) + r_2 v(r_2) - [r_2 v(r_1) + r_1 v(r_2)] \cos \theta}{d_{12}}. \quad (1.22)$$

On the other hand, if the velocity law (1.21) is isotropic, one must have

$$\dot{d}_{12} = v(d_{12}). \quad (1.23)$$

When the velocity law (1.21) is used in the identification of Eqs. (1.22) and (1.23), it is straightforward to see that  $B = 0$ . Only the first branch remains, and one has

$$v(r) = Hr, \quad (1.24)$$

where we have renamed  $H \equiv A = \dot{a}/a = \dot{r}/r$ , which can only depend on time. In a cosmological context, one recovers the Hubble law previously mentioned. In particular, it is in order to stress that it eventually does not depend on the volume scaling power index  $w$ .

We are now in a position where we can calculate the energy of the sphere. It is given by the sum of its integrated kinetic energy and its integrated potential energy, that is

$$\begin{aligned} E_{\text{Newton}} &= \int_0^a \frac{1}{2} (4\pi r^2 dr \rho) (rH)^2 - \int_0^a \frac{G}{r} (4\pi r^2 dr \rho) \left( \frac{4}{3} \pi r^3 \rho \right) \\ &= \frac{2}{5} \pi \rho a^5 H^2 - \frac{16\pi^2}{15} G \rho^2 a^5 \\ &= \frac{2}{5} \pi a^5 \rho \left( H^2 - \frac{\kappa}{3} \rho \right). \end{aligned} \quad (1.25)$$

Remembering that  $\rho$  scales as  $V^{-(w+1)} \propto a^{-3(w+1)}$ , one obtains

$$H^2 = \frac{\kappa}{3} \rho + \frac{5E_{\text{Newton}}}{2\pi\rho_0 a_0^{3(w+1)}} \frac{1}{a^{2-3w}}. \quad (1.26)$$

When the Newtonian energy vanishes, one obtains the Friedmann equation (1.17) in absence of cosmological constant and curvature, the presence of which is therefore a truly relativistic effect. In passing, let us notice that when  $E_{\text{Newton}} \neq 0$  and for ordinary matter (such that  $w = 0$ ), the second term in the right hand side of Eq. (1.26) plays a role similar to the one of curvature in Eq. (1.17), which scales as  $a^{-2}$  and which can be either positive or negative.

A last remark is in order about the conservation equation. In Newtonian mechanics, if one replaces  $v(r) = Hr$  in Eq. (1.20), one obtains the conservation equation  $\dot{\rho} + 3(w+1)H\rho = 0$ , which, in passing, matches Eq. (1.16) if  $p = w\rho$ . This relation is fairly trivial since it just states that  $\rho \propto V^{-(1+w)}$ . Thanks to this conservation law, one can check that the two equations (1.19) and (1.26) are actually equivalent when  $w = 0$ . This is just a consequence of the fact that the conservation of mechanical energy is equivalent to the second Newton law, *i.e.* that Newtonian mechanics derives from a potential. However, in the case of general relativity, the conservation equation (1.16) is not trivial at all and is required to relate the Friedmann and Raychaudhuri equations. One thus really have two independent dynamical equations.

fluid	equation of state parameter $w$	$\rho(a)$	$a(t)$
cold matter	0	$\propto a^{-3}$	$\propto t^{2/3}$
radiation	1/3	$\propto a^{-4}$	$\propto t^{1/2}$
spatial curvature	-1/3	$\propto a^{-2}$	$\propto t$
cosmological constant	-1	$\propto a^0$	$\propto \exp(Ht)$
scalar field	$-1 + 2\epsilon_1/3$	$\propto a^{-2\epsilon_1}$	$t^{1/\epsilon_1}$

Table 1.1.: Equation of state parameter  $w$  for a few fluid examples, with corresponding  $\rho(a)$  (1.27) and  $a(t)$  (1.30) profiles.

### 1.1.2.3. Constant Equations of State

It is interesting to notice that the conservation equation (1.16) can be solved in the simple case of a single ideal fluid where the energy density and the pressure are related by a constant equation of state parameter  $w \equiv p/\rho$ . One obtains

$$\rho = \rho_{\text{in}} \left( \frac{a}{a_{\text{in}}} \right)^{-3(1+w)}. \quad (1.27)$$

The equation of state parameter of cold matter is simply  $w_{\text{mat}} = 0$  so that the energy density scales as the inverse volume  $\rho_{\text{mat}} \propto a^{-3}$ , while the equation of state parameter of radiation is  $w_{\text{rad}} = 1/3$  so that the associated energy density scales as  $\rho_{\text{rad}} \propto a^{-4}$ , which includes both volume dilution effect ( $\propto a^{-3}$ ) and wavelength redshift (1.8) ( $\propto a^{-1}$ ). From the Friedmann equation (1.17), one can also associate an energy density to curvature  $\rho_{\mathcal{K}} \equiv -3\mathcal{K}/(\kappa a^2)$  and to the cosmological constant  $\rho_{\Lambda} \equiv \Lambda/\kappa$ , so that the Friedmann equation reads

$$H^2 = \frac{\kappa}{3} (\rho_{\text{matter}} + \rho_{\mathcal{K}} + \rho_{\Lambda}) \equiv \frac{\kappa}{3} \rho_{\text{T}}, \quad (1.28)$$

where  $\rho_{\text{T}}$  denotes the “total” energy density. Here,  $\rho_{\text{matter}}$  can include ordinary cold matter, radiation, or any other Universe constituent. Since  $\rho_{\mathcal{K}} \propto a^{-2}$ , this means that curvature can be viewed as a fluid constituent with equation of state parameter  $w_{\mathcal{K}} = -1/3$ . In the same manner,  $\rho_{\Lambda}$  is constant and can be viewed as a fluid constituent<sup>5</sup> with equation of state parameter  $w_{\Lambda} = -1$ . These values for the equation of state parameters are summarized in table 1.1. The last entry corresponds to a scalar field and will be further explicated in chapter 2.

Interestingly enough, since  $p_{\Lambda} = w_{\Lambda}\rho_{\Lambda} = -\rho_{\Lambda}$ , the  $\Lambda/3$  term in the right hand side of Eq. (1.18) can also be written  $-\kappa/6(\rho_{\Lambda} + 3p_{\Lambda})$ . In the same manner, since  $p_{\mathcal{K}} = -\rho_{\mathcal{K}}/3$ , adding a  $-\kappa/6(\rho_{\mathcal{K}} + 3p_{\mathcal{K}}) = 0$  to the right hand side of Eq. (1.18) does not change it, so that similarly to Eq. (1.28), the Raychaudhuri equation can be written as

$$\frac{\ddot{a}}{a} = -\frac{\kappa}{6} [\rho_{\text{matter}} + \rho_{\Lambda} + \rho_{\mathcal{K}} + 3(p_{\text{matter}} + p_{\Lambda} + p_{\mathcal{K}})] = -\frac{\kappa}{6} (\rho_{\text{T}} + 3p_{\text{T}}), \quad (1.29)$$

where  $p_{\text{T}}$  denotes the “total” pressure. This is why, as far as the two dynamical equations (1.17) and (1.18) are concerned, the curvature can be viewed as an ideal fluid constituent with equation

<sup>5</sup>This should not come as a surprise since the conservation relation  $\nabla_{\mu}T^{\mu\nu} = 0$  is invariant under the redefinition  $T_{\mu\nu} \rightarrow T_{\mu\nu} + \Lambda g_{\mu\nu}$ . This is the reason why a cosmological constant can actually be thought of as being part of the matter side of the Einstein equations.

of state parameter  $w_\kappa = -1/3$  and the cosmological constant can be viewed as an ideal fluid constituent with equation of state parameter  $w_\Lambda = -1$ .

If the scale factor  $a$  evolves monotonously with time, the right hand side of the Friedmann equation (1.28) soon gets dominated by a single fluid (the one with the smallest  $w$  if space expands, or the one with the largest  $w$  if space contracts). In this limit, it can be integrated, leading to

$$a(t) = \begin{cases} a_{\text{in}} \left[ 1 \pm \frac{3}{2} (1+w) \sqrt{\frac{\rho_{\text{in}}}{3} \frac{t - t_{\text{in}}}{M_{\text{Pl}}}} \right]^{\frac{2}{3(1+w)}} & \text{if } w \neq -1 \\ a_{\text{in}} \exp\left(\pm \sqrt{\frac{\rho_{\text{in}}}{3} \frac{t - t_{\text{in}}}{M_{\text{Pl}}}}\right) & \text{if } w = -1 \end{cases}, \quad (1.30)$$

where  $a_{\text{in}}$  and  $t_{\text{in}}$  are two integration constants. The sign  $\pm$  depends on whether space is expanding (plus sign,  $H > 0$ ) or contracting (minus sign,  $H < 0$ ). In what follows, only the case of an expanding space will be considered. The  $\rho(a)$  shape (1.27) and the  $a(t)$  shape (1.30) are also given in table 1.1 for the fluids mentioned so far.

Finally, it is interesting to notice that the conservation equation (1.16) can also be integrated when the Universe is made of a collection of ideal independent fluids with equations of state  $w_i = p_i/\rho_i$ . In this case indeed, the conservation equation gives rise to

$$\sum_i [\dot{\rho}_i + 3H(1+w_i)\rho_i] = 0. \quad (1.31)$$

One of the solutions is of course when all the terms of the above sum vanish. Physically, this corresponds to a situation of non interacting independent fluids, where there is no energy transfer from one fluid to another. Obviously, in this case the scaling solution (1.27) applies for all the fluids, and the total energy density is given by

$$\rho_{\text{T}} = \sum_i \rho_i^{\text{in}} \left( \frac{a}{a_{\text{in}}} \right)^{-3(1+w_i)}. \quad (1.32)$$

Unfortunately however, in this case the Friedmann equation  $H^2 = \kappa\rho_{\text{T}}/3$  cannot be integrated analytically.

## 1.2. The Present Composition of the Universe

Thanks to Eq. (1.32), we now know how the energy density of each constituent of the Universe evolves with time, at least provided its equation of state parameter is constant. Therefore, up to potential energy transfer between constituents, it is enough to know the energy densities at a single time (most conveniently, now) to derive their value at any other time. This is why we now discuss the present composition of the Universe.

To this end, we first define the critical density  $\rho_{\text{crit}}$  with respect to the Hubble parameter,

$$\rho_{\text{crit}} = \frac{3}{\kappa} H^2. \quad (1.33)$$

The total energy density  $\rho_{\text{tot}}$  is the sum of all contributions but the curvature one,  $\rho_{\text{tot}} = \rho_{\text{T}} - \rho_{\kappa}$ . If one writes  $\rho_{\text{tot}} = \sum_i \rho_i$ , each part  $\rho_i$  stands for an ideal fluid  $i$  with its own equation of state

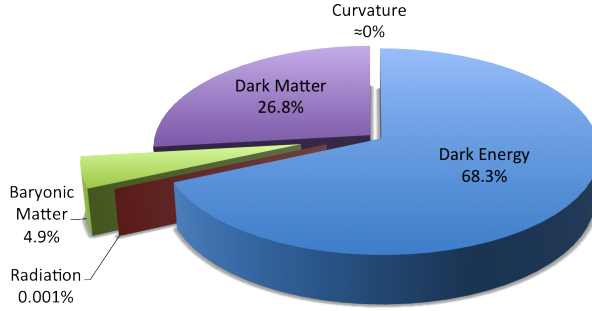


Figure 1.4.: Current Energy Composition of the Universe.

parameter  $w_i$ . The dimensionless quantities  $\Omega_i = \rho_i/\rho_{\text{crit}}$  then allow to re-write the Friedmann equation (1.28) simply as

$$\Omega_{\text{tot}} = \sum_i \Omega_i = 1 - \Omega_{\mathcal{K}}, \quad (1.34)$$

where we stress again that the curvature term (which, contrary to the others, can be either positive or negative) is treated separately. In the present Universe, the components contributing to this relation have the following weights.<sup>6</sup>

### Radiation

Most of the photons present in the Universe belong to the Cosmic Microwave Background, see section 1.3.3. They represent a tiny fraction of  $\rho_{\text{tot}}$ , with [15]  $\Omega_{\text{rad}}^{(0)} \approx 9.3 \times 10^{-5}$ .

### Baryonic Matter

The contribution from ordinary matter (*i.e.* the one we find in atoms, nuclei, *etc.*) to  $\Omega_{\text{tot}}$  is dominated by cold baryons (strongly interacting composite subatomic particles made up of three quarks) which are much heavier than leptons (elementary spin 1/2 particles that do not undergo strong interaction, such as electrons or neutrinos). However, they only amount to [15]  $\Omega_{\text{b}}^{(0)} \approx 0.049$ .

### Nonbaryonic (or “Dark”) Matter

In order to consistently explain many observational facts, ranging from galaxy rotation curves and large scale structure formation to the CMB statistics, it is common to postulate the existence of another non-relativistic matter component in the Universe, with  $w = 0$  as well, referred to as “dark matter”. Its current contribution is [15]  $\Omega_{\text{dm}}^{(0)} \approx 0.268$  and therefore, it strongly dominates over ordinary matter. The nature of dark matter is obviously the subject of active study.

<sup>6</sup>All quantities referring to their current (present-day) value are designated by a subscript (or occasionally a superscript) “0” or “(0)”.

## Curvature

When  $\mathcal{K} = 0$ , the Universe is globally flat. If  $\mathcal{K} = \pm 1$  however ( $\mathcal{K} = 1$  corresponds to a closed universe while  $\mathcal{K} = -1$  corresponds to an infinite universe), there should be a curvature component in the current Universe energy budget. However, it has not been detected yet, and all the observations made so far are still consistent with  $\Omega_{\mathcal{K}}^{(0)} \simeq 0$ . The current constraints give [15]  $100\Omega_{\mathcal{K}}^{(0)} = -0.10_{-0.65}^{+0.62}$  at 95% confidence level.

## Dark Energy

Evidently, after summing over radiation, baryonic and non-baryonic matter, the bulk part of the Universe’s energy density is still missing. Together with evidence from a recent acceleration in the expansion of the Universe, this motivates the introduction of a missing fluid named “dark energy”, with an equation of state parameter  $w \simeq -1$ . This is why the cosmological constant  $\Lambda$  (for which  $w = -1$  exactly) is one of the candidates for dark energy, even if as for dark matter, the nature of dark energy is the subject of active study (for a nice review, see Ref. [42]). It accounts for the major contribution to  $\Omega_{\text{tot}}^{(0)}$ , *i.e.* [15]  $\Omega_{\text{de}}^{(0)} \approx 0.683$ .

The values mentioned here are given in table 1.2. The relative contributions of these constituents is also displayed in Fig. 1.4. One can see that the Universe is currently dominated by fluids the physical nature of which is still not well understood (dark matter and dark energy). This gives us an idea of the theoretical effort still needed to build a complete and standard description of cosmology.

## 1.3. The History of the Universe: the Hot Big Bang Model

In the previous section, we have stated the current values of the energy fractions  $\Omega_i^{(0)}$  for the Universe main components. Combined with the dynamical considerations of section 1.1.2, this enables us to now infer the main lines of the history of the Universe.

### 1.3.1. Dominant Constituent

Plugging the previously given values for  $\Omega_i^{(0)}$  in Eq. (1.32),  $\rho_{\text{tot}}/\rho_{\text{cri}} = \sum_i \Omega_i^{(0)} (a/a_0)^{-3(1+w_i)}$ , allows us to discuss the way  $\rho_{\text{tot}}$  varies with  $a$ . The result is displayed in the left panel of Fig. 1.5. The black dashed line stands for the total sum, while the coloured lines follow each of its components. Because of the different scalings with  $a$ , each component of the Universe dominates its content at a different epoch (called “eras” in what follows).

The Universe is currently dominated by dark energy which means that  $\rho_{\text{tot}} \simeq \text{constant}$ . Since cold matter  $\rho_{\text{mat}} \equiv \rho_{\text{dm}} + \rho_{\text{b}}$  scales as  $a^{-3}$ , its contribution increases when moving backwards in time and becomes larger than the one of dark energy at some point  $a_{\text{acc}}$  defined by  $\rho_{\text{mat}}(a_{\text{acc}}) = \rho_{\text{de}}(a_{\text{acc}})$ , *i.e.*  $a_{\text{acc}}/a_0 = \left[ \Omega_{\text{mat}}^{(0)}/\Omega_{\text{de}}^{(0)} \right]^{1/3}$ . Here, the subscript “acc” stands for the onset of the dark energy phase.<sup>7</sup> When  $a < a_{\text{acc}}$ , the Universe is dominated by cold matter and one has

<sup>7</sup>One should note that contrary to what the notation may suggest, acceleration of the expansion does not begin

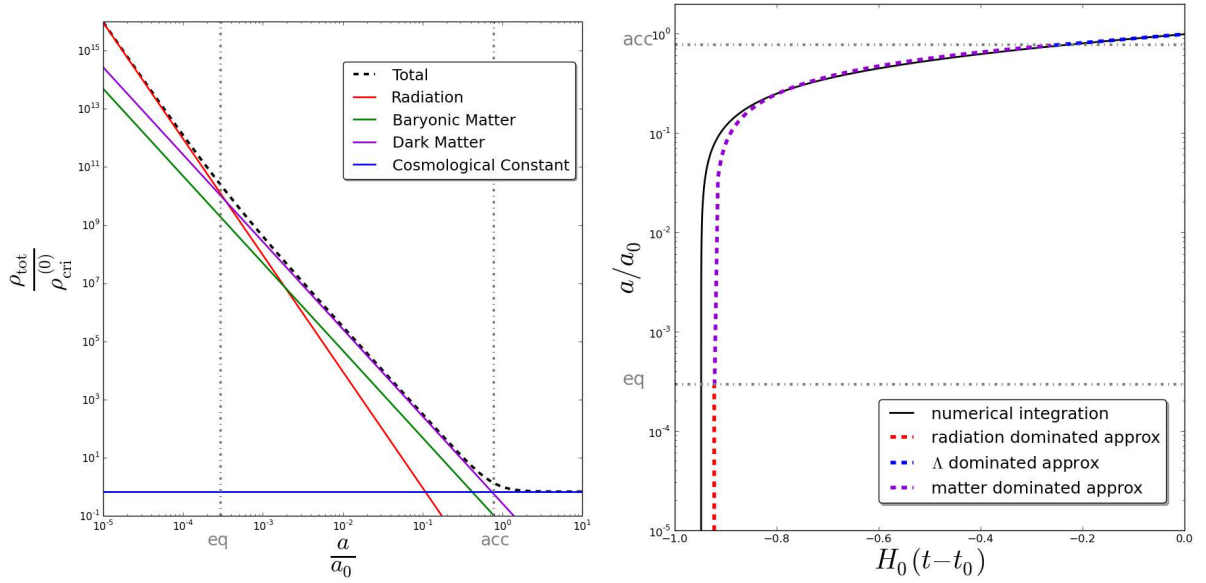


Figure 1.5.: Left panel: energy density (1.32) of the Universe constituents [scaled by the current critical density  $\rho_{\text{cri}}^{(0)}$ ] as a function of the scale factor  $a$ . The black dashed line stands for the sum of all contributions. The Universe history is made of a radiation era ( $a < a_{\text{eq}}$ ), followed by a matter era ( $a_{\text{eq}} < a < a_{\text{acc}}$ ) and more recently a cosmological constant era ( $a > a_{\text{acc}}$ ). Right panel: scale factor  $a$  as a function of cosmic time  $t$ . The black line corresponds to the numerical integration of Eq. (1.42), and the coloured lines stand for the piecewise approximated solution (1.38). Both panels make use of  $\Omega_{\mathcal{K}}^{(0)} = 0$  and the values of  $\Omega_i^{(0)}$  recalled in table 1.2, and dark energy is described by means of a cosmological constant ( $w_{\text{de}} = w_{\Lambda} = -1$ ).

$\rho_{\text{tot}} \propto a^{-3}$  and  $a \propto t^{2/3}$ , see Eq. (1.30).

It can be more convenient to label time  $t$  with the redshift  $z$  of a photon emitted at time  $t$  and reaching its observer now, defined in Eq. (1.8) as

$$1 + z = \frac{a_0}{a}. \quad (1.35)$$

With this definition, the transition redshift between matter and dark energy eras is given by

$$z_{\text{acc}} = \left[ \frac{\Omega_{\text{de}}^{(0)}}{\Omega_{\text{mat}}^{(0)}} \right]^{1/3} - 1. \quad (1.36)$$

With the values of  $\Omega_i^{(0)}$  recalled in table 1.2, one obtains  $z_{\text{acc}} \simeq 0.29$ .

Then, since radiation decays faster ( $\rho_{\text{rad}} \propto 1/a^4$ ) than matter, its contribution with respect to matter increases when moving backwards in time. Therefore, it dominates the Universe content when  $a < a_{\text{eq}}$ , where  $a_{\text{eq}}$  is defined by  $\rho_{\text{mat}}(a_{\text{eq}}) = \rho_{\text{rad}}(a_{\text{eq}})$ , giving rise to

$$z_{\text{eq}} = \frac{\Omega_{\text{mat}}^{(0)}}{\Omega_{\text{rad}}^{(0)}} - 1. \quad (1.37)$$

---

at  $a_{\text{acc}}$  exactly, since this occurs slightly before when  $\rho_{\text{de}} = \rho_{\text{mat}}/2$ .

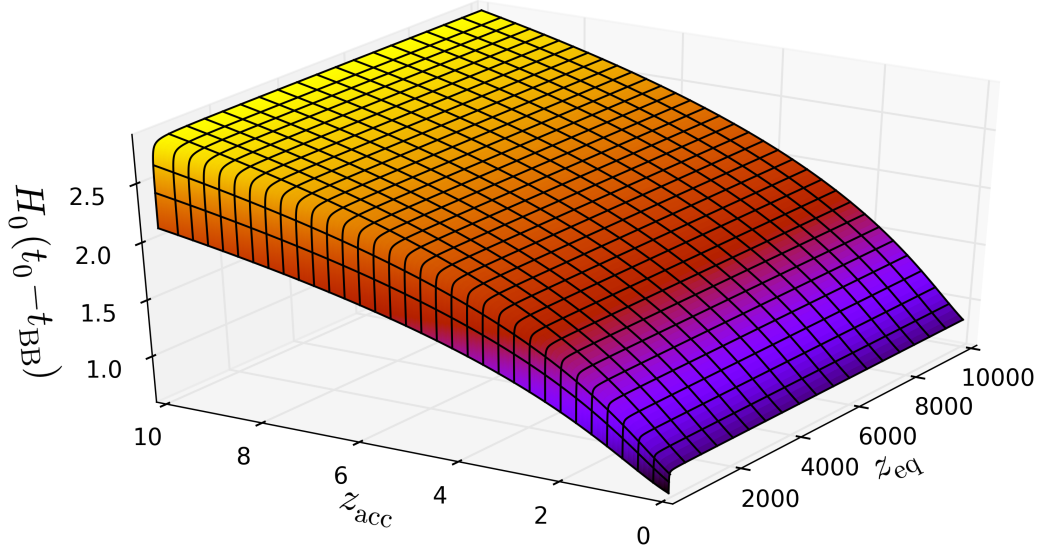


Figure 1.6.: Age of a flat universe as a function of  $z_{\text{eq}}$  and  $z_{\text{acc}}$ . The displayed value correspond to a numerical integration of Eq. (1.43).

With the values of  $\Omega_i^{(0)}$  recalled in table 1.2, one obtains  $z_{\text{eq}} \simeq 3402$ . Here, the subscript “eq” stands for “equality” between matter and radiation. When  $a < a_{\text{eq}}$  (or equivalently  $z > z_{\text{eq}}$ ), the Universe is dominated by radiation,  $\rho_{\text{tot}} \propto a^{-4}$  and  $a \propto t^{1/2}$ .

To conclude, the Universe history is made of three main phases: a radiation era for  $z > z_{\text{eq}}$  during which  $\rho_{\text{tot}} \propto 1/a^4$  and  $a \propto t^{1/2}$ , a matter era for  $z_{\text{acc}} < z < z_{\text{eq}}$  during which  $\rho_{\text{tot}} \propto 1/a^3$  and  $a \propto t^{2/3}$ , and a dark energy era for  $z < z_{\text{acc}}$  during which  $\rho_{\text{tot}} \simeq \text{constant}$  and  $a \propto e^{Ht}$ . These three eras can clearly be seen on the left panel of Fig. 1.5. In this discussion, the role played by curvature has not been included. Indeed, since  $\rho_{\mathcal{K}}$  decays slower than, say,  $\rho_{\text{mat}}$ ,  $\rho_{\mathcal{K}}^{(0)} \ll \rho_{\text{mat}}^{(0)}$  implies that this inequality holds at any previous time, and curvature can never have dominated the Universe content. This is why in Fig. 1.5 and in this section 1.3, we consider a flat universe for which  $\Omega_{\mathcal{K}}^{(0)} = 0$ .

### 1.3.2. Age of the Universe

When the Universe is dominated by an ideal fluid, the  $a(t)$  profile has been derived in Eq. (1.30). Neglecting the transition phases between the three above mentioned eras (during which there are two equally important main constituents), we can therefore derive an approximated piecewise form for  $a(t)$  spanning the whole Universe history. The integration constants  $\rho_{\text{in}}$  and  $t_{\text{in}}$  appearing in Eq. (1.30) can be set by requiring continuity of  $a$  and  $\dot{a}$  at the transition times (so

that  $H$  is continuous), and one obtains

$$\frac{a(t)}{a_0} \simeq \begin{cases} \exp[H_0(t-t_0)] & \text{if } t > t_{\text{acc}} \\ \frac{1}{1+z_{\text{acc}}} \left[1 + \frac{3}{2}H_0(t-t_{\text{acc}})\right]^{2/3} & \text{if } t_{\text{eq}} < t < t_{\text{acc}} \\ \frac{1}{1+z_{\text{eq}}} \left[1 + 2\left(\frac{1+z_{\text{eq}}}{1+z_{\text{acc}}}\right)^{3/2} H_0(t-t_{\text{eq}})\right]^{1/2} & \text{if } t_{\text{BB}} < t < t_{\text{eq}} \end{cases} . \quad (1.38)$$

Here,  $t_{\text{acc}}$  is the transition time between the matter era and the dark energy era and  $t_{\text{eq}}$  is the transition time between the radiation era and the matter era. They are such that

$$H_0(t_0 - t_{\text{acc}}) = \ln(1 + z_{\text{acc}}) , \quad (1.39)$$

$$H_0(t_{\text{acc}} - t_{\text{eq}}) = \frac{2}{3} - \frac{2}{3} \left(\frac{1+z_{\text{acc}}}{1+z_{\text{eq}}}\right)^{3/2} . \quad (1.40)$$

The piecewise function  $a(t)$  defined by Eq. (1.38) is displayed in the right panel of Fig. 1.5 (coloured lines, each colour corresponds to a different era). It is interesting to notice that when moving backwards in time,  $a$  goes to 0 in a finite amount of time. The corresponding singularity is called the Big Bang. Looking at Eq. (1.38), it occurs at the time  $t_{\text{BB}}$  given by

$$t_0 - t_{\text{BB}} \simeq H_0^{-1} \left[ \frac{2}{3} + \ln(1 + z_{\text{acc}}) - \frac{1}{6} \left(\frac{1+z_{\text{acc}}}{1+z_{\text{eq}}}\right)^{3/2} \right] . \quad (1.41)$$

One can see that as mentioned in section 1.1.1, the age of the Universe is of the order of the Hubble time  $H_0^{-1}$ . More precisely, with the values given in table 1.2, one obtains  $t_0 - t_{\text{BB}} \simeq 0.92H_0^{-1} \simeq 1.33 \times 10^{10}$  year.

Obviously, the Friedmann equation (1.28) can also be solved exactly, that is the integral

$$t - t_0 = H_0^{-1} \int_1^{a/a_0} \frac{d(\tilde{a}/a_0)}{\sqrt{\sum_i \Omega_i^{(0)} \left(\frac{\tilde{a}}{a_0}\right)^{-1-3w_i}}} \quad (1.42)$$

can be computed numerically. The result is displayed with the black line in the right panel of Fig. 1.5. The matching with the piecewise approximation is fairly good. With the parameter values recalled in table 1.2, this leads to a slightly different value for the age of the Universe, that is  $t_0 - t_{\text{BB}} \simeq 0.95H_0^{-1} \simeq 1.37 \times 10^{10}$  year. Actually, since the approximated expression (1.41) for the age of the Universe is given in terms of  $z_{\text{eq}}$  and  $z_{\text{acc}}$ , it can be useful to express the integral (1.42) in terms of these two variables only. One obtains for the age of the Universe

$$t_0 - t_{\text{BB}} = H_0^{-1} \sqrt{1 + \frac{1}{1+z_{\text{eq}}} + (1+z_{\text{acc}})^3} \times \int_0^\infty dz \left[ (1+z)^5 + \frac{1}{1+z_{\text{eq}}} (1+z)^6 + (1+z_{\text{acc}})^3 (1+z)^2 \right]^{-1/2} . \quad (1.43)$$

One can numerically check that Eqs. (1.41) and (1.43) give similar results as soon as  $z_{\text{eq}} > z_{\text{acc}}$ , and that the age of the Universe increases only mildly with  $z_{\text{eq}}$ , and more notably with  $z_{\text{acc}}$ . The integral (1.43) is displayed in Fig. 1.6 as a function of  $z_{\text{eq}}$  and  $z_{\text{acc}}$ .

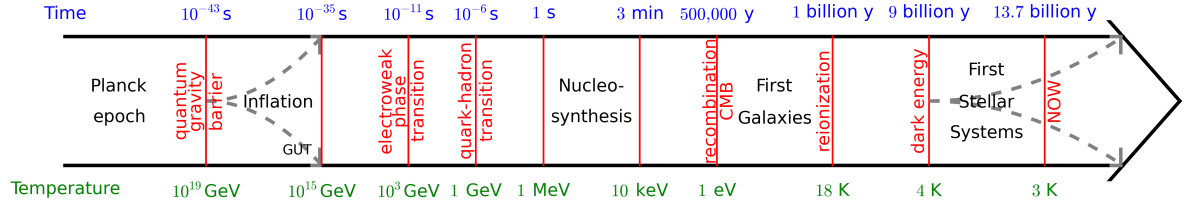


Figure 1.7.: Main events in the Cosmological Standard Scenario.

### 1.3.3. A Brief Cosmological History

The cosmological redshift (1.8) gives a rule for the behaviour of a black-body spectrum of radiation with temperature  $T_\gamma$ . Indeed, since all photons redshift as exactly the same rate  $\lambda \propto a^{-1}$ , a system which starts out as a black-body stays as a black-body, with a temperature that decreases with expansion,

$$T_\gamma \propto a^{-1}. \quad (1.44)$$

Therefore, when one goes backwards in time during the radiation era, temperature increases as  $1/a$ . In particular, this means that the initial singularity is also a point of infinite temperature. This leads us to the standard hot Big Bang picture of the Universe: a cosmological singularity at finite time in the past, followed by a hot, radiation dominated expansion, during which the Universe gradually cools down as  $T \propto a^{-1}$  and the radiation dilutes, followed by a period of matter dominated expansion during which galaxies, stars and planets form. Finally, the vacuum energy inevitably dominates and the Universe enters a state of exponential expansion.

This simple picture allows us to infer the presence of a few notable events that we now briefly recap, and that are summarized in Fig. 1.7 with orders of magnitude about time, energy and temperature at which these events occur. As one goes backwards in time, one can check that energy or temperature increases.

Inflation takes place at  $t \lesssim 10^{-35}$  s and is the object of section 1.4 and chapter 2 (in this section, times are given as elapsed since the initial singularity). This is why we start out our description afterwards, when the Universe is made of a hot plasma containing the fundamental particles of the standard model, at  $t \sim 10^{-35}$  s.

At  $t \sim 10^{-11}$  s occurs the electroweak phase transition which breaks the  $SU(2) \times U(1)$  symmetry of the electroweak field into the  $U(1)$  symmetry of the present day electromagnetic field [43, 44, 45, 46, 47, 48, 49]. This transition may be important to understanding the asymmetry between the amount of matter and antimatter in the present Universe through a process of baryogenesis [50, 51, 52, 53, 54]. It occurs at the electroweak scale which is often taken to be at the Higgs  $vev$ , around 246 GeV.

In the same manner, around  $t \sim 10^{-6}$  s, a phase transition (associated with chiral symmetry breaking) occurs that converts a plasma of free quarks and gluons into hadrons [55, 56, 57, 58, 59, 60]. This quark-hadron transition may play an important role in the generation of primordial magnetic fields [61]. It may also give rise to important baryon number inhomogeneities which can affect the distribution of light element abundances from primordial Big Bang nucleosynthesis [62] (see below). It occurs when the temperature drops below the rest energy of nucleons, around 938 MeV.

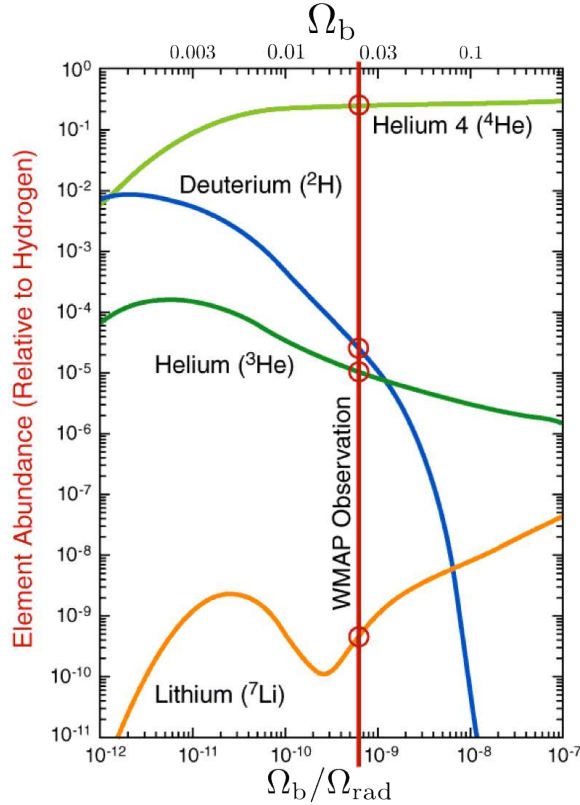


Figure 1.8.: Big Bang Nucleosynthesis. Light elements abundances (relative to hydrogen) as a function of the density of ordinary matter  $\Omega_b$  and of its density relative to photons  $\Omega_b/\Omega_{\text{rad}}$  at time of nucleosynthesis. The WMAP satellite has been able to directly measure this ordinary matter density and found a value [63] of  $4.6\%(\pm 0.2\%)$ , indicated by the vertical red line. This leads to predicted abundances shown by the circles in the graph, which are in good agreement with observed abundances. Image Credit: NASA/WMAP101087.

From there, nuclear fusion begins at  $t \sim 0.01$  s and big bang nucleosynthesis proceeds at  $t \sim 3$  min. This phase is when light elements (mostly H, D, He, Li and Be) are formed [64, 65, 66, 67]. Reproducing the observed abundances of elements from nuclear physics calculations places tight constraints on the environment it took place in [68, 69, 70, 71, 72, 73, 74, 75]. For example, in Fig. 1.8 are displayed the abundances of early produced light elements as a function of the density of ordinary matter relative to photons,  $\Omega_b/\Omega_{\text{rad}}$ . One can see that measures of elements abundances allow to set tight constraints on this ratio, and conversely. Nucleosynthesis begins at temperatures of around 10 MeV (which is the order of magnitude of nuclear binding energies) and ends at temperatures below 100 keV. The corresponding time interval is from a few tenths of a second to up to  $10^3$  seconds. Heavier elements are only formed later through stellar nucleosynthesis in evolving and exploding stars.

The Universe keeps on cooling down, until it reaches the point where charged electrons and protons become bound to form electrically neutral hydrogen atoms. This phase is often called “recombination” (although nuclei and electrons have never combined before). Since the photon-atom cross section (the Rayleigh cross-section) is much smaller than the photon-electron cross-section (Thomson cross-section), the Universe becomes transparent shortly after when photons decouple from matter (photon decoupling) and travel freely in the Universe. The associated

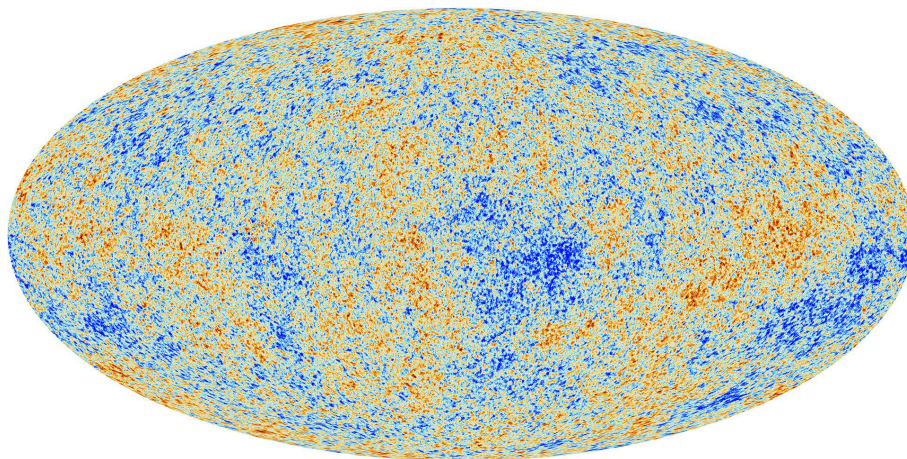


Figure 1.9.: Cosmic Microwave Background temperature fluctuations, as seen by the Planck satellite [76]. Colours encode temperature deviations from the mean temperature (blue points are colder whereas red points are hotter). Image Credit: Planck Collaboration.

relic radiation is called cosmic microwave background (CMB) and is the oldest photograph of the Universe one can get [77]. Its emission occurs at energies around 1 eV, at  $t \sim 500,000$  y. It reaches us today with the same shape of temperature distribution, *i.e.* a perfect black-body spectrum, with its central temperature redshifted by the amount of expansion  $\mathcal{O}(10^3)$  that has occurred since then, to reach the average value  $T_{\text{CMB}} = 2.725$  K. This temperature is the same for all direction in the sky, up to tiny fluctuations of the order  $10^{-5}$ . This tells us that at recombination time, the Universe is homogeneous and isotropic on all scales up to the present horizon (see section 1.4.1) to at least one part in 100,000. The statistics of the deviations from homogeneity of this radiation is a key prediction of the theory of inflation that we discuss in chapter 2. For illustrative purpose, the spatial map of the CMB temperature fluctuations measured by the Planck satellite is displayed in Fig. 1.9.

Galaxies then start to form, and inside them objects energetic enough to ionize neutral hydrogen. This is the so-called reionization epoch [78, 79, 80, 81]. As these objects form and radiate energy, the Universe indeed goes from being neutral back to being an ionized plasma, between 150 million and one billion years after the Big Bang. Compared with before recombination however, matter is much more diluted because of the expansion of the Universe, and scattering interactions are much less frequent than at this time. This is why the subsequent Universe, full of low density ionized hydrogen, remains transparent, as is the case today.

At  $t \sim 9$  billion years, dark energy starts to dominate and the expansion accelerates [84, 85]. First stellar systems form, and large scale structures continue to develop until today. Large scale structures constitute another observational pillar of modern cosmology, since the way they develop is related to the content of the Universe, the physical nature of its dark sector, the underlying theory of gravitation, and the initial cosmological perturbations they start from. For example, in Fig. 1.10 is displayed the result of simulated dark matter distributions for different cosmological models. The left panel is when structures develop in the standard cosmology described so far, the middle panel is when no dark energy is introduced in the model ( $\Omega_{\text{de}} = 0$ ), and the right panel is when warm dark matter (*i.e.* such that  $w_{\text{de}} > 0$ ) is used instead of cold dark matter. One can see that the features of the structures are different. For example, when no dark energy is present, the Universe expansion does not accelerate at late times, which allows faster structure formation. In this manner, measuring the distribution of matter around us

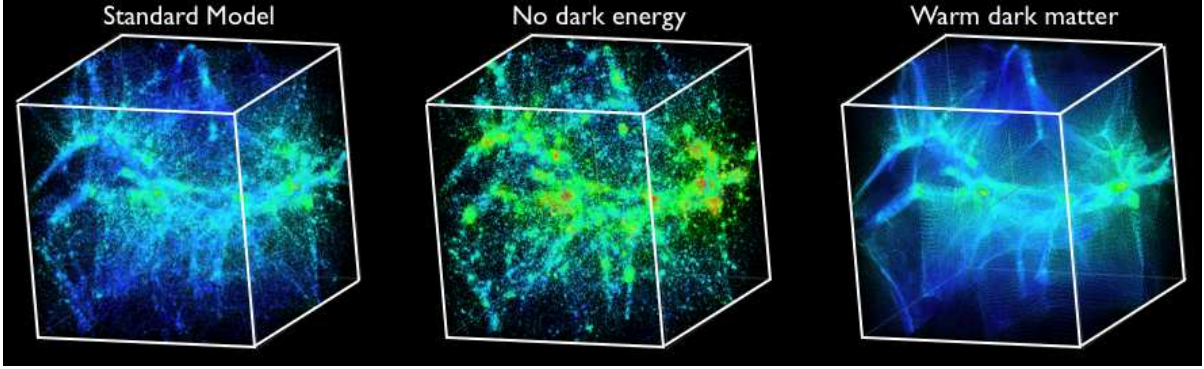


Figure 1.10.: Simulated dark matter distributions for different cosmological models. The colours encode velocities. Left panel: standard cosmological model. Middle panel: without dark energy ( $\Omega_m = 1$ ,  $\Omega_\Lambda = 0$ ,  $h = 0.7$ ). Right panel: with warm (instead of cold) dark matter in form of a sterile neutrino. Produced with the MC<sup>2</sup> code [82] run over a small simulation [containing  $32^3$  particles, with a box size of  $(32 \text{ Mpc}/h)^3$ ].

Image Credit: Ref. [83].

and understanding, notably by the means of numerical simulations and statistical tools, how it depends on the physical properties of our Universe, is a way to test these properties in the large scales regime.

## 1.4. The Big Bang Model Problems and Inflation

Now that we have introduced the main aspects of the standard cosmological model, it is worth mentioning that it raises unanswered questions, known as the hot big bang model problems. The horizon problem and the flatness problem deal with the fact that, interpreted within the standard model, observations lead to the conclusion that the Universe must have been extremely flat at early times, and homogeneous even over causally disconnected physical scales. They are not definite impossibility problems, but still serious fine-tuning issues. The monopole problem deals with the density of topological defects arising from symmetry breaking in the early Universe. Described in the standard model, these defects should be well visible at present time, which is in contradiction with experimental investigation for them. In this section, we describe in details these three problems, and we show that even if very different in nature, they can all be solved by the introduction of a phase of accelerated expansion in the early Universe.

### 1.4.1. The Horizon Problem

One of the properties of the above described cosmology is that it is endowed with a causal horizon, *i.e.* a frontier that separates observable events from non observable ones. Said differently, the set of events causally connected to a reference point in space-time only form a bounded set. Since no physical process can act on scales larger than the horizon, we typically expect the Universe to be strongly inhomogeneous on those scales.

However, as we shall now see, within the cosmological scenario of the standard hot big bang model, the last scattering surface (with respect to us) spans over several causally disconnected

pieces of space-time, that is, the size of the cosmological horizon at time of recombination is smaller than the diameter of the last scattering surface. The last scattering surface should therefore exhibit strong deviations from homogeneity, which is not the case. In this section, we thus calculate the size of the cosmological horizon [86, 87] in a FLRW space-time, and express the angular distance of the horizon at time of recombination, as seen by a current observer on Earth. For the reasons mentioned at the end of section 1.3.1, namely the fact that curvature can never have dominated the Universe content, we consider the case of a flat universe ( $\mathcal{K} = 0$ ). We take the origin of the  $r$  coordinate to be the location of Earth, *i.e.* “our” comoving coordinate is  $r = 0$ .

#### 1.4.1.1. Cosmological Horizon

Let us consider a photon emitted at  $t_{\text{em}}$  and  $r_{\text{em}}$  and traveling towards us ( $d\theta = d\phi = 0$ ). Its trajectory is given by Eq. (1.5), that is

$$r(t) = r_{\text{em}} - \int_{t_{\text{em}}}^t \frac{d\tilde{t}}{a(\tilde{t})}. \quad (1.45)$$

At time  $t$ , the physical distance (or “proper” distance) between the photon and the origin is then given by  $d_{\text{P}}(t) = a(t)r(t)$ . The horizon is defined in the following way. If the photon is received at (or before) time  $t_{\text{rec}}$ , the horizon at time  $t_{\text{rec}}$  is the proper distance to the furthest point the photon can have been sent from. Clearly, this distance is maximized if the photon was emitted at the earliest possible time, that is  $t_{\text{em}} = t_{\text{BB}}$ , and if it is received at the latest allowed time  $t_{\text{rec}}$ , that is  $r(t_{\text{rec}}) = 0$ . When plugging these two relations in Eq. (1.45), one obtains  $r_{\text{em}} = \int_{t_{\text{BB}}}^{t_{\text{rec}}} d\tilde{t}/a(\tilde{t})$ . By definition, the size of the horizon  $d_{\text{H}}$  at time  $t_{\text{rec}}$  is then given by

$$d_{\text{H}}(t_{\text{rec}}) = a(t_{\text{rec}})r_{\text{em}} = a(t_{\text{rec}}) \int_{t_{\text{BB}}}^{t_{\text{rec}}} \frac{dt}{a(t)}. \quad (1.46)$$

If one replaces  $t_{\text{rec}}$  by the time of recombination  $t_{\text{lss}}$ , one obtains the horizon size at the last scattering surface emission time,  $d_{\text{H}}(t_{\text{lss}})$ .

#### 1.4.1.2. Angular Distance to $d_{\text{H}}(t_{\text{lss}})$

We now move on to compute the angular distance of the horizon at time of recombination, as seen by a current observer on Earth. This quantity  $\Delta\Omega_{d_{\text{H}}}(t_0)$  can be expressed as follows. The last scattering surface is an instantaneous sphere of constant radius and therefore, within the last scattering surface,  $dr = dt = 0$ . The FLRW metric then takes the form  $d_{\text{P}} = a(t_{\text{lss}})r_{\text{lss}}d\Omega$ , where  $d\Omega^2 = d\theta^2 + \sin^2\theta d\phi^2$ . Therefore, the angular extension of the horizon at time of recombination reads

$$\Delta\Omega_{d_{\text{H}}}(t_0) = \frac{d_{\text{H}}(t_{\text{lss}})}{a(t_{\text{lss}})r_{\text{lss}}}. \quad (1.47)$$

It only remains to compute  $r_{\text{lss}}$ , which can be done using the same procedure as before. Indeed, applying Eq. (1.45) between  $t_{\text{em}} = t_{\text{lss}}$  and  $t_0$ ,  $r(t_0) = 0$  leads to  $r_{\text{lss}} = \int_{t_{\text{lss}}}^{t_0} dt/a(t)$ . Together with Eq. (1.46) for  $t_{\text{rec}} = t_{\text{lss}}$ , one obtains

$$\Delta\Omega_{d_{\text{H}}}(t_0) = \frac{\int_{t_{\text{BB}}}^{t_{\text{lss}}} \frac{dt}{a(t)}}{\int_{t_{\text{lss}}}^{t_0} \frac{dt}{a(t)}}. \quad (1.48)$$

### 1.4.1.3. Formulation of the Problem

Let us now evaluate this quantity with the cosmological model of section 1.3, made of a radiation era, a matter era and a dark energy era. Recombination occurs during the matter era ( $z_{\text{lss}} \simeq 1090$ , see Ref. [15]), so that  $t_{\text{BB}} < t_{\text{eq}} < t_{\text{lss}} < t_{\text{acc}}$ . Therefore, thanks to Eq. (1.38),  $t_{\text{lss}}$  can be expressed in terms of the recombination redshift  $z_{\text{lss}}$  through  $H_0(t_0 - t_{\text{lss}}) \simeq 2/3 + \ln(1 + z_{\text{acc}}) - 2/3[(1 + z_{\text{acc}})/(1 + z_{\text{lss}})]^{3/2}$ . Another consequence of this series of events is that the integrals appearing in Eq. (1.48) can be split according to  $\int_{t_{\text{BB}}}^{t_{\text{lss}}} = \int_{t_{\text{BB}}}^{t_{\text{eq}}} + \int_{t_{\text{eq}}}^{t_{\text{lss}}}$  and  $\int_{t_{\text{lss}}}^{t_0} = \int_{t_{\text{lss}}}^{t_{\text{acc}}} + \int_{t_{\text{acc}}}^{t_0}$ . Using the piecewise approximation (1.38) for the  $a(t)$  profile, each of these integrals can be computed. One obtains

$$\begin{aligned} a_0 H_0 \int_{t_{\text{BB}}}^{t_{\text{eq}}} \frac{dt}{a} &\simeq \frac{(1 + z_{\text{acc}})^{3/2}}{\sqrt{1 + z_{\text{eq}}}}, & a_0 H_0 \int_{t_{\text{eq}}}^{t_{\text{lss}}} \frac{dt}{a} &\simeq 2(1 + z_{\text{acc}})^{3/2} \left( \frac{1}{\sqrt{1 + z_{\text{lss}}}} - \frac{1}{\sqrt{1 + z_{\text{eq}}}} \right), \\ a_0 H_0 \int_{t_{\text{acc}}}^{t_0} \frac{dt}{a} &\simeq z_{\text{acc}}, & a_0 H_0 \int_{t_{\text{lss}}}^{t_{\text{acc}}} \frac{dt}{a} &\simeq 2(1 + z_{\text{acc}})^{3/2} \left( \frac{1}{\sqrt{1 + z_{\text{acc}}}} - \frac{1}{\sqrt{1 + z_{\text{lss}}}} \right). \end{aligned} \quad (1.49)$$

These expressions allow to express  $\Delta\Omega_{d\text{H}}(t_0)$  in terms of  $z_{\text{eq}}$ ,  $z_{\text{lss}}$  and  $z_{\text{acc}}$  according to

$$\Delta\Omega_{d\text{H}}(t_0) = \frac{\frac{2}{\sqrt{1 + z_{\text{lss}}} - \frac{1}{\sqrt{1 + z_{\text{eq}}}}}{2 + 3z_{\text{acc}} - \frac{2}{(1 + z_{\text{acc}})^{3/2} - \frac{1}{\sqrt{1 + z_{\text{lss}}}}}}. \quad (1.50)$$

With the parameter values recalled in table 1.2, one obtains  $\Delta\Omega_{d\text{H}}(t_0) \simeq 0.023 \text{ rad} \simeq 1.31^\circ$ . For comparison purpose, let us remind that the angular diameter of the moon seen from the Earth is  $\simeq 0.5^\circ$ .

Beyond the piecewise approximated form of  $a(t)$ , like for the age of the Universe in section 1.3.2, an exact calculation can also be carried out using the relation

$$\int_{t_1}^{t_2} \frac{dt}{a(t)} = \frac{1}{H_0 a_0} \int_{z_2}^{z_1} \frac{dz}{\sqrt{\sum_i \Omega_i^{(0)} (1 + z)^{3(1+w_i)}}}. \quad (1.51)$$

Such an integral can be computed numerically, and one obtains

$$\Delta\Omega_{d\text{H}}(t_0) = \frac{\int_{z_{\text{lss}}}^{\infty} dz / \sqrt{\sum_i \Omega_i^{(0)} (1 + z)^{3(1+w_i)}}}{\int_0^{z_{\text{lss}}} dz / \sqrt{\sum_i \Omega_i^{(0)} (1 + z)^{3(1+w_i)}}} \simeq 0.0054 \text{ rad} \simeq 0.3^\circ \quad (1.52)$$

which is of the same order of magnitude as (but even smaller than) the above approximated result, and which represents  $\sim 1/450,000$  of the full sky coverage.

As a consequence, one expects the last scattering surface to be made of 450,000 patches whose typical physical properties are *a priori* completely different. This is in contradiction with observations which establish that up to tiny fluctuations of the order  $\delta T/T \simeq 10^{-5}$ , the CMB radiation is extremely homogeneous and isotropic across the last scattering surface. This paradox is called the horizon problem [88, 89].

A solution to this problem is of course to assume that the initial conditions were identical in all the causally disconnected patches, but it seems very difficult to justify. Another solution is to add a new phase to the standard scenario.

#### 1.4.1.4. Inflation as a Solution to the Horizon Problem

Let us assume that the epoch dominated by radiation can be interrupted during the period  $t_{\text{in}} < t < t_{\text{end}}$ , or equivalently  $z_{\text{end}} < z < z_{\text{in}}$ . During this interval, we assume that the Universe is dominated by an unknown ideal fluid  $X$  with an equation of state parameter  $w_X$ . We now wonder whether there are values of  $z_{\text{in}}$ ,  $z_{\text{end}}$  and  $w_X$  such that the horizon problem can be solved in this new scenario. Let us thus redo the horizon diameter distance calculation in this new setup.

The piecewise function  $a(t)$  now has a new piece, and is given by

$$\frac{a(t)}{a_0} \simeq \begin{cases} \exp [H_0 (t - t_0)] & \text{if } t > t_{\text{acc}} \\ \frac{1}{1+z_{\text{acc}}} \left[ 1 + \frac{3}{2} H_0 (t - t_{\text{acc}}) \right]^{2/3} & \text{if } t_{\text{eq}} < t < t_{\text{acc}} \\ \frac{1}{1+z_{\text{eq}}} \left[ 1 + 2 \left( \frac{1+z_{\text{eq}}}{1+z_{\text{acc}}} \right)^{3/2} H_0 (t - t_{\text{eq}}) \right]^{1/2} & \text{if } t_{\text{end}} < t < t_{\text{eq}} \\ \frac{1}{1+z_{\text{end}}} \left[ 1 + \frac{3}{2} (1+w_X) \left( \frac{1+z_{\text{end}}}{1+z_{\text{acc}}} \right)^2 \sqrt{\frac{1+z_{\text{acc}}}{1+z_{\text{eq}}}} H_0 (t - t_{\text{end}}) \right]^{\frac{2}{3(1+w_X)}} & \text{if } t_{\text{in}} < t < t_{\text{end}} \\ \frac{1}{1+z_{\text{in}}} \left[ 1 + 2 \left( \frac{1+z_{\text{end}}}{1+z_{\text{acc}}} \right)^2 \sqrt{\frac{1+z_{\text{acc}}}{1+z_{\text{eq}}}} \left( \frac{1+z_{\text{in}}}{1+z_{\text{end}}} \right)^{\frac{3}{2}(1+w_X)} H_0 (t - t_{\text{in}}) \right]^{1/2} & \text{if } t'_{\text{BB}} < t < t_{\text{in}} \end{cases} \quad (1.53)$$

where the expressions given for  $t_{\text{acc}}$  and  $t_{\text{eq}}$  in Eqs. (1.39) and (1.40) are still valid, and where  $t_{\text{end}}$ ,  $t_{\text{in}}$  and  $t'_{\text{BB}}$  are such that

$$H_0 (t_{\text{eq}} - t_{\text{end}}) = \frac{1}{2} \left( \frac{1+z_{\text{acc}}}{1+z_{\text{eq}}} \right)^{3/2} \left[ 1 - \left( \frac{1+z_{\text{eq}}}{1+z_{\text{end}}} \right)^2 \right], \quad (1.54)$$

$$H_0 (t_{\text{end}} - t_{\text{in}}) = \frac{2}{3(1+w_X)} \left( \frac{1+z_{\text{acc}}}{1+z_{\text{end}}} \right)^2 \sqrt{\frac{1+z_{\text{eq}}}{1+z_{\text{acc}}}} \left[ 1 - \left( \frac{1+z_{\text{end}}}{1+z_{\text{in}}} \right)^{\frac{3}{2}(1+w_X)} \right], \quad (1.55)$$

$$H_0 (t_{\text{in}} - t'_{\text{BB}}) = \frac{1}{2} \left( \frac{1+z_{\text{acc}}}{1+z_{\text{end}}} \right)^2 \sqrt{\frac{1+z_{\text{eq}}}{1+z_{\text{acc}}}} \left( \frac{1+z_{\text{end}}}{1+z_{\text{in}}} \right)^{\frac{3}{2}(1+w_X)}. \quad (1.56)$$

In this new scenario, the integral decomposition of the numerator in Eq. (1.48) now reads  $\int_{t'_{\text{BB}}}^{t_{\text{iss}}} = \int_{t'_{\text{BB}}}^{t_{\text{in}}} + \int_{t_{\text{in}}}^{t_{\text{end}}} + \int_{t_{\text{end}}}^{t_{\text{eq}}} + \int_{t_{\text{eq}}}^{t_{\text{iss}}}$ , while the integral decomposition of the denominator  $\int_{t_{\text{iss}}}^{t_0} = \int_{t_{\text{iss}}}^{t_{\text{acc}}} + \int_{t_{\text{acc}}}^{t_0}$  is unchanged. The integrals  $\int_{t_{\text{eq}}}^{t_{\text{iss}}}$ ,  $\int_{t_{\text{iss}}}^{t_{\text{acc}}}$  and  $\int_{t_{\text{acc}}}^{t_0}$  have already been calculated in Eq. (1.49) and their expression remains valid. On the other hand, the three new integrals  $\int_{t'_{\text{BB}}}^{t_{\text{in}}}$ ,  $\int_{t_{\text{in}}}^{t_{\text{end}}}$  and  $\int_{t_{\text{end}}}^{t_{\text{eq}}}$ , need to be computed. Using the piecewise approximation (1.53), they are given by

$$\begin{aligned} a_0 H_0 \int_{t'_{\text{BB}}}^{t_{\text{in}}} \frac{dt}{a} &\simeq (1+z_{\text{in}}) \left( \frac{1+z_{\text{acc}}}{1+z_{\text{end}}} \right)^2 \sqrt{\frac{1+z_{\text{eq}}}{1+z_{\text{acc}}}} \left( \frac{1+z_{\text{end}}}{1+z_{\text{in}}} \right)^{\frac{3}{2}(1+w_X)}, \\ a_0 H_0 \int_{t_{\text{in}}}^{t_{\text{end}}} \frac{dt}{a} &\simeq \frac{2}{1+3w_X} \frac{(1+z_{\text{acc}})^2}{1+z_{\text{end}}} \sqrt{\frac{1+z_{\text{eq}}}{1+z_{\text{acc}}}} \left[ 1 - \left( \frac{1+z_{\text{end}}}{1+z_{\text{in}}} \right)^{\frac{1}{2}(1+3w_X)} \right], \\ a_0 H_0 \int_{t_{\text{end}}}^{t_{\text{eq}}} \frac{dt}{a} &\simeq \frac{(1+z_{\text{acc}})^{3/2}}{\sqrt{1+z_{\text{eq}}}} \frac{z_{\text{end}} - z_{\text{eq}}}{1+z_{\text{end}}}. \end{aligned} \quad (1.57)$$

We can now express the angular extension of the horizon at time of recombination, which reads

$$\Delta\Omega'_{d_H}(t_0) = \frac{\frac{2}{\sqrt{1+z_{\text{ISS}}}} - \frac{1}{\sqrt{1+z_{\text{eq}}}} + \frac{\sqrt{1+z_{\text{eq}}}}{1+z_{\text{end}}} \frac{1-3w_X}{1+3w_X} \left[1 - e^{-\frac{1}{2}(1+3w_X)N}\right]}{\frac{2+3z_{\text{acc}}}{(1+z_{\text{acc}})^{3/2}} - \frac{2}{\sqrt{1+z_{\text{ISS}}}}} \quad (1.58)$$

$$= \Delta\Omega_{d_H}(t_0) + \frac{\frac{\sqrt{1+z_{\text{eq}}}}{1+z_{\text{end}}} \frac{1-3w_X}{1+3w_X}}{\frac{2+3z_{\text{acc}}}{(1+z_{\text{acc}})^{3/2}} - \frac{2}{\sqrt{1+z_{\text{ISS}}}}} \left[1 - e^{-\frac{1}{2}(1+3w_X)N}\right], \quad (1.59)$$

where we have defined the number of  $e$ -folds of the new phase  $N \equiv \ln(a_{\text{end}}/a_{\text{in}}) = \ln \frac{1+z_{\text{in}}}{1+z_{\text{end}}}$  and where in the second line, the standard result (1.52) has been singled out. A first remark is that when  $w_X = 1/3$  (*i.e.* the new phase cannot be distinguished from the radiation era in which it intervenes) or when  $N = 0$  (*i.e.* the new phase does not exist), one re-obtains Eq. (1.50) as expected. However, when this new phase is switched on, an extra term appears in the angular size of the horizon that can make it much larger, provided

$$w_X < -1/3. \quad (1.60)$$

Indeed, if  $1 + 3w_X > 0$ , then the argument of the exponential term in Eq. (1.59) is negative and the correction coming from the phase driven by the unknown fluid becomes negligible. If  $1 + 3w_X < 0$  on the other hand, then the correction may be important enough to reach the full sky coverage  $\Delta\Omega_{d_H}(t_0) > 4\pi$ , depending of course on the number of  $e$ -folds  $N$ .

Let us give some numbers, for the values recalled in table 1.2. If  $z_{\text{end}} = z_{\text{GUT}} \simeq 10^{28}$  (where ‘‘GUT’’ stands for the Grand Unification Theory breaking scale, see section 1.4.3),  $\Delta\Omega_{d_H}(t_0) > 4\pi$  when  $N > 125$  for  $w = -2/3$  and when  $N > 63$  for  $w = -1$ . If  $z_{\text{end}} = 10^{10}$ , *i.e.* two orders of magnitude above nucleosynthesis,  $\Delta\Omega_{d_H}(t_0) > 4\pi$  when  $N > 42$  for  $w = -2/3$  and when  $N > 21$  for  $w = -1$ . Values of the minimum number of  $e$ -folds  $N_{\text{min}}$  required to have  $\Delta\Omega_{d_H} > 4\pi$  are displayed in Fig. 1.11 as a function of  $w_X$  and for a few values of  $z_{\text{end}}$ .

To sum up this discussion and in order to get a clear formula that is easy to handle, one can simplify Eq. (1.59) in the limit where  $z_{\text{ISS}} \gg 1$  and  $z_{\text{acc}} \ll 1$ . One obtains that the horizon problem is solved provided  $w_X < -1/3$  and

$$N \gtrsim -\frac{2}{1+3w_X} \ln \left( \frac{4\pi z_{\text{end}}}{\sqrt{z_{\text{eq}}}} \right). \quad (1.61)$$

One can check in Fig. 1.11 that this indeed provides a good approximation for the minimum numbers of  $e$ -folds.

Finally, from Eq. (1.30),  $a \propto t^{\frac{2}{3(1+w)}}$ , one can see that the condition  $w_X < -1/3$  is equivalent to requiring that the expansion of the Universe is accelerating, that is  $\ddot{a} > 0$ . This is why the new phase we have introduced in the cosmological standard history is called ‘‘inflation’’ [90, 91].

#### 1.4.1.5. Heuristic Understanding: Conformal Diagrams

Let us try to understand more intuitively what happened. A heuristic way of understanding why a phase of inflation can solve the horizon problem is by means of conformal diagrams. The

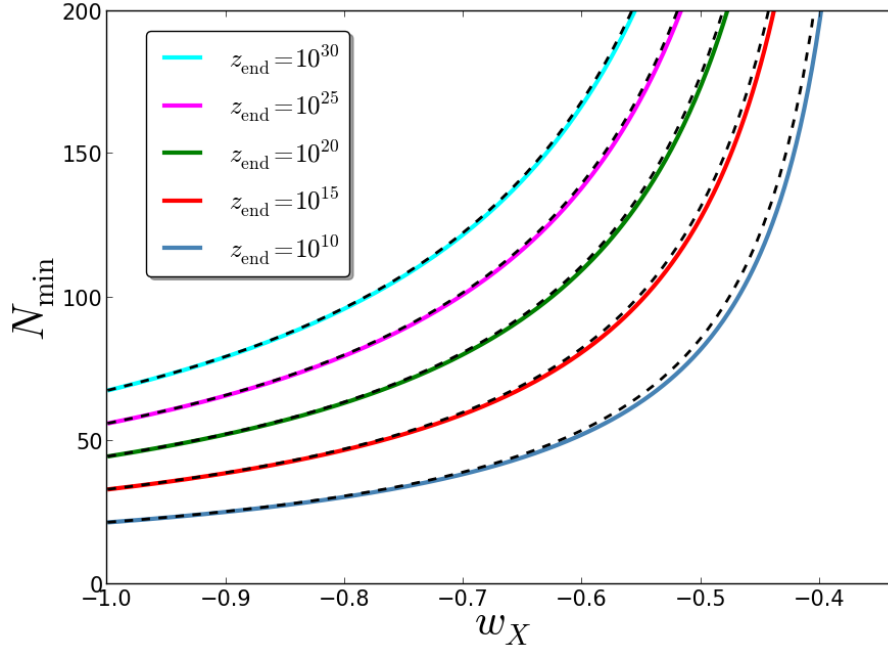


Figure 1.11.: Minimum number of  $e$ -folds in order to obtain  $\Delta\Omega_{dH}(t_0) > 4\pi$  from Eq. (1.59), as a function of  $w_X$  and for a few values of  $z_{\text{end}}$ , with parameter values given in table 1.2 (coloured lines). The black dotted lines correspond to the approximation (1.61).

conformal time  $\eta$  is defined as

$$dt = a d\eta, \quad (1.62)$$

so that the flat FLRW metric is given by  $ds^2 = a^2(d\eta^2 - dr^2)$  (where angular coordinates are omitted). In this time parameterization, null geodesics for the propagation of photons follow the very simple trajectory  $d\eta = dr$ . Therefore, the size of the horizon at time  $\eta$  is straightforwardly given by

$$d_H(\eta) = a(\eta) (\eta - \eta_{\text{BB}}). \quad (1.63)$$

When the Universe is dominated by a single ideal fluid with equation of state parameter  $w$ , the  $a(t)$  profile is given by Eq. (1.30), which, if one sets the origins of time  $t_{\text{BB}} = 0$ , reads

$$a(t) = a_0 \left( \frac{t}{t_0} \right)^{\frac{2}{3(1+w)}}. \quad (1.64)$$

From here, integrating Eq. (1.62), one obtains

$$\eta = \frac{3}{a_0 t_0} \frac{1+w}{3w+1} \left( \frac{t}{t_0} \right)^{\frac{3w+1}{3(w+1)}}, \quad (1.65)$$

where we have set the origins of conformal times such that its current value is given by  $\eta_0 = -3(a_0 t_0)^{-1}(1+w)/(3w+1)$ . The calculation of Eq. (1.63) now proceeds along two different cases:

If  $w > -1/3$ , when  $t \rightarrow 0$ ,  $\eta \rightarrow 0$  in Eq. (1.65), hence  $\eta_{\text{BB}} = 0$  and the size of the horizon given by Eq. (1.63) is finite, equal to  $d_H = a\eta$ . This is why in this case, a horizon problem can occur. This corresponds the left panel of Fig. 1.12.

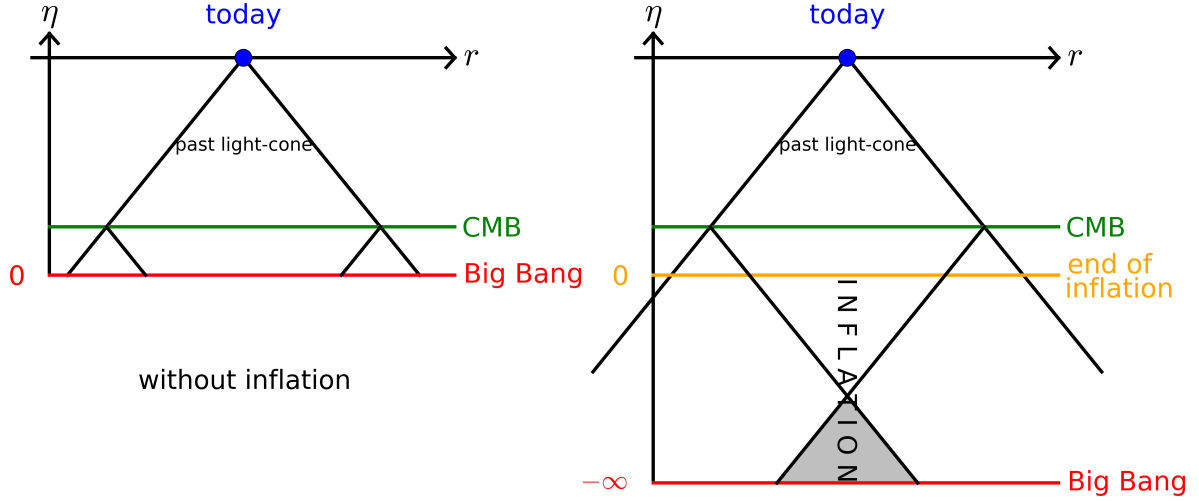


Figure 1.12.: Conformal diagrams. In the  $(\eta, r)$  plane, light propagates along straight lines. The left panel corresponds to the standard Big Bang cosmology. The CMB at last scattering consists of  $\sim 10^5$  causally disconnected regions, that is regions the past light cones of which do not intersect because at  $\eta = 0$  lies an initial singularity. The right panel corresponds to the inflationary cosmology. Inflation extends conformal time to negative values, so that past light cones of any two points on the CMB surface intersect (grey shaded area).

If  $w < -1/3$ , when  $t \rightarrow 0$ ,  $\eta \rightarrow -\infty$  in Eq. (1.65), hence  $\eta_{\text{BB}} = -\infty$  and the size of the horizon given by Eq. (1.63) is infinite. This is the case displayed in the right panel of Fig. 1.12. The singularity  $a = 0$  is pushed to the infinite past  $\eta \rightarrow -\infty$ , because  $w < -1/3$  allows  $\eta$  to reach negative values. This is why in this case, there is no horizon problem. Actually when  $w < -1/3$ , the scale factor blows up in the infinite future  $t \rightarrow \infty$  at  $\eta = 0$ . This is because in this case, we assume a phase of inflation ( $w < -1/3$ ) which lasts for ever. In practice, inflation ends at some finite time  $-1 \ll \eta_{\text{end}} < 0$  and the surface  $\eta = 0^-$  corresponds to the end of inflation, as displayed in Fig. 1.12.

This is why inflation succeeds in making the size of the horizon expand so much that it is sufficiently large at time of recombination to explain the current homogeneity of the Universe [90].

### 1.4.2. The Flatness Problem

The flatness problem is also a fine-tuning problem that arises from the observational constraint on  $1 - \Omega_{\text{tot}} = \Omega_{\mathcal{K}}$ . When  $\Omega_{\text{tot}} = 1$  (or  $\mathcal{K} = 0$ ), the Universe is globally flat, at the border line between a closed finite universe ( $\Omega_{\text{tot}} > 1$ , or  $\mathcal{K} = 1$ ) and an open, infinite universe ( $\Omega_{\text{tot}} < 1$  or  $\mathcal{K} = -1$ ). Since  $\mathcal{K}$  is a constant, the sign of  $1 - \Omega_{\text{tot}}$  cannot change during the cosmic evolution. Observational constraints put  $\Omega_{\text{tot}}^{(0)}$  well close to 1,  $100\Omega_{\mathcal{K}}^{(0)} = -0.10_{-0.65}^{+0.62}$  at 95% [15]. However,  $\Omega_{\text{tot}} = 1$  is an unstable equilibrium point. In order for  $\Omega_{\text{tot}}$  to fall within the given constraints today, it had to be equal to 1 within an extremely high level of fine-tuning in the early Universe. The flatness problem [92, 93] is the puzzle of explaining why the early Universe exhibits such fine-tuning in the value of this parameter.

### 1.4.2.1. Formulation of the Problem

From the definition (1.33) of  $\rho_{\text{cri}}$  and of the rescaled variables  $\Omega_i$ , the deviation from unity of the total rescaled energy density is given by

$$1 - \Omega_{\text{tot}} = \Omega_{\mathcal{K}} = \frac{1}{1 + \frac{\sum \Omega_i}{\Omega_{\mathcal{K}}}}. \quad (1.66)$$

From table 1.1, let us remember that  $\Omega_{\text{rad}} \propto a^{-4}$  and  $\Omega_{\mathcal{K}} \propto a^{-2}$ . This is why, when evaluating this quantity in the early Universe where radiation is the dominant constituent ( $\sum \Omega_i \simeq \Omega_{\text{rad}}$ ), one obtains

$$1 - \Omega_{\text{tot}} \simeq \frac{1}{1 + \frac{\Omega_{\text{rad}}^{(0)}}{1 - \Omega_{\text{tot}}^{(0)}} \left(\frac{a_0}{a}\right)^2} \simeq \frac{1 - \Omega_{\text{tot}}^{(0)}}{\Omega_{\text{rad}}^{(0)}} \left(\frac{1}{1 + z}\right)^2. \quad (1.67)$$

If one takes  $|\Omega_{\mathcal{K}}^{(0)}| \simeq 10^{-3}$  and  $\Omega_{\text{rad}}^{(0)} \simeq 10^{-4}$  (according to the values given in section 1.2), one obtains  $|1 - \Omega_{\text{tot}}| \simeq 10^{-15}$  for  $z \simeq 10^{10}$  and  $|1 - \Omega_{\text{tot}}| \simeq 10^{-55}$  for  $z = z_{\text{GUT}} \simeq 10^{28}$ . As a consequence, one can see that the deviation from a flat universe  $|1 - \Omega_{\text{tot}}|$  has to be fine-tuned to a tiny value at early time in order to explain the current flatness of the Universe. This is the so-called flatness problem [92, 93].

### 1.4.2.2. Inflation as a Solution to the Flatness Problem

As for the horizon problem, a possible explanation consists in adding a new phase which interrupts the radiation epoch between two times  $t_{\text{in}}$  and  $t_{\text{end}}$ , and where the Universe content is dominated by an ideal fluid  $X$  with equation of state  $w_X$ . Let us calculate the initial deviation from flatness  $|1 - \Omega_{\text{tot}}|$  required in this new scenario, sketched by Eq. (1.53). Similarly to Eq. (1.67), during this phase, one has

$$1 - \Omega_{\text{tot}}^{\text{end}} = \frac{1}{1 + \frac{\Omega_X^{\text{in}}}{1 - \Omega_{\text{tot}}^{\text{in}}} \left(\frac{a_{\text{end}}}{a_{\text{in}}}\right)^{-1-3w_X}}. \quad (1.68)$$

The purpose of this new phase is that starting from a sizable value of  $1 - \Omega_{\text{tot}}^{\text{in}}$ , it should drive this quantity to a tiny value,  $1 - \Omega_{\text{tot}}^{\text{end}}$ . Since  $a_{\text{end}}/a_{\text{in}} \gg 1$ , this is achieved provided  $-1 - 3w_X > 0$ , that is  $w_X < -1/3$ , exactly the same condition (1.60) as the one coming from the horizon problem and characterizing an inflationary phase where the expansion is accelerating.

More precisely, let us calculate the minimum number of  $e$ -folds  $N = \ln(a_{\text{end}}/a_{\text{in}})$  required to solve the flatness problem. Relating  $1 - \Omega_{\text{tot}}^{\text{end}}$  to  $1 - \Omega_{\text{tot}}^{(0)}$  thanks to Eq. (1.67), it is straightforward to write

$$N = \frac{1}{1 + 3w_X} \ln \left[ \frac{\Omega_X^{\text{in}}}{1 - \Omega_{\text{tot}}^{\text{in}}} \frac{1 - \Omega_{\text{tot}}^{(0)}}{\Omega_{\text{rad}}^{(0)}} \left(\frac{1}{1 + z_{\text{end}}}\right)^2 \right]. \quad (1.69)$$

To avoid initial fine-tuning of the Universe flatness, one takes  $\Omega_X^{\text{in}} \propto 1 - \Omega_{\text{tot}}^{\text{in}}$ , so that the flatness problem is solved provided

$$N \gtrsim -\frac{2}{1 + 3w_X} \ln \left[ z_{\text{end}} \sqrt{\frac{\Omega_{\text{rad}}^{(0)}}{|1 - \Omega_{\text{tot}}^{(0)}|}} \right]. \quad (1.70)$$

Note that the similarity with Eq. (1.61) is striking. More precisely, from the values for  $\Omega_i^{(0)}$  given in table 1.2, the pre-factors in front of  $z_{\text{end}}$  in the logarithms of Eqs. (1.61) and (1.70) are such that  $4\pi/\sqrt{z_{\text{eq}}} \sim \sqrt{\Omega_{\text{rad}}^{(0)}/(1 - \Omega_{\text{tot}}^{(0)})}$ . Therefore, the values of  $N_{\text{min}}$  displayed in Fig. 1.11 are such that the flatness problem is also solved.

Let us try to understand more intuitively why it is so. The flatness problem arises because curvature energy density decays slower than the one of matter or radiation. Therefore, if it is small today, it must have been even smaller before. The only way to escape from this fine-tuning issue is to have some phase during which the energy density decays even smaller than curvature. Since  $w_{\mathcal{K}} = -1/3$  (see table 1.1), this implies that this phase is driven by a new fluid the equation of state parameter of which is such that  $w_X < -1/3$ . When this new component dominates the Universe content, curvature decays faster than this new fluid, and is therefore dynamically driven to very small values. If the energy content of this new component  $X$  is then transferred to radiation, curvature is automatically subdominant with respect to radiation at the end of this new phase, in a sufficiently large extent provided the duration of inflation  $N$  is large enough.

### 1.4.3. The Monopole Problem

In Grand Unified Theories [94, 95, 96] (GUT), local symmetry under some simple symmetry group is spontaneously broken at an energy  $M_{\text{GUT}} \simeq 10^{16}$  GeV to the gauge symmetry of the Standard Model under the group  $SU(3) \times SU(2) \times U(1)$ . In all such cases, the field that breaks the symmetry can be left in twisted configurations that carry non-zero magnetic charge. These topological glitches in the vacuum configuration of gauge fields are magnetic monopoles [97, 98]. Such monopoles are expected to be copiously produced in Grand Unified Theories at high temperature [99, 100], and they should have persisted to the present day, to such an extent that they would become the primary constituent of the Universe [101, 102]. Not only is that not the case, but all searches for them have so far turned out fruitless, placing stringent limits on the density of relic magnetic monopoles in the Universe [103, 104, 105, 106, 107, 108]. These searches show that at present time, monopoles must be typically fewer than  $\sim 10^{-30}$  per nucleon.

#### 1.4.3.1. Formulation of the Problem

Let us estimate the current monopole density, in the standard cosmological model sketched in Eq. (1.38). At time  $t_{\text{GUT}}$  of GUT phase transition, the field that dynamically realizes the symmetry breaking cannot be correlated at length larger than the causal horizon. Therefore, when created, the mean distance  $D_{\text{mon}}$  between two neighbor monopoles must be smaller than  $d_{\text{H}}(t_{\text{GUT}})$ . If monopoles do not find each other to annihilate, this distance is stretched to the current  $D_{\text{mon}}^{(0)} = a_0/a_{\text{GUT}} d_{\text{H}}(t_{\text{GUT}})$ . Using Eq. (1.46) to express the horizon distance, one obtains

$$D_{\text{mon}}^{(0)} = \int_{t_{\text{BB}}}^{t_{\text{GUT}}} \frac{dt}{a/a_0}. \quad (1.71)$$

Making use of Eq. (1.38), this integral can easily be calculated (since the GUT phase transition occurs at energies larger than the one at equivalence, one has  $t_{\text{BB}} < t_{\text{GUT}} < t_{\text{eq}}$ ), and one obtains

$$D_{\text{mon}}^{(0)} = \frac{\sqrt{1 + z_{\text{eq}}} (1 + z_{\text{acc}})^{3/2}}{1 + z_{\text{GUT}}} H_0^{-1}. \quad (1.72)$$

In passing, the value  $z_{\text{GUT}} \sim 10^{28}$  that has been used so far and that we need here one more time can now be better justified. Indeed, GUT phase transition occurs when  $\rho \sim M_{\text{GUT}}^4$ , hence  $H_{\text{GUT}} \sim M_{\text{GUT}}^2/M_{\text{Pl}} \sim 10^{13}$  GeV. During the radiation phase, the time behaviour of  $H = \dot{a}/a$  can be calculated from Eq. (1.38), hence  $t_{\text{GUT}}$  can be expressed in terms of  $H_{\text{GUT}}$ . Using again Eq. (1.38), one then has  $a_{\text{GUT}}$  in terms of  $H_{\text{GUT}}$  and in the limit where  $z_{\text{GUT}} > z_{\text{eq}} \gg 1$ , this gives rise to

$$z_{\text{GUT}} \sim z_{\text{eq}}^{1/4} \sqrt{\frac{H_{\text{GUT}}}{H_0}} \sim 10^{28}. \quad (1.73)$$

This indeed corresponds to the value mentioned before.

Back to the current monopole density calculation, together with the values of  $z_{\text{eq}}$  and  $z_{\text{acc}}$  recalled in table 1.2, this allows us to evaluate Eq. (1.72) and one obtains  $D_{\text{mon}}^{(0)} \simeq 1$  m. Therefore, there should be about one magnetic monopole per cube meter in our vicinity neighborhood.

In order to better understand this order of magnitude, let us calculate the corresponding rescaled monopole density  $\Omega_{\text{mon}}^{(0)}$ . If the mass of each monopole is of the order  $M_{\text{GUT}}$ , and remembering that the critical energy density is given by Eq. (1.33), this rescaled quantity is given by

$$\Omega_{\text{mon}}^{(0)} = \frac{M}{3H_0^2 M_{\text{Pl}}^2 [D_{\text{mon}}^{(0)}]^3} \simeq 10^{15}. \quad (1.74)$$

Magnetic monopoles should therefore be the dominant constituent of our current Universe, which is in obvious contradiction with observations. To estimate how far we are from the observational constraints mentioned above (namely less than a monopole per  $10^{30}$  nucleon), one can also calculate the ratio of monopole and nucleon number densities  $\eta$ ,

$$\frac{\eta_{\text{mon}}^{(0)}}{\eta_{\text{nuc}}^{(0)}} = \frac{\Omega_{\text{mon}}^{(0)} m_{\text{nuc}}}{\Omega_{\text{m}}^{(0)} M_{\text{GUT}}} \simeq 5, \quad (1.75)$$

where we have assumed that visible cold matter is essentially made of nucleons, and where we have taken the mass of nucleons to be of the order of  $m_{\text{nuc}} \simeq 938$  MeV. As a consequence, there should be  $\mathcal{O}(1)$  magnetic monopole per nucleon, while observations establish that there is less than a monopole per  $10^{30}$  nucleon. This is the so-called monopole problem. Obviously, since magnetic monopoles are supposed to be produced at very high energy where particle physics remains elusive, one can always imagine that the associated symmetry breakings do not occur. However, another elegant solution is again to add a phase of inflation.

### 1.4.3.2. Inflation as a Solution to the Monopole Problem

If a phase of inflation is added after the GUT phase transition, one may hope to dilute monopoles to such an extent that they would not be visible today. In this case, Eq. (1.71) still applies, but the integral now has to be calculated with Eq. (1.53). Since the GUT phase transition occurs before inflation, one has  $t_{\text{BB}} < t_{\text{GUT}} < t_{\text{in}}$  and one obtains

$$D_{\text{mon}}^{(0)'} = \frac{\sqrt{1+z_{\text{eq}}}(1+z_{\text{acc}})^{3/2}}{1+z_{\text{GUT}}} H_0^{-1} e^{(1-3w_X)\frac{N}{2}}, \quad (1.76)$$

where again,  $N$  is the amount of  $e$ -folds during inflation. Several comments are in order. First, one notices that at first sight, the standard result (1.72) is only modified by the exponential term. When  $w_X = 1/3$  or  $N = 0$ , as before, the standard result (1.72) is recovered. However, the

value of  $z_{\text{GUT}}$  is actually also modified since the derivation of Eq. (1.73) relies on the standard scenario (1.38). Using this time the modified scheme (1.53) in the calculation of  $z_{\text{GUT}}$ , one obtains

$$z_{\text{GUT}} \sim z_{\text{eq}}^{1/4} \sqrt{\frac{H_{\text{GUT}}}{H_0}} e^{(1-3w_X)\frac{N}{4}}. \quad (1.77)$$

Here also, the standard result is modified by an exponential term, and  $z_{\text{GUT}}$  actually also depends on the number of  $e$ -folds realized during inflation. Plugging back this expression into Eq. (1.76), one finally obtains

$$D_{\text{mon}}^{(0)} \simeq z_{\text{eq}}^{1/4} \sqrt{\frac{H_0}{H_{\text{GUT}}}} H_0^{-1} e^{(1-3w_X)\frac{N}{4}}. \quad (1.78)$$

From here, one can see that the condition on  $w_X$  for the new phase to provide a possible solution to the monopole problem is  $w_X < 1/3$ . This condition is less stringent than the one arisen from the horizon and flatness problems,  $w_X < -1/3$ . Here, a phase of more rapid expansion than the one driven by radiation is sufficient, and acceleration in itself is a priori not a necessary condition. Obviously, this also depends on the number of inflationary  $e$ -folds  $N$ .

Let us see which typical numbers of  $e$ -folds are required. A first strong requirement would be that there is no magnetic monopole in our entire observable Universe. Since we cannot see beyond the last scattering surface, its size is given by  $d_{\text{obs}} = a_0 r_{\text{ISS}} = a_0 \int_{t_{\text{ISS}}}^{t_0} dt/a$ . This integral can be computed making use of Eq. (1.53), and one obtains  $d_{\text{obs}} \simeq 2/H_0$ . This confirms that as mentioned in section 1.1.1 the size of the observable Universe is of the order of the Hubble length. Therefore, requiring that  $D_{\text{mon}}^{(0)} > d_{\text{obs}}$  leads to

$$N > \frac{2}{1-3w_X} \ln \left( \frac{H_{\text{GUT}}}{H_0} \sqrt{\frac{2}{z_{\text{eq}}}} \right). \quad (1.79)$$

With the values recalled in table 1.2 for  $z_{\text{eq}}$ ,  $H_{\text{GUT}}$  and  $H_0$ , one typically obtains  $N > 61$  for  $w_X = -1$  or  $N > 246$  for  $w_X = 0$ . A less strict requirement is just to meet the observational constraint on  $\eta_{\text{mon}}^{(0)}/\eta_{\text{nucl}}^{(0)}$ . This ratio can be calculated as in Eq. (1.75), and one obtains

$$N > \frac{2}{1-3w_X} \ln \left\{ \frac{H_{\text{GUT}}}{H_0} \sqrt{\frac{1}{z_{\text{eq}}}} \left( \frac{m_{\text{nucl}} H_0}{3M_{\text{Pl}}^2 \Omega_{\text{m}}} \right)^{2/3} \left[ \frac{\eta_{\text{nucl}}^{(0)}}{\eta_{\text{mon}}^{(0)}} \right]_{\text{min}}^{2/3} \right\}. \quad (1.80)$$

Using the same values as before together with  $\eta_{\text{nucl}}^{(0)}/\eta_{\text{mon}}^{(0)} > 10^{30}$ , this gives  $N > 24.5$  for  $w_X = -1$  or  $N > 98$  for  $w_X = 0$ .

A last consistency check remains to be done. Indeed, in order for a phase with  $w < 1/3$  to solve the monopole problem, its  $e$ -folds must be realized after the GUT scale transition and before, say, the equivalence time. One should make sure that there is enough time between these two times for this new phase to proceed, that is

$$\frac{1+z_{\text{in}}}{1+z_{\text{end}}} < \frac{1+z_{\text{GUT}}}{1+z_{\text{eq}}}. \quad (1.81)$$

The left hand side of the previous relation is simply given by  $e^N$ , while  $z_{\text{GUT}}$  appearing in the right hand side depends on  $N$  through Eq. (1.77). This is why the previous relation translates into a constraint on  $N$  itself, which reads

$$N < \frac{2}{3(1+w_X)} \ln \left( \frac{H_{\text{GUT}}}{H_0} z_{\text{eq}}^{-3/4} \right). \quad (1.82)$$

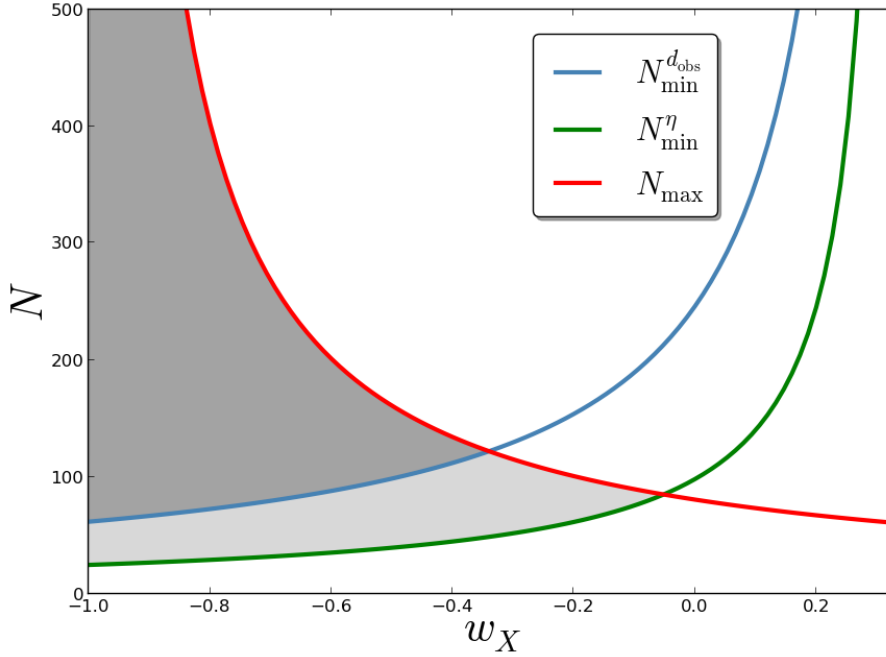


Figure 1.13.: Number of inflationary  $e$ -folds required to solve the monopole problem, as a function of  $w_X$ . The blue line stands for the minimum number of  $e$ -folds in order to dilute the monopoles further than our observable Universe and corresponds to Eq. (1.79). The green line stands for the minimum number of  $e$ -folds in order to dilute the monopoles so that the experimental constraint on  $\eta_{\text{nucl}}/\eta_{\text{mon}}$  is satisfied and corresponds to Eq. (1.80). Finally, the red line stands for the maximum number of  $e$ -folds between the GUT phase transition and equivalence and corresponds to Eq. (1.82). The shaded areas correspond to when both constraints  $N > N_{\text{min}}$  and  $N < N_{\text{max}}$  are satisfied, the darker area being when the stricter constraint on the presence of monopoles in our observable Universe is used. The parameter values used here are the ones of table 1.2.

Obviously, a viable scenario is when Eqs. (1.79) and (1.82) [or Eqs. (1.80) and (1.82)] are satisfied at the same time. Such bounding values of  $N$  are displayed in Fig. 1.13. The shaded area stands for values of  $w_X$  and  $N$  such that both constraints are simultaneously satisfied. Since the maximal value for  $N$  given by Eq. (1.82) blows up when  $w_X \rightarrow -1$ , it is always possible to solve the monopole problem, provided  $w_X$  is close enough to  $-1$ . More precisely, if the criterion (1.80) is adopted, one obtains  $w_X < -0.052$ , whereas if the criterion (1.79) is adopted, one obtains  $w_X < -0.34$ . It is remarkable that this last condition is very similar to the one  $w_X < -1/3$  that comes from the horizon and flatness problems. Therefore, even for the monopole problem, an accelerating phase seems to be required.

## 1.A. FLRW Christoffel symbols, Einstein tensor and Geodesics

In this appendix, we give the Christoffel symbols and the Ricci and Einstein tensors of the FLRW metric, and comment on the geodesic equations in comoving coordinate. Starting from the FLRW metric (1.1),

$$ds^2 = g_{\mu\nu} dx^\mu dx^\nu = -dt^2 + a^2(t) \left[ \frac{dr^2}{1 - \mathcal{K}r^2} + r^2 (d\theta^2 + \sin^2 \theta d\phi^2) \right], \quad (1.83)$$

the Christoffel symbols are formally given by

$$\Gamma_{\mu\nu}^\rho = \frac{1}{2} g^{\rho\lambda} (\partial_\nu g_{\lambda\mu} + \partial_\mu g_{\lambda\nu} - \partial_\lambda g_{\mu\nu}). \quad (1.84)$$

One can check that they are symmetrical in their lower indices, that is  $\Gamma_{\mu\nu}^\rho = \Gamma_{\nu\mu}^\rho$ . After a straightforward calculation, up to this symmetry, the only non vanishing Christoffel symbols of the FLRW metric are given by

$$\begin{aligned} \Gamma_{11}^0 &= \frac{a\dot{a}}{1 - \mathcal{K}r^2}, & \Gamma_{22}^0 &= a\dot{a}r^2, \\ \Gamma_{33}^0 &= a\dot{a}r^2 \sin^2 \theta, & \Gamma_{11}^1 &= \frac{\mathcal{K}r}{1 - \mathcal{K}r^2}, \\ \Gamma_{22}^1 &= -r(1 - \mathcal{K}r^2), & \Gamma_{33}^1 &= -r(1 - \mathcal{K}r^2) \sin^2 \theta, \\ \Gamma_{33}^2 &= -\sin \theta \cos \theta, & \Gamma_{01}^1 &= \Gamma_{02}^2 = \Gamma_{03}^3 = \frac{\dot{a}}{a}, \\ \Gamma_{12}^2 &= \Gamma_{13}^3 = \frac{1}{r}, & \Gamma_{23}^3 &= \cot \theta, \end{aligned} \quad (1.85)$$

where index 0 is for time  $t$ , 1 is for  $r$ , 2 is for  $\theta$  and 3 is for  $\phi$ . The Ricci tensor is formally expressed as

$$R_{\mu\nu} = 2\Gamma_{\mu[\nu,\rho]}^\rho + 2\Gamma_{\lambda[\rho}^\rho \Gamma_{\nu]\mu}^\lambda, \quad (1.86)$$

where the brackets mean anti-symmetrization under the indices. From the Christoffel symbols (1.85), one can check that its non-zero components are the diagonal ones, given by

$$\begin{aligned} R_{00} &= -3\frac{\ddot{a}}{a}, & R_{11} &= \frac{a\ddot{a} + 2\dot{a}^2 + 2\mathcal{K}}{1 - \mathcal{K}r^2}, \\ R_{22} &= r^2 (a\ddot{a} + 2\dot{a}^2 + 2\mathcal{K}), & R_{33} &= r^2 (a\ddot{a} + 2\dot{a}^2 + 2\mathcal{K}) \sin^2 \theta. \end{aligned} \quad (1.87)$$

The Ricci curvature scalar is just the contraction of the Ricci tensor with the metric,  $R = g^{\mu\nu} R_{\mu\nu}$ , and is given by

$$R = 6 \left[ \left( \frac{\dot{a}}{a} \right)^2 + \frac{\ddot{a}}{a} + \frac{\mathcal{K}}{a^2} \right]. \quad (1.88)$$

Finally, the Einstein tensor  $G_{\mu\nu} = R_{\mu\nu} - R/2g_{\mu\nu}$  has non vanishing components

$$\begin{aligned} G_{00} &= 3 \left[ \left( \frac{\dot{a}}{a} \right)^2 + \frac{\mathcal{K}}{a^2} \right], & G_{11} &= - \left[ \left( \frac{\dot{a}}{a} \right)^2 + 2\frac{\ddot{a}}{a} + \frac{\mathcal{K}}{a^2} \right] \frac{a^2}{1 - \mathcal{K}r^2}, \\ G_{22} &= - \left[ \left( \frac{\dot{a}}{a} \right)^2 + 2\frac{\ddot{a}}{a} + \frac{\mathcal{K}}{a^2} \right] a^2 r^2, & G_{33} &= - \left[ \left( \frac{\dot{a}}{a} \right)^2 + 2\frac{\ddot{a}}{a} + \frac{\mathcal{K}}{a^2} \right] a^2 r^2 \sin^2 \theta. \end{aligned} \quad (1.89)$$

One can check that this matches the formula (1.14) given in section 1.1.1.3.

Finally, it is interesting to say a few words about the geodesic equation

$$\frac{d^2 x^\mu}{ds^2} + \Gamma_{\nu\rho}^\mu \frac{dx^\nu}{ds} \frac{dx^\rho}{ds} = 0. \quad (1.90)$$

Because the FLRW geometry is isotropic with respect to every point, it is always possible to choose a local coordinate system such that a given geodesic initially has a purely radial part, that is  $d\theta/ds = d\phi/ds = 0$  at initial time. Then it is straightforward to see that the geodesic equations for  $\theta$  and  $\phi$  [ $\mu = 2$  or  $3$  in Eq. (1.90)] imply that it remains so at any later time. In this case, the geodesic equations for  $t$  and  $r$  are

$$\frac{d^2 t}{ds^2} + \frac{a\dot{a}}{1 - \mathcal{K}r^2} \left( \frac{dr}{ds} \right)^2 = 0, \quad (1.91)$$

$$\frac{d^2 r}{ds^2} + \frac{\mathcal{K}r}{1 - \mathcal{K}r^2} \left( \frac{dr}{ds} \right)^2 + 2 \frac{\dot{a}}{a} \frac{dt}{ds} \frac{dr}{ds} = 0. \quad (1.92)$$

One can check that a static particle such that  $dt/ds = 1$  and  $dr/dt = 0$  is a solution of the above system, which means that still particles in the comoving coordinate system are indeed solutions of the geodesic equations. If one is interested in the more general trajectory  $r(t)$  associated with this system, one can work out its solution as

$$\frac{dt}{ds} = \left[ 1 + \left( \frac{b_0}{a} \right)^2 \right]^{1/2}, \quad (1.93)$$

$$\frac{dr}{ds} = \sqrt{1 - \mathcal{K}r^2} \frac{b_0}{a^2}, \quad (1.94)$$

where  $b_0$  is an integration constant that depends on initial conditions (for example,  $b_0 = 0$  for still particles and  $b_0 = \infty$  for photons). From here, the physical impulsion  $p$  can be obtained,

$$\frac{p}{m} = \sqrt{g_{ij} \frac{dx^i}{ds} \frac{dx^j}{ds}} = \frac{a}{\sqrt{1 - \mathcal{K}r^2}} \frac{dr}{ds} = \frac{b_0}{a}, \quad (1.95)$$

which confirms the rule  $p \propto 1/a$  otherwise derived in section 1.1.1.2. More precisely, the solution for  $dr/dt$  is given by

$$\frac{dr}{dt} = \sqrt{1 - \mathcal{K}r^2} \frac{b_0}{a^2} \left[ 1 + \left( \frac{b_0}{a} \right)^2 \right]^{-1/2}, \quad (1.96)$$

which means that as time proceeds and  $a$  increases (in an expanding universe),  $dr/dt \propto 1/a^2 \rightarrow 0$  for massive particles. Therefore, massive particles asymptotically come to rest relative to the comoving coordinate system, as mentioned in section 1.1.1.2. More precisely,  $dr/dt \propto 1/a^2$  means that  $r$  reaches a finite value in the asymptotic future if  $a$  grows strictly faster than  $a \propto \sqrt{t}$ . This is the case in a matter era, an inflationary era or a dark energy era, but not during a radiation era where  $dr/dt \rightarrow 0$  but  $r \rightarrow \infty$  if  $\mathcal{K} = 0$  or  $-1$  and  $r \rightarrow 1$  if  $\mathcal{K} = 1$ .

To be explicit, once the  $a(t)$  profile known [see for example Eq. (1.30)], one can calculate

$$r(t) = r_{\text{in}} + \begin{cases} \sin(\mathcal{I}) & \text{if } K = 1 \\ \mathcal{I} & \text{if } K = 0 \\ \sinh(\mathcal{I}) & \text{if } K = -1 \end{cases}, \quad (1.97)$$

where  $\mathcal{I}$  is given by

$$\mathcal{I} = b_0 \int_{t_{\text{in}}}^t \frac{d\tilde{t}}{a^2 \sqrt{1 + \left(\frac{b_0}{a}\right)^2}}. \quad (1.98)$$

Finally, let us mention that for massless particles ( $b_0 = \infty$ ), Eq. (1.98) gives  $\mathcal{I} = \int dt/a$ , which is in agreement with Eq. (1.5).

## 1.B. Numerical Values of Cosmological Parameters

Physical Quantity	Numerical Value
$M_{\text{Pl}}$	$2.435 \times 10^{18}$ GeV
$H_0$	67.3 km/sec/Mpc
$H_0^{-1}$	$4.55 \times 10^{17}$ sec
$H_0^{-1}$	$1.36 \times 10^{26}$ m
$w_{\text{dm}}$	0
$w_{\text{mat}}$	0
$w_{\text{rad}}$	1/3
$w_{\mathcal{K}}$	-1/3
$w_{\Lambda}$	-1
$\Omega_{\text{rad}}^{(0)}$	$9.3 \times 10^{-5}$
$\Omega_{\text{b}}^{(0)}$	0.049
$\Omega_{\text{dm}}^{(0)}$	0.268
$\Omega_{\text{de}}^{(0)}$	0.683
$ \Omega_{\mathcal{K}} $	$\lesssim 10^{-3}$
$z_{\text{acc}}$	0.29
$z_{\text{ISS}}$	1090
$z_{\text{eq}}$	3402
$z_{\text{GUT}}$ (without inflation)	$10^{28}$
$M_{\text{GUT}}$	$10^{16}$ GeV
$H_{\text{GUT}}$	$10^{13}$ GeV

Table 1.2.: Numerical values of cosmological parameters used in section 1.





## 2. Cosmological Inflation

*In this chapter, we review some aspects of cosmological inflation, the physical setups it relies on, the predictions it makes and the fundamental issues it raises. Our purpose is mainly to provide the reader with an understanding of the theoretical and technical tools used in part II where the results obtained during this thesis are presented. This is why in this section, only a brief overview of the physics of inflation is given, the various aspects of which are further detailed in a broad range of textbooks [109, 110, 111, 4, 112, 113, 7, 8].*

In chapter 1, we reviewed the cornerstones of the cosmological hot big bang model and the problems it raises. In particular, in section 1.4, we saw that a phase of inflation during which the scale factor accelerates  $\ddot{a} > 0$  can solve the hot big bang problems if it occurs prior to (or during) the radiation era [91, 114, 115, 116, 117, 118, 119]. However, we have not discussed which kind of matter component can drive such a phase of inflation. From the the Raychaudhuri equation (1.18),  $\ddot{a} > 0$  implies that  $\rho + 3p < 0$ , hence the pressure must necessarily be negative. One therefore needs to find a physical system able to produce such a negative pressure.

The inflationary phase takes place at very high energy, typically between  $10^3$  and  $10^{15}$  GeV [120]. At such high energies, field theory is the relevant framework to describe matter, and a natural way to try and realize inflation is therefore to consider that a real scalar field  $\phi$  (dubbed the “inflaton” field) dominates the energy density budget of matter in the early Universe. Moreover, this assumption is compatible with the observed homogeneity, isotropy and flatness of the early Universe. Quite remarkably, it turns out that if the potential  $V(\phi)$  of this scalar field is sufficiently flat  $dV/d\phi \ll V/M_{\text{Pl}}$  so that the field moves slowly, then the corresponding pressure is negative. This is why it is believed that inflation is driven by one (or several) scalar field(s). However, the physical nature of the inflaton and its relation with the standard model of particle physics and its extensions is still unclear. This is not surprising since the inflationary mechanism takes place at energy scales where particle physics remains elusive and has not been tested in accelerators. This is why the shape of its potential is *a priori* not known except that it must be sufficiently flat to support a phase of inflation.

Nonetheless, one of the great achievements of inflation is that, combined with quantum mechanics, it provides a convincing mechanism for the origin of the cosmological fluctuations, the seeds of the CMB anisotropies and of the galaxies. Inflation predicts that their spectrum should be almost scale invariant (*i.e.* equal power on all spatial scales) [121, 122, 123, 124, 125, 126, 127, 128, 129, 130], which is fully consistent with the observations. In passing, this part of the scenario is particularly remarkable since it makes us of General Relativity and Quantum Mechanics [131, 132, 133, 134, 135, 136, 137, 138, 139, 138], two theories that are notoriously difficult to combine. In fact, inflation is probably the only case in physics where an effect based on General Relativity and Quantum Mechanics leads to predictions that, given our present day technological capabilities, can be tested experimentally. Given the confirmation of these predictions by observations and given the fact that, despite many efforts, inflation has not been superseded by its various challengers [140, 29, 141, 27, 142, 143, 144, 145, 146, 147, 148, 149,

150, 31, 34, 151, 152, 153, 154, 32, 155, 156, 157, 158, 159, 160, 161, 162], this scenario has gradually become a crucial part of modern cosmology.

What strongly motivates the investigation of the inflationary period is that there is now a flow of increasingly accurate astrophysical data which gives us a unique opportunity to learn more about inflation. In particular, the recently released Planck satellite data [76, 163, 15], and if confirmed to be of primordial origin, the  $B$ -mode detection by the BICEP2 experiment [164], play a crucial role in this process. These missions complement and improve upon observations made by the NASA WMAP satellite [165, 166] and are a major source of information relevant to several cosmological issues including inflation [167, 168]. The CMB small angular scales of Planck are already complemented by ground-based microwave telescopes such as the Atacama Cosmology Telescope [169, 170] or the South Pole Telescope [171, 172] while ultra-sensitive polarization dedicated experiments are on their way [173, 174, 175, 176, 177, 178].

Let us also mention that even if this is what we focus on in this thesis, the flow of new data does not only concern the CMB. The supernovae projects [179, 180, 181, 182] continue to measure the distances to the nearby exploding SN1A stars while the large scale galaxy surveys such as the Sloan Digital Sky Survey (SDSS) [183, 184] are providing an unprecedented picture of the structure of the universe. The “lever arm” in length scales between CMB and galaxy power spectra increases the sensitivity to the small deviations from scale invariance, and thus should be extremely powerful to constrain inflationary models. For this reason, the future Euclid satellite will be another step forward in our understanding of inflation [185]. The possibility of direct detection of the primordial gravitational waves is also currently discussed for high energy inflationary models on large scales [186, 187, 188, 189, 190, 191, 192, 193, 194, 195] and also on small scales [196, 197]. Finally, in a foreseeable future, the yet unexplored length scales are expected to be unveiled by the 21 cm cosmological telescopes. These ones will be sensitive to the redshifted 21 cm line absorbed by hydrogen clouds before the formation of galaxies [198, 199, 200, 201, 202, 203, 204]. With such data, we will have a complete tomography of the universe history from the time of CMB emission at the surface of last scattering to the distribution of galaxies today.

Our ability to see through the inflationary window is crucial since it turns the early universe into a laboratory for ultra-high energy physics, at scales entirely inaccessible to conventional experimentation. In other words, this window offers a unique opportunity to learn about the very early universe and about physics in a regime that cannot be tested otherwise, even in accelerators such as the Large Hadron Collider. In this chapter, we discuss a few aspects that play a key role in this enterprise, and we introduce some of the theoretical and technical tools that are widely used in part II where the results of this thesis are presented. It is organized as follows. In section 2.1, we explain why and under which conditions a single scalar field can support a phase of inflation. In section 2.2, we present a frame of approximation, the “slow-roll approximation”, which enables to solve its dynamics perturbatively. It also provides us with a convenient scheme of calculation to compare inflationary predictions with observational data, which we make widely use of in Ref. [205], section 3.2, in Ref. [206], section 3.3 and in Ref. [207], section 3.4. The slow-roll inflationary trajectories are also the subject of Ref. [208], section 3.1, and for this reason it seems important to review the main aspects of this formalism in the present chapter. Then, in section 2.3, we turn to the description of inflationary perturbations. We show how cosmological perturbations need to be quantized, and for illustrative purpose, we provide a detailed calculation of the power spectrum of scalar perturbations. Since such a calculation is modified when extensions to standard quantum mechanics are included in Ref. [138], section 4.3, it is important to first understand how it proceeds in the standard approach. We then specify the obtained result at leading order in the slow-roll approximation. Indeed, in Ref. [209], section 3.5,

this calculation is extended to next-to-leading order in slow roll, and it is generalized in the case where not only the potential but also the kinetic term is a free function. This is why details of the calculation for the leading order in slow roll with canonical kinetic term for the inflaton field may be useful to get acquainted with the employed technique. Finally, in section 2.4, we devote a large part of this introductory chapter to the presentation of the stochastic inflation formalism which is used in Ref. [210], section 4.1 and in Ref. [211], section 4.2. We first present a detailed heuristic derivation of the Langevin equation which is at the heart of this formalism. This allows us to discuss its nature and the assumptions it rests on. Then, we turn to the question of the time variable that should be used when solving such equations, in order to reproduce results from Quantum Field Theories (QFT). Lastly, we address the issue of the calculation of physical observable quantities in stochastic inflation, such as the power spectrum of adiabatic perturbations. We show that the stochastic setup allows us to reproduce the standard result of section 2.3, before providing complete solutions which do not rely on an expansion in the noise term. To our knowledge, this is the first time such a non perturbative calculation of the power spectrum in stochastic inflation is presented, and we plan to further discuss it in a forthcoming article.

## 2.1. Single-Field Inflation

What makes the inflationary idea quite natural is that the negative pressure condition can simply be met with a single scalar field  $\phi$ , the inflaton field, minimally coupled to gravity. The action of such a system is given by

$$S_\phi = - \int d^4x \sqrt{-g} \left[ \frac{1}{2} g^{\mu\nu} \partial_\mu \phi \partial_\nu \phi + V(\phi) \right]. \quad (2.1)$$

The function  $V(\phi)$  is a potential term for the scalar field, that is left unspecified for the moment. Indeed, the physical nature of the inflaton field is still unknown (there are many candidates) and, as a consequence,  $V(\phi)$  can have different shapes. From Eq. (1.12), the energy-momentum tensor associated with this action can be derived, and one obtains

$$T_{\mu\nu}^{(\phi)} = \partial_\mu \phi \partial_\nu \phi + g_{\mu\nu} \left[ -\frac{1}{2} g^{\rho\sigma} \partial_\rho \phi \partial_\sigma \phi + V(\phi) \right]. \quad (2.2)$$

At the background level, since FRLW space-times are homogeneous and isotropic,  $\phi$  must be homogeneous as well and can only depend on time. Interestingly enough, in such a case, the energy-momentum tensor can be expressed in the form of Eq. (1.15) if one lets

$$\rho = \frac{\dot{\phi}^2}{2} + V, \quad (2.3)$$

$$p = \frac{\dot{\phi}^2}{2} - V. \quad (2.4)$$

As a consequence, for an homogeneous scalar field, the condition for the acceleration of the scale factor is fulfilled,  $\rho + 3p < 0$ , as soon as

$$V > \dot{\phi}^2. \quad (2.5)$$

This is the condition for inflation to take place. This means that inflation can be obtained provided the inflaton slowly rolls down its potential, so that its potential energy dominates over its kinetic energy. This also shows that the inflaton potential must be sufficiently flat,

a requirement which is not always easy to obtain in realistic situations and which makes the inflationary model building problem a difficult issue [212].

The dynamics of  $\phi$  can be obtained if one plugs the expressions (2.3) and (2.4) into the conservation equation (1.16). Doing so, one gets the Klein-Gordon equation

$$\ddot{\phi} + 3H\dot{\phi} + V' = 0, \quad (2.6)$$

where a prime denotes a derivative with respect to  $\phi$ . On the other hand, the Friedmann equation (1.17) gives rise to

$$3M_{\text{Pl}}^2 H^2 = V + \frac{\dot{\phi}^2}{2}. \quad (2.7)$$

This last quantity is important since it sets the energy scale at which inflation takes place. In section 2.3, we will see that its measurement requires to detect primordial gravity waves. Without such a detection, one can only constrain  $\rho^{1/4} \propto \sqrt{M_{\text{Pl}} H}$  to be between the Grand Unified Theory (GUT) scale, that is to say  $\sim 10^{15}$  GeV, and  $\sim 10^3$  GeV [120]. However, if the measurement of the  $B$  mode polarization of the CMB by the BICEP2 experiment [164] is of primordial origin, the inflationary energy scale should lie close the GUT scale, see the discussion at the end of section 2.3.

The Klein-Gordon equation (2.6) and the Friedmann equation (2.7) form a closed system that can be integrated for any potential  $V(\phi)$  and given initial conditions  $\phi_{\text{in}}$  and  $\dot{\phi}_{\text{in}}$ . A few numerical solutions of this set of equations when  $V(\phi) = m^2\phi^2/2$  are displayed in Fig. 2.1 for illustrative purpose. In this figure, the light blue area stands for the region where the condition (2.5) is fulfilled and where inflation takes place. One can see that even if the initial velocity of the inflaton field is too large, it is quickly damped to sufficiently small values so that inflation starts and proceeds. Then, at some point, the system exits the light blue area and inflation naturally stops. Subsequently, the field quickly oscillates at the bottom of the potential, the amplitude of these oscillations being damped due to the expansion, through the term  $\propto H\dot{\phi}$  in Eq. (2.6). During this phase, possible coupling between  $\phi$  and other fields can efficiently make the inflaton field parametrically decay into radiation, hence smoothly connecting inflation to the radiation-dominated epoch [213, 214, 215, 216, 217, 218, 219, 196, 220]. This is the so-called reheating period [221, 222, 223, 224, 225].

## 2.2. The Slow-Roll Approximation

Beyond the numerical solutions of Fig. 2.1, analytical solutions can also be obtained, in the limit where the condition (2.5) is saturated, that is when  $V \gg \dot{\phi}^2$ . In this limit, one has  $p \simeq -\rho$ , so that the conservation equation  $\dot{\rho} = -3H(\rho + p)$  implies that  $\rho$  is almost constant in time. Thanks to the Friedmann equation (1.17), this means that  $H = \dot{a}/a$  is almost constant in time too, which implies that space-time is close to the de Sitter universe for which

$$a(t) = a_{\text{in}} \exp [H(t - t_{\text{in}})]. \quad (2.8)$$

This is why it is interesting to derive solutions to Eqs. (2.6) and (2.7) in the limit<sup>1</sup> where the Universe is perturbatively close to the one of Eq. (2.8). The “slow-roll approximation” refers to this limit, in which the velocity of the inflaton is small  $\dot{\phi} \ll \sqrt{V}$  and the field “slowly rolls” down its potential. At the technical level, the strategy is to define a set of parameters that quantify the deviation from de Sitter space-times, and to perform an expansion in these parameters.

<sup>1</sup>As will be shown in section 2.3.4, such an assumption can be justified *a posteriori*, e.g. by the fact that only small deviations from scale invariance are measured, with tight constraints on the level of gravity waves.

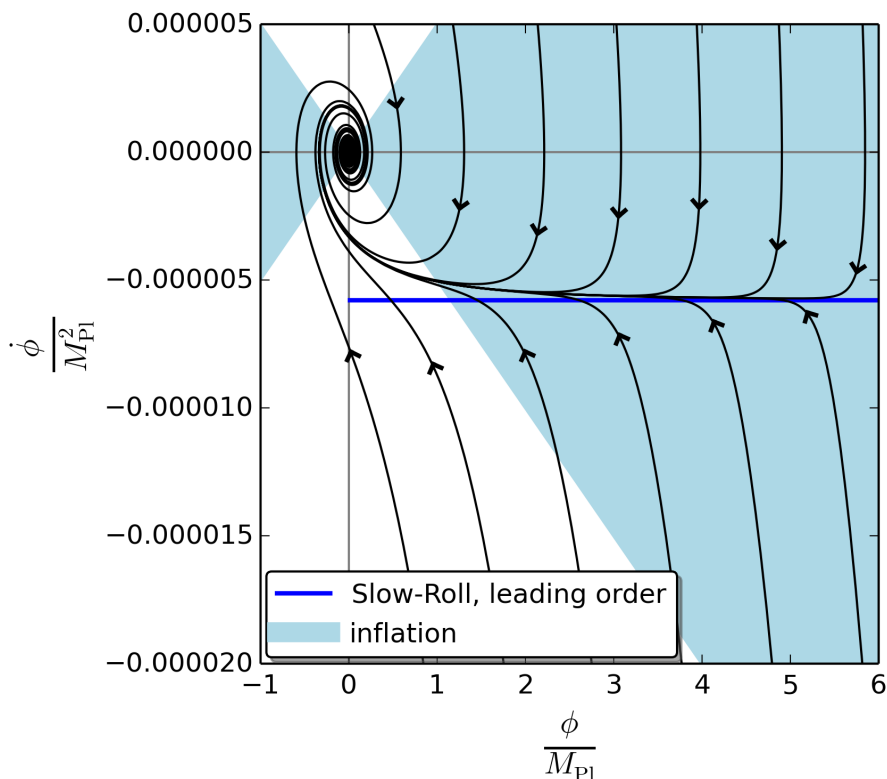


Figure 2.1.: Phase space diagram of the inflaton trajectory for  $V = m^2\phi^2/2$ , with  $m \simeq 7 \times 10^{-6}M_{\text{Pl}}$ . The black lines correspond to numerical solutions of Eqs. (2.6) and (2.7) with different initial conditions. The arrows indicate in which direction the system evolves. The light blue area stands for the region in phase space where inflation proceeds, that is where the condition (2.5),  $V > \dot{\phi}^2$ , is fulfilled. Finally, the blue solid line displays the slow-roll trajectory at leading order  $\dot{\phi} \simeq -V'/(3H)$ , with  $H^2 \simeq V/(3M_{\text{Pl}}^2)$ . One can see that as long as the slow-roll condition  $V \gg \dot{\phi}^2$  is met (*i.e.* when one is well inside the light blue area), this trajectory represents an attractor solution.

### 2.2.1. The Slow-Roll Parameters

Although there are several possible sets of slow-roll parameters, here we choose to introduce the Hubble-flow parameters  $\{\epsilon_n\}$  defined by the flow equations [226, 227]. If one lets  $\epsilon_0 \equiv H_{\text{in}}/H$ , this parameter  $\epsilon_0$  is constant for a de Sitter space (and equal to 1), so that its time derivatives should be small in the limit we are interested in. This is why, labelling time with the number of  $e$ -folds  $N \equiv \ln a$ , starting from  $\epsilon_0$ , one iteratively defines

$$\epsilon_{n+1} = \frac{d \ln |\epsilon_n|}{dN}. \quad (2.9)$$

In this hierarchy, all the  $\epsilon_n$  are typically of the same order of magnitude. By definition, one has *slow-roll* inflation as long as  $|\epsilon_n| \ll 1$ , for all  $n > 0$ . For example, the first slow-roll parameter is given by  $\epsilon_1 = -\dot{H}/H^2 = 1 - \ddot{a}/(aH^2)$ , which implies that inflation ( $\ddot{a} > 0$ ) takes place provided  $\epsilon_1 < 1$ .

### 2.2.2. The Slow-Roll Trajectory

Now, let us see how the system formed by Eqs. (2.6) and (2.7) can be solved perturbatively in the slow-roll limit. Inserting the Klein-Gordon equation in the time derivative of the Friedmann equation, one obtains  $\dot{H} = -\dot{\phi}^2/(2M_{\text{Pl}}^2)$ , hence<sup>2</sup>

$$\epsilon_1 = -\frac{\dot{H}}{H^2} = 3\frac{\dot{\phi}^2/2}{V(\phi) + \dot{\phi}^2/2}. \quad (2.10)$$

The condition  $\epsilon_1 \ll 1$  thus implies that the kinetic energy of the inflaton is much smaller than its potential energy, which is clearly the limit under study. Under this condition, the Friedmann equation simplifies and gives, at leading order in slow roll,  $H^2 \simeq V/(3M_{\text{Pl}}^2)$ .

One can keep on and play the same game with  $\epsilon_2$ . Inserting the Klein-Gordon equation (2.6) in the time derivative of the relation  $\dot{H} = -\dot{\phi}^2/(2M_{\text{Pl}}^2)$  previously obtained, one gets  $\ddot{H} = 3H\dot{\phi}^2/M_{\text{Pl}}^2 + \dot{\phi}V'/M_{\text{Pl}}^2$ , and

$$\epsilon_2 = \frac{\ddot{H}}{H\dot{H}} - 2\frac{\dot{H}}{H^2} = 6\left(\frac{\epsilon_1}{3} - \frac{V'}{3H\dot{\phi}} - 1\right). \quad (2.11)$$

The condition  $\epsilon_2 \ll 1$  thus implies that, at leading order in slow roll,  $\dot{\phi} \simeq -V'/(3H)$ , which means that the acceleration term can be neglected in the Klein-Gordon equation (2.6) (such a limit solution is displayed by the solid blue line in Fig. 2.1). This is particularly interesting since it lowers by one the order of the differential equation satisfied by  $\phi$ . As a consequence, it removes the dependency on the initial conditions by singling out a specific trajectory in phase space, and it allows to derive analytical solutions in most cases.

More explicitly, since  $dN = Hdt$ , at leading order in slow roll, the Klein-Gordon equation reads  $dN = -3H^2 d\phi/V'$ . Plugging in the slow-roll leading order of the Friedmann equation  $H_{\text{SR,LO}}^2 = V/(3M_{\text{Pl}}^2)$ , one obtains

$$\Delta N^{\text{SR,LO}} = -\frac{1}{M_{\text{Pl}}^2} \int_{\phi_{\text{in}}}^{\phi_{\text{end}}} \frac{V}{V'} d\phi, \quad (2.12)$$

where  $\Delta N \equiv N_{\text{end}} - N_{\text{in}}$ ,  $\phi_{\text{in}}$  is the value of  $\phi$  at some initial time  $N_{\text{in}}$ , and  $\phi_{\text{end}}$  is the value of  $\phi$  at some final time  $N_{\text{end}}$ . This represents the leading order (LO) of the slow-roll (SR) trajectory. Inverting this relation yields the value of  $\phi$  as a function of time  $N$ .

If one worked at next-to-leading order in slow roll, see section 2.2.3, one would obtain a slightly modified trajectory, so on and so forth, and *the* slow-roll trajectory is by definition the limit towards which this perturbative process converges. It singles out a specific solution to Eqs. (2.6) and (2.7). It is worth mentioning that as can be seen in Fig. 2.1, this slow-roll trajectory is actually a powerful attractor [228] of the inflationary dynamics, that is to say, starting from a large basin of possible initial conditions  $\phi_{\text{in}}$  and  $\dot{\phi}_{\text{in}}$ , the system quickly converges towards the slow-roll trajectory. This property makes the slow-roll scheme of approximation both convenient and physically well-motivated.

It is also interesting to remark that under the slow-roll approximation, the slow-roll hierarchy can easily be expressed in terms of  $V$  and its derivatives. Indeed, making use of Eq. (2.12), one

<sup>2</sup>Notice that with Eq. (2.10), Eqs. (2.3) and (2.4) give rise to  $\omega = p/\rho = -1 + 2\epsilon_1/3$ , which is consistent with what we displayed in table 1.1.

has

$$\left. \frac{d}{dN} \right|^{SR,LO} = -M_{Pl}^2 \frac{V'}{V} \frac{d}{d\phi}. \quad (2.13)$$

Repeatedly applying this identity starting from  $\epsilon_0 = H_{in}/H \simeq H_{in} \sqrt{3M_{Pl}^2/V}$ , one obtains, at leading order in slow roll,

$$\epsilon_0^{LO} = H_{in} \sqrt{\frac{3M_{Pl}^2}{V}}, \quad (2.14)$$

$$\epsilon_1^{LO} = \frac{M_{Pl}^2}{2} \left( \frac{V'}{V} \right)^2, \quad (2.15)$$

$$\epsilon_2^{LO} = 2M_{Pl}^2 \left[ \left( \frac{V'}{V} \right)^2 - \frac{V''}{V} \right], \quad (2.16)$$

$$\epsilon_3^{LO} = \frac{2M_{Pl}^4}{\epsilon_2^{LO}} \left[ \frac{V'''V'}{V^2} - 3 \frac{V''V'^2}{V^3} + 2 \left( \frac{V'}{V} \right)^4 \right], \quad (2.17)$$

and the following slow-roll parameters can be computed in the same manner. One can see that as mentioned above, in order for the first slow-roll parameter to be small and for inflation to take place, the potential needs to be sufficiently flat, and more precisely its logarithm,  $(d/d\phi) \ln V \ll 1/M_{Pl}$ .

### 2.2.3. Next-to-Leading Orders in Slow Roll

Most of the time, the leading order of the slow-roll trajectory is sufficiently accurate, but given the precision of observations, it can be useful (and sometimes necessary) to work at higher order in slow roll. Here we explain how the higher contributions can be derived, and as an example, we establish the next-to-leading order (NLO) and the next-to-next-to-leading order (NNLO) versions of the previous expressions. The starting point is to combine equations (2.7) and (2.10) into

$$H^2 = \frac{V}{3M_{Pl}^2} \left( 1 - \frac{\epsilon_1}{3} \right)^{-1}, \quad (2.18)$$

which is exact. Together with the Friedmann equation (2.7), this gives rise to  $\dot{\phi}^2 = 2V\epsilon_1/(3-\epsilon_1)$ . These two formulas allow us to recast  $dN = Hd\phi/\dot{\phi}$  as

$$dN = \pm \frac{1}{M_{Pl}} \frac{d\phi}{\sqrt{2\epsilon_1}}, \quad (2.19)$$

which is again an exact relation. From here the slow-roll parameters at next-to-leading order can be obtained as follows. Rewriting Eq. (2.18) as  $\epsilon_0 = \epsilon_0^{LO} \sqrt{1 - \epsilon_1/3}$ , and iteratively applying

$$\left. \frac{d}{dN} \right|^{SR,NLO} = \sqrt{\frac{\epsilon_1^{NLO}}{\epsilon_1^{LO}}} \left. \frac{d}{dN} \right|^{SR,LO} \quad (2.20)$$

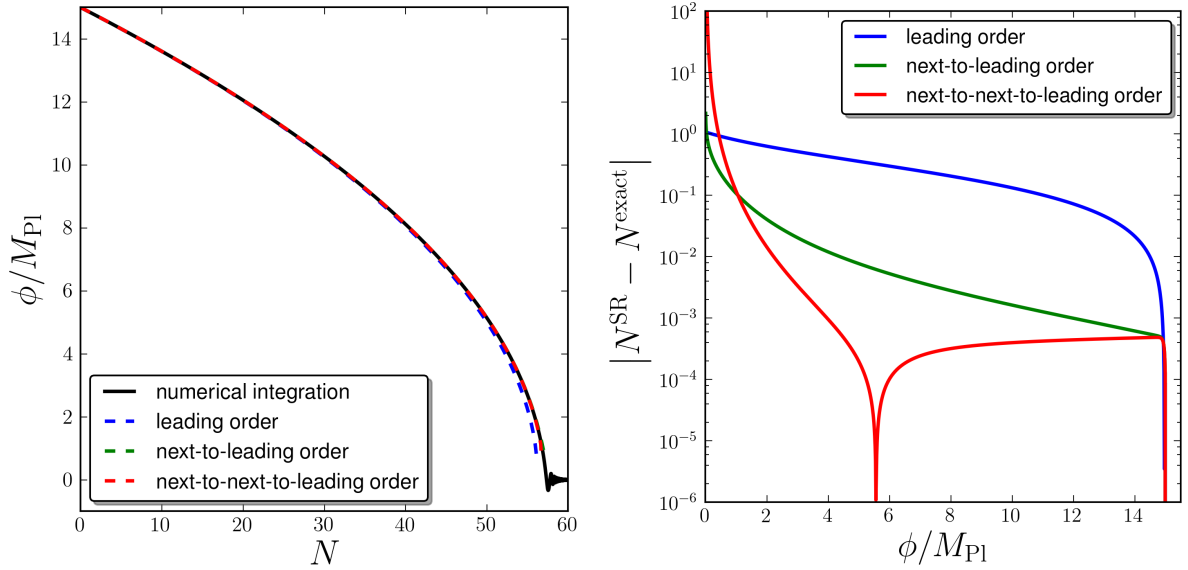


Figure 2.2.: Leading order, next-to-leading order and next-to-next-to leading order of the slow-roll trajectory for  $V = m^2\phi^2/2$ , with  $m \simeq 7 \times 10^{-6}M_{\text{Pl}}$ . All the trajectories start at  $\phi_{\text{in}} = 15M_{\text{Pl}}$ . In the left panel, the black solid line stands for the numerical solution of Eq. (2.6) where  $d\phi/dN|_{\text{in}}$  is set according to Eq. (2.12). The blue dashed line stand for the leading order slow-roll solution (2.12), the green dashed line stand for the next-to-leading order slow-roll solution (2.30), and the red dashed line stand for the next-to-next-to-leading order slow-roll solution (2.31). One can check that the slow-roll solutions are good approximations to the exact solution. More precisely, in the right panel, the distances from the slow-roll approximations to the exact solution is displayed at each order. Since  $\phi$  decreases during inflation, this plot should be read from the right to the left. Each slow-roll solution is compared with the exact solution of Eq. (2.6) that shares the same initial condition  $d\phi/dN|_{\text{in}}$  at  $N = 0$  and  $\phi_{\text{in}} = 15M_{\text{Pl}}$  (so that the distance to the exact solution exactly vanishes at  $\phi = \phi_{\text{in}}$  in all three cases). One can check that at each order, the distance to the exact solution is smaller.

which comes from Eq. (2.19), one obtains an expression for the slow-roll parameters at next-to-leading order in terms of the slow-roll parameters at leading order, which reads

$$\epsilon_0^{\text{NLO}} = \epsilon_0^{\text{LO}} \left( 1 - \frac{\epsilon_1^{\text{LO}}}{6} \right), \quad (2.21)$$

$$\epsilon_1^{\text{NLO}} = \epsilon_1^{\text{LO}} \left( 1 - \frac{\epsilon_2^{\text{LO}}}{3} \right), \quad (2.22)$$

$$\epsilon_2^{\text{NLO}} = \epsilon_2^{\text{LO}} \left( 1 - \frac{\epsilon_2^{\text{LO}}}{6} - \frac{\epsilon_3^{\text{LO}}}{3} \right), \quad (2.23)$$

$$\epsilon_3^{\text{NLO}} = \epsilon_3^{\text{LO}} \left( 1 - \frac{\epsilon_2^{\text{LO}}}{3} - \frac{\epsilon_4^{\text{LO}}}{3} \right), \quad (2.24)$$

where the following slow-roll parameters can be computed in the same manner, and where the slow-roll parameters at leading order in the right hand sides are given by Eqs. (2.14)-(2.17). In the same manner, to go to next-to-next-to-leading order, one starts again from

$\epsilon_0 = \epsilon_0^{\text{LO}} \sqrt{1 - \epsilon_1/3}$ , and iteratively applies

$$\left. \frac{d}{dN} \right|_{\text{SR,NNLO}} = \sqrt{\frac{\epsilon_1^{\text{NNLO}}}{\epsilon_1^{\text{LO}}}} \left. \frac{d}{dN} \right|_{\text{SR,LO}} \quad (2.25)$$

which is again a direct consequence of Eq. (2.19). Doing so, one obtains

$$\epsilon_0^{\text{NNLO}} = \epsilon_0^{\text{LO}} \left[ 1 - \frac{\epsilon_1^{\text{LO}}}{6} + \frac{\epsilon_1^{\text{LO}} \epsilon_2^{\text{LO}}}{18} - \frac{(\epsilon_1^{\text{LO}})^2}{72} \right], \quad (2.26)$$

$$\epsilon_1^{\text{NNLO}} = \epsilon_1^{\text{LO}} \left[ 1 - \frac{\epsilon_2^{\text{LO}}}{3} + \frac{5}{36} (\epsilon_2^{\text{LO}})^2 - \frac{\epsilon_1^{\text{LO}} \epsilon_2^{\text{LO}}}{9} + \frac{\epsilon_2^{\text{LO}} \epsilon_3^{\text{LO}}}{9} \right], \quad (2.27)$$

$$\begin{aligned} \epsilon_2^{\text{NNLO}} = \epsilon_2^{\text{LO}} \left[ 1 - \frac{\epsilon_2^{\text{LO}}}{6} - \frac{\epsilon_3^{\text{LO}}}{3} + \frac{(\epsilon_2^{\text{LO}})^2}{18} + \frac{(\epsilon_3^{\text{LO}})^2}{9} \right. \\ \left. - \frac{\epsilon_1^{\text{LO}} \epsilon_2^{\text{LO}}}{6} + \frac{5}{18} \epsilon_2^{\text{LO}} \epsilon_3^{\text{LO}} - \frac{\epsilon_1^{\text{LO}} \epsilon_3^{\text{LO}}}{9} + \frac{\epsilon_3^{\text{LO}} \epsilon_4^{\text{LO}}}{9} \right], \end{aligned} \quad (2.28)$$

$$\begin{aligned} \epsilon_3^{\text{NNLO}} = \epsilon_3^{\text{LO}} \left[ 1 - \frac{\epsilon_2^{\text{LO}}}{3} - \frac{\epsilon_4^{\text{LO}}}{3} + \frac{(\epsilon_2^{\text{LO}})^2}{6} + \frac{(\epsilon_4^{\text{LO}})^2}{9} - \frac{\epsilon_1^{\text{LO}} \epsilon_2^{\text{LO}}}{3} + \frac{5}{12} \epsilon_2^{\text{LO}} \epsilon_3^{\text{LO}} - \frac{\epsilon_1^{\text{LO}} \epsilon_4^{\text{LO}}}{9} \right. \\ \left. + \frac{5}{18} \epsilon_3^{\text{LO}} \epsilon_4^{\text{LO}} + \frac{\epsilon_3^{\text{LO}} \epsilon_4^{\text{LO}}}{9} + \frac{\epsilon_4^{\text{LO}} \epsilon_5^{\text{LO}}}{9} - \frac{\epsilon_1^{\text{LO}} (\epsilon_2^{\text{LO}})^2}{\epsilon_3^{\text{LO}}} \right], \end{aligned} \quad (2.29)$$

so on and so forth.

Let us move on to the slow-roll trajectory. At next-to-leading order, it proceeds from combining Eq. (2.19) and Eq. (2.22), which gives rise to

$$\Delta N^{\text{SR,NLO}} = -\frac{1}{M_{\text{Pl}}^2} \int_{\phi_{\text{in}}}^{\phi_{\text{end}}} \frac{V}{V'} d\phi + \frac{1}{3} \ln \left( \frac{V'_{\text{end}}/V_{\text{end}}}{V'_{\text{in}}/V_{\text{in}}} \right). \quad (2.30)$$

In the same manner, the next-to-next-to-leading order of the slow-roll trajectory can be obtained from combining Eq. (2.19) and Eq. (2.27), and one gets

$$\begin{aligned} \Delta N^{\text{SR,NNLO}} = & -\frac{1}{M_{\text{Pl}}^2} \int_{\phi_{\text{in}}}^{\phi_{\text{end}}} \frac{V}{V'} d\phi + \frac{1}{3} \ln \left( \frac{V'_{\text{end}}/V_{\text{end}}}{V'_{\text{in}}/V_{\text{in}}} \right) \\ & + \frac{M_{\text{Pl}}^2}{18} \int_{\phi_{\text{in}}}^{\phi_{\text{end}}} \left[ 5 \left( \frac{V'}{V} \right)^3 + 2 \frac{(V'')^2}{VV'} - 9 \frac{V'V''}{V^2} + 2 \frac{V'''}{V} \right] d\phi. \end{aligned} \quad (2.31)$$

The slow-roll solutions at leading order (2.12), next-to-leading order (2.30), and next-to-next-to-leading order (2.31) are displayed in Fig. 2.2 for the potential  $V(\phi) = m^2 \phi^2/2$ . In the left panel, they are superimposed to a numerical solution of Eq. (2.6). As already seen in Fig. 2.1, the inflaton rolls down the potential and eventually rapidly oscillates around its minimum, and the slow-roll solutions provide good approximations to the exact trajectory as long as the slow-roll condition is fulfilled. However, it is difficult to distinguish by eye between the different slow-roll orders in this figure. This is why in the right panel, this difference between the slow-roll approximations and the actual trajectory is displayed, in terms of the number of  $e$ -folds realized at  $\phi$ , as a function of  $\phi$  (since  $\phi$  decreases during inflation in this model, this plot should be read from the right to the left). Each slow-roll solution is actually compared with the numerical exact solution of Eq. (2.6) that shares the same initial condition  $d\phi/dN|_{\text{in}}$ , so that the difference with the exact solution exactly vanishes at  $\phi = \phi_{\text{in}}$  in all three cases. One can check that at each order, the distance to the exact solution is smaller. Therefore, the slow-roll strategy does provide a perturbative procedure that converges towards a solution (in fact, the attractor solution) of the dynamical system formed by Eqs. (2.6) and (2.7).

## 2.3. Inflationary Perturbations

What makes inflation appealing is that on top of solving the hot big bang problems, this new phase in the cosmological scenario, combined with quantum mechanics, naturally explains the origin of the CMB anisotropies and of the large-scale structures. In the inflationary paradigm indeed, these deviations from homogeneity and isotropy originate from the unavoidable zero-point quantum fluctuations of the coupled inflaton and gravitational fields. Statistically, the fluctuations are characterized by their two-point correlation function or power spectrum. The observations [229, 230, 120, 231, 232, 15, 163, 164] indicate that it is close to the Harrison-Zel'dovich, scale invariant, power spectrum with equal power on all scales. That this power spectrum represents a good fit to the astrophysical data was in fact realized before the advent of inflation, but no convincing fundamental theory was known to explain this result.

One of the main successes of inflation is that it precisely predicts an almost scale invariant power spectrum, the small deviations from scale invariance being connected to the micro-physics of inflation [122, 123, 124, 125, 126, 127]. The fact that different types of inflationary scenarios lead to a power spectrum which is, at leading order, always close to scale invariance is connected with the fact that the inflationary background is always close to the de Sitter solution (see above) or, equivalently, with the fact that the inflaton potential is always almost flat. The deviations from scale invariance are related to the deviations from a flat potential and, therefore, depend on the detailed shape of the potential. As a consequence, measuring the statistical moments of the cosmological perturbations with accuracy allows us to say something about  $V(\phi)$  and there is currently an important effort in this direction, using the high accuracy CMB data that have been released in the past years [233, 234, 235, 236, 237, 205, 206].

Thus in this section, we turn to the description of inflationary perturbations and we see how the results reviewed above can be derived. We show how and why cosmological perturbations need to be quantized, we derive their power spectrum and we verify that it is indeed almost scale invariant. This allows us to highlight some fundamental aspects about the nature of cosmological perturbations and the way they must be dealt with.

### 2.3.1. Basic Formalism

Clearly, in order to model the cosmological fluctuations, one needs to go beyond homogeneity and isotropy. The most general metric describing small fluctuations on top of a FLRW universe can be written as [129, 8]

$$ds^2 = a^2(\eta) \left[ -(1 + 2\alpha) d\eta^2 + 2B_i dx^i d\eta + (\gamma_{ij} + h_{ij}) dx^i dx^j \right]. \quad (2.32)$$

Notice that here, the metric is written in terms of conformal time  $\eta$  introduced in Eq. (1.62), and that  $\gamma_{ij}$  stands for the spatial part of the unperturbed FLRW metric that can be directly read off from Eq. (1.1). In Eq. (2.32), the three functions  $\alpha$ ,  $B_i$  and  $h_{ij}$  are functions of time and space since we consider an inhomogeneous and anisotropic situation.

#### 2.3.1.1. SVT Decomposition

In order to track the dynamics of these cosmological perturbations, it can be useful to decompose them into scalar, vector and tensor components [238] (thereof realizing a ‘‘SVT decomposition’’).

Indeed, any vector field can be decomposed into the divergence of a scalar and a vector with vanishing divergence, that is<sup>3</sup>

$$B_i = \partial_i B + \bar{B}_i, \quad \text{with} \quad \partial^i \bar{B}_i = 0. \quad (2.33)$$

In the same manner, any tensor field can be decomposed into

$$h_{ij} = -2\psi\gamma_{ij} + 2\partial_i\partial_j E + 2\partial_{(i}\bar{E}_{j)} + 2\bar{E}_{ij}, \quad \text{with} \quad \partial_i\bar{E}^{ij} = 0 \quad \text{and} \quad \bar{E}_i^i = 0. \quad (2.34)$$

It can be shown that vector modes are rapidly suppressed during inflation [129, 8]. This is why they are often disregarded. Tensor perturbations (*i.e.* gravity waves) and scalar perturbations are instead usually focused on. If one first studies scalar perturbations at linear order, one then has to consider

$$ds^2|_{\text{scal}} = a^2(\eta) \left\{ -(1 + 2\alpha) d\eta^2 + 2(\partial_i B) dx^i d\eta + [(1 - 2\psi)\delta_{ij} + 2\partial_i\partial_j E] dx^i dx^j \right\}, \quad (2.35)$$

where we take the case of a flat FLRW background for which  $\gamma_{ij} = \delta_{ij}$ , for the reasons mentioned at the end of section 1.3.1 (namely the fact that the observed spatial curvature is negligible).

### 2.3.1.2. Gauge Invariant Variables

As is well known, the above approach is redundant because of gauge freedom [129, 239, 240] under space-time diffeomorphisms. A careful study of this question shows that, in the absence of anisotropic stress, the gravitational sector can in fact be described by a single, gauge-invariant, quantity, the Bardeen potential  $\Phi_B$  defined by [239]

$$\Phi_B(\eta, \mathbf{x}) = -\alpha + \frac{1}{a} [a(B - E')]', \quad (2.36)$$

where a prime denotes a derivative with respect to the conformal time  $\eta$ . In the same manner, the matter sector can be modelled by the gauge-invariant fluctuation of the scalar field

$$\delta\phi^{(\text{gi})}(\eta, \mathbf{x}) = \delta\phi + \phi'(B - E'). \quad (2.37)$$

The two quantities  $\Phi_B$  and  $\delta\phi^{(\text{gi})}$  are related by a perturbed Einstein constraint. This implies that the scalar sector can in fact be described by a single quantity. For this reason, it is useful to introduce the so-called Mukhanov-Sasaki variable [122, 241, 242] which is a combination of the Bardeen potential and of the gauge-invariant field,

$$v(\eta, \mathbf{x}) = a \left[ \delta\phi^{(\text{gi})} + \phi' \frac{\Phi_B}{\mathcal{H}} \right], \quad (2.38)$$

where  $\mathcal{H} \equiv a'/a$ . All the other physical scalar quantities can be expressed in terms of  $v(\eta, \mathbf{x})$  which, therefore, fully characterizes the scalar sector.

### 2.3.1.3. Equation of Motion for the Perturbations

The next step consists in deriving an equation of motion for  $v(\eta, \mathbf{x})$ . Let us first establish the action for the quantity  $v(\eta, \mathbf{x})$ . Expanding the action of the system [*i.e.* Einstein-Hilbert

<sup>3</sup>For the quantities introduced here, the indexes must be lowered or raised with the unperturbed metric  $\gamma_{ij}$ . For example,  $\bar{B}^i = \gamma^{ij}\bar{B}_j$ .

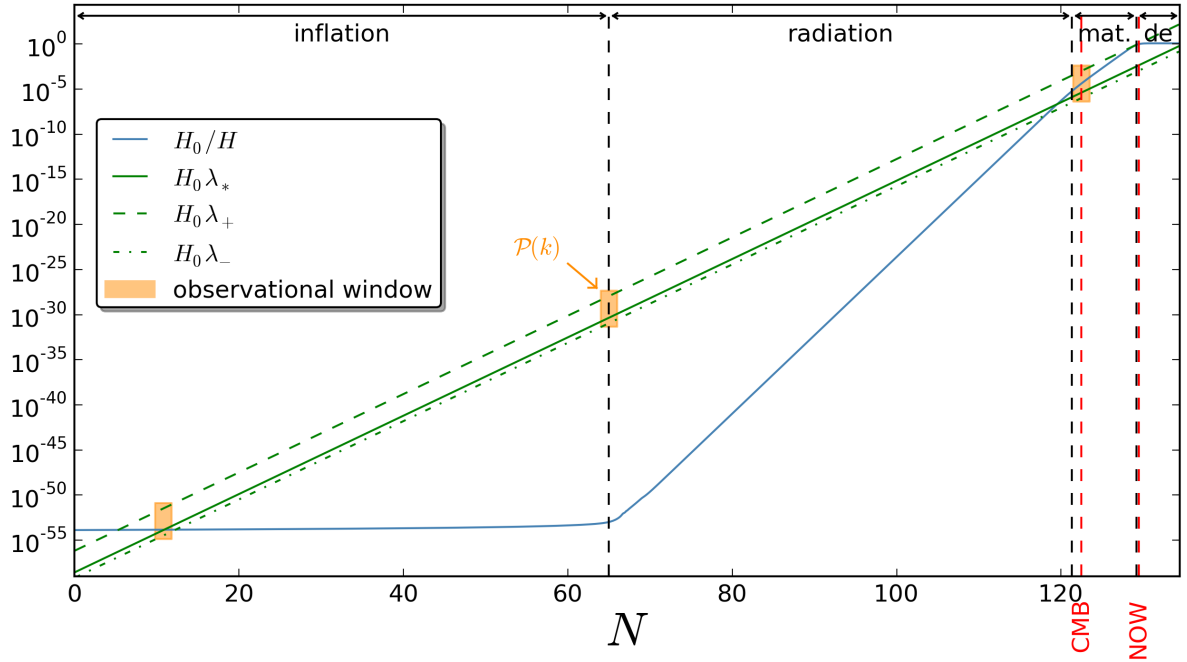


Figure 2.3.: Length scales evolution in the cosmological standard model including a phase of inflation. The blue curve stands for the Hubble radius normalized to its current value,  $H_0/H$ . The inflationary phase is implemented with a large field potential  $V(\phi) = m^2\phi^2/2$ , where  $m$  is normalized to the amplitude of the CMB power spectrum  $m \simeq 7 \times 10^{-6} M_{\text{Pl}}$  (see below), while radiation, cold matter and dark energy components follow the values of table 1.2. As expected, the Hubble radius is roughly constant during inflation and increases afterwards. The green lines stand for the physical length scales probed in the CMB, normalized to the current Hubble radius. They get stretched according to  $\lambda = a/k$ , as the expansion of the Universe proceeds. The pivot scale  $\lambda_*$  corresponds to  $k_* = 0.05 \text{ Mpc}^{-1}$ , and  $[\lambda_-, \lambda_+]$  defines the scales directly observed in the CMB, with  $k_+ \simeq 0.0002 \text{ Mpc}^{-1}$  and  $k_- \simeq 0.2 \text{ Mpc}^{-1}$ . These scales frame the observational window displayed in orange. They cross the Hubble radius during inflation, and at more recent time.

action (1.10) plus the action of the inflaton scalar field (2.1)] up to second order in the perturbations, one obtains [129]

$${}^{(2)}\delta S = \frac{1}{2} \int d^4x \left[ (v')^2 - \delta^{ij} \partial_i v \partial_j v + \frac{(a\sqrt{\epsilon_1})''}{a\sqrt{\epsilon_1}} v^2 \right], \quad (2.39)$$

where  $\epsilon_1$  is defined in Eq. (2.10). The next move consists in Fourier transforming the quantity  $v(\eta, \mathbf{x})$ . We follow such a strategy because we work with a linear theory and, as a consequence, all the modes evolve independently. We have

$$v(\eta, \mathbf{x}) = \frac{1}{(2\pi)^{3/2}} \int_{\mathbb{R}^3} d^3\mathbf{k} v_{\mathbf{k}}(\eta) e^{i\mathbf{k}\cdot\mathbf{x}}, \quad (2.40)$$

with  $v_{-\mathbf{k}} = v_{\mathbf{k}}^*$  because  $v(\eta, \mathbf{x})$  is real. Then, inserting this expansion into Eq. (2.39), one arrives at [129]

$${}^{(2)}\delta S = \int d\eta \int_{\mathbb{R}^+ \times \mathbb{R}^2} d^3\mathbf{k} \left\{ v'_{\mathbf{k}} v_{\mathbf{k}}^{*'} + v_{\mathbf{k}} v_{\mathbf{k}}^* \left[ \frac{(a\sqrt{\epsilon_1})''}{a\sqrt{\epsilon_1}} - k^2 \right] \right\}, \quad (2.41)$$

where one can see that the integral over  $\mathbf{k}$  is taken over  $\mathbb{R}^+ \times \mathbb{R}^2$ , *i.e.* half the Fourier space only, precisely because of the redundancy  $v_{-\mathbf{k}} = v_{\mathbf{k}}^*$ . For the same reason, the overall factor 1/2 has been cancelled. This allows us to define  $p_{\mathbf{k}}$ , the variable canonically conjugate to  $v_{\mathbf{k}}$ ,

$$p_{\mathbf{k}} = \frac{\delta \mathcal{L}}{\delta v_{\mathbf{k}}^*} = v'_{\mathbf{k}}, \quad (2.42)$$

where  $\mathcal{L}$  is the Lagrangian density in Fourier space that can be read off from Eq. (2.41),  ${}^{(2)}\delta S = \int d\eta \mathcal{L}$ . This gives rise to the Hamiltonian density  $\mathcal{H}$  (not to be confused with the Hubble parameter), defined by the Legendre transform  $\mathcal{H} = \int d^3\mathbf{k} v'_{\mathbf{k}} p_{\mathbf{k}} - \mathcal{L}$ , which reads

$$\mathcal{H} = \int_{\mathbb{R}^+ \times \mathbb{R}^2} d^3\mathbf{k} \left\{ p_{\mathbf{k}} p_{\mathbf{k}}^* + v_{\mathbf{k}} v_{\mathbf{k}}^* \left[ k^2 - \frac{(a\sqrt{\epsilon_1})''}{a\sqrt{\epsilon_1}} \right] \right\}. \quad (2.43)$$

This Hamiltonian density represents a collection of parametric oscillators, with one oscillator per mode  $\mathbf{k}$ , the time-dependent frequency of which can be expressed as

$$\omega^2(\eta, \mathbf{k}) = k^2 - \frac{(a\sqrt{\epsilon_1})''}{a\sqrt{\epsilon_1}}. \quad (2.44)$$

We see that the frequency depends on the scale factor and its derivatives (up to the fourth). This means that different inflationary backgrounds (*i.e.* different inflaton potentials) lead to different  $\omega(\eta, \mathbf{k})$  and, therefore, to different behaviours for  $v_{\mathbf{k}}(\eta)$ . Since Eq. (2.41) gives rise to  $\mathcal{L} = \int d^3\mathbf{k} (p_{\mathbf{k}} p_{\mathbf{k}}^* - \omega^2 v_{\mathbf{k}} v_{\mathbf{k}}^*)$ , the equation of motion for the Mukhanov-Sasaki variable can be derived from the variational relation  $\partial \mathcal{L} / \partial v_{\mathbf{k}}^* = \partial_{\eta}(\partial \mathcal{L} / \partial p_{\mathbf{k}}^*)$ . The same result can be obtained making use of Eq. (2.43),  $\mathcal{H} = \int d^3\mathbf{k} (p_{\mathbf{k}} p_{\mathbf{k}}^* + \omega^2 v_{\mathbf{k}} v_{\mathbf{k}}^*)$ , and of Hamilton's relation  $p'_{\mathbf{k}} = -\partial \mathcal{H} / \partial v_{\mathbf{k}}^*$ . In either case, one obtains

$$v''_{\mathbf{k}} + \omega^2(\eta, \mathbf{k}) v_{\mathbf{k}} = 0, \quad (2.45)$$

which confirms that each mode behaves as a parametric oscillator.

Let us comment on the structure of this equation. In the case where  $\epsilon_1$  is constant,  $\omega^2 = k^2 - a''/a$ , and since  $a \sim e^{Ht} \propto -1/(\eta H)$ , one roughly obtains  $\omega^2 \simeq k^2 - 2/\eta^2$ . Remember that during inflation,  $\eta$  increases in the range  $[-\infty, 0^-]$ , see Fig. 1.12. As a consequence, the system undergoes two different regimes. At early time, when  $\eta \ll -1/k$ , one has  $\omega^2 \simeq k^2$  which corresponds to an harmonic oscillator. In this case the Mukhanov-Sasaki variable oscillates with constant amplitude,  $v_{\mathbf{k}} \propto \cos(k\eta)$ , like in Minkowski space-time. On the contrary, at late time when  $\eta \gg -1/k$ , one has  $\omega^2 \simeq -2/\eta^2$  which corresponds to a forced harmonic oscillator, or parametric oscillator. The Mukhanov-Sasaki variable grows as  $v_{\mathbf{k}} \propto -1/\eta + \eta^2 \simeq -1/\eta$ , where the growing mode dominates over the decaying mode in the limit  $\eta \rightarrow 0^-$ . In this regime, curvature of space-time sources the parametric amplification of the cosmological perturbations.

The situation can be better understood looking at Fig. 2.3. In this figure, we have plotted the Hubble radius of a universe made of radiation, cold matter and a cosmological constant according to the values of table 1.2, and which also contains an inflaton field with potential  $V(\phi) = m^2 \phi^2/2$  (in this discussion, the precise shape of  $V$  has no importance). One can check that the Hubble radius is roughly constant during inflation, and increases afterwards during the radiation era and the matter era. On the other hand, the physical length scales  $\lambda$  associated with cosmological perturbations get stretched according to  $\lambda = a/k$  (where  $k$  is the comoving wavenumber), and always increase as the expansion of the Universe proceeds. As a consequence, at the beginning of inflation, scales of astrophysical interest today are “sub-Hubble”, which means that they are smaller than the Hubble radius. Since space-time is locally flat, of the Minkowski type, length

scales far inside the Hubble scale follow harmonic oscillator equations. At some point during inflation, they cross the Hubble radius and become “super-Hubble”. From this point on they are impacted by the curvature of space-time, and they undergo parametric amplification. Note that they cross the Hubble radius a second time, at some point between the CMB emission and now, so that they are currently sub-Hubble again.

To go beyond this schematic description, one has of course to work within a specified inflationary model. Once a potential  $V(\phi)$  is chosen, the background equations (2.6) and (2.7) can be solved and the corresponding scale factor  $a(\eta)$  is inferred. This, in turn, allows us to determine  $\omega^2(\eta, \mathbf{k})$  and, then, one can solve the equation of motion (2.45) for the Fourier component of the Mukhanov-Sasaki variable  $v_{\mathbf{k}}$ . However, in order to fully specify the solution for  $v_{\mathbf{k}}$ , one also needs to set initial conditions. Classically, there does not seem to exist a natural criterion to choose them. However, as we shall now see, when quantization is performed, if one assumes that the perturbations are sourced by the zero-point fluctuations of the theory, it leads to well-defined initial conditions. We now turn to these questions.

### 2.3.2. Quantization in the Schrödinger Picture

In this section, we review how the cosmological perturbations must be quantized. Very often in the literature, the quantization is done in the Heisenberg picture. Here, we carry out the quantization in the Schrödinger picture [135, 138] to show that one obtains the same results doing so. In order to properly quantize the system, it is more convenient to work with real variables. Therefore, we introduce the following decompositions

$$v_{\mathbf{k}} \equiv \frac{1}{\sqrt{2}} (v_{\mathbf{k}}^{\text{R}} + i v_{\mathbf{k}}^{\text{I}}), \quad p_{\mathbf{k}} \equiv \frac{1}{\sqrt{2}} (p_{\mathbf{k}}^{\text{R}} + i p_{\mathbf{k}}^{\text{I}}), \quad (2.46)$$

where  $v_{\mathbf{k}}^{\text{R}}, v_{\mathbf{k}}^{\text{I}}, p_{\mathbf{k}}^{\text{R}}$  and  $p_{\mathbf{k}}^{\text{I}}$  are real quantities. In the Schrödinger approach, the quantum state of the system is described by a wavefunctional,  $\Psi[v(\eta, \mathbf{x})]$ . Since we work in Fourier space, and since the theory is free (*i.e.* without mode mixing terms) in the sense that it does not contain terms with power higher than two in the Lagrangian, the wavefunctional can also be factorized into mode components as

$$\Psi[v(\eta, \mathbf{x})] = \prod_{\mathbf{k} \in \mathbb{R}^+ \times \mathbb{R}^2} \Psi_{\mathbf{k}}(v_{\mathbf{k}}^{\text{R}}, v_{\mathbf{k}}^{\text{I}}) = \prod_{\mathbf{k} \in \mathbb{R}^+ \times \mathbb{R}^2} \Psi_{\mathbf{k}}^{\text{R}}(v_{\mathbf{k}}^{\text{R}}) \Psi_{\mathbf{k}}^{\text{I}}(v_{\mathbf{k}}^{\text{I}}). \quad (2.47)$$

Quantization is achieved by promoting  $v_{\mathbf{k}}$  and  $p_{\mathbf{k}}$  to quantum operators,  $\hat{v}_{\mathbf{k}}$  and  $\hat{p}_{\mathbf{k}}$ , and by requiring the canonical commutation relations

$$[\hat{v}_{\mathbf{k}}^{\text{R}}, \hat{p}_{\mathbf{q}}^{\text{R}}] = i\delta(\mathbf{k} - \mathbf{q}), \quad [\hat{v}_{\mathbf{k}}^{\text{I}}, \hat{p}_{\mathbf{q}}^{\text{I}}] = i\delta(\mathbf{k} - \mathbf{q}), \quad (2.48)$$

with  $[\hat{v}_{\mathbf{k}}^{\text{R}}, \hat{p}_{\mathbf{q}}^{\text{I}}] = [\hat{v}_{\mathbf{k}}^{\text{I}}, \hat{p}_{\mathbf{q}}^{\text{R}}] = 0$ . These relations admit the following representation

$$\hat{v}_{\mathbf{k}}^{\text{R,I}} \Psi = v_{\mathbf{k}}^{\text{R,I}} \Psi, \quad (2.49)$$

$$\hat{p}_{\mathbf{k}}^{\text{R,I}} \Psi = -i \frac{\partial \Psi}{\partial v_{\mathbf{k}}^{\text{R,I}}}. \quad (2.50)$$

The wavefunctional  $\Psi[v(\eta, \mathbf{x})]$  obeys the Schrödinger equation which, in this context, is a functional differential equation. However, since each mode evolves independently, this functional

differential equation can be reduced to an infinite number of differential equations for each  $\Psi_{\mathbf{k}}^{\text{R,I}}$ . Concretely, we have

$$i \frac{\Psi_{\mathbf{k}}^{\text{R,I}}}{\partial \eta} = \hat{\mathcal{H}}_{\mathbf{k}}^{\text{R,I}} \Psi_{\mathbf{k}}^{\text{R,I}}, \quad (2.51)$$

where the Hamiltonian densities  $\hat{\mathcal{H}}_{\mathbf{k}}^{\text{R,I}}$  are related to the direct space Hamiltonian density  $\hat{\mathcal{H}}$  by the Fourier expansion  $\hat{\mathcal{H}} = \int_{\mathbb{R}^3} d^3 \mathbf{k} \left( \hat{\mathcal{H}}_{\mathbf{k}}^{\text{R}} + \hat{\mathcal{H}}_{\mathbf{k}}^{\text{I}} \right)$ . Looking at Eq. (2.43), they can be expressed as

$$\hat{\mathcal{H}}_{\mathbf{k}}^{\text{R,I}} = -\frac{1}{2} \frac{\partial^2}{\partial (v_{\mathbf{k}}^{\text{R,I}})^2} + \frac{1}{2} \omega^2(\eta, \mathbf{k}) \left( \hat{v}_{\mathbf{k}}^{\text{R,I}} \right)^2, \quad (2.52)$$

where we have made use of the representations (2.49) and (2.50), and where the factor 1/2 accounts for the fact that the  $\hat{\mathcal{H}}_{\mathbf{k}}$  densities are defined through an integral over  $\mathbb{R}^3$  while Eq. (2.43) makes use of an integral over  $\mathbb{R}^+ \times \mathbb{R}^2$ .

We are now in a position where we can solve the Schrödinger equation. Let us consider the following Gaussian state

$$\Psi_{\mathbf{k}}^{\text{R,I}} \left( \eta, v_{\mathbf{k}}^{\text{R,I}} \right) = N_{\mathbf{k}}(\eta) e^{-\Omega_{\mathbf{k}}(\eta) (v_{\mathbf{k}}^{\text{R,I}})^2}. \quad (2.53)$$

The functions  $N_{\mathbf{k}}(\eta)$  and  $\Omega_{\mathbf{k}}(\eta)$  are time dependent and do not carry the superscripts ‘‘R’’ or ‘‘I’’ because as shown below, they are the same for the wavefunctions of the real and imaginary parts. Inserting the state  $\Psi_{\mathbf{k}}$  given by Eq. (2.53) into the Schrödinger equation (2.51), one can see that such a Gaussian state is a solution of the Schrödinger equation. This is why at linear order in perturbation theory, if the initial state is Gaussian, perturbations remain Gaussian. More precisely, this is the case provided  $N_{\mathbf{k}}$  and  $\Omega_{\mathbf{k}}$  obey the following differential equations

$$i \frac{N'_{\mathbf{k}}}{N_{\mathbf{k}}} = \Omega_{\mathbf{k}} \quad \text{and} \quad \Omega'_{\mathbf{k}} = -2i \Omega_{\mathbf{k}}^2 + \frac{i}{2} \omega^2(\eta, \mathbf{k}). \quad (2.54)$$

The solutions can be easily found and read

$$|N_{\mathbf{k}}| = \left( \frac{2 \Re \Omega_{\mathbf{k}}}{\pi} \right)^{1/4} \quad \text{and} \quad \Omega_{\mathbf{k}} = -\frac{i}{2} \frac{f'_{\mathbf{k}}}{f_{\mathbf{k}}}, \quad (2.55)$$

where  $f_{\mathbf{k}}$  is a function obeying the equation  $f''_{\mathbf{k}} + \omega^2 f_{\mathbf{k}} = 0$ , that is to say exactly Eq. (2.45). The first equation (2.55) guarantees that the wavefunction is properly normalized, *i.e.* that we have

$$\int_{-\infty}^{\infty} \Psi_{\mathbf{k}}^{\text{R,I}} \Psi_{\mathbf{k}}^{\text{R,I}*} dv_{\mathbf{k}}^{\text{R,I}} = 1. \quad (2.56)$$

Let us now discuss the initial conditions. A rather natural assumption to make is that the perturbations are initially in their ground state, so that they are only sourced by the zero-point quantum fluctuations. According to the discussion following Fig. 2.3, at the beginning of inflation, all the modes of astrophysical interest today have a physical wavelength which is smaller than the Hubble radius, *i.e.*  $k/(aH) \rightarrow \infty$ . In this regime, one has  $\omega^2(\eta, \mathbf{k}) \rightarrow k^2$  and each mode behaves as an harmonic oscillator (as opposed to a parametric oscillator in the generic case) with frequency  $\omega = k$ . As a consequence, the differential equation for  $f_{\mathbf{k}}(\eta)$  can easily be solved and the solution reads  $f_{\mathbf{k}} = A_{\mathbf{k}} e^{ik\eta} + B_{\mathbf{k}} e^{-ik\eta}$ ,  $A_{\mathbf{k}}$  and  $B_{\mathbf{k}}$  being integration constants. Upon using the second equation (2.55), one then has

$$\Omega_{\mathbf{k}} \rightarrow \frac{k}{2} \frac{A_{\mathbf{k}} e^{ik\eta} - B_{\mathbf{k}} e^{-ik\eta}}{A_{\mathbf{k}} e^{ik\eta} + B_{\mathbf{k}} e^{-ik\eta}} \quad (2.57)$$

in this limit. On the other hand, let us calculate the ground state wavefunction of the harmonic oscillator under consideration. The number of particle operator  $\hat{n}_{\mathbf{k}} = \hat{a}_{\mathbf{k}}^\dagger \hat{a}_{\mathbf{k}}$  for the harmonic oscillator with  $\omega \sim k$  can be expressed in terms of the creation and annihilation operators  $\hat{a}_{\mathbf{k}}^\dagger$  and  $\hat{a}_{\mathbf{k}}$ , defined by [243]

$$\hat{a}_{\mathbf{k}} = \sqrt{\frac{k}{2}} \left( \hat{v}_{\mathbf{k}} + \frac{i}{k} \hat{p}_{\mathbf{k}} \right), \quad (2.58)$$

$$\hat{a}_{\mathbf{k}}^\dagger = \sqrt{\frac{k}{2}} \left( \hat{v}_{\mathbf{k}} - \frac{i}{k} \hat{p}_{\mathbf{k}} \right), \quad (2.59)$$

so that one has  $\hat{n}_{\mathbf{k}} = k/2(\hat{v}_{\mathbf{k}}^2 + \hat{p}_{\mathbf{k}}^2/k^2 + i/k[v_{\mathbf{k}}, p_{\mathbf{k}}]) = k/2(\hat{v}_{\mathbf{k}}^2 + \hat{p}_{\mathbf{k}}^2/k^2 - 1/k)$ , where one has made use of the canonical commutation relations (2.48). Here the superscripts ‘‘R’’ and ‘‘I’’ have been removed for simplicity. Making use of the representations (2.49) and (2.50), this allows us to calculate the mean number of particles present in the state (2.53), and one obtains

$$\langle \Psi_{\mathbf{k}} | \hat{n}_{\mathbf{k}} | \Psi_{\mathbf{k}} \rangle = \frac{k}{2} \left[ \langle \Psi_{\mathbf{k}} | \hat{v}_{\mathbf{k}}^2 | \Psi_{\mathbf{k}} \rangle \left( 1 - 4 \frac{\Omega_{\mathbf{k}}^2}{k^2} \right) + 2 \frac{\Omega_{\mathbf{k}}}{k^2} - \frac{1}{k} \right], \quad (2.60)$$

where the quantum mean value of  $v_{\mathbf{k}}^2$  is just given by the Gaussian integral

$$\begin{aligned} \langle \Psi_{\mathbf{k}} | \hat{v}_{\mathbf{k}}^2 | \Psi_{\mathbf{k}} \rangle &= \int_{-\infty}^{\infty} dv_{\mathbf{k}} \Psi_{\mathbf{k}}(\eta, v_{\mathbf{k}}) \Psi_{\mathbf{k}}^*(\eta, v_{\mathbf{k}}) v_{\mathbf{k}}^2 \\ &= \sqrt{\frac{2\Re(\Omega_{\mathbf{k}})}{\pi}} \int_{-\infty}^{\infty} dv_{\mathbf{k}} e^{-2\Re(\Omega_{\mathbf{k}})v_{\mathbf{k}}^2} v_{\mathbf{k}}^2 \\ &= \frac{1}{4\Re(\Omega_{\mathbf{k}})}. \end{aligned} \quad (2.61)$$

Combining the two previous equations together yields an expression for the mean number of particles in the Gaussian state  $\Psi_{\mathbf{k}}$ , only in terms of  $\Omega_{\mathbf{k}}$ . Requiring that this number vanishes, so that  $\Psi_{\mathbf{k}}$  coincides with the ground state of the Minkowski harmonic oscillator at early time, gives rise to  $\Im\Omega_{\mathbf{k}} = 0$  and  $\Re\Omega_{\mathbf{k}} = k/2$ . Looking back at Eq. (2.57), this means that one must set the initial conditions such that  $B_{\mathbf{k}} = 0$ .

Moreover, it is easy to check that the Wronskian  $W \equiv f_{\mathbf{k}}' f_{\mathbf{k}}^* - f_{\mathbf{k}}'^* f_{\mathbf{k}}$  is a conserved quantity,  $dW/d\eta = 0$ , thanks to the equation of motion (2.45) of  $f_{\mathbf{k}}$ . At early time, since  $f_{\mathbf{k}} = A_{\mathbf{k}} e^{ik\eta} + B_{\mathbf{k}} e^{-ik\eta}$ , one has  $W = 2ik(|A_{\mathbf{k}}|^2 - |B_{\mathbf{k}}|^2)$ . In the Heisenberg picture, the canonical commutation relations require that  $W = i$ . Even if in the Schrödinger picture presently used, the specific value of  $W$  is irrelevant since it cancels out in all calculable physical quantities, this value is conventionally adopted, which amounts to setting  $A_{\mathbf{k}} = 1/\sqrt{2k}$  on top of  $B_{\mathbf{k}} = 0$ . However, we insist that a different value of  $A_{\mathbf{k}}$  can be worked with without modifying the results obtained below, as long as  $B_{\mathbf{k}} = 0$ . The equation for  $f_{\mathbf{k}}$  (2.45) will thus be solved with the initial condition

$$\lim_{k/(aH) \rightarrow +\infty} f_{\mathbf{k}} = \frac{1}{\sqrt{2k}} e^{ik\eta}. \quad (2.62)$$

Such an initial state is often referred to as the Bunch-Davies vacuum [244, 245]. Obviously, if excited states of the harmonic oscillator are chosen as initial conditions instead, one obtains different results [246, 247, 248, 249, 250, 251, 252, 253, 254, 255, 256, 257, 258, 259, 260, 261, 262, 263, 264, 265, 266] and the inflationary predictions are dependent on what one assumes for the initial state of the perturbations.

Once an initial value for  $f_{\mathbf{k}}$  is chosen, the quantum state for the perturbations is completely specified. Indeed, the wavefunction  $\Psi$  is given by Eq. (2.53) and depends on a single parameter

$\Omega_{\mathbf{k}}$ , for which we know what is the initial state and the equation of motion. We therefore completely know the wavefunction, from which we can further study the quantum state of the perturbations. For example, in section 4.3, we show that on super-Hubble scales, the quantum state is a squeezed one, and we discuss how this squeezing can account for a quantum-to-classical transition of the perturbations. Another relevant quantity to compute is of course the two-point correlation function in the quantum state  $\Psi$ , *i.e.* the power spectrum.

### 2.3.3. The Power Spectrum

Let us now turn to the calculation of the power spectrum. We first introduce the two-point correlation function, defined by  $\langle \Psi | \hat{v}(\eta, \mathbf{x}) \hat{v}(\eta, \mathbf{x} + \mathbf{r}) | \Psi \rangle$ . Making use of the Fourier transform of the Mukhanov-Sasaki variable, Eq. (2.40), and of the mode decomposition of the wavefunction, Eq. (2.47), one has

$$\langle \Psi | \hat{v}(\eta, \mathbf{x}) \hat{v}(\eta, \mathbf{x} + \mathbf{r}) | \Psi \rangle = \frac{1}{(2\pi)^3} \int_{\mathbb{R}^3} d\mathbf{p} e^{i\mathbf{p}\cdot\mathbf{x}} \int_{\mathbb{R}^3} d\mathbf{q} e^{i\mathbf{q}\cdot(\mathbf{x}+\mathbf{r})} \langle \Psi | \hat{v}_{\mathbf{p}} \hat{v}_{\mathbf{q}} | \Psi \rangle \quad (2.63)$$

$$= \frac{1}{(2\pi)^3} \int_{\mathbb{R}^3} d\mathbf{p} e^{i\mathbf{p}\cdot\mathbf{x}} \int_{\mathbb{R}^3} d\mathbf{q} e^{i\mathbf{q}\cdot(\mathbf{x}+\mathbf{r})} \prod_{\mathbf{k} \in \mathbb{R}^+ \times \mathbb{R}^2} \prod_{\mathbf{k}' \in \mathbb{R}^+ \times \mathbb{R}^2} \langle \Psi_{\mathbf{k}} | \hat{v}_{\mathbf{p}} \hat{v}_{\mathbf{q}} | \Psi_{\mathbf{k}'} \rangle. \quad (2.64)$$

In the above expression, one can see that  $\mathbf{k}$  and  $\mathbf{k}'$  take value in  $\mathbb{R}^+ \times \mathbb{R}^2$  while  $\mathbf{p}$  and  $\mathbf{q}$  take value in  $\mathbb{R}^3$ . In order to have the same integration domain for all variables, it is useful to notice that the  $\mathbf{p}$ -integration (or, in the same manner, the  $\mathbf{q}$ -integration) can be expressed as

$$\int_{\mathbb{R}^3} d\mathbf{p} e^{i\mathbf{p}\cdot\mathbf{x}} \hat{v}_{\mathbf{p}} = \int_{\mathbb{R}^+ \times \mathbb{R}^2} d\mathbf{p} e^{i\mathbf{p}\cdot\mathbf{x}} \hat{v}_{\mathbf{p}} + \int_{\mathbb{R}^- \times \mathbb{R}^2} d\mathbf{p} e^{i\mathbf{p}\cdot\mathbf{x}} \hat{v}_{\mathbf{p}} \quad (2.65)$$

$$= \int_{\mathbb{R}^+ \times \mathbb{R}^2} d\mathbf{p} e^{i\mathbf{p}\cdot\mathbf{x}} \hat{v}_{\mathbf{p}} + \int_{\mathbb{R}^+ \times \mathbb{R}^2} d\mathbf{p} e^{-i\mathbf{p}\cdot\mathbf{x}} \hat{v}_{-\mathbf{p}} \quad (2.66)$$

$$= \int_{\mathbb{R}^+ \times \mathbb{R}^2} d\mathbf{p} e^{i\mathbf{p}\cdot\mathbf{x}} \hat{v}_{\mathbf{p}} + \int_{\mathbb{R}^+ \times \mathbb{R}^2} d\mathbf{p} e^{-i\mathbf{p}\cdot\mathbf{x}} \hat{v}_{\mathbf{p}}^* \quad (2.67)$$

$$= \int_{\mathbb{R}^+ \times \mathbb{R}^2} d\mathbf{p} (e^{i\mathbf{p}\cdot\mathbf{x}} \hat{v}_{\mathbf{p}} + e^{-i\mathbf{p}\cdot\mathbf{x}} \hat{v}_{\mathbf{p}}^*), \quad (2.68)$$

where between the second and the third line we have used the relation  $\hat{v}_{-\mathbf{p}} = \hat{v}_{\mathbf{p}}^*$  mentioned above which comes from the fact that  $\hat{v}$  is a real operator in physical space. Plugging the obtained expression in Eq. (2.64), one obtains

$$\begin{aligned} \langle \Psi | \hat{v}(\eta, \mathbf{x}) \hat{v}(\eta, \mathbf{x} + \mathbf{r}) | \Psi \rangle &= \frac{1}{(2\pi)^3} \int_{\mathbb{R}^+ \times \mathbb{R}^2} d\mathbf{p} \int_{\mathbb{R}^+ \times \mathbb{R}^2} d\mathbf{q} \prod_{\mathbf{k} \in \mathbb{R}^+ \times \mathbb{R}^2} \prod_{\mathbf{k}' \in \mathbb{R}^+ \times \mathbb{R}^2} \\ &\quad \left\langle \Psi_{\mathbf{k}} \left| \left[ e^{i\mathbf{p}\cdot\mathbf{x}} \hat{v}_{\mathbf{p}} + e^{-i\mathbf{p}\cdot\mathbf{x}} \hat{v}_{\mathbf{p}}^* \right] \left[ e^{i\mathbf{q}\cdot(\mathbf{x}+\mathbf{r})} \hat{v}_{\mathbf{q}} + e^{-i\mathbf{q}\cdot(\mathbf{x}+\mathbf{r})} \hat{v}_{\mathbf{q}}^* \right] \right| \Psi_{\mathbf{k}'} \right\rangle. \end{aligned} \quad (2.69)$$

Since the Hilbert spaces associated with each mode are independent at linear order in perturbation theory, and since the  $|\Psi_{\mathbf{k}}\rangle$  wavefunctions are normalized,  $\langle \Psi_{\mathbf{k}} | \Psi_{\mathbf{k}'} \rangle = \delta(\mathbf{k} - \mathbf{k}')$ , in the above expression the product terms can be written as

$$\left\langle \Psi_{\mathbf{k}} \left| \hat{v}_{\mathbf{p}}^{(*)} \hat{v}_{\mathbf{q}}^{(*)} \right| \Psi_{\mathbf{k}'} \right\rangle = \delta(\mathbf{p} - \mathbf{q}) \delta(\mathbf{p} - \mathbf{k}) \delta(\mathbf{q} - \mathbf{k}') \left\langle \Psi_{\mathbf{k}} \left| \hat{v}_{\mathbf{p}}^{(*)} \hat{v}_{\mathbf{q}}^{(*)} \right| \Psi_{\mathbf{k}'} \right\rangle, \quad (2.70)$$

where the superscripts “(\*)” mean that stars may or may not be present. The delta functions allow to calculate all integrals and products (since they are performed on the same domains) but one, and one obtains

$$\begin{aligned} \langle \Psi | \hat{v}(\eta, \mathbf{x}) \hat{v}(\eta, \mathbf{x} + \mathbf{r}) | \Psi \rangle &= \frac{1}{(2\pi)^3} \int_{\mathbb{R}^+ \times \mathbb{R}^2} d\mathbf{p} \\ &\quad \left\langle \Psi_{\mathbf{p}} \left| [e^{i\mathbf{p}\cdot\mathbf{x}} \hat{v}_{\mathbf{p}} + e^{-i\mathbf{p}\cdot\mathbf{x}} \hat{v}_{\mathbf{p}}^*] [e^{i\mathbf{p}\cdot(\mathbf{x}+\mathbf{r})} \hat{v}_{\mathbf{p}} + e^{-i\mathbf{p}\cdot(\mathbf{x}+\mathbf{r})} \hat{v}_{\mathbf{p}}^*] \right| \Psi_{\mathbf{p}} \right\rangle. \end{aligned} \quad (2.71)$$

Let us now decompose the product terms into real parts and imaginary parts. Making use of Eq. (2.46), and since  $\hat{v}_{\mathbf{p}}^{\text{R}}$  and  $\hat{v}_{\mathbf{p}}^{\text{I}}$  act on independent Hilbert spaces again,  $|\Psi_{\mathbf{k}}\rangle = |\Psi_{\mathbf{k}}^{\text{R}}\rangle |\Psi_{\mathbf{k}}^{\text{I}}\rangle$ , one has for example

$$\langle \Psi_{\mathbf{p}} | \hat{v}_{\mathbf{p}}^2 | \Psi_{\mathbf{p}} \rangle = \frac{1}{2} \langle \Psi_{\mathbf{p}} | (\hat{v}_{\mathbf{p}}^{\text{R}} + i\hat{v}_{\mathbf{p}}^{\text{I}})^2 | \Psi_{\mathbf{p}} \rangle \quad (2.72)$$

$$= \frac{1}{2} \langle \Psi_{\mathbf{p}}^{\text{R}} | (\hat{v}_{\mathbf{p}}^{\text{R}})^2 | \Psi_{\mathbf{p}}^{\text{R}} \rangle - \frac{1}{2} \langle \Psi_{\mathbf{p}}^{\text{I}} | (\hat{v}_{\mathbf{p}}^{\text{I}})^2 | \Psi_{\mathbf{p}}^{\text{I}} \rangle, \quad (2.73)$$

and in the same manner

$$\langle \Psi_{\mathbf{p}} | \hat{v}_{\mathbf{p}} \hat{v}_{\mathbf{p}}^* | \Psi_{\mathbf{p}} \rangle = \langle \Psi_{\mathbf{p}} | \hat{v}_{\mathbf{p}}^* \hat{v}_{\mathbf{p}} | \Psi_{\mathbf{p}} \rangle = \frac{1}{2} \langle \Psi_{\mathbf{p}}^{\text{R}} | (\hat{v}_{\mathbf{p}}^{\text{R}})^2 | \Psi_{\mathbf{p}}^{\text{R}} \rangle + \frac{1}{2} \langle \Psi_{\mathbf{p}}^{\text{I}} | (\hat{v}_{\mathbf{p}}^{\text{I}})^2 | \Psi_{\mathbf{p}}^{\text{I}} \rangle, \quad (2.74)$$

$$\langle \Psi_{\mathbf{p}} | (\hat{v}_{\mathbf{p}}^*)^2 | \Psi_{\mathbf{p}} \rangle = \frac{1}{2} \langle \Psi_{\mathbf{p}}^{\text{R}} | (\hat{v}_{\mathbf{p}}^{\text{R}})^2 | \Psi_{\mathbf{p}}^{\text{R}} \rangle - \frac{1}{2} \langle \Psi_{\mathbf{p}}^{\text{I}} | (\hat{v}_{\mathbf{p}}^{\text{I}})^2 | \Psi_{\mathbf{p}}^{\text{I}} \rangle. \quad (2.75)$$

Plugging these relations into Eq. (2.71), one obtains

$$\begin{aligned} \langle \Psi | \hat{v}(\eta, \mathbf{x}) \hat{v}(\eta, \mathbf{x} + \mathbf{r}) | \Psi \rangle &= \frac{1}{(2\pi)^3} \int_{\mathbb{R}^+ \times \mathbb{R}^2} d\mathbf{p} \left\{ [\cos(\mathbf{p}\cdot\mathbf{r}) + \cos(2\mathbf{p}\cdot\mathbf{x} + \mathbf{p}\cdot\mathbf{r})] \langle \Psi_{\mathbf{p}}^{\text{R}} | (\hat{v}_{\mathbf{p}}^{\text{R}})^2 | \Psi_{\mathbf{p}}^{\text{R}} \rangle \right. \\ &\quad \left. + [\cos(\mathbf{p}\cdot\mathbf{r}) - \cos(2\mathbf{p}\cdot\mathbf{x} + \mathbf{p}\cdot\mathbf{r})] \langle \Psi_{\mathbf{p}}^{\text{I}} | (\hat{v}_{\mathbf{p}}^{\text{I}})^2 | \Psi_{\mathbf{p}}^{\text{I}} \rangle \right\}. \end{aligned} \quad (2.76)$$

The mean values of  $(\hat{v}_{\mathbf{p}}^{\text{R}})^2$  and  $(\hat{v}_{\mathbf{p}}^{\text{I}})^2$  are the same, and given by Eq. (2.61). This is why the previous expression reduces to

$$\langle \Psi | \hat{v}(\eta, \mathbf{x}) \hat{v}(\eta, \mathbf{x} + \mathbf{r}) | \Psi \rangle = \frac{1}{2(2\pi)^3} \int_{\mathbb{R}^+ \times \mathbb{R}^2} d\mathbf{p} \frac{\cos(\mathbf{p}\cdot\mathbf{r})}{\Re(\Omega_{\mathbf{p}})}. \quad (2.77)$$

Now, let us see how the angular part of the  $\mathbf{p}$ -integral can be performed. When  $p$  denotes the module of  $\mathbf{p}$  and  $r$  denotes the module of  $\mathbf{r}$ , let  $\theta$  be the angle between  $\mathbf{r}$  and  $\mathbf{p}$ . With these notations, one has  $\mathbf{p}\cdot\mathbf{r} = pr \cos \theta$ , and from what precedes,<sup>4</sup>  $\Omega_{\mathbf{p}}$  only depends on  $p$  and we use the notation  $\Omega_p$ . The  $\mathbf{p}$ -integral can be decomposed into radial and angular parts,  $d\mathbf{p} = p^2 \sin \theta dp d\theta d\varphi$ . Because  $\mathbf{p}$  takes its values in  $\mathbb{R}^+ \times \mathbb{R}^2$ ,  $\varphi$  only varies in  $[0, \pi]$ , and one has

$$\langle \Psi | \hat{v}(\eta, \mathbf{x}) \hat{v}(\eta, \mathbf{x} + \mathbf{r}) | \Psi \rangle = \frac{1}{2(2\pi)^3} \int_0^\pi d\varphi \int_0^\pi d\theta \sin \theta \int_0^\infty dp p^2 \frac{\cos(pr \cos \theta)}{\Re(\Omega_p)} \quad (2.78)$$

$$= \frac{1}{16\pi^2} \int_0^\pi d\theta \sin \theta \int_0^\infty dp p^2 \frac{\cos(pr \cos \theta)}{\Re(\Omega_p)} \quad (2.79)$$

$$= \frac{1}{16\pi^2} \int_0^\infty dp p^2 \frac{1}{\Re(\Omega_p)} \left[ \frac{\sin(pr \cos \theta)}{-pr} \right]_{\theta=0}^{\theta=\pi} \quad (2.80)$$

$$= \frac{1}{8\pi^2} \int_0^\infty dp \frac{\sin(pr)}{p} \frac{p^3}{pr \Re(\Omega_p)}. \quad (2.81)$$

<sup>4</sup>Indeed,  $f_{\mathbf{p}}$  is initiated in the state (2.62) which only depends on the radial part  $p$  of  $\mathbf{p}$ , and follows an equation of motion (2.45) that only depends on  $p$  as well. Hence  $f_{\mathbf{p}} = f_p$ , and  $\Omega_{\mathbf{p}} = \Omega_p$ .

We are now in a position where an expression for the power spectrum can be given. The power spectrum  $\mathcal{P}_v(\mathbf{k})$  is defined as the square of the Fourier amplitude per logarithmic interval at a given scale  $\mathbf{k}$ , *i.e.* it is such that

$$\langle \Psi | \hat{v}(\eta, \mathbf{x}) \hat{v}(\eta, \mathbf{x} + \mathbf{r}) | \Psi \rangle \equiv \int_0^\infty \frac{dk \sin(kr)}{k \quad kr} \mathcal{P}_v(\mathbf{k}) . \quad (2.82)$$

By identifying Eqs. (2.81) and (2.82), it is straightforward to obtain

$$\mathcal{P}_v(\mathbf{k}) = \frac{k^3}{8\pi^2} \frac{1}{\Re(\Omega_{\mathbf{k}})} . \quad (2.83)$$

Finally, let us express  $\Re(\Omega_{\mathbf{k}})$  in terms of the function  $f_{\mathbf{k}}$ . From the second Eq. (2.55), one easily shows that

$$\Re(\Omega_{\mathbf{k}}) = -\frac{i}{4} \frac{W}{|f_{\mathbf{k}}|^2} . \quad (2.84)$$

One can check that only the ratio  $W/|f_{\mathbf{k}}|^2$  is involved, so that as announced above, the absolute normalization of  $f_{\mathbf{k}}$  does not play any role in the Schrödinger picture. Since the initial condition (2.62) is associated with the choice  $W = i$ , one eventually obtains

$$\mathcal{P}_v(k) = \frac{k^3}{2\pi^2} |f_{\mathbf{k}}|^2 . \quad (2.85)$$

A last remark is in order. Instead of calculating the power spectrum of the Mukhanov variable  $\mathcal{P}_v$ , it often proves more convenient to discuss the power spectrum of curvature perturbations  $\mathcal{P}_\zeta$ . The quantity  $\zeta$  is related to the Bardeen potential defined in Eq. (2.36) through the following expression [129, 267, 240]

$$\zeta = \frac{2}{3} \frac{\mathcal{H}^{-1} \Phi'_B + \Phi_B}{1 + w} + \Phi_B , \quad (2.86)$$

where  $w \equiv p/\rho$  is the equation of state parameter. The importance of  $\zeta$  lies in the fact that it is a conserved quantity on large scales [267, 240]. Therefore, its spectrum, calculated at the end of inflation, can directly be propagated to the recombination time as it is not sensitive to the details of the cosmological evolution, in particular to those of the complicated reheating era [268, 223, 214, 225, 219]. The curvature perturbation can also be expressed in terms of the Mukhanov-Sasaki variable as [267]

$$\zeta = \frac{1}{a\sqrt{2\epsilon_1}} \frac{v}{M_{\text{Pl}}} . \quad (2.87)$$

Making use of Eq. (2.85), one then has

$$\mathcal{P}_\zeta(k) = \frac{1}{2a^2 M_{\text{Pl}}^2 \epsilon_1} \mathcal{P}_v(k) = \frac{k^3}{4\pi^2 a^2 \epsilon_1 M_{\text{Pl}}^2} |f_{\mathbf{k}}|^2 , \quad (2.88)$$

and it only remains to calculate  $|f_{\mathbf{k}}|^2$ .

### 2.3.4. Power Spectrum at Leading Order in Slow Roll

In the last section, we saw that the calculation of the scalar power spectrum  $\mathcal{P}_\zeta(k)$  boils down to solving the differential equation (2.45) for  $f_{\mathbf{k}}$ , with initial condition given by Eq. (2.62). In Eq. (2.45),  $\omega^2(\eta, \mathbf{k}) = (a\sqrt{\epsilon_1})''/(a\sqrt{\epsilon_1})$  depends on the background function  $a(\eta)$ , hence on  $V(\phi)$  and on the solution of the Klein-Gordon equation (2.6). In practice, it must be solved numerically

once these quantities are specified. However, in the slow-roll approximation, as explained in section 2.2,  $a(\eta)$  is close to the de Sitter profile  $a(\eta) \propto -1/(H\eta)$ , and at the technical level, the slow-roll parameters quantify the deviation of  $a(\eta)$  from this de Sitter solution. A priori,  $\omega^2(\eta, \mathbf{k})$  can therefore be expressed in terms of the slow-roll parameters and Eq. (2.45) can be solved accordingly. This is why in this section, in order to gain some insight on the shape of the power spectrum, we solve Eq. (2.45) at first order in slow roll and we calculate the power spectrum  $\mathcal{P}_\zeta(k)$  around some pivot scale  $k_*$  at this same order in slow roll.

The first step consists in working out an expression for  $a(\eta)$  at first order in slow roll. One can start from the definition of  $\eta$ , given by Eq. (1.62), and write

$$\eta = \int \frac{dt}{a} = \int \frac{da}{a\mathcal{H}}, \quad (2.89)$$

where we denote  $\mathcal{H} \equiv a'/a = aH$ . Writing the last integrand as  $1/(a\mathcal{H}) = (d/da)a \times 1/(a\mathcal{H})$ , the last integral can be integrated by parts and one obtains

$$\int \frac{da}{a\mathcal{H}} = \frac{1}{\mathcal{H}} + \int \frac{da}{a\mathcal{H}}(2 - \epsilon_1), \quad (2.90)$$

where  $\epsilon_1 = 1 - \dot{H}/H^2 = -\mathcal{H}'/\mathcal{H}^2$  has been defined in Eq. (2.10). The above expression gives rise to

$$\int \frac{da}{a\mathcal{H}} \epsilon_1 = -\frac{1}{\mathcal{H}} + \int \frac{da}{a\mathcal{H}} \epsilon_1. \quad (2.91)$$

Again, the integral in the right hand side can be integrated by parts. Indeed, its integrand can be written as  $\epsilon_1/(a\mathcal{H}) = 1/(a\mathcal{H}) \times \epsilon_1 = (d/da)[-1/\mathcal{H} + \int da\epsilon_1/(a\mathcal{H})] \times \epsilon_1$ , where we have made use of Eq. (2.91) itself to integrate  $1/(a\mathcal{H})$ . Therefore, one obtains

$$\int \frac{da}{a\mathcal{H}} \epsilon_1 = -\frac{\epsilon_1}{\mathcal{H}} + \epsilon_1 \int \frac{\epsilon_1 da}{a\mathcal{H}} + \int \frac{\epsilon_1 \epsilon_2 da}{a\mathcal{H}} - \int \left[ \frac{d}{da}(\epsilon_1) \int \frac{\epsilon_1 d\bar{a}}{\bar{a}\mathcal{H}} \right] da \quad (2.92)$$

$$= -\frac{\epsilon_1}{\mathcal{H}} + \epsilon_1 \int \frac{\epsilon_1 da}{a\mathcal{H}} + \int \frac{\epsilon_1 \epsilon_2 da}{a\mathcal{H}} - \epsilon_1 \int \frac{\epsilon_1 da}{a\mathcal{H}} + \int \frac{\epsilon_1^2 da}{a\mathcal{H}} \quad (2.93)$$

$$= -\frac{\epsilon_1}{\mathcal{H}} + \int \left[ \frac{\epsilon_1}{a\mathcal{H}} (\epsilon_1 + \epsilon_2) \right] da, \quad (2.94)$$

where between the first and the second line the last term has been integrated by parts. Plugging Eq. (2.94) into Eq. (2.91) yields an expression for  $\eta$ , namely

$$\eta = -\frac{1 + \epsilon_1}{\mathcal{H}} + \int \frac{da}{a\mathcal{H}} (\epsilon_1^2 + \epsilon_1 \epsilon_2). \quad (2.95)$$

Since we want to work at first order in slow roll, the last integral can be dropped and one simply has  $\eta \simeq -(1 + \epsilon_1)/\mathcal{H}$ . However, let us notice that if one wanted to derive higher order in slow-roll terms, the same strategy could be used. The integral in the right hand side of Eq. (2.95) could be integrated by parts making use of Eq. (2.94), noticing that its integrand can be written as  $\epsilon_1/(a\mathcal{H}) \times (\epsilon_1 + \epsilon_2)$  and that Eq. (2.94) precisely provides us with a formal integral of the first term  $\epsilon_1/(a\mathcal{H})$ , so on and so forth. At second order in slow roll for example, one would obtain Eq. (2.5) of Ref. [209], see section 3.5. Here however, we work at first order in slow roll and we have

$$\mathcal{H} \simeq -\frac{1 + \epsilon_{1*}}{\eta}. \quad (2.96)$$

In the above expression, the first slow-roll parameter has been evaluated at the time  $\eta_*$  where the pivot scale  $k_*$  crosses the Hubble radius since as will be shown in Eq. (2.99), deviations of  $\epsilon_1$

from this value are slow-roll suppressed quantities. If one integrates the above expression along  $d\eta$ , one obtains

$$\ln\left(\frac{a}{a_*}\right) \simeq (1 + \epsilon_{1*}) \ln\left(\frac{\eta_*}{\eta}\right) \quad (2.97)$$

from which one has after exponentiation, and at first order in slow roll,  $a/a_* = \eta_*/\eta[1 - \epsilon_{1*} \ln(\eta/\eta_*)]$ . Looking at Eq. (2.96), the time  $\eta_*$  can be expressed as  $\eta_* = -(1 + \epsilon_{1*})/\mathcal{H}_*$ , so that one eventually has

$$a \simeq -\frac{1}{H_*\eta} \left[ 1 + \epsilon_{1*} - \epsilon_{1*} \ln\left(\frac{\eta}{\eta_*}\right) \right]. \quad (2.98)$$

We have therefore reached our first goal, namely to find an expression for  $a(\eta)$  at first order in slow roll. Notice that when  $\epsilon_{1*} = 0$ , one recovers the de Sitter profile  $a(\eta) = -1/(H\eta)$ . Now we need to calculate the corresponding behaviour of  $\omega^2(\eta, \mathbf{k}) = (a\sqrt{\epsilon_1})''/(a\sqrt{\epsilon_1})$  at leading order in slow roll. The first slow-roll parameter  $\epsilon_1$  can be expanded at first order in slow roll around the time  $\eta_*$ , and one has

$$\begin{aligned} \epsilon_1 &\simeq \epsilon_{1*} + \left. \frac{d\epsilon_1}{dN} \right|_{\eta_*} (N - N_*) \simeq \epsilon_{1*} + \epsilon_{1*}\epsilon_{2*} \ln\left(\frac{a}{a_*}\right) \\ &\simeq \epsilon_{1*} - \epsilon_{1*}\epsilon_{2*} (1 + \epsilon_{1*}) \ln\left(\frac{\eta}{\eta_*}\right) \\ &\simeq \epsilon_{1*} \left[ 1 - \epsilon_{2*} \ln\left(\frac{\eta}{\eta_*}\right) \right], \end{aligned} \quad (2.99)$$

where in the second line we have used Eq. (2.97) to express  $\ln(a)$  in terms of  $\eta$ . At this point, with Eqs. (2.98) and (2.99), we are in a position where we can calculate  $\omega^2$  at first order in slow roll. After a straightforward calculation, one obtains

$$\frac{(a\sqrt{\epsilon_1})''}{a\sqrt{\epsilon_1}} \simeq \frac{2}{\eta^2} \left( 1 + \frac{3}{2}\epsilon_{1*} + \frac{3}{4}\epsilon_{2*} \right). \quad (2.100)$$

In particular, one notices that the logarithmic terms in  $\eta$  cancel out at first order in slow roll, which makes the previous expression quite simple and easy to handle. Indeed, at this order, Eq. (2.45) reads

$$f_{\mathbf{k}}'' + \left[ k^2 - \frac{2}{\eta^2} \left( 1 + \frac{3}{2}\epsilon_{1*} + \frac{3}{4}\epsilon_{2*} \right) \right] f_{\mathbf{k}} = 0. \quad (2.101)$$

Conveniently enough, such a differential equation can be solved in terms of Hankel functions, and one obtains

$$f_{\mathbf{k}} = C_{\mathbf{k}} \sqrt{-k\eta} H_{\nu}^{(1)}(-k\eta) + D_{\mathbf{k}} \sqrt{-k\eta} H_{\nu}^{(2)}(-k\eta), \quad (2.102)$$

with

$$\nu = \frac{3}{2} \sqrt{1 + \frac{4}{3}\epsilon_{1*} + \frac{2}{3}\epsilon_{2*}} \quad (2.103)$$

$$\simeq \frac{3}{2} + \epsilon_{1*} + \frac{\epsilon_{2*}}{2}. \quad (2.104)$$

In Eq. (2.102),  $H_{\nu}^{(1)}$  and  $H_{\nu}^{(2)}$  are Hankel functions [269] (also called Bessel functions of the third kind), and  $C_{\mathbf{k}}$  and  $D_{\mathbf{k}}$  are integration constants.

These constants can be set so that the Bunch-Davies vacuum (2.62) is recovered at early time. In Eq. (2.62) the limit  $k/(aH) \rightarrow +\infty$  actually corresponds to  $k\eta \rightarrow -\infty$  since from Eq. (2.96)

one has  $k/(aH) = k/\mathcal{H} \simeq -k\eta/(1 + \epsilon_{1*})$ . Since one has [269]  $H_\nu^{(1)}(z) \simeq \sqrt{2/(\pi z)} \exp[i(z - \nu\pi/2 - \pi/4)]$  and  $H_\nu^{(2)}(z) \simeq \sqrt{2/(\pi z)} \exp[-i(z - \nu\pi/2 - \pi/4)]$  when  $z \gg 1$ , one obtains

$$f_{\mathbf{k}} \xrightarrow[k\eta \rightarrow -\infty]{} C_{\mathbf{k}} \sqrt{\frac{2}{\pi}} \exp\left[-i\left(k\eta + \frac{\nu\pi}{2} + \frac{\pi}{4}\right)\right] + D_{\mathbf{k}} \sqrt{\frac{2}{\pi}} \exp\left[i\left(k\eta + \frac{\nu\pi}{2} + \frac{\pi}{4}\right)\right]. \quad (2.105)$$

This is why in order to match Eq. (2.62), one must set  $C_{\mathbf{k}} = 0$  and  $D_{\mathbf{k}} = \sqrt{\pi/k} \exp[-i\pi/2(\nu + 1/2)]/2$ . One eventually has

$$f_{\mathbf{k}} = \frac{1}{2} \sqrt{\frac{\pi}{k}} \sqrt{-k\eta} e^{-i\frac{\pi}{2}(\nu + \frac{1}{2})} H_\nu^{(2)}(-k\eta). \quad (2.106)$$

At the end of inflation, the pivot scale  $k_*$  around which we are expanding the power spectrum and which is of astrophysical interest today, is much larger than the Hubble radius, *i.e.*  $k_*/(a_{\text{end}}H_{\text{end}}) \ll 1$ . In Fig. 2.3, this corresponds to the observational window located at the end of inflation where  $\mathcal{P}(k)$  is calculated. Since we have shown that  $k/(aH) \simeq -k\eta$ , this means that the power spectrum (2.88), which scales as  $|f_{\mathbf{k}}|^2$ , can be approximated at the end of inflation in the limit  $k\eta \rightarrow 0^-$ . Since one has [269]  $H_\nu^{(2)}(z) \simeq -i(2/z)^\nu \Gamma(\nu)/\pi$  when  $z \rightarrow 0$ , one obtains

$$|f_{\mathbf{k}}|^2 \xrightarrow[k\eta \rightarrow 0^-]{} \frac{-k\eta}{4k} \left(\frac{2}{-k\eta}\right)^{2\nu} \frac{\Gamma^2(\nu)}{\pi}. \quad (2.107)$$

In order to be consistent with our first order in slow roll expansion, the slow-roll parameters appearing in  $\nu$ , see Eq. (2.104), should now be expanded too. One has  $\Gamma(\nu) = \Gamma(3/2) + \Gamma'(3/2)(\epsilon_{1*} + \epsilon_{2*}/2)$ , where [269]  $\Gamma'(3/2) = \Gamma(3/2)(2 - 2\ln 2 - \gamma_E)$  and  $\Gamma(3/2) = \sqrt{\pi}/2$ ,  $\gamma_E$  being the Euler-Mascheroni constant. On the other hand, one can write  $[-2/(k\eta)]^{2\nu} = e^{2\nu \ln[-2/(k\eta)]} \simeq [-2/(k\eta)]^3 \{1 + (2\epsilon_{1*} + \epsilon_{2*}) \ln[-2/(k\eta)]\}$ . Plugging these expressions in Eq. (2.107), one obtains

$$|f_{\mathbf{k}}|^2 \xrightarrow[k\eta \rightarrow 0^-]{} \frac{1}{2k} \frac{1}{(k\eta)^2} \{1 + (2\epsilon_{1*} + \epsilon_{2*}) [2 - \ln 2 - \gamma_E - \ln(-k\eta)]\}. \quad (2.108)$$

We now have everything one needs to calculate the power spectrum  $\mathcal{P}_\zeta$  at first order in slow roll. In Eq. (2.88), let us replace  $a$  by Eq. (2.98),  $\epsilon_1$  by Eq. (2.99), and  $|f_{\mathbf{k}}|^2$  by Eq. (2.108). One obtains, at first order in slow roll,

$$\mathcal{P}_\zeta(k) = \frac{H_*^2}{8\pi^2 \epsilon_{1*} M_{\text{Pl}}^2} [2(1 - \ln 2 - \gamma_E) \epsilon_{1*} + (2 - \ln 2 - \gamma_E) \epsilon_{2*} - (2\epsilon_{1*} + \epsilon_{2*}) \ln(-k\eta_*)]. \quad (2.109)$$

One can see that quite remarkably, the dependence in  $\eta$  has cancelled out since, as announced, the curvature perturbations are constant on large scales. The time  $\eta_*$  can be expressed in terms of  $k_*$  since by definition, it is such that  $k_*/(a_*H_*) = 1$ . Since Eq. (2.96) gives  $k/(aH) = k/\mathcal{H} = -k\eta(1 + \epsilon_{1*})$ , one simply has  $-k\eta_* = (k/k_*)(1 + \epsilon_{1*})^{-1}$ . Denoting  $C \equiv \ln 2 + \gamma_E - 2 \simeq -0.7296$  for simplicity, the power spectrum of curvature perturbations calculated at the end of inflation, at first order in slow roll, is finally given by

$$\mathcal{P}_\zeta(k) = \frac{H_*^2}{8\pi^2 \epsilon_{1*} M_{\text{Pl}}^2} \left[1 - 2(C + 1) \epsilon_{1*} - C \epsilon_{2*} - (2\epsilon_{1*} + \epsilon_{2*}) \ln\left(\frac{k}{k_*}\right)\right]. \quad (2.110)$$

This result was derived for the first time in Ref. [128], where the corresponding formula for gravity waves was obtained too. Indeed, the same procedure as the one presented here can be employed to calculate the power spectrum of tensor perturbations  $\mathcal{P}_h$ . Instead of Eq. (2.45), one has to solve an equation of the form  $h'' + (k^2 - a''/a)h = 0$ , and one obtains

$$\mathcal{P}_h(k) = \frac{2H_*^2}{\pi^2 M_{\text{Pl}}^2} \left[1 - 2(C + 1) \epsilon_{1*} - 2\epsilon_{1*} \ln\left(\frac{k}{k_*}\right)\right]. \quad (2.111)$$

Before that, scalar perturbations during inflation were first integrated in Refs. [270, 242] and tensor perturbations in Ref. [121].<sup>5</sup> The same result (2.110) was later re-derived using the Green function method in Ref. [272], using the Wentzel-Kramers-Brillouin (WKB) method in Ref. [273] and using the uniform approximation in Refs. [274, 275]. In fact, the Green function method of Ref. [272] made possible the first determination of the scalar power spectrum at second order in slow roll, since at second order, the mode equation (2.45) describing the evolution of the cosmological perturbations can no longer be solved exactly, hence the need for a new method of approximation.<sup>6</sup> Finally, the first derivation of the tensor power spectrum at second order in slow roll using the Green function method was presented in Ref. [278].

A few comments are in order regarding Eqs. (2.110) and (2.111). First of all, as announced, at leading order in slow roll, these two spectra are scale invariant, that is the power on each scale  $k$  does not depend on  $k$ . For scalar perturbations, the overall amplitude is measured to be [163, 167]  $\mathcal{P}_\zeta(k_*) \simeq 2.203 \times 10^{-9}$ . More precisely, the small deviations from scale invariance appear through the logarithm of  $k$ , and are controlled by the slow-roll parameters, which quantify the deviation of space-time from de Sitter, see Eq. (2.9), or equivalently the non flatness of the potential, see Eqs. (2.14)-(2.17). As a consequence, measuring the scale dependence of the power spectrum is a way of constraining the inflationary potential  $V(\phi)$ . For scalar perturbations, the deviation from scale invariance of the power spectrum is often described in terms of the scalar spectral index  $n_s$ , defined as

$$n_s \equiv 1 + \frac{d \ln \mathcal{P}_\zeta}{d \ln k}, \quad (2.112)$$

where  $n_s = 1$  for exact scale invariance. At first order in slow roll, from Eq. (2.110), it is given by  $n_s = 1 - 2\epsilon_{1*} - \epsilon_{2*}$ . By definition, the first slow-roll parameter  $\epsilon_1 = -\dot{H}/H^2$  is always positive. The second slow-roll parameter is proportional to its time derivative,  $\epsilon_2 = (d\epsilon_1/dN)/\epsilon_1$ . Inflation takes place as long as  $\epsilon_1 < 1$ , and if it ends with a “graceful exit” when  $\epsilon_1 = 1$ , it is natural to assume that  $\epsilon_1$  increases during inflation, and therefore that  $\epsilon_2$  is positive too. As a consequence, a rather natural prediction [122, 279] of slow-roll inflation is that the scalar power spectrum should be almost scale invariant but slightly red, *i.e.* “ $n_s < 1$ ” (as opposed to “blue”, for which  $n_s > 1$ ). This is why it is quite remarkable that the most recent observations [163, 167] strongly favour a red scalar spectrum,  $n_s = 0.9619 \pm 0.0073$ , which excludes exact scale invariance  $n_s = 1$  at more than the  $5\sigma$  confidence level. As for tensors, the deviation from scale invariance is usually described in terms of the tensor spectral index

$$n_T \equiv \frac{d \ln \mathcal{P}_h}{d \ln k}, \quad (2.113)$$

where  $n_T = 0$  for exact scale invariance. At first order in slow roll, from Eq. (2.111), it is given by  $n_T = -2\epsilon_{1*}$ . Since  $\epsilon_1$  is always positive, this means that the tensor spectral index is generically red ( $n_T < 0$ ) in slow-roll inflation. The sign of  $n_T$  has not been measured so far, but one can see that it would be an additional test for slow-roll inflation. If one ever finds that a blue spectrum  $n_T > 0$  is favoured, this would be difficult to explain in the framework presented here, and alternatives such as, for instance, string gas cosmology which predicts a blue spectrum [280], would be a possible solution. Another useful quantity to calculate is the ratio  $r$  between the amplitude of both power spectra,

$$r \equiv \frac{\mathcal{P}_h(k_*)}{\mathcal{P}_\zeta(k_*)} \simeq 16\epsilon_{1*}, \quad (2.114)$$

<sup>5</sup>In Ref. [271], it was also realized that the power spectrum can be evaluated exactly in the case of power-law inflation, for which  $a(\eta) \propto |\eta|^\beta$ .

<sup>6</sup>In Refs. [276, 277], it was also shown how to improve the WKB method by adding more adiabatic terms. This improved WKB method has allowed a re-derivation of the scalar and tensor power spectra at second order and confirmed the results of the Green function approach.

where its first order expression in slow roll has been derived thanks to Eqs. (2.110) and (2.111). Since  $\epsilon_1$  is a small parameter in slow-roll inflation, this means that tensor perturbations are generically suppressed with respect to scalar perturbations. This is why in practice, it seems difficult to directly measure the gravitational primordial power spectrum. However, tensor perturbations leave an indirect imprint in the polarization pattern of the CMB through its rotational component (dubbed “ $B$  mode”) that scalar cannot, by definition, produce. Recently the BICEP2 experiment [164] has reported the detection of this  $B$  mode signal. If it is of primordial origin, the associated value for  $r$  is found to be  $r = 0.16_{-0.05}^{+0.06}$ . This value carries important physical consequences, notably, it allows to constrain the energy scale  $\rho_* = 3M_{\text{Pl}}^2 H_*^2$  of inflation. Indeed, combining Eqs. (2.110), (2.111) and (2.114), one obtains

$$\rho_*^{1/4} = 2.0 \times 10^{16} \left( \frac{r}{0.16} \right)^{1/4} \left( \frac{\mathcal{P}}{2.2 \times 10^{-9}} \right)^{1/4} \text{ GeV}, \quad (2.115)$$

which corresponds to GUT energy scales. If such a detection is confirmed, therefore, inflation is a high energy phenomenon by Particle Physics standard. Such a value of  $r$  also implies a large field excursion. Indeed, because of the relation (2.19), one has  $\Delta\phi/M_{\text{Pl}} \sim \sqrt{2\epsilon_1} M_{\text{Pl}} \Delta N = \mathcal{O}(1) (r/0.16)^{1/2}$  [281, 282], which indicates that the excursion of the field during inflation is necessarily super-Planckian. This raises model building issues since most inflationary theoretical setups arise as effective field theories relying on sub-Planckian expansions [283].

Finally, a last comment is in order concerning the value of  $\mathcal{P}_\zeta \sim 10^{-9}$ . Indeed, during the typical inflationary time scale of one  $e$ -fold, as just mentioned, the field excursion  $\Delta\phi_{\text{cl}}$  under the “classical” Klein-Gordon equation (2.6) is given by  $\Delta\phi_{\text{cl}} \sim \sqrt{2\epsilon_1} M_{\text{Pl}}$ . On the other hand, as we will see in the next section, quantum fluctuations in the scalar sector modify the inflaton dynamics, which translates into a quantum excursion  $\Delta\phi_{\text{qu}} = H/(2\pi)$ . As a consequence, the ratio between these two field excursions, which roughly quantifies how much the quantum effects modify the inflationary dynamics, is given by  $\Delta\phi_{\text{qu}}/\Delta\phi_{\text{cl}} = H/\sqrt{8\pi^2 M_{\text{Pl}}^2 \epsilon_1} = \sqrt{\mathcal{P}_\zeta}$ . As a consequence, the small measured value of  $\mathcal{P}_\zeta$  indicates that the quantum effects on the inflaton dynamics are small, at least at Hubble exit time of the modes of astrophysical interest today. Hence the classical trajectory (2.6) can safely be used as a first approximation. In the next section, we discuss in more details the implementation of quantum effects on the inflationary dynamics, notably by means of the “stochastic inflation” formalism.

## 2.4. Stochastic Inflation

As explained in section 2.3, in the standard description of inflation, the homogeneous parts of the fields are usually assumed to behave classically, while the small deviations from homogeneity and isotropy over this classical background are treated quantum mechanically. However, one expects quantum corrections to the classical trajectory to modify the way the background evolves [284, 285, 286, 287, 288, 289]. The stochastic inflation formalism [290, 291, 292, 293, 294, 295, 296, 297, 289, 298] aims at modeling this physics. The idea is to treat the dynamics of the inflaton field coarse-grained over length scales larger than the Hubble radius, by integrating out the sub-Hubble degrees of freedom. It amounts to working out the effective theory for an open quantum system made of the large scale modes of the field operators. When such a theory is derived, it can be shown that the dynamics of the coarse-grained field  $\varphi$  is modified by the presence of a stochastic term, so that its slow-roll equation of motion  $d\varphi/dN = -V'/(3H^2)$  is modified and becomes a Langevin equation of the form [290]

$$\frac{d\varphi}{dN} = -\frac{V'}{3H^2} + \frac{H}{2\pi} \xi(N), \quad (2.116)$$

where  $\xi$  is a normalized white Gaussian noise, such that  $\langle \xi(N) \rangle = 0$  and  $\langle \xi(N_1)\xi(N_2) \rangle = \delta(N_1 - N_2)$ . What makes this formalism very appealing is that it reproduces results from quantum field theory in curved space-times, even beyond the perturbative level [298, 299, 300, 301]. For example, in Ref. [302], it is shown that stochastic inflation reproduces perturbative calculations of quantum field theories with non-conformal fields, in particular its secular effects which take the form of “infrared logarithms”. Not only stochastic inflation accounts for the leading infrared logarithms at each order in perturbation theory, but it can even describe the regimes where inflation proceeds so long that the large logarithms overwhelm small coupling constants. In Refs. [303, 304], this technique was extended to scalar quantum electrodynamics on a de Sitter background. As one can see, stochastic inflation is therefore more than just a qualitative description of some backreaction effects, but it provides us with a very powerful and straightforward frame of calculation for quantum field theoretic effects on inflationary space-times.

This section is organized as follows. First, in section 2.4.1, we detail an heuristic derivation of the Langevin equations of stochastic inflation. This allows us to emphasize a few important aspects of the nature of the formalism and of the assumptions it rests on. Then, in section 2.4.2, we elaborate on the reasons why this equation needs to be written and solved with the number of  $e$ -folds as the time variable. Since it happens quite often that a different time variable is used in the literature, it seems important to stress why it is *a priori* wrong to do so. Finally, in section 2.4.3 we address the issue of the calculation of physical observable quantities in stochastic inflation such as the power spectrum of adiabatic perturbations. Making use of the  $\delta N$  formalism, we show that the stochastic setup enables to reproduce the standard result (derived in section 2.3) of linear perturbation theory, in a “classical” limit that we carefully define. Then, we provide complete solutions which do not rely on an expansion in the noise terms and which are therefore valid even when the stochastic effects are large. Generic formulas are provided that can be straightforwardly applied to any single field potential, and as an example, the case of a large field potential  $V \propto \phi^p$  is completely worked out. To our knowledge, it is the first time such a non perturbative calculation of the power spectrum in stochastic inflation is presented.

### 2.4.1. Heuristic Derivation of the Langevin Equations

The basic strategy of stochastic inflation is to introduce a cutoff in Fourier space through a suitable time-dependent window function that filters out the modes whose frequency is higher than the comoving horizon size. The inflaton field is thus split in two differently behaving parts: the short-wavelength part which is treated as a fully quantum operator, and the coarse-grained one which collects the remaining super-horizon modes and which is treated as classical. A Langevin equation of motion for the long-wavelength part can be obtained, where the sub-horizon modes enter as a classical stochastic noise term that perturbs the dynamics of the coarse-grained field. In this section, we give a detailed derivation of such a stochastic equation of motion for the coarse-grained field, based on a heuristic argument dealing with the equation of motion only.

However, it is worth mentioning that a more general approach can be followed that exploits the influence functional method [305, 306] and operates the frequency splitting at the action level, getting rid of the high frequencies via a path-integral over the sub-horizon part of the field. The effective action obtained by this process contains some extra terms that can be interpreted as the coupling of the super-horizon field with a classical random noise source, whose configurations are statistically weighted by an appropriate functional probability distribution, becoming the

origin of the stochastic character of the Langevin equation of motion. In some sense, stochastic inflation is therefore nothing more than a direct application of the well-known non equilibrium quantum field theories for open quantum systems, to inflationary cosmologies.

### 2.4.1.1. Coarse-Grained Field

The starting point of the stochastic formalism is to divide the inflaton field  $\phi$  into two pieces,  $\phi = \varphi + \phi_{>}$ . The coarse-grained field  $\varphi$  contains all wavelengths much larger than the Hubble radius, *i.e.* such that  $k < \sigma aH$ , where  $\sigma \ll 1$  is a fixed parameter that sets the coarse-graining scale. On the other hand,  $\phi_{>}$  collects the small wavelength modes, and can be written as

$$\phi_{>}(\mathbf{x}, N) = \int \frac{d\mathbf{k}}{(2\pi)^{\frac{3}{2}}} W\left(\frac{k}{\sigma aH}\right) \left[ e^{-i\mathbf{k}\cdot\mathbf{x}} \phi_{\mathbf{k}}(N) a_{\mathbf{k}} + e^{i\mathbf{k}\cdot\mathbf{x}} \phi_{\mathbf{k}}^*(N) a_{\mathbf{k}}^\dagger \right], \quad (2.117)$$

where  $W$  is a filter function so that  $W \simeq 0$  when its argument is small,  $k/(\sigma aH) \ll 1$ , and  $W \simeq 1$  when its argument is large,  $k/(\sigma aH) \gg 1$ . The idea is to derive an effective equation of motion for  $\varphi$ , integrating out the degrees of freedom contained in  $\phi_{>}$ .

The time dependence in the argument of the window function translates the fact that modes are continuously leaving the small wavelength part of the field  $\phi_{>}$  to source the coarse-grained part  $\varphi$ . Therefore, one expects the dynamics of the coarse-grained field to be kicked by the inflow of modes which cross the Hubble radius during inflation. It is important to stress that the effect one shall obtain is only due to this continuous Hubble crossing of modes, rather than to some fundamental coupling between super-Hubble and sub-Hubble modes.<sup>7</sup>

### 2.4.1.2. Split Klein-Gordon Equation

We start from the Klein-Gordon equation of the field  $\phi(\mathbf{x}, t)$  given by Eq. (2.6), but we rewrite it in terms of the number of  $e$ -folds  $N \equiv \ln a$ , that is

$$\frac{\partial^2 \phi(\mathbf{x}, N)}{\partial N^2} + (3 - \epsilon_1) \frac{\partial \phi(\mathbf{x}, N)}{\partial N} - \frac{\nabla^2}{a^2 H^2} \phi(\mathbf{x}, N) + \frac{V'[\phi(\mathbf{x}, N)]}{H^2} = 0. \quad (2.118)$$

The reasons why it is crucial to work with  $N$  as the time variable are explained in section 2.4.2. It is important to stress that in the stochastic inflationary setup, the short wavelength perturbations are taken to be test perturbations, in the sense that the background functions  $H$ ,  $aH$  and  $\epsilon_1$  appearing in Eq. (2.118) are to be evaluated at the coarse-grained field  $\varphi$  only, through the Friedmann equation (2.7). Written in terms of  $\varphi$  and  $\partial\varphi/\partial N$  only, the latter is given by

$$H^2 = \frac{V(\varphi)}{3M_{\text{Pl}}^2 - \frac{1}{2} \left( \frac{d\varphi}{dN} \right)^2}. \quad (2.119)$$

Here we have not displayed any gradient term since it is  $\sigma$ -suppressed for  $\varphi$ . In the same manner, the first slow-roll parameter  $\epsilon_1 = -(dH/dN)/H$  can simply be expressed in terms of  $d\varphi/dN$  as  $\epsilon_1 = (d\varphi/dN)^2/(2M_{\text{Pl}}^2)$ , see Eq. (2.15).

Let us now plug the decomposition  $\phi = \varphi + \phi_{>}$  into the Klein-Gordon equation (2.118), and expand the obtained result at first order in  $\phi_{>}$ . One obtains

$$\frac{\partial^2 \varphi}{\partial N^2} + (3 - \epsilon_1) \frac{\partial \varphi}{\partial N} + \frac{V'(\varphi)}{H^2} = -\frac{\partial^2 \phi_{>}}{\partial N^2} - (3 - \epsilon_1) \frac{\partial \phi_{>}}{\partial N} + \frac{\nabla^2 \phi_{>}}{(aH)^2} - \frac{V''(\varphi)}{H^2} \phi_{>}, \quad (2.120)$$

<sup>7</sup>Such couplings would need to be taken into account *e.g.* beyond linear order in perturbation theory.

where the gradient term for  $\varphi$  has been dropped for the same reason as above. Again,  $H$  and  $\epsilon_1$  have to be understood as functions of  $\varphi$  and  $\partial\varphi/\partial N$ . The right hand side of this equation can be written with the Fourier expansion (2.117). Before doing so, to simplify notations, we first introduce the hermitian operators  $A_{\mathbf{k}}$ , defined as

$$A_{\mathbf{k}}(\mathbf{x}, N) = e^{-i\mathbf{k}\cdot\mathbf{x}} \phi_{\mathbf{k}}(N) a_{\mathbf{k}} + e^{i\mathbf{k}\cdot\mathbf{x}} \phi_{\mathbf{k}}^*(N) a_{\mathbf{k}}^\dagger, \quad (2.121)$$

so that for example, the Fourier expansion of  $\phi$  is simply given by  $(2\pi)^{-3/2}\phi = \int d\mathbf{k} A_{\mathbf{k}}$ . One obtains

$$\begin{aligned} \frac{\partial^2 \varphi}{\partial N^2} + (3 - \epsilon_1) \frac{\partial \varphi}{\partial N} + \frac{V'(\varphi)}{H^2} = & - \int \frac{d\mathbf{k}}{(2\pi)^{3/2}} \left\{ \frac{\partial}{\partial N} W\left(\frac{k}{\sigma a H}\right) \left[ 2 \frac{\partial A_{\mathbf{k}}}{\partial N} + (3 - \epsilon_1) A_{\mathbf{k}} \right] \right. \\ & \left. + \frac{\partial^2}{\partial N^2} W\left(\frac{k}{\sigma a H}\right) A_{\mathbf{k}} + W\left(\frac{k}{\sigma a H}\right) \left[ \frac{\partial^2 A_{\mathbf{k}}}{\partial N^2} + (3 - \epsilon_1) \frac{\partial A_{\mathbf{k}}}{\partial N} + \left( \frac{V''}{H^2} + \frac{k^2}{a^2 H^2} \right) A_{\mathbf{k}} \right] \right\}. \end{aligned} \quad (2.122)$$

In this equation, it is clear that the last bracketed term vanishes since from the definition (2.121) of the  $A_{\mathbf{k}}$  operators, it involves the equation of motion for  $\phi_{\mathbf{k}}$  and for  $\phi_{\mathbf{k}}^*$  that one obtains by Fourier expanding Eq. (2.118). This is why, if one lets

$$\xi_1 = - \int \frac{d\mathbf{k}}{(2\pi)^{3/2}} \frac{\partial}{\partial N} \left[ W\left(\frac{k}{\sigma a H}\right) \right] A_{\mathbf{k}} \quad (2.123)$$

and

$$\xi_2 = - \int \frac{d\mathbf{k}}{(2\pi)^{3/2}} \frac{\partial}{\partial N} \left[ W\left(\frac{k}{\sigma a H}\right) \right] \frac{\partial A_{\mathbf{k}}}{\partial N}, \quad (2.124)$$

the split Klein-Gordon equation can be written as

$$\frac{\partial^2 \varphi}{\partial N^2} + (3 - \epsilon_1) \frac{\partial \varphi}{\partial N} + \frac{V'(\varphi)}{H^2} = (3 - \epsilon_1) \xi_1 + \frac{\partial \xi_1}{\partial N} - \xi_2. \quad (2.125)$$

### 2.4.1.3. Stochastic Processes

A crucial ingredient of the stochastic inflationary setup is the statement that the coarse-grained field can be described in terms of a classical stochastic quantity. Indeed, it can be shown that as the cosmological perturbations cross the Hubble radius, they evolve from a coherent vacuum state to a strongly squeezed state [131], the corresponding squeezing being much more important than whatever can be realized in the laboratory [307]. In this limit, the predictions of the quantum formalism are indistinguishable from that of a theory where the fluctuations are just assumed to be realizations of a classical stochastic process [308, 132, 309, 310]. The classical limit is a subtle concept in quantum mechanics but, in this sense, such a system can be characterized as being classical [136]. Moreover, the large-scale cosmological perturbations are not isolated and, as a consequence, the phenomenon of decoherence [311, 312, 313] is relevant for them, which is also considered as playing a role in their quantum-to-classical transition [132, 314, 309, 315, 133, 316, 317, 318, 319].

This is why in the  $\sigma \ll 1$  limit where  $\varphi$  contains only super-Hubble, largely squeezed modes, the terms  $\xi_1$  and  $\xi_2$  can be treated<sup>8</sup> as classical noise sources acting on a stochastic coarse-grained field  $\varphi$ , through a split Klein-Gordon equation which becomes a Langevin equation for  $\varphi$ . This

<sup>8</sup>This is rigorously showed within the Keldysh formalism, see Refs. [305, 306]

is the stochastic inflationary setup. The mapping between  $\xi_1$  and  $\xi_2$  (which are, strictly speaking, quantum operators) and their classical noise counterparts is made by identifying quantum expectation values with stochastic moments, *i.e.* by requiring that

$$\left\langle \xi_i^p(\mathbf{x}_1, N_1) \xi_j^q(\mathbf{x}_2, N_2) \right\rangle = \left\langle 0 \left| T \left[ \xi_i^p(\mathbf{x}_1, N_1) \xi_j^q(\mathbf{x}_2, N_2) \right] \right| 0 \right\rangle, \quad (2.126)$$

where  $i$  and  $j$  stand for 1 or 2,  $p$  and  $q$  are natural integers, and where the  $T$ -product is the time ordering product. Note that in the left hand side of the above, the angle brackets stand for stochastic average while in the right hand side, they denote the bra and the ket of the vacuum state  $|0\rangle$ .

#### 2.4.1.4. Noise Moments

Since the field fluctuations  $\phi_{\mathbf{k}}$  are Gaussian to a good level of approximation, and since  $\xi_1$  and  $\xi_2$  are linearly constructed out of them, they also follow Gaussian statistics and it is enough to calculate their second moments to fully characterize them. First of all,  $T$ -products of  $A_{\mathbf{k}}$ 's and  $\partial A_{\mathbf{k}}/\partial N$ 's need to be worked out. Making use of the canonical relations  $\langle 0 | T [a_{\mathbf{k}_1} a_{\mathbf{k}_2}^\dagger] | 0 \rangle = \delta(\mathbf{k}_1 - \mathbf{k}_2)$  and  $\langle 0 | T [a_{\mathbf{k}_1} a_{\mathbf{k}_2}] | 0 \rangle = \langle 0 | T [a_{\mathbf{k}_1}^\dagger a_{\mathbf{k}_2}^\dagger] | 0 \rangle = \langle 0 | T [a_{\mathbf{k}_1}^\dagger a_{\mathbf{k}_2}] | 0 \rangle = 0$ , from the definition (2.121) one obtains

$$\langle A_{\mathbf{k}_1}(\mathbf{x}_1, N_1) A_{\mathbf{k}_2}(\mathbf{x}_2, N_2) \rangle = \phi_{\mathbf{k}_1}(N_1) \phi_{\mathbf{k}_2}^*(N_2) e^{i\mathbf{k}_1 \cdot (\mathbf{x}_2 - \mathbf{x}_1)} \delta(\mathbf{k}_1 - \mathbf{k}_2), \quad (2.127)$$

$$\left\langle A_{\mathbf{k}_1}(\mathbf{x}_1, N_1) \frac{\partial A_{\mathbf{k}_2}}{\partial N}(\mathbf{x}_2, N_2) \right\rangle = \phi_{\mathbf{k}_1}(N_1) \frac{\partial \phi_{\mathbf{k}_2}^*}{\partial N}(N_2) e^{i\mathbf{k}_1 \cdot (\mathbf{x}_2 - \mathbf{x}_1)} \delta(\mathbf{k}_1 - \mathbf{k}_2), \quad (2.128)$$

$$\left\langle \frac{\partial A_{\mathbf{k}_1}}{\partial N}(\mathbf{x}_1, N_1) \frac{\partial A_{\mathbf{k}_2}}{\partial N}(\mathbf{x}_2, N_2) \right\rangle = \frac{\partial \phi_{\mathbf{k}_1}}{\partial N}(N_1) \frac{\partial \phi_{\mathbf{k}_2}^*}{\partial N}(N_2) e^{i\mathbf{k}_1 \cdot (\mathbf{x}_2 - \mathbf{x}_1)} \delta(\mathbf{k}_1 - \mathbf{k}_2). \quad (2.129)$$

Let us proceed with the details of the calculation for  $\langle \xi_1 \xi_1 \rangle$ , since the expressions for  $\langle \xi_1 \xi_2 \rangle$  and  $\langle \xi_2 \xi_2 \rangle$  will follow accordingly. Making use of Eq. (2.127), one obtains

$$\begin{aligned} \langle \xi_1(\mathbf{x}_1, N_1) \xi_1(\mathbf{x}_2, N_2) \rangle &= \int \frac{d\mathbf{k}_1 d\mathbf{k}_2}{(2\pi)^3} \frac{\partial}{\partial N} W \left[ \frac{k_1}{\sigma a(N_1) H(N_1)} \right] \frac{\partial}{\partial N} W \left[ \frac{k_2}{\sigma a(N_2) H(N_2)} \right] \\ &\quad \times \phi_{\mathbf{k}_1}(N_1) \phi_{\mathbf{k}_2}^*(N_2) e^{i\mathbf{k}_1 \cdot (\mathbf{x}_2 - \mathbf{x}_1)} \delta(\mathbf{k}_1 - \mathbf{k}_2) \end{aligned} \quad (2.130)$$

$$= \int \frac{d\mathbf{k}}{(2\pi)^3} \frac{\partial}{\partial N} W \left[ \frac{k}{\sigma a(N_1) H(N_1)} \right] \frac{\partial}{\partial N} W \left[ \frac{k}{\sigma a(N_2) H(N_2)} \right] \phi_{\mathbf{k}}(N_1) \phi_{\mathbf{k}}^*(N_2) e^{i\mathbf{k} \cdot (\mathbf{x}_2 - \mathbf{x}_1)}. \quad (2.131)$$

Let  $\theta$  be the angle between  $\mathbf{k}$  and  $\mathbf{x}_2 - \mathbf{x}_1$ , so that  $\mathbf{k} \cdot (\mathbf{x}_2 - \mathbf{x}_1) = kr \cos(\theta)$ , where  $r \equiv |\mathbf{x}_2 - \mathbf{x}_1|$  and  $k = |\mathbf{k}|$ . Decomposing  $d\mathbf{k} = k^2 dk \sin(\theta) d\theta d\phi$ , the  $\phi$  integration can be factorized out and just gives a  $2\pi$  factor. The  $\theta$  integral can also be performed, since one has

$$\int_0^\pi d\theta \sin(\theta) e^{ikr \cos(\theta)} = \left[ -\frac{e^{ikr \cos(\theta)}}{ikr} \right]_0^\pi = 2 \frac{\sin(kr)}{kr}. \quad (2.132)$$

It only remains the  $k$ -integral, and one has

$$\begin{aligned} \langle \xi_1(\mathbf{x}_1, N_1) \xi_1(\mathbf{x}_2, N_2) \rangle &= \\ &= \int \frac{k^2 dk}{(2\pi)^2} \frac{\partial}{\partial N} W \left[ \frac{k}{\sigma a(N_1) H(N_1)} \right] \frac{\partial}{\partial N} W \left[ \frac{k}{\sigma a(N_2) H(N_2)} \right] \phi_{\mathbf{k}}(N_1) \phi_{\mathbf{k}}^*(N_2) \frac{\sin(kr)}{kr}. \end{aligned} \quad (2.133)$$

Another quantity we need to compute is  $\partial W/\partial N$ . One has

$$\frac{\partial}{\partial N} W \left( \frac{k}{\sigma a H} \right) = \frac{\partial}{\partial N} \left( \frac{k}{\sigma a H} \right) W' \left( \frac{k}{\sigma a H} \right) = \frac{k(\epsilon_1 - 1)}{\sigma a H} W' \left( \frac{k}{\sigma a H} \right). \quad (2.134)$$

This is why to proceed, one needs to specify the window function.

### 2.4.1.5. Window Function and Coloured Noises

A very simple choice for the window function consists in taking a Heaviside step function  $W(s) = \theta(s - 1)$ , so that  $W \equiv 1$  when  $k \geq \sigma a H$  and  $W \equiv 0$  when  $k < \sigma a H$ . In this case, one has

$$\begin{aligned} W' \left( \frac{k}{\sigma a H} \right) &= \theta' \left( \frac{k}{\sigma a H} - 1 \right) = \delta \left( \frac{k}{\sigma a H} - 1 \right) \\ &= \sigma a H \delta(k - \sigma a H) . \end{aligned} \quad (2.135)$$

Combining this relation with Eq. (2.134), one obtains

$$\begin{aligned} &\frac{\partial}{\partial N} W \left[ \frac{k}{\sigma a(N_1) H(N_1)} \right] \frac{\partial}{\partial N} W \left[ \frac{k}{\sigma a(N_2) H(N_2)} \right] \\ &= \sigma^2 a(N_1) H(N_1) a(N_2) H(N_2) \delta[k - \sigma a(N_1) H(N_1)] \delta[k - \sigma a(N_2) H(N_2)] \\ &= \sigma^2 a(N_1) H(N_1) a(N_2) H(N_2) \delta[k - \sigma a(N_1) H(N_1)] \delta[\sigma a(N_1) H(N_1) - \sigma a(N_2) H(N_2)] \\ &= \sigma^2 a(N_1) H(N_1) a(N_2) H(N_2) \delta[k - \sigma a(N_1) H(N_1)] \frac{\delta(N_1 - N_2)}{(1 - \epsilon_1) \sigma a(N_1) H(N_1)} \\ &= \frac{\sigma a(N_1) H(N_1)}{1 - \epsilon_1} \delta[k - \sigma a(N_1) H(N_1)] \delta(N_1 - N_2) . \end{aligned} \quad (2.136)$$

One can see that due to the presence of the  $\delta(N_1 - N_2)$  term,  $\xi_1$  and  $\xi_2$  are white noises, which means that the value they take at time  $N_1$  is uncorrelated with any of their previous (or future) realizations at times  $N_2$ , or said differently, that the noises have no memory of their previous history. Thanks to this property,  $\varphi$  describes a Markovian process.

However, one should note that this is directly due to our choice of a step function as the window function. If smooth window functions were considered instead, one would obtain coloured noises, and consequently non-Markovian processes [320, 321, 322]. This has important physical implications, since coloured noises directly affect the shape of the power spectrum [322] and provide an extra source to the production of non-Gaussianities [323]. Even though their treatment is more challenging, coloured noises can be argued to be better motivated, since a sharp cutoff in momentum space gives rise to a rather unnatural window function in position space, and since a wide class of smooth window functions give rise to the same asymptotic coloured noise, so that physical quantities remain independent of the exact shape of the window function.

More precisely, it was shown in Ref. [324] that the final correlations of the coarse-grained field are independent of the window function if it satisfies two properties. First, when written in position space, it must be chosen to be spherically symmetric and  $\mathbf{x}$ -dependent only through the combination  $|\mathbf{x}|/R$ , where  $R = 1/(\sigma a H)$  is the length scale over which coarse graining is performed. In this way,  $W$  is constrained to have the form  $W(x, N) \propto R^{-3} w(|x|/R)$ , when represented in position space. Second, the function  $w(s)$  must decrease at least as  $s^{-6}$  for  $s \gg 1$ . This is not the case for the Heaviside step window function which gives, after Fourier transform,

$$w_{\text{Heav}}(s) = \frac{\sin(s) - s \cos(s)}{2\pi^2 s^3} . \quad (2.137)$$

Such a window function is not everywhere positive and decays too slowly at large distances to satisfy the criterion mentioned above. For simplicity in the following, we will still work with the Heaviside step window function, but one may keep in mind that this choice is not without consequences.

Working with a Heaviside window function, one then obtains

$$\langle \xi_1(\mathbf{x}_1, N_1) \xi_1(\mathbf{x}_2, N_2) \rangle = \frac{(\sigma a H)^3}{2\pi^2} (1 - \epsilon_1) |\phi_{\mathbf{k}}|_{k=\sigma a H}^2 \frac{\sin(\sigma a H r)}{\sigma a H r} \delta(N_1 - N_2) . \quad (2.138)$$

Similarly, one gets for  $\langle \xi_2 \xi_2 \rangle$  and  $\langle \xi_1 \xi_2 \rangle$  the following expressions,

$$\langle \xi_2(\mathbf{x}_1, N_1) \xi_2(\mathbf{x}_2, N_2) \rangle = \frac{(\sigma a H)^3}{2\pi^2} (1 - \epsilon_1) \left| \frac{\partial \phi_{\mathbf{k}}}{\partial N} \right|_{k=\sigma a H}^2 \frac{\sin(\sigma a H r)}{\sigma a H r} \delta(N_1 - N_2), \quad (2.139)$$

$$\langle \xi_1(\mathbf{x}_1, N_1) \xi_2(\mathbf{x}_2, N_2) \rangle = \frac{(\sigma a H)^3}{2\pi^2} (1 - \epsilon_1) \left( \phi_{\mathbf{k}} \frac{\partial \phi_{\mathbf{k}}^*}{\partial N} \right)_{k=\sigma a H} \frac{\sin(\sigma a H r)}{\sigma a H r} \delta(N_1 - N_2), \quad (2.140)$$

and  $\langle \xi_2 \xi_1 \rangle$  is simply given by  $\langle \xi_1 \xi_2 \rangle^*$ .

#### 2.4.1.6. Case of a de Sitter Background

In practice, from here, one needs to calculate the amplitude of the Fourier modes  $\phi_{\mathbf{k}}$  over the background under consideration to work out the correlations of the noises  $\xi_1$  and  $\xi_2$ . This must be done by solving the equation of motion for the modes  $\phi_{\mathbf{k}}$ , which is given by the last bracketed term of Eq. (2.122). Here we give the solution in the specific case of a de Sitter background. When writing the equation for the modes in term of the time variable  $z \equiv k/(aH)$ , one obtains

$$\frac{d^2 \phi_{\mathbf{k}}}{dz^2} - \frac{2}{z} \frac{d\phi_{\mathbf{k}}}{dz} + \left( 1 + \frac{V''}{H^2 z^2} \right) \phi_{\mathbf{k}}. \quad (2.141)$$

If  $V''$  is taken to be constant, then the solutions of this equation are given by

$$\phi_{\mathbf{k}} = A_{\mathbf{k}} z^{3/2} H_{\nu}^{(1)}(z) + B_{\mathbf{k}} z^{3/2} H_{\nu}^{(2)}(z), \quad (2.142)$$

where  $H_{\nu}^{(1)}$  and  $H_{\nu}^{(2)}$  are the Hankel functions [269] of the first and second class respectively,  $A_{\mathbf{k}}$  and  $B_{\mathbf{k}}$  are integration constants, and

$$\nu = \frac{3}{2} \sqrt{1 - \frac{4V''}{9H^2}}. \quad (2.143)$$

As explained in section 2.3.2, the integration constants can be set by requiring that the perturbations are initiated in their Bunch-Davies vacuum state  $a\phi_{\mathbf{k}} = e^{-ik\eta}/\sqrt{2k}$ , see Eq. (2.62), when they are well inside the Hubble radius. Remember that  $\eta$  is the conformal time defined in Eq. (1.62). This amounts to choosing

$$\phi_{\mathbf{k}} \xrightarrow{z \gg 1} \frac{zH}{\sqrt{2kk}} e^{-iz}. \quad (2.144)$$

Since one has [269]  $H_{\nu}^{(1)}(z) \simeq \sqrt{2/(\pi z)} \exp[i(z - \nu\pi/2 - \pi/4)]$  and  $H_{\nu}^{(2)}(z) \simeq \sqrt{2/(\pi z)} \exp[-i(z - \nu\pi/2 - \pi/4)]$  when  $z \gg 1$ , this sets the integration constants to be  $A_{\mathbf{k}} = 0$  and  $B_{\mathbf{k}} = \sqrt{\pi}/2H/k^{3/2} \exp[-i\pi/2(\nu + 1/2)]$ , so that one has

$$\phi_{\mathbf{k}} = \frac{\sqrt{\pi}}{2} H \left( \frac{z}{k} \right)^{3/2} \exp \left[ -i \frac{\pi}{2} \left( \nu + \frac{1}{2} \right) \right] H_{\nu}^{(2)}(z). \quad (2.145)$$

This allows to evaluate  $\phi_{\mathbf{k}}$  when  $k = \sigma a H$ , that is when  $z = \sigma$ . Since one has [269]  $H_{\nu}^{(2)}(\sigma) \simeq i/\pi \Gamma(\nu) (\sigma/2)^{-\nu}$  when  $\sigma \ll 1$ , where  $\Gamma$  is the Euler Gamma function, one can write

$$(\sigma a H)^3 |\phi_{\mathbf{k}}|_{k=\sigma a H}^2 \simeq \frac{H^2}{4\pi} \Gamma^2(\nu) 2^{2\nu} \sigma^{3-2\nu}. \quad (2.146)$$

In the same manner, making use of the relation [269]  $dH_\nu^{(2)}(z)/dz = H_{\nu-1}^{(2)}(z) - \nu/zH_\nu^{(2)}(z) \simeq -\nu/zH_\nu^{(2)}(z)$  when  $z \ll 1$ , and since  $d/dN = -zd/dz$ , one has  $d\phi_{\mathbf{k}}/dN \simeq (\nu - 3/2)\phi_{\mathbf{k}}$  in this same limit, so that one obtains

$$(\sigma a H)^3 \left| \frac{d\phi_{\mathbf{k}}}{dN} \right|_{k=\sigma a H}^2 \simeq \frac{H^2}{4\pi} \Gamma^2(\nu) \left( \nu - \frac{3}{2} \right)^2 2^{2\nu} \sigma^{3-2\nu}, \quad (2.147)$$

$$(\sigma a H)^3 \left( \phi_{\mathbf{k}} \frac{d\phi_{\mathbf{k}}^*}{dN} \right)_{k=\sigma a H} \simeq \frac{H^2}{4\pi} \Gamma^2(\nu) \left( \nu - \frac{3}{2} \right) 2^{2\nu} \sigma^{3-2\nu}. \quad (2.148)$$

From here, when evaluated at the same point  $\mathbf{x}$  in space, the cross correlations (2.138)-(2.140) of the noises simply read

$$\langle \xi_1(N_1) \xi_1(N_2) \rangle = \left( \frac{H}{2\pi} \right)^2 \left( \frac{\sigma}{2} \right)^{3-2\nu} \frac{4\Gamma^2(\nu)}{\pi} \delta(N_1 - N_2), \quad (2.149)$$

$$\langle \xi_2(N_1) \xi_2(N_2) \rangle = \left( \frac{H}{2\pi} \right)^2 \left( \nu - \frac{3}{2} \right)^2 \left( \frac{\sigma}{2} \right)^{3-2\nu} \frac{4\Gamma^2(\nu)}{\pi} \delta(N_1 - N_2), \quad (2.150)$$

$$\langle \xi_1(N_1) \xi_2(N_2) \rangle = \left( \frac{H}{2\pi} \right)^2 \left( \nu - \frac{3}{2} \right) \left( \frac{\sigma}{2} \right)^{3-2\nu} \frac{4\Gamma^2(\nu)}{\pi} \delta(N_1 - N_2). \quad (2.151)$$

#### 2.4.1.7. Case of a Light Field

We now specify the noises amplitudes when the field is assumed to be light compared to the Hubble factor, that is when  $V'' \ll H$ . In this case, from Eq. (2.143), one has  $\nu \simeq 3/2$ . Looking back at Eqs. (2.149)-(2.151), this means that one simply has  $\xi_2 = 0$ , and that

$$\langle \xi_1(N_1) \xi_1(N_2) \rangle = \left( \frac{H}{2\pi} \right)^2 \delta(N_1 - N_2). \quad (2.152)$$

This is why it is convenient to express  $\xi_1$  in terms of a normalized white Gaussian noise  $\xi$  through  $\xi_1 = H/(2\pi)\xi$ , so that the Langevin equation for the coarse-grained field is simply given by

$$\frac{\partial^2 \varphi}{\partial N^2} + 3 \frac{\partial \varphi}{\partial N} + \frac{V'(\varphi)}{H^2} = 3 \frac{H}{2\pi} \xi. \quad (2.153)$$

#### 2.4.1.8. Case of a Slow-Rolling Field

Finally, if the field is experiencing slow roll, then as usual the second time derivative can be neglected in the equation of motion and one finally obtains

$$\frac{\partial \varphi}{\partial N} + \frac{V'(\varphi)}{3H^2} = \frac{H}{2\pi} \xi, \quad (2.154)$$

which corresponds to the announced equation (2.116) and which was first derived in Ref. [290].

### 2.4.2. Why should we use the Number of $e$ -folds as the Time Variable in the Langevin equations?

In section 2.4.1, the Langevin equation has been worked out in terms of the number of  $e$ -folds  $N$ . A priori, another time variable could have been used, such as cosmic time  $t$  for example.

Indeed, in a number of papers (see *e.g.* Refs. [325, 326, 289, 327, 324, 328, 329, 330, 331]), the Langevin equation is written and solved in terms of  $t$  instead of  $N$ . However, this choice is not without consequences since the transformation from  $t$  to  $N$  makes use of the stochastic function  $H[\varphi(t)]$  and as a consequence, leads to a physically different stochastic process with different probability distributions.

### 2.4.2.1. Steady-State Distributions

The claim we just made can be easily established [289, 332, 333] when deriving *e.g.* the steady-state distribution associated with the stochastic process under study, for different time variables. This distribution can be obtained writing the Fokker-Planck equation for  $P(\phi, N)$ , which is the probability density for the coarse-grained field to take the value  $\phi$  at time  $N$ . If one starts from the Langevin equation (2.116) written in terms of  $N$ , in the Itô interpretation [334], one obtains

$$\frac{\partial}{\partial N} P(\phi, N) = \frac{\partial}{\partial \phi} \left[ \frac{V'}{3H^2} P(\phi, N) \right] + \frac{\partial^2}{\partial \phi^2} \left[ \frac{H^2}{8\pi^2} P(\phi, N) \right]. \quad (2.155)$$

If we denote the steady-state probability distribution by  $P_{\text{stat}}(\phi)$ , the equation for  $P_{\text{stat}}(\phi)$  is simply given by  $\partial P_{\text{stat}}(\phi)/\partial N = 0$ , that is

$$\frac{\partial}{\partial \phi} \left\{ \frac{V'}{3H^2} P_{\text{stat}}(\phi) + \frac{\partial}{\partial \phi} \left[ \frac{H^2}{8\pi^2} P_{\text{stat}}(\phi) \right] \right\} \equiv \frac{\partial J}{\partial \phi} = 0, \quad (2.156)$$

where  $J$  denotes the probability current. This current thus needs to be independent of  $\phi$  in the steady-state case. In most interesting cases, it is actually 0. For example, if  $\phi$  can take unbounded values, since  $\int P_{\text{stat}}(\phi) d\phi = 1$ ,  $P_{\text{stat}}(\phi)$  needs to decrease at infinity strictly faster than  $|\phi|^{-1}$ . In this case,  $P_{\text{stat}}(\phi)$  and  $\partial P_{\text{stat}}(\phi)/\partial \phi$  vanish at infinity and  $J$  is 0 at infinity, hence everywhere. This yields quite a simple equation to solve for  $P_{\text{stat}}(\phi)$ , and one obtains

$$P_{\text{stat}}(\phi) \propto \frac{24\pi^2 M_{\text{Pl}}^4}{V(\phi)} \exp \left[ \frac{24\pi^2 M_{\text{Pl}}^4}{V(\phi)} \right], \quad (2.157)$$

where there is an overall integration constant chosen so that the distribution is normalized,  $\int P_{\text{stat}}(\phi) d\phi = 1$ , and that for simplicity we do not display here. Now, let us redo the same calculation, but starting this time from the Langevin equation written in terms of cosmic time  $t$ . Performing a simple change of time variable in Eq. (2.116), the later is given by

$$\frac{d\tilde{\phi}}{dt} = -\frac{V'}{3H} + \frac{H^{3/2}}{2\pi} \xi(t), \quad (2.158)$$

where we use the notation  $\tilde{\phi}$  to stress the fact that *a priori*,  $\tilde{\phi}$  is not the same stochastic process as  $\phi$ . The Fokker-Planck equation corresponding to the above equation reads

$$\frac{\partial}{\partial t} \tilde{P}(\tilde{\phi}, N) = \frac{\partial}{\partial \tilde{\phi}} \left[ \frac{V'}{3H} \tilde{P}(\tilde{\phi}, N) \right] + \frac{\partial^2}{\partial \tilde{\phi}^2} \left[ \frac{H^3}{8\pi^2} \tilde{P}(\tilde{\phi}, N) \right]. \quad (2.159)$$

In the same manner as before, this equation can be written as  $\partial \tilde{P}/\partial t = \partial \tilde{J}/\partial \tilde{\phi}$ , and requiring that the current  $\tilde{J}$  vanishes gives rise to a differential equation for the steady-state distribution  $\tilde{P}_{\text{stat}}(\tilde{\phi})$  that can easily be solved, and one obtains

$$\tilde{P}_{\text{stat}}(\tilde{\phi}) \propto \left[ \frac{24\pi^2 M_{\text{Pl}}^4}{V(\tilde{\phi})} \right]^{3/2} \exp \left[ \frac{24\pi^2 M_{\text{Pl}}^4}{V(\tilde{\phi})} \right]. \quad (2.160)$$

This is, as announced, explicitly different from Eq. (2.157). In this calculation, it can also be made explicit that this difference is intimately related with the fact that the amplitude of the noise depends on the coarse grained field through the function  $H(\phi)$ . Indeed, if one does the same calculation but assume that  $H$  is a constant, then one obtains the same stationary distribution for the two time variables,  $P_{\text{stat}} = \tilde{P}_{\text{stat}} \propto \exp(24\pi^2 M_{\text{Pl}}^4/V)$ .

In any case, with the example of the steady-state distribution, we have shown that different time variables for the Langevin equation correspond to different stochastic processes. This is why, in the following, we identify the correct time variable one must work with when dealing with stochastic inflation.

### 2.4.2.2. Perturbations Equation derived from the Background Equation

As suggested in Ref. [335], since the Langevin equation was obtained in section 2.4.1 by performing an expansion in  $\phi_{>}$  in the equation of motion directly, the correct time variable should be the one such that the equations for the perturbations, which must be established at the action level, can correctly be obtained from varying the equation of motion for the background itself, when written in terms of this time variable. In this section, we establish that this condition selects out  $N$  as the time variable. This is of course an heuristic argument only, and a more rigorous derivation of this result will be presented in section 2.4.2.3 where it will be shown that  $N$  only allows to reproduce results from Quantum Field Theories.

In the case where inflation is driven by a single scalar field  $\phi$ , the action we start from,  $S = S_{\text{grav}} + S_{\phi}$  where  $S_{\text{grav}}$  is given by Eq. (1.10) and  $S_{\phi}$  is given by Eq. (2.1), reads

$$S = \int d^4x \sqrt{-g} \left[ \frac{M_{\text{Pl}}^2}{2} R - \frac{1}{2} g^{\mu\nu} \partial_{\mu} \phi \partial_{\nu} \phi - V(\phi) \right]. \quad (2.161)$$

From this action (and this action only), we first want to derive equations of motion for the scalar perturbations, that can be compared with what will be obtained below from varying the equation of motion itself. To make our point even more convincing, we go up to second order in the perturbations. This is why we expand the background fields  $\{\phi, g_{\mu\nu}\}$  at second order in the non-homogeneous scalar perturbations, without fixing any gauge for the moment. With the same notations as in section 2.3.1, when the time variable in the metric is the conformal time  $\eta$ , one has

$$\begin{aligned} \phi(\eta, \vec{x}) &= \phi^{(0)}(\eta) + \phi^{(1)}(\eta, \vec{x}) + \frac{1}{2} \phi^{(2)}(\eta, \vec{x}), \\ g_{00} &= a^2 \left[ -1 - 2\alpha^{(1)} - \alpha^{(2)} \right], & g_{i0} &= -a^2 \left[ \partial_i B^{(1)} + \frac{1}{2} \partial_i B^{(2)} \right], \\ g_{ij} &= a^2 \left\{ \delta_{ij} \left[ 1 - 2\psi^{(1)} - \psi^{(2)} \right] + 2\partial_i \partial_j \left[ E^{(1)} + \frac{1}{2} E^{(2)} \right] \right\}. \end{aligned} \quad (2.162)$$

Here we have not displayed vector and tensor perturbations, as in Eq. (2.35). As explained in section 2.3.1, the degrees of freedom introduced above are partially redundant and in absence of anisotropic stress, the scalar sector can be described in terms of a single gauge invariant variable. One possible choice is the Mukhanov-Sasaki variable [122, 241, 242]  $v$ , which can be defined, order by order, as the scalar field fluctuation  $\phi^{(n)}$  on uniform curvature hypersurfaces [336]. To

first and second orders, after a lengthy but straightforward calculation, one obtains [337]

$$v^{(1)} = \phi^{(1)} + \frac{(\phi^{(0)})'}{\mathcal{H}} \psi^{(1)}, \quad (2.163)$$

$$\begin{aligned} v^{(2)} = & \phi^{(2)} + \frac{(\phi^{(0)})'}{\mathcal{H}} \psi^{(2)} + \left(\frac{\psi_1}{\mathcal{H}}\right)^2 \left[ (\phi^{(0)})'' + 2\mathcal{H} (\phi^{(0)})' - \frac{\mathcal{H}'}{\mathcal{H}} (\phi^{(0)})' \right] \\ & + 2 \frac{(\phi^{(0)})'}{\mathcal{H}^2} \psi_1' \psi_1 + 2 \frac{\psi_1}{\mathcal{H}} (\phi^{(1)})'. \end{aligned} \quad (2.164)$$

From varying the expanded action, one can derive an equation of motion for the scalar perturbations, and in particular for a gauge invariant combination of them, say the Mukhanov-Sasaki variable. In this section, we want to compare this action-based equation of motion for the scalar perturbations with an equation of motion for the perturbation in  $\phi$  coming from varying the background Klein-Gordon equation. It is therefore important to work in a gauge where these two quantities,  $v$  and the perturbation in  $\phi$ , can be identified. By definition of the Mukhanov-Sasaki variable, this is the case in the Uniform Curvature Gauge, for which one has

$$v^{(n)} = \phi^{(n)} \quad (2.165)$$

to all orders. In this gauge, one notably has  $\psi = 0$  to all orders, which indeed gives Eq. (2.165) at first and second order starting from Eqs. (2.163) and (2.164).

The equation of motion for the scalar perturbations  $\phi^{(1)}$  and  $\phi^{(2)}$  is therefore given by the one for  $v^{(1)}$  and  $v^{(2)}$  in this gauge. At leading order in the slow-roll approximation, and in the long wavelength limit, they read<sup>9</sup>

$$3H\dot{\phi}^{(1)} + \left( V'' - \frac{V'^2}{3H^2 M_{\text{Pl}}^2} \right) \phi^{(1)} = 0, \quad (2.166)$$

$$3H\dot{\phi}^{(2)} + \left( V'' - \frac{V'^2}{3H^2 M_{\text{Pl}}^2} \right) \phi^{(2)} = -\frac{1}{2} \left( V''' - \frac{V'V''}{H^2 M_{\text{Pl}}^2} + \frac{2V'^3}{9H^4 M_{\text{Pl}}^4} \right) \phi^{(1)2}. \quad (2.167)$$

We now need to compare these equations with the ones that arise when varying the equation of motion for the background, and find out for which time variable they match.

### If $t$ is used

When cosmic time  $t$  is used, the leading order of the slow-roll approximation for the Klein-Gordon equation for the background is given by Eq. (2.12),

$$\frac{d\phi}{dt} = -\frac{V'}{3H(\phi)}, \quad (2.168)$$

<sup>9</sup>In spite of the complexity of the field equations at second order, see *e.g.* Ref. [338], in the long wavelength limit, it is sufficient [339] to use the local conservation of energy-momentum to establish Eqs. (2.166) and (2.167). Because this is not the main subject of this section, the corresponding calculations are not reproduced here but they can be found in Refs. [339, 336].

where we take  $H^2 \simeq V/(3M_{\text{Pl}}^2)$  at leading order in slow roll. When plugging  $\phi = \phi^{(0)} + \phi^{(1)} + \phi^{(2)}$  in this equation, one obtains at first and second order in the perturbations

$$3H\ddot{\phi}^{(1)} + \left( V'' - \frac{V'^2}{6H^2M_{\text{Pl}}^2} \right) \tilde{\phi}^{(1)} = 0, \quad (2.169)$$

$$3H\ddot{\phi}^{(2)} + \left( V'' - \frac{V'^2}{6H^2M_{\text{Pl}}^2} \right) \tilde{\phi}^{(2)} = -\frac{1}{2} \left( V''' - \frac{V'V''}{2H^2M_{\text{Pl}}^2} + \frac{V'^3}{12H^4M_{\text{Pl}}^4} \right) \tilde{\phi}^{(1)2}. \quad (2.170)$$

One should stress that these equations do not apply to  $\phi^{(1)}$  and  $\phi^{(2)}$  since they are different from Eqs. (2.166) and (2.167), which is why we use the notation  $\tilde{\phi}^{(1,2)}$  instead of  $\phi^{(1,2)}$ . The differences with Eqs. (2.166) and (2.167) are displayed in red. One can see that several factors do not match. This is because in general, the equations for the perturbations must be derived from the action itself and cannot be obtained by simply varying the equation of motion for the background.

### If $ds = H^p a^q dt$ is used

For this reason, let us look for a time variable  $s$  which is such that the equations for the perturbations arise from varying the equation of motion for the background when written in terms of  $s$ . Let us assume that  $s$  is related to  $t$  thanks to a relation of the form

$$ds = H^p(\phi) a^q(\phi) dt, \quad (2.171)$$

where  $p$  and  $q$  are power indexes that we try to determine. For example, when  $p = 0$  and  $q = 0$ ,  $s$  is the cosmic time  $t$ , when  $p = 1$  and  $q = 0$ ,  $s$  is the number of  $e$ -folds  $N$ , while when  $p = 0$  and  $q = -1$ ,  $s$  is the conformal time  $\eta$ . In terms of  $s$ , the equation of motion for the background is given by

$$\frac{d\phi}{ds} = -\frac{V'}{3H^{p+1}(\phi)}, \quad (2.172)$$

where again we take  $H^2 \simeq V/(3M_{\text{Pl}}^2)$  at leading order in slow roll. When plugging  $\phi = \phi^{(0)} + \phi^{(1)} + \phi^{(2)}$ , one obtains at first and second order in the perturbations

$$3H\dot{\tilde{\phi}}^{(1)} + \left( V'' - \frac{p+1}{6} \frac{V'^2}{H^2M_{\text{Pl}}^2} + 3qH^2 \right) \tilde{\phi}^{(1)} = 0, \quad (2.173)$$

$$3H\dot{\tilde{\phi}}^{(2)} + \left( V'' - \frac{p+1}{6} \frac{V'^2}{H^2M_{\text{Pl}}^2} + 3qH^2 \right) \tilde{\phi}^{(2)} = -\frac{1}{2} \left[ V''' - \frac{p+1}{2} \frac{V'V''}{H^2M_{\text{Pl}}^2} + \frac{(p+1)(p+3)}{36} \frac{V'^3}{H^4M_{\text{Pl}}^4} + 3q \frac{H^2V''}{V'} - pq \frac{V'}{M_{\text{Pl}}^2} - 18q \frac{H^4}{V'} \right] \tilde{\phi}^{(1)2}. \quad (2.174)$$

Again, these equations do not apply to  $\phi^{(1)}$  and  $\phi^{(2)}$  in general since the correct ones are given by Eqs. (2.166) and (2.167) which is why we use the notation  $\tilde{\phi}^{(1,2)}$ . The differences between these two sets of equations are displayed in red. In order for the above to match Eqs. (2.166) and (2.167), one must have  $q = 0$  and  $(p+1)/6 = 1/3$  which gives  $p = 1$ ,  $(p+1)/2 = 1$  which also gives  $p = 1$ , and  $(p+1)(p+3)/36 = 2/9$  which gives  $p = 1$  or  $p = -5$ . As a conclusion, with  $p = 1$  and  $q = 0$  only, the equations for the perturbations (from what is shown here, up to second order in perturbation theory) can be seen as if they were derived from varying the equation of motion for the background. This choice corresponds to the number of  $e$ -folds  $N$ .

### 2.4.2.3. Stochastic Inflation and QFT on Curved Space-Times

To go beyond this heuristic argument, one can explicitly show [299, 300] that  $N$  is the time variable which allows to consistently connect stochastic inflation with results of QFT on curved space-times. For example, let us consider the leading order of the fluctuations  $\delta\phi = \varphi - \phi_{\text{cl}}$  in the coarse-grained inflaton field about its classical background value  $\phi_{\text{cl}}$ . By “classical”, we mean that  $\phi_{\text{cl}}$  is the solution of the equation of motion without the noise term. We want to compute the mean square value of  $\delta\phi$  and compare what we obtain to results coming from QFT calculations. For example, in Ref. [340], with renormalization obtained by employing the adiabatic subtraction prescription on inflationary backgrounds, it was shown that in quadratic inflation where  $V = m^2\phi^2/2$ , if  $\delta\phi = 0$  at time  $t_0$ , one has at leading order see Eq. (48) of Ref. [340]

$$\langle (\phi - \phi_{\text{cl}})^2 \rangle = \frac{H_0^6 - H^6}{8\pi^2 m^2 H^2}, \quad (2.175)$$

where  $H$  means  $H(\phi_{\text{cl}})$  and  $H_0$  means  $H$  evaluated at time  $t_0$ . In the same manner, in Ref. [341], it was shown that in power-law inflation where  $a(t) \propto t^p$  with  $p \gg 1$ , the same quantity is given by see Eq. (29) of Ref. [341]

$$\langle (\phi - \phi_{\text{cl}})^2 \rangle = \frac{p}{8\pi^2} (H_0^2 - H^2). \quad (2.176)$$

Let us see how these results can be derived in the stochastic inflationary framework. We start from the Langevin equation (2.116) that we write

$$\frac{d\varphi}{dN} = -2M_{\text{Pl}}^2 \frac{H'}{H} + \frac{H}{2\pi} \xi(N) \quad (2.177)$$

where we have used  $H^2 \simeq V/(3M_{\text{Pl}}^2)$  and where a prime denotes a derivative with respect to the inflaton field. Since  $\phi_{\text{cl}}$  is the solution of the above equation without the noise term, the noise term can be considered as a perturbation captured in  $\delta\phi$ . After expanding Eq. (2.177) in powers of  $\delta\phi$ , one gets for the leading order  $\delta\phi^{(1)}$

$$\frac{d\delta\phi^{(1)}}{dN} + 2M_{\text{Pl}}^2 \left( \frac{H'}{H} \right)' \delta\phi^{(1)} = \frac{H}{2\pi} \xi. \quad (2.178)$$

Multiplying this equation by  $\delta\phi^{(1)}$  and taking the stochastic average leads to

$$\frac{d\langle \delta\phi^{(1)2} \rangle}{dN} + 4M_{\text{Pl}}^2 \left( \frac{H'}{H} \right)' \langle \delta\phi^{(1)2} \rangle = \frac{H}{\pi} \langle \xi \delta\phi^{(1)} \rangle. \quad (2.179)$$

In order to obtain a differential equation for  $\langle \delta\phi^{(1)2} \rangle$  only, one needs to evaluate the right hand side of the previous equation. This can be done as follows. Letting  $\delta\phi^{(1)} = 0$  at time  $N_0$ , a formal solution of Eq. (2.178) is given by

$$\delta\phi^{(1)} = \exp \left[ -2M_{\text{Pl}}^2 \int_{N_0}^N \left( \frac{H'}{H} \right)' dn \right] \int_{N_0}^N \left\{ \frac{H}{2\pi} \xi(n) \exp \left[ 2M_{\text{Pl}}^2 \int_{N_0}^n \left( \frac{H'}{H} \right)' d\bar{n} \right] \right\} dn. \quad (2.180)$$

From this expression, since  $\langle \xi(N) \xi(N') \rangle = \delta(N - N')$ , it is straightforward to see that<sup>10</sup>

$$\langle \xi \delta\phi^{(1)} \rangle = \frac{H}{4\pi}. \quad (2.181)$$

<sup>10</sup>The 1/2 factor comes from the rule  $\int_{x_1}^{x_2} f(x)\delta(x - x_2)dx = f(x_2)/2$  when the Dirac function is centred at a boundary of the integral.

This is why one obtains

$$\frac{d\langle\delta\phi^{(1)2}\rangle}{dN} + 4M_{\text{Pl}}^2 \left(\frac{H'}{H}\right)' \langle\delta\phi^{(1)2}\rangle = \frac{H^2}{4\pi^2}. \quad (2.182)$$

Since the equation of motion for  $\phi_{\text{cl}}$  is simply given by  $dN = -H/(2H'M_{\text{Pl}}^2)d\phi_{\text{cl}}$ , one can change the time variable from  $N$  to  $\phi_{\text{cl}}$  and the formal solution of the above equation can be written as

$$\langle\delta\phi^{(1)2}\rangle = -\frac{1}{8\pi^2 M_{\text{Pl}}^2} \frac{H'^2}{H^2} \int \frac{H^5}{H'^3} d\phi_{\text{cl}}. \quad (2.183)$$

For quadratic inflation where  $H = m\phi/(\sqrt{6}M_{\text{Pl}})$ , this exactly gives rise to Eq. (2.175) while for power-law inflation where<sup>11</sup>  $H = H_0 \exp[-1/\sqrt{2p}(\phi - \phi_0)/M_{\text{Pl}}]$ , one exactly obtains Eq. (2.176). Therefore, stochastic and standard field-theoretical approaches to inflation produce the same results for the amount of field fluctuations. Here we have established this property at leading order in perturbation theory. However, as shown in Refs. [290, 298], the stochastic approach can reproduce QFT results for any finite number of scalar loops and even beyond.

To emphasize the specificity of  $N$  as a preferred time variable choice, let us repeat the same procedure using the Langevin equation written in terms of  $t$ ,

$$\frac{d\tilde{\phi}}{dt} = -2M_{\text{Pl}}^2 H' + \frac{H^{3/2}}{2\pi} \xi(t). \quad (2.184)$$

Since this corresponds to a different stochastic process as the one written in terms of  $N$ , we use again the notation  $\tilde{\phi}$  instead of  $\phi$ . At leading order in the noise, one obtains for  $\delta\tilde{\phi}^{(1)}$

$$\frac{d\delta\tilde{\phi}^{(1)}}{dt} + 2M_{\text{Pl}}^2 H'' \delta\tilde{\phi}^{(1)} = \frac{H^{3/2}}{2\pi} \xi(t). \quad (2.185)$$

Again, multiplying this equation by  $\delta\tilde{\phi}^{(1)}$  and taking the stochastic average leads to

$$\frac{d\langle\delta\tilde{\phi}^{(1)2}\rangle}{dt} + 4M_{\text{Pl}}^2 H'' \langle\delta\tilde{\phi}^{(1)2}\rangle = \frac{H^{3/2}}{\pi} \langle\xi(t) \delta\tilde{\phi}^{(1)}\rangle. \quad (2.186)$$

In the same manner as before, making use of the formal solution to Eq. (2.185),

$$\delta\tilde{\phi}^{(1)} = \exp\left[-2M_{\text{Pl}}^2 \int_{t_0}^t H'' du\right] \int_{t_0}^t \left\{ \frac{H^{3/2}}{2\pi} \xi(u) \exp\left[2M_{\text{Pl}}^2 \int_{t_0}^u H'' dv\right] \right\} du, \quad (2.187)$$

one can show that  $\langle\xi(t) \delta\tilde{\phi}^{(1)}\rangle = H^{3/2}/(4\pi)$ , so that one needs to solve

$$\frac{d\langle\delta\tilde{\phi}^{(1)2}\rangle}{dt} + 4M_{\text{Pl}}^2 H'' \langle\delta\tilde{\phi}^{(1)2}\rangle = \frac{H^3}{4\pi^2}. \quad (2.188)$$

Making use of the classical trajectory  $dt = -d\phi_{\text{cl}}/(2M_{\text{Pl}}^2 H')$ , one obtains<sup>12</sup>

$$\langle\delta\tilde{\phi}^{(1)2}\rangle = -\frac{H'^2}{8\pi^2 M_{\text{Pl}}^2} \int \frac{H^3}{H'^3} d\phi_{\text{cl}} \quad (2.189)$$

<sup>11</sup>In section 3.2, it is shown that the potential associated with power-law inflation, for which  $a(t) \propto t^p$ , is given by  $V(\phi) \propto e^{-\sqrt{2/p}\phi/M_{\text{Pl}}}$ . Since  $H^2 = V(\phi)/(3M_{\text{Pl}}^2)$  at leading order in slow roll, one obtains the given  $H(\phi)$  profile.

<sup>12</sup>This equation (2.189) also matches Eq. (13) of Ref. [328] where perturbative solutions of stochastic inflation are derived when formulated in terms of the cosmic time.

which is clearly different from Eq. (2.183).<sup>13</sup> For example, for quadratic inflation, it reduces to  $\langle \delta\tilde{\phi}^{(1)2} \rangle = 3(H_0^4 - H^4)/(16\pi^2 m^2)$  which does not coincide with Eq. (2.175) and for power-law inflation, it reduces to  $\langle \delta\tilde{\phi}^{(1)2} \rangle = p H^2 / (4\pi^2) \ln(H_0/H)$  which does not coincide with Eq. (2.176).

Finally and in passing, let us derive the corresponding results for the leading order of the mean fluctuation  $\langle \delta\phi \rangle$ . Since from Eq. (2.178) it is clear that  $\langle \delta\phi^{(1)} \rangle = 0$ , one has to work out  $\langle \delta\phi^{(2)} \rangle$ . Expanding  $\varphi = \phi_{\text{cl}} + \delta\phi^{(1)} + \delta\phi^{(2)}$  in Eq. (2.177), one obtains

$$\frac{d\delta\phi^{(2)}}{dN} + 2M_{\text{Pl}}^2 \left( \frac{H'}{H} \right)' \delta\phi^{(2)} + M_{\text{Pl}}^2 \left( \frac{H'}{H} \right)'' \delta\phi^{(1)2} = \frac{H'}{2\pi} \delta\phi^{(1)} \xi(N). \quad (2.190)$$

When taking the stochastic average of the above equation,  $\langle \delta\phi^{(1)2} \rangle$  is given by Eq. (2.183) and  $\langle \delta\phi^{(1)} \xi \rangle$  is given by Eq. (2.181), so that one obtains

$$\frac{d\langle \delta\phi^{(2)} \rangle}{dN} + 2M_{\text{Pl}}^2 \left( \frac{H'}{H} \right)' \langle \delta\phi^{(2)} \rangle = \frac{1}{8\pi^2} \left( \frac{H'}{H} \right)'' \left( \frac{H'}{H} \right)^2 \int \frac{H^5}{H'^3} d\phi + \frac{HH'}{8\pi^2}. \quad (2.191)$$

Using the classical trajectory  $d\phi_{\text{cl}} = -2M_{\text{Pl}}^2 H' / H dN$ , this equation can be written in terms of  $\phi_{\text{cl}}$ , and after integration by parts, this gives rise to

$$\langle \delta\phi^{(2)} \rangle = \frac{1}{2} \frac{(H'/H)'}{H'/H} \langle \delta\phi^{(1)2} \rangle + \frac{1}{32M_{\text{Pl}}^2 \pi^2} \frac{H'}{H} \left( \frac{H_0^4}{H_0'^2} - \frac{H^4}{H'^2} \right), \quad (2.192)$$

where  $\langle \delta\phi^{(1)2} \rangle$  is given by Eq. (2.181). For example, when applied to quadratic inflation where  $V = m^2 \phi^2 / 2$ , one obtains

$$\langle \delta\phi^{(2)} \rangle = \frac{\sqrt{6}}{96\pi^2 m M_{\text{Pl}} H} \left[ \frac{H^6 - H_0^6}{H^2} - 3(H^4 - H_0^4) \right], \quad (2.193)$$

which corresponds to Eq. (49) of Ref. [299]. However, it is again worth noting that one would have obtained a completely different result starting from the Langevin equation written in terms of cosmic time  $t$ , namely<sup>14</sup>

$$\langle \delta\tilde{\phi}^{(2)} \rangle = \frac{1}{2} \frac{H''}{H'} \langle \delta\tilde{\phi}^{(1)2} \rangle + \frac{H'}{32\pi^2 M_{\text{Pl}}^2} \left( \frac{H_0^3}{H_0'^2} - \frac{H^3}{H'^2} \right). \quad (2.194)$$

This obviously differs from Eq. (2.192).

To summarize the discussion, different time variables in the Langevin equation lead to different stochastic processes, and the only time variable which allows the stochastic inflation formalism to reproduce QFT calculations is the number of  $e$ -folds  $N$ . One should therefore always work with  $N$  when dealing with stochastic inflation.

### 2.4.3. Stochastic Inflation and the Scalar Power Spectrum

In the previous section, we saw that stochastic inflation is able to reproduce QFT results, and we mentioned that this is even true beyond the linear order [298, 302, 299, 300, 301] in

<sup>13</sup>As shown below in section 2.4.3.1, this difference is crucial since it leads *e.g.* to an incorrect result for the power spectrum of scalar perturbations.

<sup>14</sup>This equation (2.194) matches Eq. (15) of Ref. [328] where perturbative solutions of the Langevin equation are derived when formulated in terms of the cosmic time.

perturbations theory. Let us see how this interesting property shall be used. The calculation of the corrections to the power spectrum that arise when perturbations are worked out beyond the linear order [342, 343, 344] is a difficult task, see for example Refs. [345, 346]. Indeed, already at second order, the perturbed Einstein equations  $\delta G_{\mu\nu} = \delta T_{\mu\nu}$  are cumbersome. However, as we saw explicitly in sections 2.4.2.2 and 2.4.2.3, stochastic inflation can lead to the same results as the ones coming from a  $\delta G_{\mu\nu} = \delta T_{\mu\nu}$  calculation, by means of a Langevin Klein-Gordon equation. This is why in this section, we calculate the power spectrum of scalar adiabatic perturbations, starting from the Langevin equation, and at any order in the noise term.

At linear order, this problem has been treated in Refs. [327, 322, 331] by expanding the coarse-grained field about its classical counterpart at first order,  $\varphi = \phi_{\text{cl}} + \delta\phi^{(1)}$ , where  $\phi_{\text{cl}}$  is the solution of the Langevin equation (2.116) without the noise term, and by calculating the statistical moments of  $\delta\phi^{(1)}$  making use of the same techniques as in section 2.4.2.3. The correlation functions of  $\delta\phi^{(1)}$  are related to the power spectrum  $\mathcal{P}_\zeta$  of curvature perturbations thanks to the relation [331]

$$\mathcal{P}_\zeta \simeq \frac{1}{H(\phi_{\text{cl}})} \frac{d}{dt} \left\{ \left[ \frac{H(\phi_{\text{cl}})}{\dot{\phi}_{\text{cl}}} \right]^2 \left\langle [\delta\phi^{(1)}]^2 \right\rangle \right\}. \quad (2.195)$$

In this expression, the right hand side needs to be evaluated when the scale associated with the wavenumber  $k$  (for which the power spectrum is calculated) exits the Hubble radius. In the references mentioned above, it is important to stress that the Langevin equations are solved in terms of  $t$  as the time variable, whereas we have shown in section 2.4.2 that the number of  $e$ -folds  $N$  must be used instead. This has important consequences. Indeed, if one plugs the expression (2.183) obtained for  $\langle \delta\phi^{(1)2} \rangle$  using the number of  $e$ -folds as the time variable into Eq. (2.195), one obtains for the power spectrum  $\mathcal{P}_\zeta$  evaluated at the wavenumber  $k$

$$\mathcal{P}_\zeta \simeq \left[ \frac{H(\phi_{\text{cl}})}{2\pi} \right]^2 \frac{1}{2M_{\text{Pl}}^2 \epsilon_1(\phi_{\text{cl}})}, \quad (2.196)$$

where as above,  $\phi_{\text{cl}}$  needs to be evaluated when the scale associated with the wavenumber  $k$  (for which the power spectrum is calculated) exits the Hubble radius. This expression exactly matches the standard result (2.110) recovered below, see Eq. (2.205). However, if one makes use of the cosmic time  $t$  as the time variable and plugs Eq. (2.189) into Eq. (2.195), one obtains instead

$$\mathcal{P}_{\tilde{\zeta}} \simeq \left[ \frac{H(\phi_{\text{cl}})}{2\pi} \right]^2 \frac{1}{2M_{\text{Pl}}^2 \epsilon_1(\phi_{\text{cl}})} \left\{ 1 + 2 \left[ \frac{H'(\phi_{\text{cl}})}{H(\phi_{\text{cl}})} \right]^2 \int^{\phi_{\text{cl}}} \left[ \frac{H(\phi_{\text{cl}})}{H'(\phi_{\text{cl}})} \right]^3 d\phi \right\} \quad (2.197)$$

$$= \mathcal{P}_\zeta \left\{ 1 + 2 \left[ \frac{H'(\phi_{\text{cl}})}{H(\phi_{\text{cl}})} \right]^2 \int^{\phi_{\text{cl}}} \left[ \frac{H(\phi_{\text{cl}})}{H'(\phi_{\text{cl}})} \right]^3 d\phi \right\}. \quad (2.198)$$

Here we have adopted the same notation as in section 2.4.2 where a tilde stresses that not the same quantity is actually worked out and  $\zeta$  is not  $\tilde{\zeta}$ . This result exactly matches Eq (2.11) of Ref. [331]. However, when in this work it is concluded that, because of the second term in the braces of Eq. (2.198) which is always negative, “the amplitude of the spectrum in the stochastic approach is in general reduced with respect to the amplitude in the standard approach”, one can see that such a statement is incorrect since the extra term in Eq. (2.198) is entirely due to a bad choice of time variable. This is why, if such an approach were to be followed and generalized to higher orders, it would again be crucial to work with  $N$  as the time variable contrary to what is done in the references mentioned above.

Another strategy is followed in Refs. [347, 348, 349], where methods of statistical physics, such as replica field theory, are employed in a stochastic inflationary context in the case of a free test

field evolving in a de Sitter or power-law background. In particular, dependence on the window function  $W$  is studied and it is shown that the effects associated with the choice of the window function vanish at late time so that the power spectrum calculated at the end of inflation is rather independent on  $W$ .

Finally, in Refs. [350, 351], the  $\delta N$  formalism is used to relate the curvature perturbations to the number of  $e$ -folds perturbations. The Langevin equation is solved numerically over a large number of realizations, and the power spectrum is computed in this manner, numerically, for quadratic potentials and hybrid potentials.

This is this last route that we chose to follow here, since it does not rely on a perturbative expansion in the noise terms and it therefore allows us to describe regimes where the stochastic effects are large. The  $\delta N$  formalism proves very helpful since it relates the scalar power spectrum to stochastic properties of a family of background trajectories, and it is thus well suited to address the issue of stochastic effects on the scalar power spectrum. For the first time, we derive fully analytical and non perturbative results that apply to any single-field potential, and which do not require a numerical solution of the Langevin equation. These results allow us to prove that the usual power spectrum is recovered in the classical limit, for any potential, and to discuss qualitatively and quantitatively the modifications to the standard result that arise due to the stochastic effects. The work presented here has not been pre-printed or published yet since it has been derived in the course of drafting this manuscript.

In this section, we first briefly describe how the  $\delta N$  formalism proceeds. We then turn to the stochastic inflation equations for which we provide generic formal results about ending points probabilities, mean number of  $e$ -folds and dispersion in the number of  $e$ -folds. For each quantity, we derive analytical non perturbative results that we compute explicitly for the “large field” potential ( $V \propto \phi^p$ ) as an illustrative example. We then derive the generic curvature perturbations power spectrum computed in stochastic inflation, again without using any expansion in the noise term. We make sure that in the classical limit (that we pay attention to carefully define), the standard result (2.110) is recovered. Finally, we completely work out the large field example for which we precisely calculate and discuss the stochastic effects on the scalar power spectrum and its tilt.

### 2.4.3.1. The $\delta N$ Formalism

Based on generic considerations, the  $\delta N$  formalism [125, 352, 353, 354, 355, 356] enables to relate statistical properties of cosmological perturbations to the distributions of number of  $e$ -folds in some family of homogeneous universes. This leads the way to a very powerful frame of calculation that we now briefly describe. As explained in section 2.3.1, starting from the Friedmann-Lemaître-Robertson-Walker line element  $ds^2 = -dt^2 + a^2(t)\delta_{ij}dx^i dx^j$ , deviations from homogeneity and isotropy can be included in a more general metric, which contains some gauge redundancy. A specific gauge choice consists in setting the fixed  $t$ -slices of space-time to have uniform energy density, and the fixed  $x$ -worldlines to be comoving. When doing so, the perturbed metric becomes [357, 288]

$$ds^2 = -dt^2 + a^2(t)e^{2\zeta(t,\mathbf{x})}\gamma_{ij}(t,\mathbf{x}), \quad (2.199)$$

where  $\zeta$  is the curvature perturbation. This allows to define a local scale factor  $\tilde{a}(t,\mathbf{x}) = a(t)e^{\zeta(t,\mathbf{x})}$ . Starting from an initial flat slice of space-time at time  $t_{\text{in}}$ , the amount of expansion  $N(t,\mathbf{x}) \equiv \ln[\tilde{a}(t,\mathbf{x})/a(t_{\text{in}})]$  to a final slice of uniform energy density is straightforwardly related

to the curvature perturbation

$$\zeta(t, \mathbf{x}) = N(t, \mathbf{x}) - N_0(t) \equiv \delta N, \quad (2.200)$$

where  $N_0(t) \equiv \ln[a(t)/a(t_{\text{in}})]$  is the unperturbed amount of expansion. This result leads to the  $\delta N$  formalism if one further assumes that on super-Hubble scales, the evolution of the Universe at each position is independent and well-approximated by the evolution of an unperturbed universe. This is the so-called ‘‘separate universe’’ assumption [355, 339, 358]. It implies that  $N(t, \mathbf{x})$  is the amount of expansion in unperturbed universes, so that  $\zeta$  can be calculated from the knowledge of the evolution of a family of such universes. Written in terms of the inflaton field  $\phi(\mathbf{x}) = \phi + \delta\phi(\mathbf{x})$ , made of an unperturbed homogeneous piece  $\phi$  and a perturbation  $\delta\phi$  originating from vacuum quantum dispersion, Eq. (2.200) gives rise to

$$\zeta(t, \mathbf{x}) = N[\rho(t), \phi(\mathbf{x})] - N[\rho(t), \phi], \quad (2.201)$$

where  $N$  is evaluated in unperturbed universes from an initial epoch when the inflaton field has an assigned value  $\phi$  to a final epoch when the energy density has an assigned value  $\rho$ . Since the observed curvature perturbations are almost Gaussian, at leading order in perturbation theory, one has

$$\zeta(t, \mathbf{x}) = \delta N \simeq \frac{\partial N}{\partial \phi} \delta\phi, \quad (2.202)$$

where  $N(\phi)$  is evaluated with the classical formula

$$N(\phi) = \frac{1}{M_{\text{Pl}}} \int \frac{d\phi}{\sqrt{2\epsilon_1}}. \quad (2.203)$$

Once  $\zeta$  is decomposed into Fourier components,  $\zeta_{\mathbf{k}} = (2\pi)^{-3/2} \int d^3\mathbf{k}' \zeta(t, \mathbf{k}') \exp(i\mathbf{k} \cdot \mathbf{x})$ , the power spectrum  $\mathcal{P}_\zeta$ , defined with the quantum expected value  $\langle \zeta_{\mathbf{k}} \zeta_{\mathbf{k}'} \rangle \equiv (2\pi)^3 \mathcal{P}_\zeta(k) \delta(\mathbf{k} + \mathbf{k}')$  and  $\mathcal{P}_\zeta(k) \equiv \frac{k^3}{2\pi^2} P_\zeta(k)$ , can be expressed in terms of the power-spectrum of  $\delta\phi$  (defined by similar relations) thanks to Eq. (2.202). For quasi de Sitter inflation, and when the curvature of the inflaton potential is much smaller than  $H$ , on super-Hubble scales, the later is given by<sup>15</sup> [244]

$$\mathcal{P}_{\delta\phi}(k) \simeq \left[ \frac{H(k)}{2\pi} \right]^2, \quad (2.204)$$

where  $H(k)$  means  $H$  evaluated at the time when the  $k$  mode crosses the Hubble radius, *i.e.* when  $aH = k$ . Together with Eq. (2.203), one therefore obtains

$$\mathcal{P}_\zeta = \left[ \frac{H(k)}{2\pi} \right]^2 \frac{1}{2M_{\text{Pl}}^2 \epsilon_1(k)}, \quad (2.205)$$

where again, functions must be evaluated at the time when the corresponding mode  $k$  crosses the Hubble radius. This result matches the one coming from the usual calculation [128] presented in section 2.3. Indeed, in the slow-roll approximation, around some pivot scale  $k_*$  well chosen in the range of scales probed by the CMB, one has  $H \simeq H_* [1 - \epsilon_{1*} \ln(k/k_*)]$  and  $\epsilon_1 \simeq \epsilon_{1*} [1 + \epsilon_{2*} \ln(k/k_*)]$ , where we use the second slow-roll parameter  $\epsilon_2 \equiv (d\epsilon_1/dN)/\epsilon_1$ . This gives rise to

$$\mathcal{P}_\zeta = \frac{H_*^2}{8\pi^2 M_{\text{Pl}}^2 \epsilon_{1*}} \left[ 1 - (2\epsilon_{1*} + \epsilon_{2*}) \ln \left( \frac{k}{k_*} \right) + \dots \right]. \quad (2.206)$$

The standard result (2.110) is retrieved, except that the slow-roll correction to the overall amplitude  $1 - 2(C+1)\epsilon_{1*} - C\epsilon_{2*}$  obtained in Eq. (2.110) is not present here. This is because the

<sup>15</sup>The de Sitter spectrum for  $\delta\phi$  (2.204) can be obtained *e.g.* letting  $\nu = 3/2$  in Eq. (2.146), since with the above definitions  $\mathcal{P}_{\delta\phi}(k) = k^3/2\pi^2 |\phi_{\mathbf{k}}|^2$ .

de Sitter spectrum (2.204) has been used for  $\mathcal{P}_{\delta\phi}$  while the slow-roll corrected spectrum should have<sup>16</sup>. However, one can see that this approximation only affects the overall amplitude by a subleading correction, and that the shape of the power spectrum is correctly described. For example, the spectral index, defined in Eq. (2.112), is correctly given by  $n_s = 1 - 2\epsilon_{1*} - \epsilon_{2*}$  at first order in slow roll.

A fundamental remark is that in the above calculation, the separate universe approximation is assorted with the assumption that once  $k_*$  crosses the Hubble radius, the evolution of the inflaton field is governed by its classical equation of motion (2.203). The stochastic dispersion in the number of  $e$ -folds thus only comes from the field dispersion at Hubble crossing  $\delta\phi_*$ . In most cases, this is a good approximation for the following reason. Looking at the Langevin equation (2.116), one can see that during the typical time scale of one  $e$ -fold, the classical drift of the inflaton field is of the order  $\Delta\phi_{\text{cl}} = V'/(3H^2) = \sqrt{2\epsilon_1}M_{\text{Pl}}$ , while the quantum noise is of the order  $\Delta\phi_{\text{qu}} = H/(2\pi)$ . As in the end of section 2.3.4, this allows us to define a criterion  $\eta \equiv \Delta\phi_{\text{qu}}/\Delta\phi_{\text{cl}}$  that measures the amplitude of the stochastic corrections to the classical trajectory. Looking back at Eqs. (2.205), one can see that this stochastic criterion  $\eta$  can be expressed as

$$\eta = \frac{\Delta\phi_{\text{qu}}}{\Delta\phi_{\text{cl}}} = \sqrt{\mathcal{P}_\zeta}. \quad (2.207)$$

Since  $\mathcal{P}_\zeta(k_*) \sim 2 \times 10^{-9}$ , in single field inflation with canonical kinetic term,  $\eta$  is already small when  $k_*$  crosses the Hubble radius. If one further assumes that inflation ends “naturally” (*i.e.* by slow-roll violation when  $\epsilon_1$  reaches 1) so that  $\epsilon_1$  grows during the last stages of inflation,  $\mathcal{P}_\zeta \propto H^2/\epsilon_1$  decreases (since  $H$  can only decrease) and one is therefore ensured that the stochastic correction to the inflaton trajectory is small after  $k_*$  crosses the Hubble radius.

However, it can happen that  $\epsilon_1$  decreases after the Hubble crossing time of modes of astrophysical interest today. For example, when the potential has an inflection point [359, 360, 361, 362, 363, 364, 365, 366, 367, 368, 369, 370], see also Refs. [371, 372, 373],  $\epsilon_1$  decreases before crossing the inflection point and increases afterwards, so that a transient phase where the stochastic effects can play a non negligible role may happen at some point during the last 60  $e$ -folds. In some other cases, inflation does not end naturally but is triggered *e.g.* by tachyonic instability involving another field, like in hybrid inflation [374, 212, 375, 376, 377, 378]. In such models  $\epsilon_1$  monotonously decreases during inflation and the last  $e$ -folds may be stochastic dominated. It can also happen, for instance in string theoretical contexts where the inflaton stands for the distance between two branes and evolves in a throat [379, 380, 381, 382], that the inflaton field is allowed to vary only in a bounded interval of values, and that inflation ends by brane annihilation when  $\phi$  reaches a bound of this interval. In these cases again,  $\epsilon_1$  may decrease as inflation proceeds, and even if  $\eta$  is small when  $k_*$  crosses the Hubble radius, it does not necessarily remain so since it keeps increasing afterwards.<sup>17</sup>

In these cases, it is crucial to study the dispersion  $\delta N$  that arises not only from  $\delta\phi_*$  but from the complete stochastic history of the coarse-grained field. In the next sections, we therefore calculate the first statistical moments of the number of  $e$ -folds realized between fixed points.

<sup>16</sup>The calculation of  $\mathcal{P}_{\delta\phi}$  relies on the de Sitter spectrum (2.204), because the amplitude of the noise term in Eq. (2.116) also relies on it, see sections 2.4.1.6 and 2.4.1.7. This is why in the following, only the leading contributions in slow roll will be derived, and the obtained results should be compared with the reference classical spectrum (2.206). If one wants to go beyond, one needs to add slow-roll corrections to the noise amplitudes.

<sup>17</sup>Another situation of interest is  $k$ -inflation [383, 384] for which  $\eta \propto \sqrt{\mathcal{P}_\zeta\gamma}$  where  $\gamma > 1$  is the Lorentz factor. It can easily happen that  $\gamma \gg 1$  in which case  $\mathcal{P}_\zeta(k_*) \sim 10^{-9}$  does not necessarily mean that  $\eta \ll 1$ .

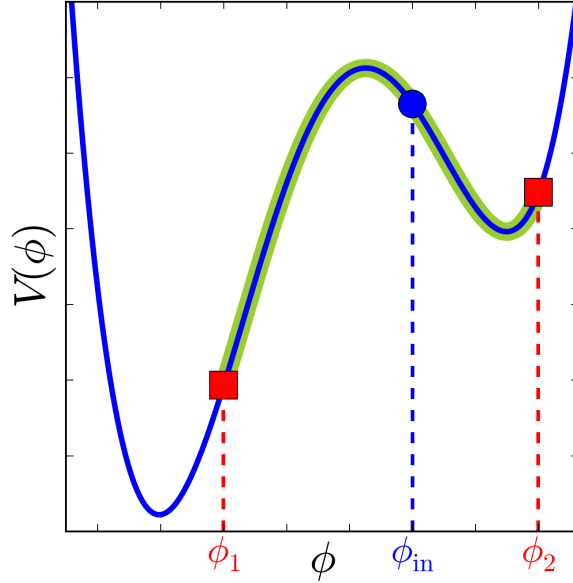


Figure 2.4.: Sketch of the dynamics solved in section 2.4.3. If the inflaton is initially located at  $\phi_{\text{in}}$ , it evolves along some potential  $V(\phi)$  thanks to the stochastic Langevin equation (2.208), until it reaches one of the two values  $\phi_1$  or  $\phi_2$  where it stops.

### 2.4.3.2. Stochastic Inflation and Number of $e$ -folds

Let us start from the slow-roll Langevin equation (2.116),

$$\frac{d\phi}{dN} = -\frac{V'}{3H^2} + \frac{H}{2\pi}\xi(N), \quad (2.208)$$

and work at leading order in slow roll so that  $H^2 \simeq V/(3M_{\text{Pl}}^2)$ . In what follows, we make use of stochastic analysis common tools, introduced *e.g.* in Ref. [385] (see notably p.108 and below). In any case, all the quantities introduced below are self consistently defined. We calculate the mean number of  $e$ -folds realized between two points, the dispersion in the number of  $e$ -folds realized between two points, and the ending point probability which allows to quantify how much the inflaton can climb up its potential under stochastic effects.

More precisely, let us consider the situation described in Fig. 2.4, where the inflaton is initially located at  $\phi_{\text{in}}$  and evolves in some potential  $V(\phi)$  under Eq. (2.208). Usually, the inflationary dynamics is stopped when the inflaton reaches some ending value. In the stochastic setup however, since the inflaton can a priori explore any part of the potential thanks to stochastic effects, it makes sense to introduce two possible ending points, located at  $\phi_1$  and  $\phi_2$  on each side of  $\phi_{\text{in}}$ . We assume that inflation stops when  $\phi$  reaches  $\phi_1$  or  $\phi_2$ . Let  $\mathcal{N}$  be the number of  $e$ -folds realized when this happens. Obviously,  $\mathcal{N}$  is a stochastic quantity, which means that it is different from one realization to another. In what follows, we compute its first and second moments, as well as the probability that inflation ends at  $\phi_1$  (or  $\phi_2$ ).

A first useful result to establish is the Itô lemma, which is a relation verified by any smooth function  $f$  of  $\phi$ . The Taylor expansion of such a function at second order gives  $f(\phi + d\phi) = f(\phi) + f'(\phi)d\phi + f''(\phi)/2 d\phi^2 + \mathcal{O}(d\phi^3)$ . Now, if  $\phi$  is a realization of the stochastic process

under study,  $d\phi$  is given by Eq. (2.208) and at first order in  $dN$ , one obtains

$$\begin{aligned} df[\phi(N)] &= f'[\phi(N)] \frac{\sqrt{V}[\phi(N)]}{2\pi\sqrt{3}M_{\text{Pl}}} \xi(N) dN \\ &\quad - f'[\phi(N)] \frac{V'[\phi(N)]}{V[\phi(N)]} M_{\text{Pl}}^2 dN + \frac{1}{24\pi^2 M_{\text{Pl}}^2} f''[\phi(N)] V[\phi(N)] dN. \end{aligned} \quad (2.209)$$

Integrating this relation between  $N = 0$  where  $\phi = \phi_{\text{in}}$  and  $N = \mathcal{N}$  where  $\phi = \phi_1$  or  $\phi_2$ , one gets the Itô lemma [386]

$$\begin{aligned} f(\phi_1 \text{ or } \phi_2) - f(\phi_{\text{in}}) &= \int_0^{\mathcal{N}} f'[\phi(N)] \frac{\sqrt{V}[\phi(N)]}{2\pi\sqrt{3}M_{\text{Pl}}} \xi(N) dN \\ &\quad + \int_0^{\mathcal{N}} \left\{ \frac{1}{24\pi^2 M_{\text{Pl}}^2} f''[\phi(N)] V[\phi(N)] - f'[\phi(N)] \frac{V'[\phi(N)]}{V[\phi(N)]} M_{\text{Pl}}^2 \right\} dN. \end{aligned} \quad (2.210)$$

### 2.4.3.3. Ending Point Probability

In this section we calculate the probability  $p_1$  that the inflaton field first reaches the ending point located at  $\phi_1$  [*i.e.*  $\phi(\mathcal{N}) = \phi_1$ ], or equivalently the probability  $p_2 = 1 - p_1$  that the inflaton field first reaches the ending point located at  $\phi_2$  [*i.e.*  $\phi(\mathcal{N}) = \phi_2$ ]. First of all, let  $\psi(\phi)$  be a function that can be expressed as

$$\psi(\phi) = \frac{h(\phi) - h(\phi_2)}{h(\phi_1) - h(\phi_2)}, \quad (2.211)$$

where  $h(\phi)$  will be specified later. By construction, one has  $\psi(\phi_1) = 1$  and  $\psi(\phi_2) = 0$ . This implies that the mean value of  $\psi$  evaluated at  $\phi(\mathcal{N})$  is given by

$$\langle \psi[\phi(\mathcal{N})] \rangle = p_1 \psi(\phi_1) + p_2 \psi(\phi_2) = p_1. \quad (2.212)$$

The idea is then to find an appropriate  $h(\phi)$  function which makes easy the evaluation of the left hand side of the previous relation, to deduce  $p_1$ . In order to do so, let us apply the Itô lemma (2.210) to  $h(\phi)$ . If one requires that the integral of the second line of Eq. (2.210) vanishes, that is

$$h''(\phi) \frac{V(\phi)}{24\pi^2 M_{\text{Pl}}^4} = h'(\phi) \frac{V'(\phi)}{V(\phi)}, \quad (2.213)$$

one obtains

$$h[\phi(\mathcal{N})] - h(\phi_{\text{in}}) = \int_0^{\mathcal{N}} h'[\phi(N)] \frac{\sqrt{V}[\phi(N)]}{2\pi\sqrt{3}M_{\text{Pl}}} \xi(N) dN. \quad (2.214)$$

Using the linear relation (2.211) between  $h$  and  $\psi$ , this gives rise to the same equation for  $\psi$ . Finally, taking the stochastic average of this equation over all the realizations cancels out<sup>18</sup> its right hand side, so that one obtains

$$\langle \psi[\phi(\mathcal{N})] \rangle = \psi(\phi_{\text{in}}), \quad (2.215)$$

which is the probability  $p_1$  one is seeking for. Therefore all one needs to do is to solve Eq. (2.213) to obtain  $h(\phi)$ , then to plug the obtained expression in Eq. (2.211) to derive  $\psi(\phi)$ , and finally

<sup>18</sup>The fact that the integral in the right hand side of Eq. (2.214) vanishes when averaged is actually non trivial since both the integrand and the upper bound are stochastic quantities, but it can be shown in a rigorous way (see page 12 of Ref. [385]).

to evaluate this function at  $\phi_{\text{in}}$  to calculate  $p_1$ . A formal solution to Eq. (2.213) can straightforwardly be calculated and one obtains

$$h(\phi) = A \int_B^\phi \exp\left[-\frac{24\pi^2 M_{\text{Pl}}^4}{V(u)}\right] du, \quad (2.216)$$

where  $A$  and  $B$  are two integration constants that play no role since they cancel out when calculating  $\psi$  thanks to Eq. (2.211). Indeed, this gives rise to

$$p_1 = \frac{\int_{\phi_2}^{\phi_{\text{in}}} \exp\left[-\frac{24\pi^2 M_{\text{Pl}}^4}{V(u)}\right] du}{\int_{\phi_2}^{\phi_1} \exp\left[-\frac{24\pi^2 M_{\text{Pl}}^4}{V(u)}\right] du}. \quad (2.217)$$

A few remarks are in order about this equation. Firstly, one can check that since  $\phi_{\text{in}}$  lies between  $\phi_1$  and  $\phi_2$ , this probability is ensured to be comprised between 0 and 1. Secondly, the function appearing in the integral,  $\exp(-24\pi^2 M_{\text{Pl}}^4/V)$ , is rather natural for the problem under study, since it has already been encountered (actually, its inverse) when calculating the steady-state distribution in section 2.4.2.1, see Eq. (2.157). Thirdly, a special case that will prove useful in the following (in particular in sections 2.4.3.4 and 2.4.3.5) is when the potential is maximal at  $\phi_\infty = \pm\infty$ , and when, say,  $\phi_1 = \phi_\infty$ . In this case one is sure to first reach the ending point located at  $\phi_2$ , that is  $p_1 = 0$ . Indeed, assuming that the potential is bounded from below, the numerator of Eq. (2.217) must be finite, since a bounded function is integrated over a bounded interval. If the potential is maximal at  $\phi_1$ , and if it is monotonous over an interval of the type  $[\phi_0, \phi_1[$ , the denominator of Eq. (2.217) is on the contrary larger than the integral of a function bounded from below by a strictly positive number, over an unbounded interval  $[\phi_0, \phi_\infty]$ . This is why it diverges, and  $p_1$  vanishes.

**Example:**  $V \propto \phi^p$

For illustrative purpose, let us now see what Eq. (2.217) gives in the case where the potential  $V$  is monomial in the inflaton field  $\phi$  and is given by

$$V(\phi) = M^4 \left(\frac{\phi}{M_{\text{Pl}}}\right)^p, \quad (2.218)$$

where  $p$  is a positive parameter that sets the shape of the potential (here we take  $p > 1$ ) and  $M$  is an overall mass scale normalization. Such models are often referred to as ‘‘large field inflation’’ (LFI), or ‘‘chaotic inflation’’ (for further details about this model, including theoretical justifications, see *e.g.* section 4.2 of Ref. [205], section 3.2). In such cases, if one defines  $x \equiv V/(24\pi^2 M_{\text{Pl}}^4)$ , one obtains

$$p_1 = \frac{\Gamma\left(-\frac{1}{p}, \frac{1}{x_2}\right) - \Gamma\left(-\frac{1}{p}, \frac{1}{x_{\text{in}}}\right)}{\Gamma\left(-\frac{1}{p}, \frac{1}{x_2}\right) - \Gamma\left(-\frac{1}{p}, \frac{1}{x_1}\right)}, \quad (2.219)$$

where  $\Gamma(s, y) \equiv \int_y^\infty t^{s-1} e^{-t} dt$  is the upper incomplete gamma function [269]. It is displayed in Fig. 2.5 for a few values of  $p$ . One can check that  $p_1$  decreases monotonously between  $p_1 = 1$  when  $x_{\text{in}} = x_1$  and  $p_1 = 0$  when  $x_{\text{in}} = x_2$ . Since  $\phi_{\text{in}}$  is labelled by  $x_{\text{in}} = V(\phi_{\text{in}})/(24\pi^2 M_{\text{Pl}}^4)$  in Fig. 2.5, inflation classically proceeds from the right to the left. Therefore,  $p_1 < 1$  implies that some realizations of the stochastic process (2.208) climb up the potential and end up at  $\phi_2$ . When  $x_1 < x_{\text{in}} \ll 1$  however, one has  $p_1 \simeq 1$  [as can be seen in Fig. 2.5, or directly checked in Eq. (2.217)] which means that in this case the inflaton very seldom climbs up the potential. This actually corresponds to the classical limit, on which we elaborate below.

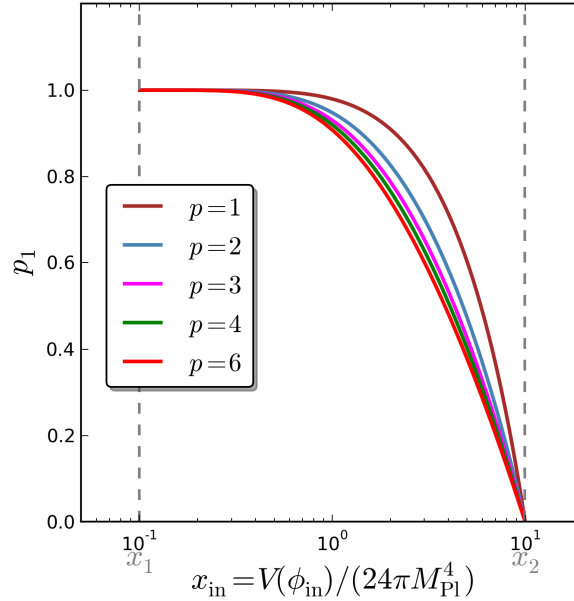


Figure 2.5.: Probability of reaching the ending point located at  $\phi_1$  first, as a function of  $\phi_{\text{in}}$  labelled by  $x_{\text{in}} = V(\phi_{\text{in}})/(24\pi^2 M_{\text{Pl}}^4)$  (so that inflation classically proceeds from the right to the left), in the large field potentials (LFI). The displayed result corresponds to  $p = 1$  (brown),  $p = 2$  (blue),  $p = 3$  (magenta),  $p = 4$  (green) and  $p = 6$  (red). It is given by Eq. (2.219). The two ending points are located at  $x_1 = 0.1$  and  $x_2 = 10$ , and are denoted by the dashed grey vertical lines.

#### 2.4.3.4. Mean Number of $e$ -folds

Let us now turn to the calculation of the mean number of  $e$ -folds  $\langle \mathcal{N} \rangle$ . As above, we want to make use of the Itô lemma (2.210). In order to do so, let us choose  $f(\phi)$  to be defined as the solution of the differential equation

$$\frac{f''(\phi)}{24\pi^2 M_{\text{Pl}}^2} V(\phi) - f'(\phi) \frac{V'(\phi)}{V(\phi)} M_{\text{Pl}}^2 = -1, \quad (2.220)$$

with boundary conditions  $f(\phi_1) = f(\phi_2) = 0$ . Such a solution will be explicitly calculated in due time. For now it is interesting to notice that thanks to this definition, the first term of the left hand side of the Itô equation (2.210),  $f(\phi_1 \text{ or } \phi_2)$ , vanishes, and that the second integrand of its right hand side is  $-1$ . Thus, the Itô equation can be rewritten as

$$\mathcal{N} = f(\phi_{\text{in}}) + \int_0^{\mathcal{N}} f'[\phi(N)] \frac{\sqrt{V}[\phi(N)]}{2\pi\sqrt{3}M_{\text{Pl}}} \xi(N) dN. \quad (2.221)$$

By averaging over all the realizations, one obtains<sup>19</sup>

$$\langle \mathcal{N} \rangle = f(\phi_{\text{in}}). \quad (2.222)$$

Therefore it is enough to solve the deterministic differential equation (2.220) for  $f$  with the associated boundary conditions, and to evaluate the obtained solution at  $\phi_{\text{in}}$ , in order to derive

<sup>19</sup>Here also, since both the integrand and the upper bound are stochastic quantities, it is a non trivial fact that the integral in the right hand side of Eq. (2.221) vanishes when averaged. However it can be shown in a rigorous way, see page 12 of Ref. [385].

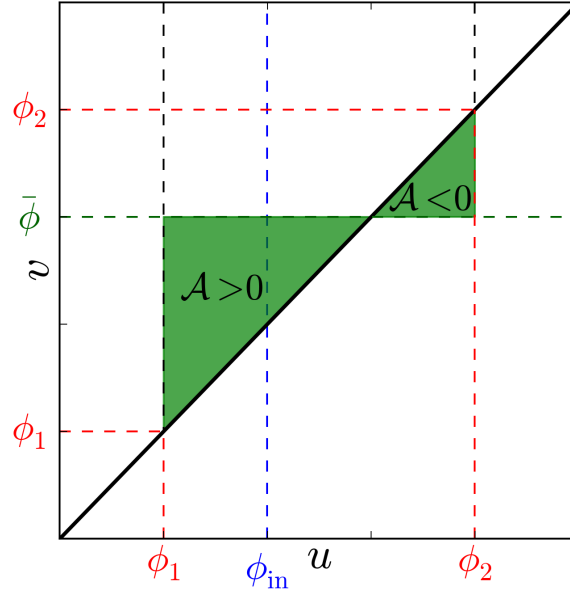


Figure 2.6.: Integration domain of Eq. (2.223) when evaluated at  $\phi = \phi_2$ , in the case  $\phi_1 < \phi_2$  (the opposite case proceeds exactly the same way). The discrete parameter  $u$  is integrated between  $\phi_1$  and  $\phi_2$ , while  $v$  varies between  $\bar{\phi}$  and  $u$ . The resulting integration domain is displayed in green. When  $u < \bar{\phi}$ , one has  $dudv < 0$  and one integrates a positive contribution [remember that a minus sign stands in front of Eq. (2.223)], and conversely when  $u > \bar{\phi}$ , one has  $dudv > 0$  and one integrates a negative contribution. This is a necessary condition in order for the overall integral to vanish. This is why  $\bar{\phi}$  must lie between  $\phi_1$  and  $\phi_2$ .

the mean value of the realized number of  $e$ -folds. Solving Eq. (2.220) gives rise to

$$f(\phi) = -24\pi^2 M_{\text{Pl}}^2 \int_{\phi_1}^{\phi} du \int_{\bar{\phi}(\phi_1, \phi_2)}^u \frac{dv}{V(v)} \exp \left\{ 24\pi^2 M_{\text{Pl}}^4 \left[ \frac{1}{V(v)} - \frac{1}{V(u)} \right] \right\}, \quad (2.223)$$

where  $\bar{\phi}$  is an integration constant that must be chosen in order to have  $f(\phi_2) = 0$ . More precisely, as can be seen in Fig. 2.6,  $\bar{\phi}$  must be such that, when  $f$  is evaluated at  $\phi_2$ , the integration domain of Eq. (2.223) possesses a positive part and a negative part, that are able to compensate for each other. This implies that  $\bar{\phi}$  lies between  $\phi_1$  and  $\phi_2$ . Another generic condition comes from splitting the  $u$ -integral in Eq. (2.223) into  $\int_{\phi_1}^{\bar{\phi}} du + \int_{\bar{\phi}}^{\phi_2} du$ . The first integral vanishes because  $f(\phi_2) = 0$ , which means that in order for  $f$  to be symmetrical in  $\phi_1 \leftrightarrow \phi_2$ ,  $\bar{\phi}(\phi_1, \phi_2)$  must abide by this symmetry too, that is

$$\bar{\phi}(\phi_1, \phi_2) = \bar{\phi}(\phi_2, \phi_1). \quad (2.224)$$

Beyond these simple conditions, the actual location of  $\bar{\phi}$  needs to be calculated for each potential  $V$  explicitly and there is no explicit generic expression for it.

However, in the special case where the potential is maximal at  $\phi_{\infty} = \pm\infty$  (which is the case notably for large field or plateau models), and if one wants to calculate the mean number of  $e$ -folds between  $\phi_{\text{in}}$  and  $\phi_1$ , things can be made clearer regarding the location of  $\bar{\phi}$ . Indeed, one can set  $\phi_2 = \phi_{\infty}$ , since in the case described here the probability to reach  $\phi_{\infty}$  vanishes, as shown in section 2.4.3.3. Therefore, the quantity we really compute is the mean number of  $e$ -folds between  $\phi_{\text{in}}$  and  $\phi_1$ . In order to make things explicit, let us assume that  $V' > 0$  (the

same line of arguments can be followed in the case  $V' < 0$ ). Inflation proceeds at  $\phi < \phi_\infty$ . In this case, the (absolute value of the) integrand of Eq. (2.226) increases with  $u$  and reaches a constant when  $u \rightarrow \phi_\infty$ , while strongly decreasing with  $v$ . Looking back at Fig. 2.6, one can convince oneself that, in order for the negative integration domain to cancel out the positive one,  $\bar{\phi}$  has therefore to be moved to  $\phi_\infty$ ,

$$\bar{\phi} = \phi_\infty. \quad (2.225)$$

Once the location of  $\bar{\phi}$  is determined, from Eqs. (2.222) and (2.223), one obtains

$$\langle \mathcal{N} \rangle = -24\pi^2 M_{\text{Pl}}^2 \int_{\phi_1}^{\phi_{\text{in}}} du \int_{\bar{\phi}(\phi_1, \phi_2)}^u \frac{dv}{V(v)} \exp \left\{ 24\pi^2 M_{\text{Pl}}^4 \left[ \frac{1}{V(v)} - \frac{1}{V(u)} \right] \right\}. \quad (2.226)$$

Here also, one recognizes the same kind of functions as the ones appearing in the steady-state distribution (2.157).

### Classical Limit

As a consistency check, let us derive the asymptotic limit of Eq. (2.226) in the classical approximation, and see whether the classical trajectory (2.12) is properly recovered. For simplicity, we consider the situation described above where the potential is maximal at  $\phi_\infty = \pm\infty$  and where we thus need to evaluate Eq. (2.226) between  $\phi_{\text{in}}$  and  $\phi_1 = \phi_{\text{end}}$ , with  $\bar{\phi} = \phi_\infty$ .

Let us first work out the  $v$ -integral, that is to say  $\int_{\bar{\phi}}^u dv/V(v) \exp[24\pi^2 M_{\text{Pl}}^4/V(v)]$ . Since the integrand varies exponentially with the potential, the strategy is to evaluate it close to its maximum, that is where the potential  $V$  is minimum. The potential being maximal at  $\phi_\infty = \bar{\phi}$ , the integrand is clearly maximal<sup>20</sup> at  $u$ . In order for the dominant contributions to the  $v$ -integral to come from the close neighbourhood of its ending point  $u$ , one needs the argument of the exponential to be large, that is

$$V(\phi_{\text{end}}) \ll 24\pi^2 M_{\text{Pl}}^4. \quad (2.227)$$

This assumption is quite natural in the classical limit since  $V/M_{\text{Pl}}^4$  controls the amplitude of the noise term in Eq. (2.208), but we come back to what it really means below. Taylor expanding  $1/V$  at first order around  $u$ ,  $1/V(v) \simeq 1/V(u) - V'(u)/V^2(u)(v-u)$ , one obtains, after integrating by parts<sup>21</sup>

$$\int_{\bar{\phi}}^u \frac{dv}{V(v)} \exp \left[ \frac{24\pi^2 M_{\text{Pl}}^4}{V(v)} \right] \simeq -\frac{1}{24\pi^2 M_{\text{Pl}}^4} \frac{V(u)}{V'(u)} \left[ 1 - \frac{V(u)}{24\pi^2 M_{\text{Pl}}^4} \right] \exp \left[ \frac{24\pi^2 M_{\text{Pl}}^4}{V(u)} \right]. \quad (2.228)$$

This is similar to a saddle-point approximation [387] (also called Laplace's method). Because of assumption (2.227), the term  $1 - V(u)/(24\pi^2 M_{\text{Pl}}^4)$  can be approximated to 1. Plugging back this expression in Eq. (2.226), one finally obtains

$$\langle \mathcal{N} \rangle|_{\text{cl}} = \int_{\phi_{\text{end}}}^{\phi_{\text{in}}} \frac{du}{M_{\text{Pl}}^2} \frac{V(u)}{V'(u)}, \quad (2.229)$$

which exactly matches the classical trajectory (2.12). The classical limit is then properly recovered.

<sup>20</sup>More generally, the calculation presented here only relies on the assumption  $V(\bar{\phi}) > V(\phi_{\text{in}})$  and on Eq. (2.227).

<sup>21</sup>Since  $V(\bar{\phi}) > V(u)$  and since  $V$  is monotonous, one can also show that  $\exp[-24\pi^2 M_{\text{Pl}}^4 V'(u)/V^2(u)(\bar{\phi} - u)]$  is exponentially vanishing.

A few remarks are in order. First, the classical trajectory appears as a saddle-point limit of the mean stochastic trajectory, analogously to what happens *e.g.* in the context of path integral calculations. The fact that the classical limit corresponds to Eq. (2.227) is also interesting, since it can be shown [388, 389] that  $V/M_{\text{Pl}}^4$  measures the amplitude of the quantum gravity corrections. Therefore, the “classical” limit needs here to be understood as the limit where corrections from quantum gravity are negligible, and the condition (2.227) is in fact very generic. For this reason, in the following and as we did in section 2.4.3.3, it is convenient to define the ratio

$$x \equiv \frac{V}{24\pi^2 M_{\text{Pl}}^4}. \quad (2.230)$$

Generic expressions in  $x$  will be derived, but the validity range of the present calculation is of course  $x < 1$  since we do not incorporate quantum gravity. In the following also, the “classical” limit shall always refer to the  $x \ll 1$  limit. Finally and in passing, the fact that  $x$  encodes the amplitude of quantum gravity possible effects can be illustrated in the calculation of the steady-state distribution, see section 2.4.2.1. In this section, we made clear that different time variables in the Langevin equation lead to different stochastic processes (and as a consequence, different steady-state distributions) because of the  $H(\phi)$  dependence, through which the amplitude of the noise depends on the coarse-grained field. In some sense, because the coarse-grained field is a stochastic quantity, so is  $H$ , *i.e.* the metric, and we understand why it has to do with “quantum gravity”. In any case, this  $H(\phi)$  dependence translates into different steady-state distributions  $P$  and  $\tilde{P}$  when computed in terms of  $N$  or in terms of  $t$  respectively. Making use of Eqs. (2.157) and (2.160), the difference between these two distributions can be studied through the ratio

$$\frac{\ln P}{\ln \tilde{P}} = \frac{1 - x \ln x}{1 - \frac{3}{2}x \ln x}, \quad (2.231)$$

from which it is clear that the two distributions are identical [and the effects coming from the  $H(\phi)$  dependence vanish] in the limit where  $x \rightarrow 0$ .

**Example:**  $V \propto \phi^p$

As an illustrative example, let us now see what Eq. (2.226) gives in the case of the large field potential (2.218). In these models, remember that the classical trajectory proceeds at decreasing values of  $\phi$ . One is interested in the mean number of  $e$ -folds realized between  $\phi_{\text{in}}$  and  $\phi_{\text{end}}$ . Since the large field potential belongs to the category mentioned above where  $V$  is maximal at  $\phi_{\infty} = \infty$ , one takes  $\phi_1 = \phi_{\text{end}}$  and  $\bar{\phi} = \phi_{\infty} = \infty$  in Eq. (2.226). One obtains, for  $p > 1$ ,

$$\langle \mathcal{N} \rangle = \frac{1}{p(p-1)} \left( \frac{24\pi^2 M_{\text{Pl}}^4}{M^4} \right)^{2/p} \int_{x_{\text{end}}}^{x_{\text{in}}} e^{-\frac{1}{x}} x^{\frac{2}{p}-2} M \left( 1 - \frac{1}{p}, 2 - \frac{1}{p}, \frac{1}{x} \right) dx, \quad (2.232)$$

where  $M$  is the Kummer’s confluent hypergeometric function [269] and where we have used the variable  $x = V/(24\pi^2 M_{\text{Pl}}^4)$ , so that the classical limit corresponds to  $x \ll 1$ . In this limit, one can make use of the asymptotic expansion [269]  $M(a, a+1, z) \simeq a \exp(z)/z$  when  $z \rightarrow \infty$ , and one exactly obtains the classical trajectory (2.12) as expected.

An explicit comparison between both trajectories is displayed in Fig. 2.7 for a few values of  $p$ . The quantity which is displayed is the derivative of the mean number of  $e$ -folds with respect to  $\phi_{\text{in}}$ , to remove the dependence on  $\phi_{\text{end}}$ . It is plotted as a function of  $\phi_{\text{in}}$ , which is labelled by  $x_{\text{in}}$  to make interpretation easier. Since the energy density must remain sub-Planckian, only the region  $x < 1$  makes really sense but we display a larger range of values for  $x$  to see how the functions

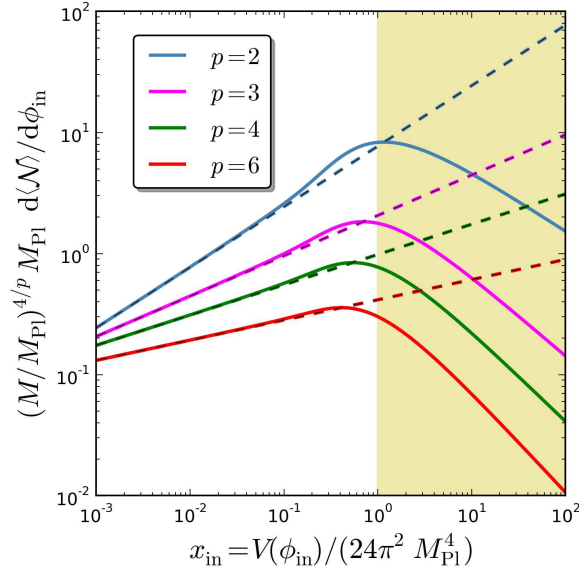


Figure 2.7.: Mean number of  $e$ -folds for the models  $V \propto \phi^p$  with  $p = 2$  (blue),  $p = 3$  (magenta),  $p = 4$  (green) and  $p = 6$  (red). The displayed quantity is the derivative of the mean number of  $e$ -folds with respect to the starting point  $\phi_{\text{in}}$ , as a function of  $\phi_{\text{in}}$  labeled by  $x_{\text{in}} = V(\phi_{\text{in}})/(24\pi^2 M_{\text{Pl}}^4)$ . The solid lines correspond to Eq. (2.232) while the dashed lines stand for the classical trajectory  $\propto V/V'$  given by Eq. (2.12). The latter provides a good approximation to the former in the regime  $x \ll 1$ , as expected. Obviously, the calculation makes sense only when  $x < 1$ , *i.e.* outside the yellow shaded area, which is displayed for information only.

involved behave in general. One can first check that when  $x_{\text{in}} \ll 1$ , the classical trajectory (2.12) provides a good approximation to the mean number of  $e$ -folds given by Eq. (2.232). On the other hand, when  $x_{\text{in}}$  is large, the deviation between these two quantities starts to be important and the mean stochastic number of  $e$ -folds is smaller than the classical one. This is due to the effect of the quantum kicks, which tend to shift the inflaton field faster than what the classical drift does at large field values. More precisely, since the confluent hypergeometric function tends to 1 when its last argument goes to 0, one has  $d\langle N \rangle / d\phi_{\text{in}} \propto x_{\text{in}}^{1/p-1}$  when  $x_{\text{in}} \gg 1$ , whereas classically  $dN/d\phi \propto x_{\text{in}}^{1/p}$ . Finally, there exists an intermediate range of values when  $x_{\text{in}} \sim 1$  for which the mean number of  $e$ -folds is slightly larger than the classical one.

#### 2.4.3.5. Number of $e$ -folds Dispersion

Let us now move on with the calculation of the dispersion in the number of  $e$ -folds, that we denote

$$\delta\mathcal{N}^2 = \langle \mathcal{N}^2 \rangle - \langle \mathcal{N} \rangle^2. \quad (2.233)$$

This quantity first requires to compute the mean squared number of  $e$ -folds  $\langle \mathcal{N}^2 \rangle$ . In order to do so, let us square Eq. (2.221), and take the stochastic average of it. One obtains<sup>22</sup>

$$\langle \mathcal{N}^2 \rangle = f^2(\phi_{\text{in}}) + \left\langle \int_0^{\mathcal{N}} f'^2[\phi(N)] \frac{V[\phi(N)]}{12\pi^2 M_{\text{Pl}}^2} dN \right\rangle. \quad (2.234)$$

<sup>22</sup>This is again a non trivial result since both the integrand and the upper bound of the integral appearing in Eq. (2.221) are stochastic quantities, but it can be shown in a rigorous way (see page 12 of Ref. [385]).

In order to make use of the Itô lemma, let  $g(\phi)$  be the function defined by

$$\frac{g''(\phi)V(\phi)}{24\pi^2 M_{\text{Pl}}^2} - g'(\phi) \frac{V'(\phi)}{V(\phi)} M_{\text{Pl}}^2 = -f'^2(\phi) \frac{V(\phi)}{12\pi^2 M_{\text{Pl}}^2}, \quad (2.235)$$

where  $f$  is the function introduced in Eq. (2.223). When applied to  $g(\phi)$ , if one further sets  $g(\phi_1) = g(\phi_2) = 0$ , the stochastic average of the Itô lemma (2.210) gives rise to

$$\begin{aligned} g(\phi_{\text{in}}) &= \left\langle \int_0^{\mathcal{N}} f'^2[\phi(N)] \frac{V[\phi(N)]}{12\pi^2 M_{\text{Pl}}^2} dN \right\rangle \\ &= \langle \mathcal{N}^2 \rangle - f^2(\phi_{\text{in}}) \\ &= \langle \mathcal{N}^2 \rangle - \langle \mathcal{N} \rangle^2, \end{aligned} \quad (2.236)$$

where the second line is just a consequence of Eq. (2.234) and where the third line is just a consequence of Eq. (2.222). Therefore, what one needs to do is to solve Eq. (2.235) with boundary conditions  $g(\phi_1) = g(\phi_2) = 0$ , and to evaluate the resulting function at  $\phi_{\text{in}}$  in order to obtain

$$\delta \mathcal{N}^2 = g(\phi_{\text{in}}). \quad (2.237)$$

The differential equation (2.235) can formally be integrated, and one obtains

$$g(\phi_{\text{in}}) = 2 \int_{\phi_{\text{in}}}^{\phi_1} d\phi \int_{\hat{\phi}(\phi_1, \phi_2)}^{\phi} d\psi f'^2(\psi) \exp \left[ \frac{24\pi^2 M_{\text{Pl}}^4}{V(\psi)} - \frac{24\pi^2 M_{\text{Pl}}^4}{V(\phi)} \right], \quad (2.238)$$

where  $\hat{\phi}(\phi_1, \phi_2)$  is an integration constant that must be chosen in order to have  $g(\phi_2) = 0$ . As for  $\bar{\phi}$ , it is straightforward to show that  $\hat{\phi}$  must lie between  $\phi_1$  and  $\phi_2$  and that it must be symmetric in  $(\phi_1, \phi_2)$ , that is

$$\hat{\phi}(\phi_1, \phi_2) = \hat{\phi}(\phi_2, \phi_1). \quad (2.239)$$

In the same manner as for  $\bar{\phi}$ , when the potential is maximal at  $\phi_{\infty} = \pm\infty$  and if  $\phi_2 = \phi_{\infty}$ , one has  $\hat{\phi} = \phi_{\infty}$ .

### Classical Limit

As was done for the mean number of  $e$ -folds in section 2.4.3.4, let us derive the classical limit  $x \ll 1$  of Eq. (2.238). Obviously, in the classical setup the trajectories are not stochastic and  $\delta \mathcal{N}^2 = 0$ , and what we mean by ‘‘classical limit’’ here is the non vanishing leading order contribution to  $\delta \mathcal{N}^2$  in the limit  $x \ll 1$ . As in section 2.4.3.4, we consider the situation where the potential is maximal at  $\phi_{\infty} = \pm\infty$  and where we thus need to evaluate Eq. (2.238) between  $\phi_{\text{in}}$  and  $\phi_1 = \phi_{\text{end}}$ , with  $\hat{\phi} = \phi_{\infty}$  and  $\bar{\phi} = \phi_{\infty}$  in the  $f'^2$  term.

Let us first work out the  $\psi$ -integral, that is to say  $\int_{\hat{\phi}}^{\phi} d\psi f'^2 \exp[24\pi^2 M_{\text{Pl}}^4/V(\psi)]$ , with a saddle-point approximation as before. Since the integrand varies exponentially with the potential, the strategy is again to evaluate it close to its maximum, that is where the potential  $V$  is minimum. The potential is maximal at  $\phi_{\infty} = \hat{\phi}$ , so the integrand is clearly maximal at  $\phi$ . Taylor expanding  $1/V$  at first order around  $\phi$ ,  $1/V(\psi) \simeq 1/V(\phi) - V'(\phi)/V^2(\phi)(\psi - \phi)$ , one obtains<sup>23</sup>

$$\int_{\hat{\phi}}^{\phi} d\psi f'^2(\psi) \exp \left[ \frac{24\pi^2 M_{\text{Pl}}^4}{V(\psi)} \right] \simeq -\frac{1}{24\pi^2 M_{\text{Pl}}^8} \frac{V^4(\phi)}{V'^3(\phi)} \exp \left[ \frac{24\pi^2 M_{\text{Pl}}^4}{V(\phi)} \right]. \quad (2.240)$$

<sup>23</sup>In the limit where  $V(\phi) \ll 24\pi^2 M_{\text{Pl}}^4$ ,  $f$  is close to the classical trajectory (2.229) as shown in section 2.4.3.4, and one can take  $f'(\psi) \simeq V(\psi)/V'(\psi) M_{\text{Pl}}^{-2}$ .

Plugging back this expression in Eq. (2.238), one obtains

$$\delta\mathcal{N}^2|_{\text{cl}} = \frac{1}{12\pi^2 M_{\text{Pl}}^8} \int_{\phi_{\text{end}}}^{\phi_{\text{in}}} d\phi \frac{V^4(\phi)}{V'^3(\phi)} \quad (2.241)$$

which we shall refer to as the classical approximation to  $\delta\mathcal{N}^2$ .

### 2.4.3.6. Scalar Power Spectrum

We are now in a position where we can calculate the power spectrum for scalar adiabatic perturbations  $\mathcal{P}_\zeta$ . The power spectrum of  $\delta\mathcal{N}$  is defined by the two-point correlator of  $\mathcal{N}$ ,

$$\mathcal{P}_{\delta\mathcal{N}}(k) = \frac{k^3}{2\pi^2} \int d^3x \langle \delta\mathcal{N}(0) \delta\mathcal{N}(x) \rangle e^{i\mathbf{k}\cdot\mathbf{x}}. \quad (2.242)$$

Since the quantity  $\delta\mathcal{N}^2$  computed between two points  $\phi_{\text{in}}$  and  $\phi_{\text{end}}$  is due to an integrated effects of all the modes crossing the Hubble radius between these two points, one has

$$\delta\mathcal{N}^2 = \int_{k_{\text{in}}}^{k_{\text{end}}} \mathcal{P}_{\delta\mathcal{N}}(k) \frac{dk}{k} = \int_{\ln k_{\text{end}} - \langle\mathcal{N}\rangle(1-\epsilon_1+\dots)}^{\ln k_{\text{end}}} \mathcal{P}_{\delta\mathcal{N}} dN, \quad (2.243)$$

where  $\langle\mathcal{N}\rangle = \ln(a_{\text{end}}/a_{\text{in}}) = \ln(k_{\text{end}}/k_{\text{in}})(1 + \epsilon_1 + \dots)$ . Here, “ $\dots$ ” refer to higher order in slow roll terms, but it is enough to keep the zeroth order only since we are just interested in the leading order contributions in slow roll. This is why the above relation leads to

$$\mathcal{P}_\zeta(k) = \mathcal{P}_{\delta\mathcal{N}}(k) = \left. \frac{d\delta\mathcal{N}^2}{d\langle\mathcal{N}\rangle} \right|_{\langle\mathcal{N}\rangle = \ln(k_{\text{end}}/k)}. \quad (2.244)$$

Since  $\delta\mathcal{N}^2$  is given by  $g(\phi)$ , see Eq. (2.237), and  $\langle\mathcal{N}\rangle$  is given by  $f(\phi)$ , see Eq. (2.222), noting that  $d/d\langle\mathcal{N}\rangle = (d\phi/d\langle\mathcal{N}\rangle)d/d\phi = (1/f')d/d\phi$ , this gives rise to

$$\mathcal{P}_\zeta(\phi) = \frac{g'(\phi)}{f'(\phi)} = 2 \int_{\phi}^{\hat{\phi}} d\psi \frac{f'^2(\psi)}{f(\phi)} \exp \left[ \frac{24\pi^2 M_{\text{Pl}}^4}{V(\psi)} - \frac{24\pi^2 M_{\text{Pl}}^4}{V(\phi)} \right], \quad (2.245)$$

where  $f$  is given by Eq. (2.223). Here, by  $\mathcal{P}_\zeta(\phi)$ , we mean the power spectrum calculated at a scale  $\mathbf{k}$  such that when it crosses the Hubble radius, the inflaton field value is  $\phi$ . This is the main result of this section since it provides, for the first time, a complete expression of the curvature perturbations power spectrum in stochastic inflation, computed in a non perturbative manner and, therefore, including the full stochastic effects.

### Classical Limit

As a consistency check, it is important to make sure that the standard result for the power spectrum (2.205) is properly recovered in the classical limit  $x \ll 1$ . Since we already derived the classical limit for  $\delta\mathcal{N}^2$ , given by Eq. (2.241), and the classical limit for  $\langle\mathcal{N}\rangle$ , given by the classical trajectory (2.229), one can plug these two expressions in Eq. (2.244). Noting again that  $d/d\langle\mathcal{N}\rangle = (d\phi/d\langle\mathcal{N}\rangle)d/d\phi = (1/f')d/d\phi$ , one obtains

$$P_\zeta|_{\text{cl}} = \frac{1}{12\pi^2 M_{\text{Pl}}^6} \frac{V^3(\phi)}{V'^2(\phi)}, \quad (2.246)$$

which exactly matches the usual result (2.205), since at leading order in slow roll one has  $H^2 \simeq V/(3M_{\text{Pl}}^2)$  and  $\epsilon_1 = M_{\text{Pl}}^2/2(V'/V)^2$ . This generalizes the result of Ref. [350], where this

correspondence is shown but only for inflationary models where the Hubble parameter varies linearly with  $\phi$ , that is for inflationary potentials of the specific form given by Eq. (50) in Ref. [208], section 3.1. Here we have extended this result to any potential is single-field slow-roll inflation.

### 2.4.3.7. Scalar Spectral Index

Finally, it can be interesting to calculate the scalar spectral index, defined in Eq. (2.112) and which characterizes the way  $\mathcal{P}_\zeta$  varies with  $k$ . Since we established in the last section how  $\mathcal{P}_\zeta$  varies with  $\phi$ , see Eq. (2.245), we first need to determine how  $\phi$  varies with  $k$ . At leading order in slow roll, one has

$$\frac{\partial}{\partial \ln(k)} \simeq (1 + \epsilon_1) \frac{\partial}{\partial N} \quad (2.247)$$

$$\simeq -\frac{1}{\partial \langle \mathcal{N} \rangle / \partial \phi} \frac{\partial}{\partial \phi} \quad (2.248)$$

$$\simeq -\frac{1}{f'(\phi)} \frac{\partial}{\partial \phi}. \quad (2.249)$$

When going from Eq. (2.247) to Eq. (2.248), the  $1 + \epsilon_1$  term has been dropped since it only gives rise to subdominant corrections in slow roll. Making use of Eq. (2.244) for  $\mathcal{P}_\zeta$ , one obtains

$$n_s = 1 - \frac{g''(\phi)}{f'(\phi)g'(\phi)} + \frac{f''(\phi)}{f'^2(\phi)}, \quad (2.250)$$

where  $f(\phi)$  is given by Eq. (2.223) and  $g(\phi)$  is given by Eq. (2.238).

#### Classical Limit

The regular classical result can also be recovered as in section 2.4.3.6. When  $f(\phi)$  is given by its classical limit (2.229) and  $g(\phi)$  is given by its classical limit (2.241), the above result (2.250) gives rise to

$$n_s|_{\text{cl}} = 1 - M_{\text{Pl}}^2 \left[ 3 \left( \frac{V'}{V} \right)^2 - 2 \frac{V''}{V} \right] = 1 - 2\epsilon_1 - \epsilon_2, \quad (2.251)$$

which matches the formula given below Eq. (2.206) since in the slow-roll approximation, the slow-roll parameters  $\epsilon_1$  and  $\epsilon_2$  can be expressed as

$$\epsilon_1 = \frac{M_{\text{Pl}}^2}{2} \left( \frac{V'}{V} \right)^2, \quad (2.252)$$

$$\epsilon_2 = 2M_{\text{Pl}}^2 \left[ \left( \frac{V'}{V} \right)^2 - \frac{V''}{V} \right], \quad (2.253)$$

see Eqs. (2.15) and (2.16).

### 2.4.3.8. A Complete Example: Large Field Inflation

In sections 2.4.3.3 and 2.4.3.4, we have exemplified the above results in the case of a large field potential. This is why, to gain some intuition on how the stochastic effects modify the power

spectrum, and in order to make clear how the calculation presented here works in practice, we now turn to the complete treatment of large field inflation. We recall that the potential of these models is given by

$$V(\phi) = M^4 \left( \frac{\phi}{M_{\text{Pl}}} \right)^p. \quad (2.254)$$

In the figures displayed below, we set the mass scale  $M^4$  to the value that fits the amplitude of the power spectrum  $P_\zeta$ , when the power spectrum is calculated with the classical formula. The classical trajectory (2.229) can be integrated as  $\phi/M_{\text{Pl}} = \sqrt{\phi_{\text{end}}^2/M_{\text{Pl}}^2 - 2p(N - N_{\text{end}})}$ , where  $\phi_{\text{end}}/M_{\text{Pl}} = p/\sqrt{2}$  is the location where  $\epsilon_1 \simeq p^2 M_{\text{Pl}}^2/(2\phi^2) = 1$ . Then, Eq. (2.205) gives rise to

$$\frac{M^4}{M_{\text{Pl}}^4} = 12\pi^2 p^2 \left( \frac{p^2}{2} + 2p\Delta N_* \right)^{-1-p/2} \mathcal{P}_{\zeta_*}, \quad (2.255)$$

where we take the measured value [163]  $\mathcal{P}_{\zeta_*} \simeq 2.203 \times 10^{-9}$  and we let  $\Delta N_* \simeq 50$ . Obviously, when the power spectrum does not match the one given by the classical calculation, this mass normalization needs to be changed accordingly (see section 2.4.3.9) but here we use this value for illustrative purpose.

The aim of this section is to see which corrections to the power spectrum arise due to stochastic effects, and also to check the validity of the formulas derived above with a numerical code that integrates a large number of realizations of the Langevin equation. In passing, it is worth noting that in order to avoid large numerical errors when doing so (due *e.g.* to the small value of  $M^4/M_{\text{Pl}}^4 \simeq 10^{-11}$ ), the Langevin equation (2.208) can be written in terms of the rescaled variables

$$y = \left( \frac{M^2}{2\pi\sqrt{3p}M_{\text{Pl}}^2} \right)^{2/p} \frac{\phi}{M_{\text{Pl}}} \quad \text{and} \quad s = p \left( \frac{M^2}{2\pi\sqrt{3p}M_{\text{Pl}}^2} \right)^{4/p} N, \quad (2.256)$$

so that it is given by the simple form

$$\frac{dy}{ds} = -\frac{1}{y} + y^{p/2} \xi(s). \quad (2.257)$$

This equation is solved a large number of times (typically  $10^6 - 10^7$  realizations are produced) and the mean values of  $\mathcal{N}$  and  $\mathcal{N}^2$  are computed over the realizations.

### Mean number of $e$ -folds

The mean number of  $e$ -folds has already been computed and is given by Eq. (2.232). In order to test both the validity of our analytical approach and the reliability of our numerical code, we compare in Fig. 2.8 the integral (2.232) with the ensemble average over a large number of numerical realizations of the Langevin equation (2.257). Since the energy density must remain sub-Planckian, values of  $x$  larger than 1 do not really make sense but here, we display them to check the agreement between our code and our calculation in a broader range. Obviously, this agreement is excellent. When the value of  $\phi_{\text{in}}$  is such that  $x_{\text{in}} \ll 1$ , the classical trajectory (2.229) provides a very good approximation to the mean stochastic trajectory. To go beyond, it proves useful at this point to derive the next-to-leading orders expressions for  $\langle \mathcal{N} \rangle$  in the  $x \ll 1$  limit, to characterize the deviations from the classical trajectory in this regime. Making use of the expansion [269]  $M(1 - 1/p, 2 - 1/p, 1/x) \simeq (1 - 1/p)e^{1/x}[x + x^2/p + (1 + p)/p^2 x^3 + \dots]$  when

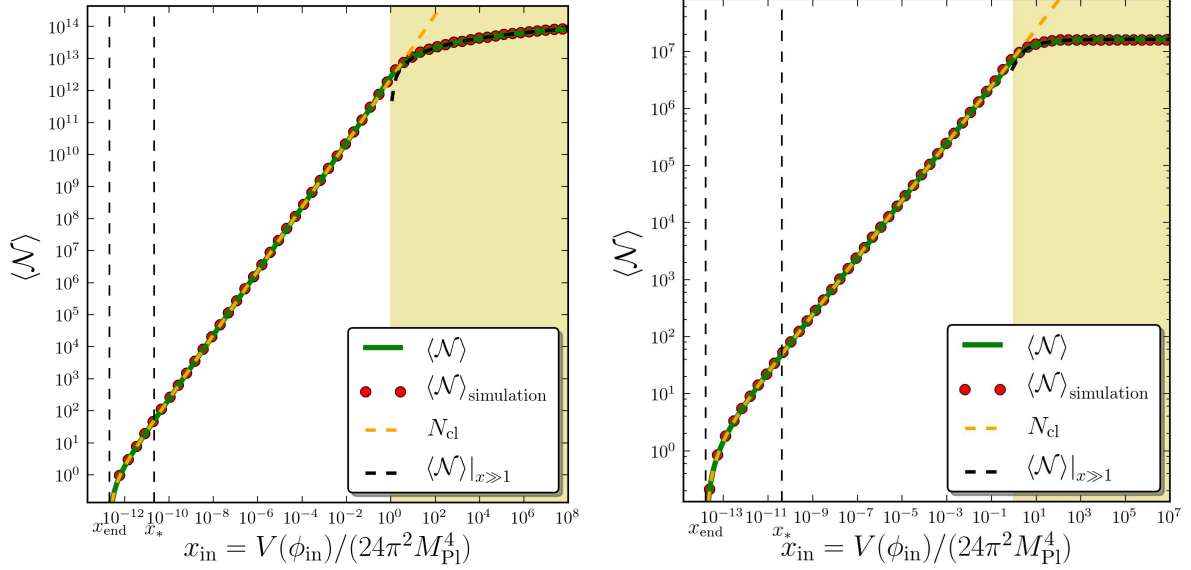


Figure 2.8.: Mean number of  $e$ -folds  $\langle \mathcal{N} \rangle$  realized in the large field potential (2.254) for  $p = 2$  (left panel) and  $p = 4$  (right panel), between  $x_{\text{in}}$  and  $x_{\text{end}}$ , as a function of  $x_{\text{in}}$ , where  $x = V/(24\pi^2 M_{\text{Pl}}^4)$ . The mass scale  $M^4$  is normalized to Eq. (2.255). The location  $x_*$  refers to the value of  $x$  for which the classical number of  $e$ -folds  $N_{\text{cl}} = 50$  and  $x_{\text{end}}$  is where  $\epsilon_1 = 1$ . The green line corresponds to the analytical exact result (2.232), and the red circles are provided by a numerical integration of the Langevin equation (2.257) where a large number of realizations are produced over which the mean value of  $\mathcal{N}$  is computed. Obviously, the agreement with the analytical formula is excellent and confirms both approaches. The orange dashed line corresponds to the classical trajectory (2.229), which provides a good approximation to the exact result when  $x_{\text{in}} \ll 1$ . Finally, the black dashed line corresponds to Eq. (2.259) which is the expansion of Eq. (2.232) in the opposite limit  $x \gg 1$ . Obviously, the calculation makes sense only when  $x < 1$ , *i.e.* outside the yellow shaded area, which is displayed for information only.

$x \ll 1$ , one obtains

$$\begin{aligned} \langle \mathcal{N} \rangle|_{x_{\text{end}} < x_{\text{in}} \ll 1} &\simeq \left( \frac{24\pi^2 M_{\text{Pl}}^4}{M^4} \right)^{2/p} \frac{1}{p^2} \left[ \frac{p}{2} \left( x_{\text{in}}^{2/p} - x_{\text{end}}^{2/p} \right) \right. \\ &\quad \left. + \frac{1}{p+2} \left( x_{\text{in}}^{2/p+1} - x_{\text{end}}^{2/p+1} \right) + \frac{1}{2p} \left( x_{\text{in}}^{2/p+2} - x_{\text{end}}^{2/p+2} \right) + \dots \right]. \end{aligned} \quad (2.258)$$

The term on the first line corresponds to the classical trajectory (2.229), and the following ones are corrections in the regime  $x_{\text{in}} \ll 1$ . Again, the opposite limit  $x \gg 1$  corresponds to super-Planckian energy densities where our calculation should not apply. However, it can be interesting to see how Eq. (2.258) breaks when  $x \gtrsim 1$ . If one expands Eq. (2.232) in the limit

where  $x_{\text{in}} \gg 1$ , one obtains

$$\langle \mathcal{N} \rangle \Big|_{x_{\text{end}} \ll 1, x_{\text{in}} \gg 1} \simeq \begin{cases} \left( \frac{24\pi^2 M_{\text{Pl}}^4}{M^4} \right)^{2/p} \frac{x_{\text{in}}^{2/p-1}}{(p-1)(2-p)} & \text{if } 1 < p < 2 \\ \frac{12\pi^2 M_{\text{Pl}}^4}{M^4} \ln(x_{\text{in}}) & \text{if } p = 2 \\ \left( \frac{24\pi^2 M_{\text{Pl}}^4}{M^4} \right)^{2/p} \left[ C(p) - \frac{x_{\text{in}}^{2/p-1}}{(p-1)(p-2)} \right] & \text{if } p > 2 \end{cases}, \quad (2.259)$$

where  $C(p)$  is a constant depending on  $p$  but which is always of order one. These expressions are also displayed in Fig. 2.8 where one can check that they provide reliable approximations to the exact result when  $x_{\text{in}} \gg 1$ . Interestingly enough, when  $p > 2$ , the mean number of  $e$ -folds that one can realize in the large field potential is always finite even if one starts from  $\phi_{\text{in}} = \infty$ , and is of the order  $\mathcal{O}(1)(M/M_{\text{Pl}})^{8/p}$ . This is not the case when  $p \leq 2$  for which the potential is flatter and the mean number of  $e$ -folds blows up with  $\phi_{\text{in}}$ .

### Number of $e$ -folds dispersion

The calculation of the power spectrum also requires to obtain the dispersion in the number of  $e$ -folds. Applying Eq. (2.238) to the potential (2.254), one gets

$$\delta \mathcal{N}^2 = \frac{2}{p^2(p-1)^2} \left( \frac{24\pi^2 M_{\text{Pl}}^4}{M^4} \right)^{4/p} \int_{x_{\text{end}}}^{x_{\text{in}}} ds \int_s^\infty dt (st^3)^{\frac{1}{p}-1} e^{-\frac{1}{s}-\frac{1}{t}} M^2 \left( 1 - \frac{1}{p}, 2 - \frac{1}{p}, \frac{1}{t} \right). \quad (2.260)$$

This expression is displayed in Fig. 2.9 together with the result of a numerical integration of the Langevin equation for a large number of realizations over which the mean values of  $\mathcal{N}$  and  $\mathcal{N}^2$  are computed, and  $\delta \mathcal{N}^2$  is obtained. Obviously, the agreement is excellent. At this point, it again proves useful to derive the asymptotic limits of Eq. (2.260) in the regimes  $x_{\text{in}} \ll 1$  and  $x_{\text{in}} \gg 1$ , even if we recall that the later is non-physical. When  $x_{\text{end}} < x_{\text{in}} \ll 1$ , if  $p > 3/2$ , one has

$$\delta \mathcal{N}^2 \Big|_{x_{\text{end}} < x_{\text{in}} \ll 1} \simeq \frac{2}{p^4} \left( \frac{24\pi^2 M_{\text{Pl}}^4}{M^4} \right)^{4/p} \left[ \frac{p}{p+4} \left( x_{\text{in}}^{4/p+1} - x_{\text{end}}^{4/p+1} \right) + \frac{p+5}{2p+4} \left( x_{\text{in}}^{4/p+2} - x_{\text{end}}^{4/p+2} \right) + \frac{2p^2+15p+18}{3p^2+4p} \left( x_{\text{in}}^{4/p+3} - x_{\text{end}}^{4/p+3} \right) \right]. \quad (2.261)$$

The first line of this expression exactly matches the classical approximation (2.241) to  $\delta \mathcal{N}^2$ , as expected, while the following terms are corrections in the regime  $x \ll 1$ . On the other hand, when  $x_{\text{end}} \ll 1$  but  $x_{\text{in}} \gg 1$ , one has

$$\delta \mathcal{N}^2 \Big|_{x_{\text{end}} \ll 1, x_{\text{in}} \gg 1} \simeq \begin{cases} \frac{1}{(p-1)^2(2-p)(2p-3)} \left( \frac{24\pi^2 M_{\text{Pl}}^4}{M^4} \right)^{\frac{4}{p}} x_{\text{in}}^{4/p-2} & \text{if } \frac{3}{2} < p < 2 \\ \left( \frac{24\pi^2 M_{\text{Pl}}^4}{M^4} \right)^2 \ln(x_{\text{in}}) & \text{if } p = 2 \\ \left( \frac{24\pi^2 M_{\text{Pl}}^4}{M^4} \right)^{4/p} \left[ \bar{C}(p) - \frac{x_{\text{in}}^{4/p-2}}{(p-1)^2(p-2)(2p-3)} \right] & \text{if } p > 2 \end{cases}, \quad (2.262)$$

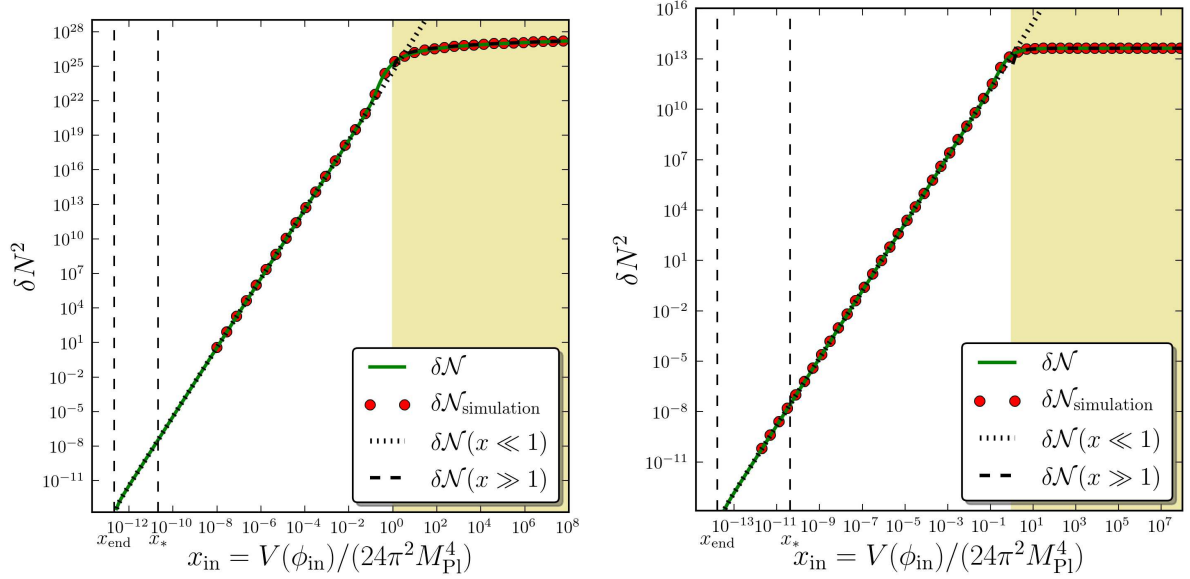


Figure 2.9.: Dispersion of the number of  $e$ -folds  $\delta\mathcal{N}^2 = \langle \mathcal{N}^2 \rangle - \langle \mathcal{N} \rangle^2$  realized in the large field potential (2.254) for  $p = 2$  (left panel) and  $p = 4$  (right panel), between  $x_{\text{in}}$  and  $x_{\text{end}}$ , as a function of  $x_{\text{in}}$ , where  $x \equiv V/(24\pi^2 M_{\text{Pl}}^4)$ . The mass scale  $M^4$  is normalized to Eq. (2.255). The location  $x_*$  refers to the value of  $x$  for which the classical number of  $e$ -folds  $N_{\text{cl}} = 50$  and  $x_{\text{end}}$  is where  $\epsilon_1 = 1$ . The green line corresponds to the analytical exact result (2.260), and the red circles are provided by a numerical integration of the Langevin equation (2.257) where a large number of realizations are produced over which the mean values of  $\mathcal{N}$  and  $\mathcal{N}^2$  are computed. Obviously, the agreement with the analytical formula is excellent and confirms both approaches. The black dotted line corresponds to the classical limit (2.241), which provides a good approximation to the exact result when  $x_{\text{in}} \ll 1$ . Finally, the black dashed line corresponds to Eq. (2.262) which is the expansion of Eq. (2.260) in the opposite limit  $x \gg 1$ . Again, this limit is non-physical since one must have  $x < 1$  in order to keep the energy densities from being super-Planckian, and the yellow shaded area is displayed only to check the agreement between the numerical code and the analytical calculation in a broader range.

where  $\bar{C}(p)$  is a constant depending on  $p$  but which is always of order one. These expressions are also displayed in Fig. 2.9 where one can check that they provide reliable approximations to the exact result. As for the mean number of  $e$ -folds, it is worth noticing that when  $p > 2$ ,  $\delta\mathcal{N}^2$  is bounded by  $\mathcal{O}(1)(M_{\text{Pl}}/M)^{16/p}$ , while when  $p \leq 2$  it can reach arbitrarily large values in principle.

### Power Spectrum

Following section 2.4.3.6, the power spectrum can now be properly computed. Making use of Eq. (2.245), one obtains for the large field potential (2.254)

$$\mathcal{P}_\zeta = \frac{2}{p(p-1)} \left( \frac{24\pi^2 M_{\text{Pl}}^4}{M^4} \right)^{2/p} \frac{x^{1-1/p}}{M \left( 1 - \frac{1}{p}, 2 - \frac{1}{p}, \frac{1}{x} \right)} \int_x^\infty t^{3/p-3} e^{-\frac{1}{t}} M^2 \left( 1 - \frac{1}{p}, 2 - \frac{1}{p}, \frac{1}{t} \right) dt. \quad (2.263)$$

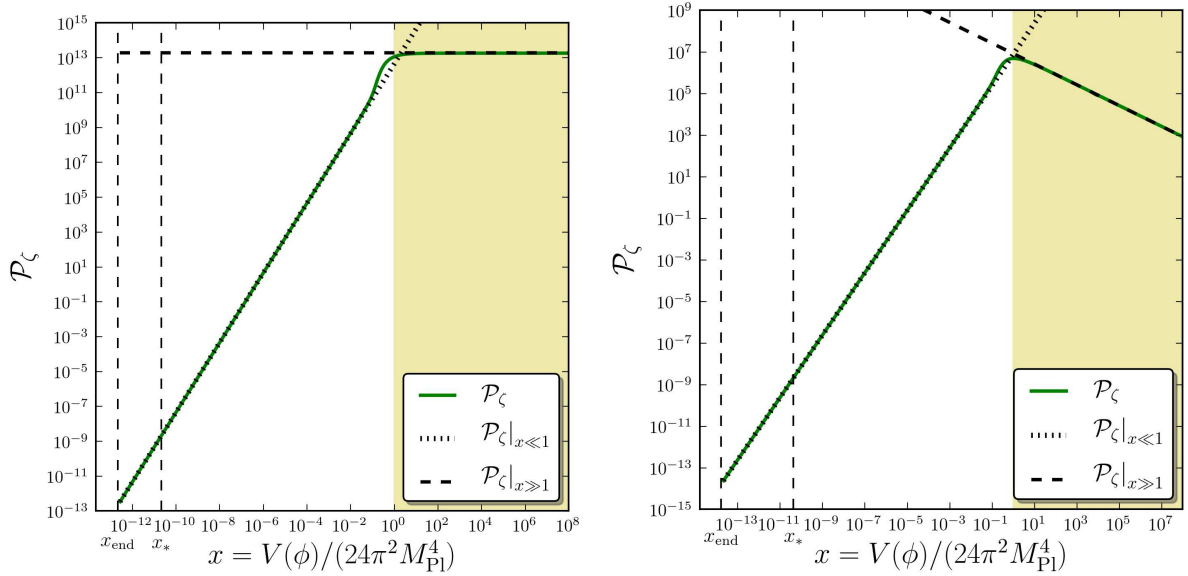


Figure 2.10.: Power Spectrum of curvature perturbations  $\mathcal{P}_\zeta$  realized in the large field potential (2.254) for  $p = 2$  (left panel) and  $p = 4$  (right panel), computed at a scale whose Hubble exit time is labelled by  $x$ , where  $x = V/(24\pi^2 M_{\text{Pl}}^4)$ , as a function of  $x$ , and where inflation terminates at  $x_{\text{end}}$ . The mass scale  $M^4$  is normalized to Eq. (2.255), so that at  $x_*$ , one can check that  $\mathcal{P} \simeq 2 \times 10^{-9}$ . The location  $x_*$  refers to the value of  $x$  for which the classical number of  $e$ -folds  $N_{\text{cl}} = 50$  and  $x_{\text{end}}$  is where  $\epsilon_1 = 1$ . The green line stands for the analytical exact result (2.263). The black dotted line corresponds to the classical limit (2.246), which provides a good approximation to the exact result when  $x \ll 1$ . Finally, the black dashed line corresponds to Eq. (2.266) which is the expansion of Eq. (2.263) in the opposite limit  $x \gg 1$ . As before, the yellow shaded area  $x > 1$  may not be physical and it is displayed for illustrative purpose only.

Here,  $x$  means the actual value of  $x$  at the Hubble exit time of the scale where the power spectrum is calculated. The classical limit of this expression can be obtained either expanding the above formula in  $x \ll 1$ , or combining Eqs. (2.258) and (2.261). In either case, one obtains

$$\mathcal{P}_\zeta|_{x_{\text{end}} < x \ll 1} \simeq \frac{2}{p^2} \left( \frac{24\pi^2 M_{\text{Pl}}^4}{M^4} \right)^{\frac{2}{p}} x^{1+\frac{2}{p}} \left[ 1 + \left( 1 + \frac{4}{p} \right) x + \left( 2 + \frac{13}{p} + \frac{13}{p^2} \right) x^2 \right] \quad (2.264)$$

$$\simeq P_{\zeta|\text{cl}} \left[ 1 + \left( 1 + \frac{4}{p} \right) x + \left( 2 + \frac{13}{p} + \frac{13}{p^2} \right) x^2 \right], \quad (2.265)$$

where  $P_{\zeta|\text{cl}}$  is given by Eq. (2.246) and exactly corresponds to the regular ‘‘classical’’ contribution to the power spectrum. To see how this result breaks when  $x \gtrsim 1$ , it can be interesting to write the opposite limit  $x \gg 1$ , where the power spectrum can be obtained combining Eqs. (2.259) and (2.262). Interestingly enough, for  $\langle \mathcal{N} \rangle$  and  $\delta \mathcal{N}^2$ , three different cases were to be distinguished according to the value of  $p$ . As far as the power spectrum is concerned, they all give rise to the same expression, namely

$$\mathcal{P}_\zeta|_{x_{\text{end}} \ll 1, x \gg 1} \simeq \frac{2}{(p-1)(2p-3)} \left( \frac{24\pi^2 M_{\text{Pl}}^4}{M^4} \right)^{2/p} x^{2/p-1}. \quad (2.266)$$

In particular, when  $p = 2$ , the power spectrum tend to be constant (*i.e.* scale invariant) in the limit  $x \gg 1$ . This is the limiting case between  $p < 2$  where the power spectrum amplitude

increases with  $\phi$  in the  $x \gg 1$  limit, and the case  $p > 2$  where the power spectrum amplitude decreases with  $\phi$ .

The three formulas (2.263), (2.246) and (2.266) are displayed together in Fig. 2.10 for  $p = 2$  and  $p = 4$ . The mass scale  $M^4$  is normalized to Eq. (2.255), *i.e.* the amplitude of the power spectrum is calibrated to  $\mathcal{P}_\zeta \simeq 2 \times 10^{-9}$  when it is computed  $\sim 50$   $e$ -folds before the location defined by  $\epsilon_1 = 1$ . Of course, if one is interested in a situation where the scales of astrophysical interest today crossed the Hubble radius at a different value of  $\phi_*$  or equivalently  $x_*$  (for example, if inflation proceeds at larger fields and ends by tachyonic instability), then the mass scale  $M^4$  needs to be calibrated differently (and the value of  $x_{\text{end}}$  has to be changed as well). In any case, Fig. 2.10 shows how the amplitude of the power spectrum varies with  $\phi$  for fixed  $M^4$ .

A few other comments are in order. First, as expected, when  $x \ll 1$ , the classical limit provides a good approximation to the exact result. Actually, from Eq. (2.265), the relative difference between the two is given by  $\delta\mathcal{P}_\zeta / \mathcal{P}_\zeta|_{\text{cl}} \simeq (1 + 4/p)x > 0$ , which means that the stochastic effects account for a slightly larger amplitude of the power spectrum in this limit.<sup>24</sup> Second, in the regular case where inflation terminates when  $\epsilon_1 = 1$  and the power spectrum is computed 50  $e$ -folds before this point, Eq. (2.255) gives rise to  $x_* \simeq 10^{-11}$  and the actual stochastic modification to the power spectrum is accordingly small. Therefore, in the large field model, only tiny corrections appear, and we will come back to this point in section 2.4.3.9.

### Scalar Spectral Index

Finally, let us calculate the spectral index  $n_s$  at a given scale whose Hubble exit time is labelled by  $x$ . It is given by Eq. (2.250) and can be computed straightforwardly. Its asymptotic limits can also be worked out making use of the previous formulas. In the limit where  $x \ll 1$ , one obtains

$$n_s|_{x_{\text{end}} < x \ll 1} - 1 \simeq - \left( \frac{M^4}{24\pi^2 M_{\text{Pl}}^4} \right)^{2/p} p(p+2) x^{-\frac{2}{p}} \left[ 1 + \left( 1 - \frac{1}{p} + \frac{2}{p+2} \right) x + \left( 3 + \frac{8}{p+2} + \frac{3}{p} - \frac{1}{p^3} \right) x^2 + \mathcal{O}(x^3) \right] \quad (2.267)$$

$$\simeq (n_s|_{\text{cl}} - 1) \left[ 1 + \left( 1 - \frac{1}{p} + \frac{2}{p+2} \right) x + \left( 3 + \frac{8}{p+2} + \frac{3}{p} - \frac{1}{p^3} \right) x^2 + \mathcal{O}(x^3) \right], \quad (2.268)$$

where one has used Eq. (2.251) to single out the classical result  $n_s|_{\text{cl}}$ . Therefore, one can check that in the classical limit, the regular result is recovered. The scalar index is red ( $n_s < 1$ ), and stochastic effects tend to make it even redder by slightly decreasing the actual value of  $n_s$ . Again, even if it corresponds to super-Planckian energy densities, it can be interesting to see how the above result breaks in the regime  $x \gtrsim 1$ , and one obtains

$$n_s|_{x_{\text{end}} \ll 1, x \gg 1} \simeq 1 - \left( \frac{M^4}{24\pi^2 M_{\text{Pl}}^4} \right)^{\frac{2}{p}} (p-1)(2-p) x^{1-\frac{2}{p}}. \quad (2.269)$$

If  $p < 2$ , the spectral index remains red and keeps increasing with  $x$  towards 1 (even if slower than in the classical regime), whereas if  $p > 2$ , the spectral index becomes blue and starts increasing with  $x$  away from 1, *i.e.* away from scale invariance. The case  $p = 2$  is singular since, at leading order, the previous expression gives  $n_s = 1$ . This is why one needs to work out

<sup>24</sup>Contrary to what is incorrectly concluded in Ref. [331], as explained in the introductory part of section 2.4.3.

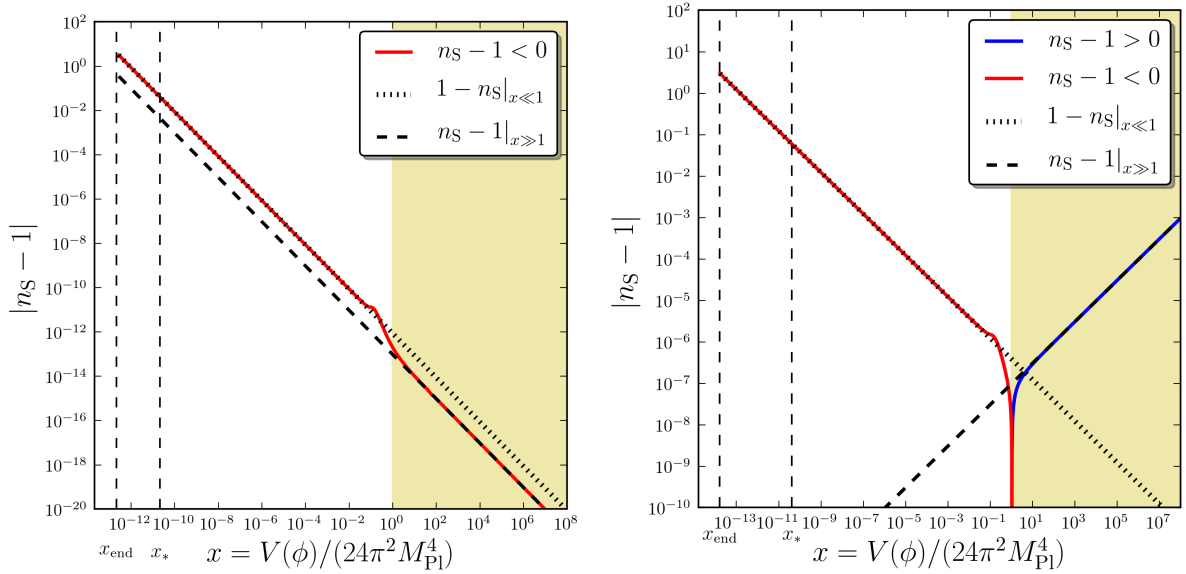


Figure 2.11.: Spectral index  $n_s$  of the power spectrum of curvature perturbations realized in the large field potential (2.254) for  $p = 2$  (left panel) and  $p = 4$  (right panel), computed at a scale whose Hubble exit time is labelled by  $x$ , where  $x = V/(24\pi^2 M_{\text{Pl}}^4)$ , as a function of  $x$ , and where inflation terminates at  $x_{\text{end}}$ . The mass scale  $M^4$  is normalized to Eq. (2.255), the location  $x_*$  corresponds to the value of  $x$  for which the classical number of  $e$ -folds  $N_{\text{cl}} = 50$  and  $x_{\text{end}}$  is where  $\epsilon_1 = 1$ . The coloured lines stand for the analytical exact result (2.250), it is blue when the spectral index is “blue” ( $n_s > 1$ ), and it is red when the spectral index is “red” ( $n_s < 1$ ). The black dotted line corresponds to the classical limit (2.251), which provides a good approximation to the exact result when  $x \ll 1$ . Finally, the black dashed line corresponds to Eqs. (2.269) and (2.270) which is the expansion of Eq. (2.250) in the opposite limit  $x \gg 1$ . As before, the yellow shaded area  $x > 1$  may not be physical and it is displayed for illustrative purpose only.

Eqs. (2.259) and (2.266) at next-to-leading order in  $1/x$ . After a straightforward calculation, one obtains

$$n_s|_{x_{\text{end}} \ll 1, x \gg 1} (p = 2) \simeq 1 - \frac{M^4}{24\pi^2 M_{\text{Pl}}^4} \frac{8}{9x}. \quad (2.270)$$

Therefore, in this case, the spectral index also remains red, and increases towards 1 at the same rate than in the classical regime. The exact result (2.250) is compared with these approximations in Fig. 2.11 for  $p = 2$  (left panel) and  $p = 4$  (right panel). If  $p = 2$ , one can see that the stochastic effects do not modify much the behaviour of  $n_s$  even when  $x \gtrsim 1$  and only add some feature around  $x \simeq 1$ . However, this case is singular and in general, the result radically changes when  $x$  approaches 1. When  $p > 2$ , the spectral index can even turn from red to blue.

#### 2.4.3.9. Discussion

At the beginning of section 2.4.3, we explained that, because of the relation  $\mathcal{P}_\zeta \propto \eta^2 \sim 2 \times 10^{-9}$ , the stochastic effects play a negligible role at the time where the scales of astrophysical today cross the Hubble radius. However, we pointed out that it does not mean that  $\eta$  remains small

during all the last  $\sim 50$   $e$ -folds of inflation, and that some substantial effects on the power spectrum may appear in models where it is not the case. The calculation we carried out in this section shows that it is not the case. Indeed, the amplitude of the corrections to the power spectrum is not controlled by  $\eta$ , but by  $x$ , which is generically small in order to keep energy densities sub-Planckian. Furthermore, contrary to  $\eta$ ,  $x$  can only decrease during inflation. For example, in the large field model we studied, one typically has  $x_* \sim 10^{-11}$ . In general, since at leading order in slow roll, the amplitude of the power spectrum is given by  $\mathcal{P}_\zeta \sim H^2/(8\pi^2 M_{\text{Pl}}^2 \epsilon_1) = x/\epsilon_1$ , one has

$$x_* \simeq \epsilon_{1*} \mathcal{P}_{\zeta*} \simeq \frac{r}{16} \mathcal{P}_{\zeta*}. \quad (2.271)$$

With  $\mathcal{P}_{\zeta*} \sim 2 \times 10^{-9}$  and since  $r < 1$  with certainty, one has  $x_* < 10^{-10}$  and the corrections to the power spectrum we have computed are at most tiny  $\sim 10^{-10}$  corrections, at least under the assumptions we made (single field and slow roll). However, we have built a scheme in which it is straightforward to calculate these corrections, at any order. Besides, our calculation is well under control even when the stochastic effects dominate the inflationary dynamics (in the sense  $\eta \gg 1$ ), as long as  $x < 1$ .

Let us mention a few prospects. In order to test the ability of stochastic inflation to reproduce results beyond the linear level, it would first be interesting to compare what we obtained with a computation of the power spectrum at second order in the perturbations, using the standard approach. Another interesting idea would be to generalize our scheme to multiple-field scenarios, since it has been shown [390] that the  $\delta N$  formalism performs very well in these situations too. Finally, a straightforward prospect would be to enlarge our procedure to the calculation of non-Gaussianities. Indeed, in the  $\delta N$  formalism and in the large scale limit, the  $f_{\text{NL}}$  parameters quantifying non-Gaussianities can be related [356, 391, 390] to the third moments of the number of  $e$ -folds  $\mathcal{N}$  thanks to

$$f_{\text{NL}}^{\text{loc}} = \frac{\delta \mathcal{N}^3}{(\delta \mathcal{N}^2)^2} = \frac{\langle (\mathcal{N} - \langle \mathcal{N} \rangle)^3 \rangle}{\langle (\mathcal{N} - \langle \mathcal{N} \rangle)^2 \rangle^2}. \quad (2.272)$$

In this expression,  $\delta \mathcal{N}^2$  has already been calculated and  $\delta \mathcal{N}^3$  can be obtained just the same way we calculated  $\langle \mathcal{N} \rangle$  and  $\langle \mathcal{N}^2 \rangle$ . In this manner, we could also study non-Gaussianities in the context of stochastic inflation. For single-field models with canonical kinetic terms, the  $f_{\text{NL}}$  parameters are already known to be small (of the order of the slow-roll parameters), but the same formalism as the one we presented here can be derived *e.g.* for DBI inflation [379, 392, 393, 394, 395, 396, 397, 398, 399, 400, 401] (or general k-inflation [383, 384]). In these models, the kinetic term is not canonical and a larger amount of non-Gaussianities can be produced. The stochastic inflation formalism has been generalized to these models [402, 403, 404, 405] where a modified Langevin equation has been obtained, and the same techniques as the one we developed here can in principle be applied.



**Part II.**

**Results and Publications**



### 3. Inflationary Predictions and Comparison with “Big Data” Observations

*Inflation has entered a “big data” era driven by the current flow of high accuracy astrophysical observations, among which are the Cosmic Microwave Background (CMB) measurements. During the time of this thesis notably, the Planck (and if confirmed BICEP2) experiments published unequalled measurements of the CMB maps. It offers an unprecedented opportunity to constrain the inflationary theory. This is however a challenging project given the size of the inflationary landscape which contains hundreds of different scenarios. The objective of this first chapter is to take full advantage of the unprecedented accuracy of the data to determine which models appear to be favoured.*

#### Publications

---

3.1. “Horizon-Flow off-track for Inflation” (article) . . . . .	106
3.2. “Encyclopædia Inflationaris” (article) . . . . .	108
3.3. “The Best Inflationary Models After Planck” (article) . . . .	110
3.4. “Compatibility of Planck and BICEP2 in the Light of Inflation” (article) . . . . .	112
3.5. “K-inflationary Power Spectra at Second Order” (article) . .	114

---

The inflationary theory contains hundreds of different scenarios. As a consequence, it is a difficult task to single out the ones that are favoured by the observations. In order to take full advantage of the unprecedented accuracy of astrophysical data, which is needed to address this problem, it is necessary to develop new tools and techniques in order to perform a change of scales in the analysis and to adopt a systematic approach.

A first attempt to carry out this programme is to make use of model independent parametrizations of inflation, such as the one of “horizon-flow”. In this approach, the analysis is run over quantities describing the way the Hubble parameter  $H$  varies with the inflaton field  $\phi$  in single-field inflation. In particular, potential reconstruction and the search for “generic” inflationary predictions have been addressed with this technique. In section 3.1, Ref. [208], we show that in fact, the horizon-flow framework implicitly samples a subclass of phenomenological inflationary

potentials, which strongly bias the analysis. Furthermore, it relies on trajectories in phase space that differ from the slow-roll, that are sometimes even unstable, and that make the horizon-flow setup blind to entire inflationary regimes. Such an approach should therefore be avoided.

On the contrary, slow roll does not suffer from these flaws and this is why in collaboration with Jérôme Martin and Christophe Ringeval, we have used this framework to systematically analyse the inflationary models one by one. For each of them, we derived the corresponding predictions and compared them to the Planck data. The results of this somewhat “industrial” project are presented in section 3.2, Ref. [205]. We focused on the simplest models, the single-field slow-roll models with minimal kinetic term, since there is currently no observational evidence for non-minimal extensions of the inflationary paradigm.

Together with this paper, we developed the publicly available library<sup>1</sup> ASPIC, which provides all fortran routines needed to quickly derive reheating consistent observable predictions for all those scenarios. From a systematic scan of the literature, we found that this amounts to including  $\sim 75$  potentials. This number should be compared with three or four representing the previous state of the art. The ASPIC library is an evolutive project and is intended to be completed as new models appear.

We then used Bayesian inference and model comparison techniques to rank the ASPIC models and find the best ones. Interfacing the ASPIC codes with a machine-learned effective likelihood and a nested sampling algorithm, we designed a numerical pipeline that provides the Bayesian evidences and complexities of  $\sim 200$  models of inflation using the Planck 2013 CMB data, from non-committal and well-studied priors. The results of this analysis are presented in section 3.3, Ref. [206]. We showed that one third of the models can now be considered as strongly disfavoured, and that the preferred potentials are of the plateau type, *i.e.* they are such that both the kinetic energy and the kinetic-to-total energy ratio increase during inflation.

When the BICEP2 experiment released its measurements of the CMB polarization, we updated our results including these data in the analysis. This can be found in section 3.4, Ref. [207]. In particular, we investigated the implications for inflation of the detection of  $B$ -modes polarization *if* it is of primordial origin. We showed that the sets of inflationary models preferred by Planck alone and BICEP2 alone are almost disjoint, indicating a clear tension between these two data sets. More precisely, we addressed this tension with a Bayesian measure of compatibility between the two data sets, showing that for the Planck-preferred as for the BICEP2-preferred models, they tend to be incompatible. This is why at this point, it seems premature to draw definitive conclusions, and one should better wait for the release of the polarization data from Planck, scheduled by the end of the year, and for a clarification of the dust contribution to the BICEP2 measured signal.

Finally, there are various possible extensions and prospects for this project. One of them is to generalize our analysis and numerical pipeline to k-inflation models [383, 384], where the speed of sound is varying, but the action for the curvature perturbations remains quadratic (see also Refs. [406, 407]). This is why in Ref. [209], presented in section 3.5, we have paved the way for including such models in the analysis, by calculating for the first time the next-to-next-to-leading order scalar and tensor primordial power spectra in k-inflation. We made use of the uniform approximation together with a second order expansion in the Hubble and sound-flow functions.

---

<sup>1</sup><http://cp3.irmp.ucl.ac.be/~ringeval/aspic.html>



**Horizon-flow off-track for inflation**

Vincent Vennin\*

*Institut d'Astrophysique de Paris, UMR 7095-CNRS, Université Pierre et Marie Curie,  
98bis boulevard Arago, 75014 Paris, France*

(Received 20 January 2014; published 10 April 2014)

Inflation can be parametrized by means of truncated flow equations. In this “horizon-flow” setup, generic results have been obtained, such as typical values for  $r/(1 - n_S)$ . They are sometimes referred to as intrinsic features of inflation itself. In this paper we first show that the phenomenological class of inflationary potentials sampled by horizon flow is directly responsible for such predictions. They are therefore anything but generic. Furthermore, the horizon-flow setup is shown to rely on trajectories in phase space that differ from the slow roll. For a given potential, we demonstrate that this renders horizon flow blind to entire relevant inflationary regimes, for which the horizon-flow trajectory is shown to be unstable. This makes horizon flow a biased parametrization of inflation.

DOI: 10.1103/PhysRevD.89.083526

PACS numbers: 98.80.Cq

**I. INTRODUCTION**

Inflation is currently the leading paradigm for explaining the physical conditions that prevailed in the very early Universe [1–5]. It describes a phase of accelerated expansion that solves the puzzles of the standard hot big bang model, and it provides a causal mechanism for generating inhomogeneities on cosmological scales [6–11]. These inhomogeneities result from the amplification of the unavoidable vacuum quantum fluctuations of the gravitational and matter fields during the accelerated expansion. In particular, inflation predicts that their spectrum should be almost scale invariant, with small deviations from scale invariance being related to the precise microphysics of inflation. This prediction is consistent with the current high precision astrophysical observations [12–15]. In particular, the recent Planck measurement [15] of the cosmic microwave background temperature map gives together with WMAP polarization data a slightly red tilted scalar spectral index  $n_S \simeq 0.96$ , ruling out exact scale invariance  $n_S = 1$  at over  $5\sigma$  and enabling us to constrain the inflationary models still allowed by the observations [16,17].

Together with the absence of primordial non-Gaussianities and of isocurvature modes [15], these results indicate that, at this stage, the full set of observations can be accounted for in the minimal setup, where inflation is driven by a single scalar field  $\phi$ , the inflaton field, minimally coupled to gravity, and evolving in some potential  $V(\phi)$ . The action for such a system is given by (hereafter  $M_{\text{Pl}}$  denotes the reduced Planck mass)

$$S = \int \left[ \frac{M_{\text{Pl}}^2}{2} R - \frac{1}{2} \partial_\mu \phi \partial^\mu \phi - V(\phi) \right] \sqrt{-g} d^4x, \quad (1)$$

where the background metric is chosen to be of the flat Friedmann-Lemaître-Robertson-Walker type, i.e. the one of

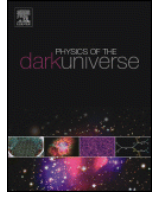
a homogeneous and isotropic expanding universe (about which fluctuations are evolved), given by  $ds^2 = -dt^2 + a^2(t)dx^2$ , where the scale factor  $a(t)$  is a free function of time. However, the physical nature of the inflaton and its relation with the standard model of particle physics and its extensions remain elusive, since the inflationary mechanism is supposed to take place at very high energies in a regime where particle physics is not known and has not been tested in accelerators. Therefore the only requirement on  $V$  is that it should be sufficiently flat to support inflation, but otherwise the multitude of inflaton candidates (with associated potentials) makes the theory as a whole hardly tractable, unless one restricts to a specific model.

If one does so, within a given inflationary model  $V(\phi)$ , there exists a frame of approximation, the slow-roll approximation, which provides a set of manageable equations to calculate an attractor solution for the dynamics arising from the action (1), and to consistently derive the statistical properties of cosmological perturbations produced during inflation. This is why, in order to constrain the inflationary scenario at a level matching the accuracy of the current data, a first approach is to scan the full set of models that have been proposed so far, and to test them one by one [16,17] making use of the slow-roll setup.

Another strategy consists in developing model independent approaches and in studying generic parametrizations of inflation. Among these parametrizations is the “horizon-flow” setup [18–22] which relies on truncated flow equations describing the inflationary dynamics. The starting point is to define a set of flow parameters, based on time derivatives of the Hubble scale  $H \equiv \dot{a}/a$  during inflation (a dot denoting a derivation with respect to cosmic time  $t$ ), and to derive a set of equations for their variation in time. A finite subset of these equations is then solved numerically. Since all the observable quantities related to inflation directly depend on  $H$  and the way it (slowly) varies with time, this is indeed a generic way to describe a full set of

\*vennin@iap.fr

To keep the size of this manuscript manageable, the rest of this article [208] is not displayed here. A full version of it can be found at <http://journals.aps.org/prd/abstract/10.1103/PhysRevD.89.083526> (published version) or at <http://arxiv.org/abs/1401.2926> (arXived version).



## Encyclopædia Inflationaris

Jérôme Martin<sup>a</sup>, Christophe Ringeval<sup>b,\*</sup>, Vincent Vennin<sup>a</sup>

<sup>a</sup>Institut d'Astrophysique de Paris, UMR 7095-CNRS, Université Pierre et Marie Curie, 98bis boulevard Arago, 75014 Paris, France

<sup>b</sup>Centre for Cosmology, Particle Physics and Phenomenology, Institute of Mathematics and Physics, Louvain University, 2 Chemin du Cyclotron, 1348 Louvain-la-Neuve, Belgium

### ARTICLE INFO

#### Article history:

Received 3 October 2013

Accepted 13 January 2014

#### Keywords:

Cosmic inflation

Slow-roll

Reheating

Cosmic microwave background

ASPIC

### ABSTRACT

The current flow of high accuracy astrophysical data, among which are the Cosmic Microwave Background (CMB) measurements by the Planck satellite, offers an unprecedented opportunity to constrain the inflationary theory. This is however a challenging project given the size of the inflationary landscape which contains hundreds of different scenarios. Given that there is currently no observational evidence for primordial non-Gaussianities, isocurvature perturbations or any other non-minimal extension of the inflationary paradigm, a reasonable approach is to consider the simplest models first, namely the slow-roll single field models with minimal kinetic terms. This still leaves us with a very populated landscape, the exploration of which requires new and efficient strategies. It has been customary to tackle this problem by means of approximate model independent methods while a more ambitious alternative is to study the inflationary scenarios one by one. We have developed the new publicly available runtime library ASPIC<sup>1</sup> to implement this last approach. The ASPIC code provides all routines needed to quickly derive reheating consistent observable predictions within this class of scenarios. ASPIC has been designed as an evolutive code which presently supports 74 different models, a number that may be compared with three or four representing the present state of the art. In this paper, for each of the ASPIC models, we present and collect new results in a systematic manner, thereby constituting the first *Encyclopædia Inflationaris*. Finally, we discuss how this procedure and ASPIC could be used to determine the best model of inflation by means of Bayesian inference.

© 2014 Published by Elsevier B.V.

### 1. Introduction

The theory of inflation [1–4] represents a cornerstone of the standard model of modern cosmology (the “hot Big-Bang model” of Lemaître and Friedmann) [5–8]. By definition, it is a phase of accelerated expansion which is supposed to take place in the very early universe, at very high energy, between Big-Bang Nucleosynthesis (BBN) and  $10^{15}$  GeV. Inflation allows us to understand several puzzles that plagued the pre-inflationary standard model (before 1981) and that could not be understood otherwise. Without inflation, the standard model of cosmology would remain incomplete and highly unsatisfactory. The most spectacular achievement of inflation is that, combined with quantum mechanics, it provides a convincing mechanism for the origin of the cosmological fluctuations (the seeds of the galaxies and of the Cosmic Microwave Background – CMB – anisotropies) and predicts that their spectrum should be almost scale invariant (i.e. equal power on all spatial scales) [9–17] which is fully consistent with the observations. Let us notice in passing that this part of the scenario is particularly remarkable since it combines General Relativity and

Quantum Mechanics [18–20, 7, 8, 21–24]. Given all these spectacular successes and given the fact that, despite many efforts, inflation has not been superseded by its various challengers [25–53], this scenario has gradually become a crucial part of modern cosmology. As can be seen in Fig. 1, the number of papers devoted to this topic and published each year is inflating since the advent of inflation.

In order to produce a phase of inflation within General Relativity, the matter content of the universe has to be dominated by a fluid with negative pressure. At very high energy, the correct description of matter is field theory, the prototypical example being a scalar field since it is compatible with the symmetries implied by the cosmological principle. Quite remarkably, if the potential of this scalar field is sufficiently flat (in fact, more precisely, its logarithm) so that the field moves slowly, then the corresponding pressure is negative. This is why it is believed that inflation is driven by one (or several) scalar field(s). For obvious reasons, this scalar field was given the name “inflaton”. However, the physical nature of the inflaton and its relation with the standard model of particle physics and its extensions remain elusive. Moreover the shape of its potential is not known except that it must be sufficiently flat. This is not so surprising since, as mentioned above, the inflationary mechanism is supposed to take place at very high energies in a regime where particle physics is not known and has not been tested in accelerators.

Another crucial aspect of the inflationary scenario is how it ends and how it is connected to the subsequent hot Big-Bang phase. It

<sup>1</sup> <http://cp3.irmp.ucl.ac.be/ringeval/aspic.html>

\* Corresponding author. Tel.: +32 10472075.

E-mail address: [christophe.ringeval@uclouvain.be](mailto:christophe.ringeval@uclouvain.be) (Christophe Ringeval).

To keep the size of this manuscript manageable, the rest of this article [205] is not displayed here. A full version of it can be found at <http://www.sciencedirect.com/science/article/pii/S2212686414000053> (published version) or at <http://arxiv.org/abs/1303.3787> (arX-ived version).

# The best inflationary models after Planck

Jérôme Martin,<sup>a</sup> Christophe Ringeval,<sup>b</sup> Roberto Trotta<sup>c</sup> and Vincent Vennin<sup>a</sup>

<sup>a</sup>Institut d'Astrophysique de Paris, UMR 7095-CNRS, Université Pierre et Marie Curie, 98bis boulevard Arago, 75014 Paris, France

<sup>b</sup>Centre for Cosmology, Particle Physics and Phenomenology, Institute of Mathematics and Physics, Louvain University, 2 Chemin du Cyclotron, 1348 Louvain-la-Neuve, Belgium

<sup>c</sup>Imperial College London, Astrophysics & Imperial Centre for Inference and Cosmology, Blackett Laboratory, Prince Consort Road, London SW7 2AZ, United Kingdom

E-mail: [jmartin@iap.fr](mailto:jmartin@iap.fr), [christophe.ringeval@uclouvain.be](mailto:christophe.ringeval@uclouvain.be), [r.trotta@imperial.ac.uk](mailto:r.trotta@imperial.ac.uk), [vennin@iap.fr](mailto:vennin@iap.fr)

Received December 20, 2013

Revised February 8, 2014

Accepted February 18, 2014

Published March 19, 2014

**Abstract.** We compute the Bayesian evidence and complexity of 193 slow-roll single-field models of inflation using the Planck 2013 Cosmic Microwave Background data, with the aim of establishing which models are favoured from a Bayesian perspective. Our calculations employ a new numerical pipeline interfacing an inflationary effective likelihood with the slow-roll library *ASPIC* and the nested sampling algorithm *MultiNest*. The models considered represent a complete and systematic scan of the entire landscape of inflationary scenarios proposed so far. Our analysis singles out the most probable models (from an Occam's razor point of view) that are compatible with Planck data, while ruling out with very strong evidence 34% of the models considered. We identify 26% of the models that are favoured by the Bayesian evidence, corresponding to 15 different potential shapes. If the Bayesian complexity is included in the analysis, only 9% of the models are preferred, corresponding to only 9 different potential shapes. These shapes are all of the plateau type.

**Keywords:** inflation, CMBR experiments, physics of the early universe, cosmological parameters from CMBR

**ArXiv ePrint:** [1312.3529](https://arxiv.org/abs/1312.3529)

To keep the size of this manuscript manageable, the rest of this article [206] is not displayed here. A full version of it can be found at <http://iopscience.iop.org/1475-7516/2014/03/039/> (published version) or at <http://arxiv.org/abs/1312.3529> (arXived version).

# Compatibility of Planck and BICEP2 in the Light of Inflation

Jérôme Martin,<sup>1,\*</sup> Christophe Ringeval,<sup>2,†</sup> Roberto Trotta,<sup>3,‡</sup> and Vincent Vennin<sup>1,§</sup>

<sup>1</sup>*Institut d'Astrophysique de Paris, UMR 7095-CNRS,*

*Université Pierre et Marie Curie, 98 bis boulevard Arago, 75014 Paris, France*

<sup>2</sup>*Centre for Cosmology, Particle Physics and Phenomenology,*

*Institute of Mathematics and Physics, Louvain University,*

*2 Chemin du Cyclotron, 1348 Louvain-la-Neuve (Belgium)*

<sup>3</sup>*Imperial College London, Astrophysics & Imperial Centre for Inference and Cosmology,*

*Blackett Laboratory, Prince Consort Road, London SW7 2AZ (United Kingdom)*

(Dated: May 29, 2014)

We investigate the implications for inflation of the detection of  $B$ -modes polarization in the Cosmic Microwave Background (CMB) by BICEP2. We show that the hypothesis of primordial origin of the measurement is only favored by the first four bandpowers, while the others would prefer unreasonably large values of the tensor-to-scalar ratio. Using only those four bandpowers, we carry out a complete analysis in the cosmological and inflationary slow-roll parameter space using the BICEP2 polarization measurements *alone* and extract the Bayesian evidences and complexities for all the *Encyclopædia Inflationaris* models. This allows us to determine the most probable and simplest BICEP2 inflationary scenarios. Although this list contains the simplest monomial potentials, it also includes many other scenarios, suggesting that focusing model building efforts on large field models only is unjustified at this stage. We demonstrate that the sets of inflationary models preferred by Planck alone and BICEP2 alone are almost disjoint, indicating a clear tension between the two data sets. We address this tension with a Bayesian measure of compatibility between BICEP2 and Planck. We find that for models favored by Planck the two data sets tend to be incompatible, whereas there is a moderate evidence of compatibility for the BICEP2 preferred models. As a result, it would be premature to draw any conclusion on the best Planck models, such as Starobinsky and/or Kähler moduli inflation. For the subset of scenarios not exhibiting data sets incompatibility, we update the evidences and complexities using both data sets together.

PACS numbers: 98.80.Cq

## I. INTRODUCTION

The recent discovery of  $B$ -mode polarization in the Cosmic Microwave Background (CMB) by BICEP2 [1], if confirmed to be of primordial origin [2], would constitute a breakthrough for our understanding of early universe cosmology. In addition to lensing,  $B$ -mode can be generated by either vector perturbations or tensor perturbations [3]. Vectors do not propagate in a Friedmann-Lemaître universe (see however Ref. [4]) and can be a potential explanation of the BICEP2 data only if they are incessantly generated by active sources such as cosmic strings [5] or magnetic fields [6]. These, however, are severely constrained by other measurements [7, 8].

Tensor modes are a natural and expected outcome of cosmic inflation although the uncertainty on their amplitude is huge (several orders of magnitude). In this context, the BICEP2 result might represent the first detection of primordial gravity waves produced in the early Universe [9, 10] and, therefore, could give us precious information about the physical conditions that prevailed

at that time. Of course, the BICEP2 result needs to be confirmed by other measurements before one can be sure that primordial  $B$ -mode have really been detected. In this paper, our working hypothesis will be that this is indeed the case. On general grounds, it is anyway always interesting to explore the implications for inflation of a non negligible level of primordial gravity waves.

The claimed amplitude of the signal corresponds to a tensor to scalar ratio of  $r = 0.2_{-0.05}^{+0.07}$  or  $r = 0.16_{-0.05}^{+0.06}$  depending on how polarized dust foregrounds are modeled and/or subtracted. Recent works [11] have however cast doubts on the modeling of the foreground dust, which could potentially lead to the amplitude of the tensor modes signal to be much lower, to the point of becoming undetectable. In the following, we shall take the BICEP2 result at face value, pending further investigation, most notably thanks to the recently released Planck dust maps [12]. The BICEP2 measurement, if, as already mentioned, interpreted as of primordial origin, has several important physical consequences that we now discuss.

Firstly, the energy scale of inflation [13–21] is fixed and roughly given by

$$\rho^{1/4} \simeq 2.2 \left( \frac{r}{0.2} \right)^{1/4} 10^{16} \text{ GeV}, \quad (1)$$

i.e. around the Grand Unified Theory (GUT) energy scale. A more accurate determination of this energy

\*Electronic address: [jmartin@iap.fr](mailto:jmartin@iap.fr)

†Electronic address: [christophe.ringeval@uclouvain.be](mailto:christophe.ringeval@uclouvain.be)

‡Electronic address: [r.trotta@imperial.ac.uk](mailto:r.trotta@imperial.ac.uk)

§Electronic address: [vennin@iap.fr](mailto:vennin@iap.fr)

### 3.4. “COMPATIBILITY OF PLANCK AND BICEP2 IN THE LIGHT OF INFLATION” (ARTICLE)

---

To keep the size of this manuscript manageable, the rest of this article [207] is not displayed here. A full version of it can be found at <http://arxiv.org/abs/1405.7272>.

# K-inflationary power spectra at second order

Jérôme Martin,<sup>a</sup> Christophe Ringeval<sup>b</sup> and Vincent Vennin<sup>a</sup>

<sup>a</sup>Institut d'Astrophysique de Paris, UMR 7095-CNRS, Université Pierre et Marie Curie, 98bis boulevard Arago, 75014 Paris, France

<sup>b</sup>Centre for Cosmology, Particle Physics and Phenomenology, Institute of Mathematics and Physics, Louvain University, 2 Chemin du Cyclotron, 1348 Louvain-la-Neuve, Belgium

E-mail: [jmartin@iap.fr](mailto:jmartin@iap.fr), [christophe.ringeval@uclouvain.be](mailto:christophe.ringeval@uclouvain.be), [vennin@iap.fr](mailto:vennin@iap.fr)

Received March 18, 2013

Revised April 23, 2013

Accepted May 30, 2013

Published June 17, 2013

**Abstract.** Within the class of inflationary models, k-inflation represents the most general single field framework that can be associated with an effective quadratic action for the curvature perturbations and a varying speed of sound. The incoming flow of high-precision cosmological data, such as those from the Planck satellite and small scale Cosmic Microwave Background (CMB) experiments, calls for greater accuracy in the inflationary predictions. In this work, we calculate for the first time the next-to-next-to-leading order scalar and tensor primordial power spectra in k-inflation needed in order to obtain robust constraints on the inflationary theory. The method used is the uniform approximation together with a second order expansion in the Hubble and sound flow functions. Our result is checked in various limits in which it reduces to already known situations.

**Keywords:** inflation, cosmological perturbation theory, physics of the early universe

**ArXiv ePrint:** [1303.2120](https://arxiv.org/abs/1303.2120)

To keep the size of this manuscript manageable, the rest of this article [209] is not displayed here. A full version of it can be found at <http://iopscience.iop.org/1475-7516/2013/06/021/> (published version) or at <http://arxiv.org/abs/1303.2120> (arXived version).



## 4. Quantum Aspects of Inflation and the Stochastic Formalism

*One of the great achievements of inflation is that, combined with quantum mechanics, it provides a convincing mechanism for the origin of the cosmological fluctuations. Such a mechanism rests on General Relativity and Quantum Mechanics, two theories that are notoriously difficult to combine, and leads to predictions that can be tested experimentally. This is why inflation is an ideal playground to discuss deep questions at the fundamental level. This second chapter aims at studying issues related to the quantum nature of the theory, and in particular the stochastic formalism which enables to address some of them.*

### Publications

---

4.1. “Stochastic Effects in Hybrid Inflation” (article) . . . . .	120
4.2. “Recursive Stochastic Effects in Valley Hybrid Inflation” (article) . . . . .	122
4.3. “Cosmological Inflation and the Quantum Measurement Problem” (article) . . . . .	124

---

In the standard description of inflation, the homogeneous parts of the fields are usually assumed to behave classically while the small deviations from homogeneity and isotropy are treated quantum mechanically over this classical background. To go beyond this “semi-classical” approach, it seems interesting to incorporate quantum corrections to the inflationary dynamics. The stochastic inflation formalism aims at describing such an effect, by deriving the effective action for the fields coarse-grained over length scales larger than the Hubble radius, and integrating out the sub-Hubble degrees of freedom. At the technical level, such an approach boils down to solving Langevin equations for the coarse-grained fields, in which an additional, stochastic term, is added.

These stochastic equations give rise to non trivial inflationary dynamics, especially in the case where multiple fields are present. In order to understand how the quantum diffusion can affect the observable predictions in such models, in section 4.1, Ref. [210], we study the stochastic effects in hybrid inflation, a two-field model where inflation ends due to an instability triggered

by an auxiliary “waterfall” field. In the neighbourhood of the critical point, the potential is very flat and the quantum fluctuations dominate over the classical drifts of the fields. In practice, one has to deal with two coupled Langevin equations, and solving the corresponding system, even at the perturbative level, is a difficult task. This is why we numerically addressed this problem by simulating a large number of realizations of the stochastic processes, and studied the associated probability distributions in the hybrid potential, discussing in particular the impact of the stochastic effects on the realized number of  $e$ -folds.

We then studied how these results get modified when further backreaction effects are implemented. In the original version of stochastic inflation indeed, the correlations of the noise in the Langevin equations are controlled by the amplitude of the perturbations, calculated over the classical, *i.e.* without the stochastic corrections, background. At next-to-leading order however, these stochastic corrections modify the amplification of the perturbations, hence the properties of the stochastic corrections, so on and so forth. In section 4.2, Ref. [211], we designed a recursive formalism that addresses this issue and applied it to the case of hybrid inflation. We showed that the method converges in the valley (before the critical point) but points towards an expected instability in the waterfall (after the critical point). Notably, we found that the typical dispersion of the waterfall field at the critical point is diminished, thus jeopardizing the possibility of a short transition, and we showed that the blue-tilt problem present in the hybrid model is even worsened by recursive stochastic effects.

Finally, as an illustration of how inflationary physics enables to discuss deep questions related to the nature of the quantum theory itself, in section 4.3, Ref. [138], we addressed the issue of the quantum-to-classical transition and the quantum measurement problem in a cosmological context. We first reviewed how the quantum-to-classical transition of the cosmological perturbations is usually accounted for by the large squeezing of the quantum state of the perturbations and the phenomenon of decoherence. However, this does not explain how a specific outcome can be produced in the early Universe in the absence of any observer (referring to the Copenhagen interpretation of Quantum Mechanics). We then studied the continuous spontaneous localization (CLS) approach to quantum mechanics which attempts to solve the quantum measurement question by causing the wavefunction collapse by means of additional non-linear and stochastic terms to the Schrödinger equation. CSL is the only falsifiable solution to the quantum measurement problem proposed so far, since it makes predictions that, in some regimes, differ from standard quantum mechanics. We applied this theory to inflation, and we showed that reaching a satisfactory degree of collapse at the end of inflation requires to strongly break the almost scale invariance of the power spectrum of the scalar perturbations, at a level which is completely excluded by observations. These results illustrate the remarkable power of inflation in particular and cosmology in general to constrain new physics, in regimes complementary to what can be achieved in lab experiments. Let us mention that following our work, other authors [408] generalized our calculation to the case where the CSL strength parameter depends on physical scales through a phenomenological power law, so as to capture the CSL amplification mechanism. In particular, they showed that there exists a power index for which the problem we pointed out can be evaded.



**Stochastic effects in hybrid inflation**Jérôme Martin<sup>\*</sup> and Vincent Vennin<sup>†</sup>*Institut d'Astrophysique de Paris, UMR 7095-CNRS, Université Pierre et Marie Curie,  
98bis boulevard Arago, 75014 Paris, France*

(Received 2 November 2011; published 22 February 2012)

Hybrid inflation is a two-field model where inflation ends due to an instability. In the neighborhood of the instability point, the potential is very flat and the quantum fluctuations dominate over the classical motion of the inflaton and waterfall fields. In this article, we study this regime in the framework of stochastic inflation. We numerically solve the two coupled Langevin equations controlling the evolution of the fields and compute the probability distributions of the total number of e-folds and of the inflation exit point. Then, we discuss the physical consequences of our results, in particular, the question of how the quantum diffusion can affect the observable predictions of hybrid inflation.

DOI: [10.1103/PhysRevD.85.043525](https://doi.org/10.1103/PhysRevD.85.043525)

PACS numbers: 98.80.Cq, 98.80.Qc

**I. INTRODUCTION**

Inflation is the leading scenario among the models attempting to describe the physical conditions that prevailed in the very early Universe. It consists in a phase of accelerated expansion which naturally solves the problems of the hot big bang theory [1–5] (for reviews, see Refs. [6–8]). In addition, it predicts an almost scale invariant power spectrum for the primordial cosmological fluctuations, the tiny deviations from scale invariance being related to the microphysics of inflation [9–14]. As is well known, this prediction turns out to be fully consistent with different types of astrophysical observations, among which is the measurement of the cosmic microwave background radiation (CMBR) anisotropies [15–19].

Inflation is usually driven by one or many scalar fields. In the context of general relativity, this represents the simplest mechanism to obtain the negative pressure necessary to produce an accelerated expansion. However, the physical nature of those scalar fields is presently unknown, and many different inflationary models have been suggested. The reason for such a situation originates from the fact that inflation is a high energy phenomenon. Indeed, the energy scale of inflation is somewhere between the TeV scale and the grand unified theory scale [15]. At those scales, particle physics remains elusive, and as a consequence there is presently a large variety of different inflationary scenarios.

However, given the extensions of the standard model of particle physics, notably those based on supersymmetry and supergravity, it is clear that some models appear to be more motivated and more generic than others. In particular, this is the case of hybrid inflation [20,21], which can be realized in various ways in the context of supersymmetry; see, for instance, the scenarios named *F*-term inflation and *D*-term inflation (among others) [22–25]. Hybrid inflation

is a two-field model such that inflation occurs along a valley in the field space and ends by tachyonic instability along the so-called waterfall field direction. Hybrid inflation is known to lead to a blue spectrum for the fluctuations, a prediction which appears to be disfavored by the most recent observations [15]. However, it was shown recently [26–28] that, in some regions of the parameter space, a significant number of e-folds can occur in the waterfall regime. In this case, it was also demonstrated that the spectral index becomes red, which therefore implies that the model is in fact totally compatible with the data [26,27].

In the context of inflation, another interesting question is the role played by the quantum corrections [29–39]. Various works have shown that they can have a crucial impact on the inflationary dynamics. This is, for instance, the case for large field inflation if one starts inflation high enough in the potential. In this case, the quantum kicks undergone by the field can be so important that the field climbs its potential instead of rolling down it as should be the case according to the classical equations of motion. In such a situation, it is likely that one enters into a regime of eternal inflation [31,40,41].

Hybrid inflation is also a model where one expects the quantum corrections to be very important. It should be the case high in the inflationary valley but also around the critical point where the tachyonic instability is triggered [26,27,42]. The goal of this article is to investigate this last question in detail. In particular, we are interested in whether the quantum effects can significantly modify the classical dynamics and affect the observational predictions of the model.

In order to carry out our study, we use the stochastic inflation formalism [30,32–39,43,44]. It consists in modeling the quantum effects by a stochastic white noise. As a consequence, the equation describing the motion of the fields becomes a Langevin equation. As mentioned previously, hybrid inflation is a genuine two-field model, which implies that one has to deal with two coupled Langevin

<sup>\*</sup>[jmartin@iap.fr](mailto:jmartin@iap.fr)<sup>†</sup>[vennin@iap.fr](mailto:vennin@iap.fr)

To keep the size of this manuscript manageable, the rest of this article [210] is not displayed here. A full version of it can be found at <http://journals.aps.org/prd/abstract/10.1103/PhysRevD.85.043525> (published version) or at <http://arxiv.org/abs/1110.2070> (arXived version).

**Recursive stochastic effects in valley hybrid inflation**

Laurence Perreault Levasseur\*

*DAMTP, Center for Mathematical Sciences, University of Cambridge, Cambridge CB3 0WA, United Kingdom*Vincent Vennin<sup>†</sup>*Institut d'Astrophysique de Paris, UMR 7095-CNRS, Université Pierre et Marie Curie, 98bis boulevard Arago, 75014 Paris, France*Robert Brandenberger<sup>‡</sup>*Department of Physics, McGill University, Montréal, Québec H3A 2T8, Canada  
(Received 26 August 2013; published 31 October 2013)*

Hybrid inflation is a two-field model where inflation ends because of a tachyonic instability, the duration of which is determined by stochastic effects and has important observational implications. Making use of the recursive approach to the stochastic formalism presented in [L. P. Levasseur, preceding article, *Phys. Rev. D* **88**, 083537 (2013)], these effects are consistently computed. Through an analysis of backreaction, this method is shown to converge in the valley but points toward an (expected) instability in the waterfall. It is further shown that the quasistationarity of the auxiliary field distribution breaks down in the case of a short-lived waterfall. We find that the typical dispersion of the waterfall field at the critical point is then diminished, thus increasing the duration of the waterfall phase and jeopardizing the possibility of a short transition. Finally, we find that stochastic effects worsen the blue tilt of the curvature perturbations by an  $\mathcal{O}(1)$  factor when compared with the usual slow-roll contribution.

DOI: [10.1103/PhysRevD.88.083538](https://doi.org/10.1103/PhysRevD.88.083538)

PACS numbers: 98.80.Cq, 98.70.Vc

**I. INTRODUCTION**

Inflation is currently the leading paradigm attempting to shed light on the physics of the very early Universe. It describes a phase of accelerated expansion, which solves many problems of the hot big bang scenario [1–8]. Inflation further provides a causal mechanism for generating fluctuations on cosmological scales, and it predicts that their spectrum should be almost scale invariant, with small deviations from scale invariance which can be traced back to the precise microphysics of inflation [9–14]. This prediction is consistent with the current astrophysical observation, such as the CMB, including the measurement of the cosmic microwave background anisotropies. For this specific observable, the latest results [15–17] give a slightly red-tilted spectral index  $n_S \simeq 0.96$ , ruling out exact scale invariance  $n_S = 1$  at over  $5\sigma$  and allowing us to constrain the inflationary models still allowed by the data [18].

With the ever-increasing precision of the experiments probing this window into the early Universe, it is now very important to develop robust and self-consistent methods for calculating inflationary predictions. For example, in the context of multifield inflation, it is complicated to disentangle the gravitational and matter degrees of freedom when describing fluctuations produced in the scalar fields using traditional methods. Typically, approximations are used to make the problem tractable, but these

approximations ignore backreaction, that is, the effects of these fluctuations on the background spacetime and field trajectory. Restoring or even assessing the importance of these neglected effects then becomes extremely nontrivial, and it has been shown that such effects can have a crucial impact on the inflationary dynamics [19–22] (see also Ref. [23] for a review of early work).

One way to resum these effects, at least partially, is to make use of the stochastic inflation formalism [24–34]. The basic strategy is to derive an effective theory for the long-wavelength part of the fields, which are “coarse grained” at a scale larger than the Hubble radius. In this framework, the small-scale quantum fluctuations play the role of a “bath” and are collected in classical noise terms which affect the dynamics of the coarse-grained fields. The super-Hubble physics can thus be described by a stochastic classical theory.

The corresponding equations can be derived by making use of the Schwinger-Keldysh closed time path formalism [35–38], where the strategy is to split the degrees of freedom of the full quantum fields in momentum space through a window function, and perform the path integral over the small-scale fluctuations. In Ref. [39], this Lagrangian formulation of the theory is used to develop a recursive method for solving the stochastic equations when the background spacetime is taken to be dynamic. It is this recursive method which we now apply to models of multifield inflation, and specifically to hybrid inflation.

At the energy scale of inflation (typically around  $10^{15}$ – $10^{16}$  GeV), particle physics remains elusive, leaving room for a large variety of different inflationary scenarios.

\*l.perreault-levasseur@damtp.cam.ac.uk

<sup>†</sup>vennin@iap.fr<sup>‡</sup>rhb@hep.physics.mcgill.ca

To keep the size of this manuscript manageable, the rest of this article [211] is not displayed here. A full version of it can be found at <http://journals.aps.org/prd/abstract/10.1103/PhysRevD.88.083538> (published version) or at <http://arxiv.org/abs/arXiv:1307.2575> (arX-ived version).

**Cosmological inflation and the quantum measurement problem**J r me Martin,<sup>\*</sup> Vincent Vennin,<sup>†</sup> and Patrick Peter<sup>‡</sup>*Institut d'Astrophysique de Paris, UMR 7095-CNRS, Universit  Pierre et Marie Curie,  
98 bis boulevard Arago, 75014 Paris, France*

(Received 17 July 2012; published 26 November 2012)

According to cosmological inflation, the inhomogeneities in our Universe are of quantum-mechanical origin. This scenario is phenomenologically very appealing as it solves the puzzles of the standard hot big bang model and naturally explains why the spectrum of cosmological perturbations is almost scale invariant. It is also an ideal playground to discuss deep questions among which is the quantum measurement problem in a cosmological context. Although the large squeezing of the quantum state of the perturbations and the phenomenon of decoherence explain many aspects of the quantum-to-classical transition, it remains to understand how a specific outcome can be produced in the early Universe, in the absence of any observer. The continuous spontaneous localization (CSL) approach to quantum mechanics attempts to solve the quantum measurement question in a general context. In this framework, the wave function collapse is caused by adding new nonlinear and stochastic terms to the Schr dinger equation. In this paper, we apply this theory to inflation, which amounts to solving the CSL parametric oscillator case. We choose the wave function collapse to occur on an eigenstate of the Mukhanov-Sasaki variable and discuss the corresponding modified Schr dinger equation. Then, we compute the power spectrum of the perturbations and show that it acquires a universal shape with two branches, one which remains scale invariant and one with  $n_S = 4$ , a spectral index in obvious contradiction with the cosmic microwave background anisotropy observations. The requirement that the non-scale-invariant part be outside the observational window puts stringent constraints on the parameter controlling the deviations from ordinary quantum mechanics. Due to the absence of a CSL amplification mechanism in field theory, this also has the consequence that the collapse mechanism of the inflationary fluctuations is not efficient. Then, we determine the collapse time. On small scales the collapse is almost instantaneous, and we recover exactly the behavior of the CSL harmonic oscillator (a case for which we present new results), whereas, on large scales, we find that the collapse is delayed and can take several e-folds to happen. We conclude that recovering the observational successes of inflation and, at the same time, reaching a satisfactory resolution of the inflationary ‘‘macro-objectification’’ issue seems problematic in the framework considered here. This work also provides a complete solution to the CSL parametric oscillator system, a topic we suggest could play a very important role to further constrain the CSL parameters. Our results illustrate the remarkable power of inflation and cosmology to constrain new physics.

DOI: [10.1103/PhysRevD.86.103524](https://doi.org/10.1103/PhysRevD.86.103524)

PACS numbers: 98.80.Cq, 98.80.Qc, 03.65.Ta, 03.65.Yz

**I. INTRODUCTION**

Inflation is currently the leading paradigm for explaining the physical conditions that prevailed in the very early Universe [1–5]. It solves the puzzles of the standard hot big bang phase and it explains the origin of the inhomogeneities in our Universe [6–11] (for reviews, see Refs. [12–18]). According to the inflationary scenario, these inhomogeneities result from the amplification of the unavoidable vacuum quantum fluctuations of the gravitational and inflaton fields during a phase of accelerated expansion. In particular, inflation predicts an almost scale invariant power spectrum for the cosmological fluctuations [19], a prediction which fits very well the high accuracy astrophysical data now at our disposal [20–26].

Often less emphasized is the fact that inflation is also particularly remarkable from the theoretical point of view. Indeed, the inflationary mechanism for the production of cosmological perturbations makes use of general relativity and quantum mechanics, two theories that are notoriously difficult to combine. Moreover, this mechanism leads to theoretical predictions that are possible to study observationally with great accuracy. In fact, inflation is probably the only case in physics where an effect based on general relativity and quantum mechanics leads to predictions that, given our present day technological capabilities, can be tested experimentally.

The situation described above can be used to investigate deep questions. Among these deep questions is how the quantum measurement problem looks in a cosmological context. According to inflation, the cosmic microwave background (CMB) radiation anisotropy [27] is an observable and is therefore described by a quantum operator. As a consequence, when one looks at a CMB map, one observes

---

<sup>\*</sup>jmartin@iap.fr  
<sup>†</sup>vennin@iap.fr  
<sup>‡</sup>peter@iap.fr

#### 4.3. “COSMOLOGICAL INFLATION AND THE QUANTUM MEASUREMENT PROBLEM” (ARTICLE)

---

To keep the size of this manuscript manageable, the rest of this article [138] is not displayed here. A full version of it can be found at <http://journals.aps.org/prd/abstract/10.1103/PhysRevD.86.103524> (published version) or at <http://arxiv.org/abs/arXiv:1207.2086> (arXived version).



# Conclusion

*The goal of this thesis was to derive observational constraints on cosmological inflation models, and to investigate some fundamental aspects related to the quantum nature of the inflationary setup. In this last section we summarize the main results we obtained, drawing a few concluding remarks and suggesting possible prospects.*

The phenomenological successes of inflation have provided the motivation for numerous efforts to establish its connection with the standard model of particle physics. Our ability to see through the inflationary window turns the early Universe into a laboratory for ultra-high energy physics, at scales entirely inaccessible to conventional experimentation. A crowd of inflationary candidates have thus been proposed, among which it is *a priori* difficult to discriminate the most promising ones since inflation takes place at energy scales where particle physics remain elusive. As a consequence, despite the fact that it has become a cornerstone, the inflationary era is not as well constrained as the other parts of the standard model of Cosmology. However, there is now a flow of increasingly accurate astrophysical data which gives us a unique opportunity to learn more about inflation. We have now entered the era of massive multi-data analysis, and a change of scale is clearly required compared to previous analyses.

The first goal of this thesis was to develop methods that allow us to constrain the inflationary scenario at a level matching the accuracy of the data. We chose to adopt a systematic and somewhat “industrial” approach of this issue. We first focused on the single-field models of inflation, with canonical kinetic terms, and studied them in the slow-roll approximation. Indeed, these are the simplest inflationary models, and there is currently no observational evidence (as would be for example the detection of substantial primordial non-Gaussianities or entropic perturbations) that forces us to consider more complicated models. Obviously, this does not mean that more complicated models are ruled out, but simply that single-field slow-roll scenarios achieve the best compromise between quality of the fit and theoretical simplicity. This still left us with a very populated landscape.

Going through the literature, we identified  $\sim 75$  different inflationary potentials that we studied one by one. Without any other approximation than slow roll, we calculated the predictions of these models. For many of them, we thus derived new results since in most cases, they were studied under additional approximations. The errors associated with these approximations cannot be ignored given the current accuracy of the data, and it is therefore necessary to do without them. We also developed a publicly available runtime library that computes the reheating consistent predictions for these models. This project is an evolutive one and it is intended to be completed as new models appear.

Then, the Planck 2013 Cosmic Microwave Background (CMB) data were released and we computed the Bayesian evidences and complexities of the  $\sim 200$  inflationary scenarios that arise from the previously studied potentials. At the technical level, we actually interfaced the slow-roll library mentioned above with a machine-learning effective likelihood and a nested sampling algorithm. Doing so, we identified the most probable models that are compatible with the Planck

data, while ruling out with very strong evidence one third of the models considered. Among the preferred models, we identified that most potentials are of the plateau type, *i.e.* they are such that the kinetic energy and the kinetic-to-total energy density ratio increase during inflation. Prototypical examples of such models are the Starobinsky model or the Kähler moduli model.

Later on in the course of this thesis, the BICEP2 experiment reported the detection of  $B$ -mode signal in the polarization of the CMB, at the level of  $r \sim 0.16$ . Beyond the strong implications that such a detection would have for inflation in general if confirmed, it was clear that it could drastically refine our analysis arising from the Planck data only. In particular, the Planck likelihood is consistent with  $r = 0$  (so far), and indicates that  $r < 0.1$  at the two-sigma confidence level. A measurement of  $r$  obviously puts further constraints on the inflationary models. This is why we re-processed the same computational pipeline, but including the BICEP2 data in the analysis. The results we obtained showed that the sets of inflationary models preferred by Planck alone and BICEP2 alone are almost disjoint, indicating a clear tension between the two data sets.

We then decided to quantify this tension with a Bayesian measure of compatibility between BICEP2 and Planck. The compatibility of these two experiments is widely discussed in the literature, but the improvement of our approach is that we quantify compatibility *under the assumption* of inflation or *under the assumption* of a specific inflationary model. In this manner, we could draw stronger and more reliable conclusions. Under the generic assumption of slow-roll inflation, we established that the Bayesian test is inconclusive, *i.e.* there is neither indication towards compatibility nor incompatibility. However, when computing the compatibility level model by model, we found that for models favoured by Planck the two data sets tend to be incompatible, whereas there is a moderate evidence of compatibility for the BICEP2 preferred models. As a result, it is premature to draw any conclusion on the best Planck models at this point, such as Starobinsky inflation or Kähler moduli inflation. Furthermore, we established that the data are strongly compatible only for models that are disfavoured by both Planck and BICEP2 separately. Indeed, both data sets agree in disfavoring those models and in this sense only, they can be said to be “compatible”. This is why one still needs to wait for some clarification about the data before being able to properly combine them and draw definitive conclusions as for the Planck best models. In particular, the polarization measurements by Planck that should be released by the end of the year, and a possible reconsideration of the dust contribution in the  $B$ -mode signal measured by BICEP2, may help to unveil the tension.

As a possible prospect of this work, the inclusion of k-inflation models in the analysis needs to be considered. Indeed, in this class of models, the action for the scalar perturbations at linear order is still quadratic, but the speed of sound  $c_s$  is now a function of time. As a consequence, there exists a frame of approximation similar to slow roll that applies to the time variation of  $c_s$ , and the same machinery can be extended to these cases without implying an unreasonable increase in its complexity level. Since the accuracy of the data requires to work at next-to-next-to leading order at least, we have calculated, for the first time, the power spectra of scalar and tensor perturbations at this order in k-inflation to pave the way for such an extension. However, such models can produce a large amount of primordial non-Gaussianities, and this observable needs also be included in the analysis to properly constrain k-inflation.

Obviously, one could go beyond and include multi-field models, non scalar-field models, *etc.* However, this represents much more complicated situations with strong dependence on the initial conditions, and where there is no such thing as a frame of approximation in which the background trajectory and the amplitude of the perturbations can be calculated perturbatively. As a consequence, one needs to numerically integrate all equations, and it seems difficult to

---

process our complete Bayesian pipeline in a realistic amount of time for such models, at least in the generic situation.

Another relevant study to carry out is the one about reheating. From the beginning, we have taken care of consistently describing reheating in the analysis, which boils down to including a single parameter combining the mean energy density and the average equation of state during reheating. From the results we obtained, it is clear that we are in a position where we can put explicit constraints on the reheating parameters, either model by model, or in a model averaged way. We are currently working on such a follow-up.

There is also an ongoing debate about what the next instrumental move should be. If the urge for a clear detection of  $r$  is obvious, the sensitivity of future experiments must be such that, in case of a non detection, the improvement in the constraint on the gravity wave level would still significantly improve our knowledge about the early Universe. This is why we are also currently examining future experiments specifications in the light of this issue. For the few ones that have been planned, we are deriving the likelihood it would provide given a fiducial model, and we are processing our Bayesian pipeline for the  $\sim 200$  inflationary models we have at hand, to determine how much the constraints on these models would improve. Repeating the analysis for a few different fiducial models, this allows us to derive clear forecasts about the actual performance of these experiments.

It is also worth mentioning that the reliability of our approach, compared with model independent parametrizations of inflation, was strengthened by our analysis of the horizon-flow framework. In this setup, inflation is parametrized by means of truncated flow equations. Typically, potential reconstruction has been investigated with the help of this technique, as well as the search for “generic” inflationary predictions. We showed that horizon flow only samples a phenomenological class of inflationary potentials, which are at the origins of such wrongly concluded generic predictions. Furthermore, we established that the horizon-flow setup rests on trajectories in phase space that differ from the slow roll one. Such trajectories are sometimes unstable, and given a potential, they render horizon flow blind to entire inflationary regimes, hence making this parametrization a biased one.

Together with this data-oriented approach of inflationary models, we also studied more fundamental aspects related to the quantum nature of the inflationary setup. In particular, we got interested in the stochastic inflation formalism which incorporates quantum corrections to the classical background by means of stochastic Langevin equations. Such a formalism is theoretically well founded and technically appealing since it is notably able to reproduce a number of results from Quantum Field Theories, even beyond the perturbative level. It gives rise to non trivial dynamics, in particular when multiple fields are present, since in these cases, due to quantum diffusion, the system can explore parts of the inflationary potential to which the classical trajectory is insensitive. This is why we studied the stochastic effects in hybrid inflation, a two-field model where inflation ends by tachyonic instability, triggered by an auxiliary “waterfall” field, close to a critical saddle point. There, the potential is very flat and the quantum fluctuations dominate over the classical drifts of the fields. The two Langevin equations become highly coupled, and their solving requires a numerical approach. It is however important to well understand what happens in this regime, since it determines the amount of  $e$ -folds that can be realized in the waterfall phase. If the scales of astrophysical interest today cross the Hubble radius before the critical point, that is if the number of  $e$ -folds realized in the waterfall is smaller than  $\sim 50$ , then the power spectrum of scalar perturbations was shown to be blue and the model is therefore ruled out. Only if the last 50  $e$ -folds are realized in the waterfall phase can this problem be evaded, and it is then crucial to properly determine the amount of  $e$ -folds realized in

the waterfall. This is why we mainly focused on this quantity, and we computed its distribution for different sets of parameters.

To go beyond, one needs to investigate more the regime of parameters for which  $\sim 50$   $e$ -folds are realized during the waterfall, and scales of astrophysical interest today cross the Hubble radius in the neighbourhood of the critical point, that is where the stochastic effects do not represent a tiny correction to the classical trajectory anymore. In such a case, the calculation of the power spectrum is more involved. In the introductory part of this manuscript, we have derived an entirely analytical method for calculating the power spectrum in stochastic inflation in a non-perturbative manner, that is without relying on an expansion in the noise term, for single-field models. If such an approach should be employed to calculate the power spectrum and the non-Gaussianity levels in some single-field models where important stochastic effects are expected to play a role, it still remains to be generalized to multiple-fields setups in order to address the case of models such as hybrid inflation.

Another issue we studied is the fact that in standard stochastic inflation, the correlations of noise terms in the Langevin equations depend on the amplitude of perturbations that are calculated over a classical background. Now, if the background is stochastically shifted, the perturbations should be affected, hence the noise correlations, hence the way the background is shifted, so on and so forth. In order to try and take into account such an effect, we designed a recursive approach to stochastic inflation that we applied to the hybrid models. As expected, such a formalism converges in the valley but blows up in the waterfall. Interestingly enough, the corresponding effects tend to increase the duration of the waterfall phase by decreasing the waterfall field dispersion at the critical point, and worsen the blue tilt problem in the valley, hence reinforcing the plausibility of long lasting waterfall scenarios.

Finally, we addressed the issue of the quantum measurement problem in a cosmological context, so as to illustrate how inflationary physics can help to discuss deep questions related to the nature of the quantum theory itself. The quantum-to-classical transition of cosmological perturbations is a subject of great interest at the fundamental level, since perturbations originate from zero point quantum fluctuation but are usually treated as purely classical quantities after inflation ends. This transition is often accounted for by the large squeezing of the quantum state of the perturbations, for which one can show that it is phenomenologically equivalent to a stochastic set of classical processes. The phenomenon of quantum decoherence is also usually mentioned as being part of the explanation. However, at the fundamental level, this does not explain how a specific outcome can be produced in the early Universe, in the absence of any observer. A possible way out is the continuous spontaneous localization (CSL) approach to quantum mechanics in which the wavefunction collapse is caused by adding non linear and stochastic terms to the Schrödinger equation. We applied this theory to inflation, and calculated both the collapse level of the wavefunction at the end of inflation and the power spectrum of perturbations. We found that reaching a satisfactory level of collapse for the scales of astrophysical interest today implies to strongly break the scale invariance of the power spectrum, hence rendering the direct application of the theory in the early Universe problematic. In a later work, other authors have extended our calculation in the case where the CSL strength parameter depends on physical scales through a phenomenological power law, and they showed that there exists a power index for which the problem we point out is evaded. In any case, this illustrates the remarkable power of inflation in particular, and Cosmology in general, to constrain new physics.

In this thesis, we have thus shown that theoretical developments and observational achievements of the past years make possible to constrain the inflationary physics and to learn more about the physical conditions that prevailed in the early Universe. However, one might fear that the

---

built-in phenomenological robustness of inflation may keep us from learning too much about its microphysical origin since inflationary predictions depend on a few generic observables and the window of scales through which we may grasp a look at early Universe physics is restricted to a few  $e$ -folds.

Actually, we may indeed be at a turning point with the possible detection of primordial gravity waves. Indeed, if the detection of  $r$  is confirmed, it is clear that we should undertake all possible and reasonable efforts to provide an accurate measurement of its value. If it is of the same order of magnitude as the one announced by BICEP2,  $r \sim 0.1 - 0.2$ , it also means that the spectral index of gravity waves,  $n_T$ , may also be measured [409] in the medium term. This would double the number of inflationary parameters for which we have a measurement, going from  $\{\mathcal{P}_{\zeta,*}, n_s\}$  to  $\{\mathcal{P}_{\zeta,*}, n_s, r, n_T\}$ . If this is the case, considering also the  $EE$  and  $TE$  signals measured by Planck and that will be released soon, it seems realistic to try and really constrain the shape of the inflationary potential and its energy scale. This is a very exciting perspective.

However, if a more accurate determination of the foregrounds contribution to the BICEP2 signal makes its detection disappear, measurement of new inflationary parameters in the short run seem quite unlikely. Indeed, some plateau models, such as Khäler moduli inflation or brane inflation, can predict tiny values of  $r$ , typically  $r < 10^{-6}$ . At the present day, it seems technologically unrealistic to try and detect such small amount of primordial gravity waves. Moreover, for single-field slow-roll models of inflation with canonical kinetic terms, the level of non-Gaussianities is very small,  $f_{\text{NL}} \sim \epsilon$ , and still beyond what we can reach observationally [410]. The same applies for entropic perturbations which may well be far beyond what we will be able to detect in the years to come if the other fields contributing to  $\rho$  during inflation are very massive. The running of the scalar power spectrum is also very small in the slow-roll regime,  $\alpha_s \sim \epsilon^2$ , and if no deviation from slow roll occurred in the observational window (as it seems to be the case so far), it is also quite unlikely to be detected in the years to come. Of course, there is still the possibility that slow roll be mildly violated at some point, or that a “massive but not so massive” auxiliary field contributes to the energy density during inflation, or that a “small but not so small” deviation from minimal coupling to gravity appear, so that the quantities mentioned above may still be measured soon, but this would represent a rather fine-tuned situation, considering what we already know. This is why in that second case, it is possible that the observational constraints on inflationary models stagnate for a decade or even more.

To continue to improve our knowledge of early universe physics, two routes may then be followed. One is to try and discriminate among models on a theoretical basis, dedicating more efforts in the model building programme, better understanding how inflationary models are sensitive to radiative corrections, how they can be connected to the standard model of particle physics and its extensions, *etc.* Another is to investigate more the connections between inflationary predictions and other astrophysical probes such as supernovae, galaxy surveys, 21 cm astrophysics, the reconstruction of the initial conditions large scale structures simulations, *etc.* For example, the “lever arm” in length scales between CMB and galaxy power spectra is huge and it increases the sensitivity to the small deviations from scale invariance.

Cosmology has now entered a “big data” era where measurements very different in nature have to be cleverly combined to derive constraints on physical processes equally different. In this manner, advances in the different fields of Cosmology and even Astrophysics are highly entangled, and the decryption of the early Universe physics is an ongoing adventure.



# List of Figures

1.1.	Hubble Diagram from the 1929 original paper by Edwin Hubble . . . . .	4
1.2.	Comparison of $H_0$ measurements . . . . .	5
1.3.	Homogeneous sphere in Newtonian radial expansion . . . . .	9
1.4.	Cosmic Pie . . . . .	13
1.5.	$\rho(a)$ and $a(t)$ in the hot big bang scenario . . . . .	15
1.6.	Age of a flat universe as a function of $z_{\text{eq}}$ and $z_{\text{acc}}$ . . . . .	16
1.7.	Main events in the Cosmological Standard Scenario . . . . .	18
1.8.	Light elements abundances according to Big Bang Nucleosynthesis . . . . .	19
1.9.	Cosmic Microwave Background temperature map . . . . .	20
1.10.	Simulated dark matter distributions for different cosmological models . . . . .	21
1.11.	Minimum number of $e$ -folds to solve the horizon problem . . . . .	26
1.12.	Space-time conformal diagrams with and without inflation . . . . .	27
1.13.	Minimum number of $e$ -folds to solve the monopole problem . . . . .	32
2.1.	Klein-Gordon phase space diagram. . . . .	43
2.2.	Next-to-leading orders of the slow-roll trajectory . . . . .	46
2.3.	Perturbations length scale and Hubble Radius . . . . .	50
2.4.	Sketch of the Langevin bounded dynamics . . . . .	81
2.5.	Ending point probability in the large field potential . . . . .	84
2.6.	Integration domain of the mean number of $e$ -folds . . . . .	85
2.7.	Mean number of $e$ -folds realized in the $V \propto \phi^p$ potential . . . . .	88
2.8.	mean number of $e$ -folds realized in the large field potential . . . . .	93
2.9.	Dispersion in the number of $e$ -folds realized in the large field potential . . . . .	95
2.10.	Scalar power spectrum in the large field potential with stochastic effects . . . . .	96
2.11.	Scalar spectral index in large field inflation with stochastic effects . . . . .	98
5.1.	A few models predictions and contours for WMAP, Planck and Planck+Bicep2 . . . . .	170
5.2.	Jeffreys models distribution with Planck, Bicep2 and Planck+Bicep2 . . . . .	172
5.3.	Probability Density in the $(\varphi, \psi)$ plane at different times $N$ in the hybrid model . . . . .	177
5.4.	Wigner function and inflationary squeezing of the quantum state . . . . .	179
5.5.	CSL power spectrum . . . . .	181



## List of Tables

1.1. $w$ , $\rho(a)$ and $a(t)$ profiles for a few perfect fluid examples . . . . .	11
1.2. Numerical values of cosmological parameters . . . . .	36



# Bibliography

- [1] E. W. Kolb and M. S. Turner, *The Early Universe*, vol. 69. Front.Phys., 1990.
- [2] P. Peebles, *Principles of physical cosmology*. Princeton University Press, 1994.
- [3] A. R. Liddle, *An introduction to modern cosmology*. Wiley, 1998.
- [4] A. R. Liddle and D. Lyth, *Cosmological inflation and large scale structure*. Cambridge, UK: Univ. Pr., 2000.
- [5] S. Dodelson, *Modern cosmology*. Amsterdam, Netherlands: Academic Pr., 2003.
- [6] V. Mukhanov, *Physical foundations of cosmology*. Cambridge, UK: Univ. Pr., 2005.
- [7] D. H. Lyth and A. R. Liddle, *The primordial density perturbation: Cosmology, inflation and the origin of structure*. Cambridge, UK: Cambridge Univ. Pr., 2009.
- [8] P. Peter and J.-P. Uzan, *Primordial cosmology*. Oxford University Press, UK, 2009.
- [9] A. Friedmann, “On the Possibility of a world with constant negative curvature of space,” *Z.Phys.* **21** (1924) 326–332.
- [10] G. Lemaitre, “A homogeneous Universe of constant mass and growing radius accounting for the radial velocity of extragalactic nebulae,” *Annales Soc.Sci.Brux.Ser.I Sci.Math.Astron.Phys.* **A47** (1927) 49–59.
- [11] H. Robertson, “Kinematics and World-Structure,” *Astrophys.J.* **82** (1935) 284–301.
- [12] A. G. Walker, “On the formal comparison of Milne’s kinematical system with the systems of general relativity,” *Mon.Not.Roy.Astron.Soc.* **95** (1935) 263–269.
- [13] E. Hubble, “A relation between distance and radial velocity among extra-galactic nebulae,” *Proc.Nat.Acad.Sci.* **15** (1929) 168–173.
- [14] A. Sandage, “Current Problems in the Extragalactic Distance Scale,” *Astrophys.J.* **127** (1958) 513–526.
- [15] **Planck Collaboration** Collaboration, P. Ade *et al.*, “Planck 2013 results. XVI. Cosmological parameters,” [arXiv:1303.5076](https://arxiv.org/abs/1303.5076) [[astro-ph.CO](https://arxiv.org/archive/astro)].
- [16] L. Verde, P. Protopapas, and R. Jimenez, “Planck and the local Universe: Quantifying the tension,” *Phys.Dark Univ.* **2** (2013) 166–175, [arXiv:1306.6766](https://arxiv.org/abs/1306.6766) [[astro-ph.CO](https://arxiv.org/archive/astro)].
- [17] J.-Q. Xia, H. Li, and X. Zhang, “Dark Energy Constraints after Planck,” *Phys.Rev.* **D88** (2013) 063501, [arXiv:1308.0188](https://arxiv.org/abs/1308.0188) [[astro-ph.CO](https://arxiv.org/archive/astro)].

- [18] A. Caramete and L. Popa, “Cosmological evidence for leptonic asymmetry after Planck,” *JCAP* **1402** (2014) 012, [arXiv:1311.3856 \[astro-ph.CO\]](#).
- [19] A. E. Romano and S. A. Vallejo, “Can the tension in the  $H_0$  estimation be solved by a local overdensity?,” [arXiv:1403.2034 \[astro-ph.CO\]](#).
- [20] L. Verde, P. Protopapas, and R. Jimenez, “The expansion rate of the intermediate Universe in light of Planck,” [arXiv:1403.2181 \[astro-ph.CO\]](#).
- [21] B. Leistedt, H. V. Peiris, and L. Verde, “No new cosmological concordance with massive sterile neutrinos,” [arXiv:1404.5950 \[astro-ph.CO\]](#).
- [22] A. Einstein, “The Field Equations of Gravitation,” *Sitzungsber.Preuss.Akad.Wiss.Berlin (Math.Phys.)* **1915** (1915) 844–847.
- [23] A. Einstein, “On the General Theory of Relativity,” *Sitzungsber.Preuss.Akad.Wiss.Berlin (Math.Phys.)* **1915** (1915) 778–786.
- [24] D. Hilbert, “Die Grundlagen der Physik. 1.,” *Gott.Nachr.* **27** (1915) 395–407.
- [25] A. Friedman, “On the Curvature of space,” *Z.Phys.* **10** (1922) 377–386.
- [26] A. Raychaudhuri, “Relativistic cosmology. 1.,” *Phys.Rev.* **98** (1955) 1123–1126.
- [27] J. Khoury, B. A. Ovrut, P. J. Steinhardt, and N. Turok, “The Ekpyrotic universe: Colliding branes and the origin of the hot big bang,” *Phys.Rev.* **D64** (2001) 123522, [arXiv:hep-th/0103239 \[hep-th\]](#).
- [28] J. Khoury, B. A. Ovrut, P. J. Steinhardt, and N. Turok, “Density perturbations in the ekpyrotic scenario,” *Phys.Rev.* **D66** (2002) 046005, [arXiv:hep-th/0109050 \[hep-th\]](#).
- [29] P. J. Steinhardt and N. Turok, “Cosmic evolution in a cyclic universe,” *Phys.Rev.* **D65** (2002) 126003, [arXiv:hep-th/0111098 \[hep-th\]](#).
- [30] M. Gasperini and G. Veneziano, “The Pre - big bang scenario in string cosmology,” *Phys.Rept.* **373** (2003) 1–212, [arXiv:hep-th/0207130 \[hep-th\]](#).
- [31] J. Martin and P. Peter, “On the causality argument in bouncing cosmologies,” *Phys.Rev.Lett.* **92** (2004) 061301, [arXiv:astro-ph/0312488 \[astro-ph\]](#).
- [32] L. R. Abramo and P. Peter, “K-Bounce,” *JCAP* **0709** (2007) 001, [arXiv:0705.2893 \[astro-ph\]](#).
- [33] P. Peter and N. Pinto-Neto, “Cosmology without inflation,” *Phys.Rev.* **D78** (2008) 063506, [arXiv:0809.2022 \[gr-qc\]](#).
- [34] J. Martin and P. Peter, “Parametric amplification of metric fluctuations through a bouncing phase,” *Phys.Rev.* **D68** (2003) 103517, [arXiv:hep-th/0307077 \[hep-th\]](#).
- [35] E. A. Milne, “A Newtonian expanding Universe,” *The Quarterly Journal of Mathematics* **5** (1934) 64–72.
- [36] W. H. McCrea and E. A. Milne, “Newtonian Universes and the curvature of space,” *The*

- Quarterly Journal of Mathematics* **5** (1934) 73–80.
- [37] C. G. Wells, “On The Equivalence of the FRW Field Equations and those of Newtonian Cosmology,” [arXiv:1405.1656 \[gr-qc\]](#).
- [38] A. Narimani, N. Afshordi, and D. Scott, “How does pressure gravitate? Cosmological constant problem confronts observational cosmology,” [arXiv:1406.0479 \[gr-qc\]](#).
- [39] S. Rappaport, J. Schwab, S. Burles, and G. Steigman, “Big Bang Nucleosynthesis Constraints on the Self-Gravity of Pressure,” *Phys.Rev.* **D77** (2008) 023515, [arXiv:0710.5300 \[astro-ph\]](#).
- [40] J. Schwab, S. A. Hughes, and S. Rappaport, “The Self-Gravity of Pressure in Neutron Stars,” [arXiv:0806.0798 \[astro-ph\]](#).
- [41] F. Kamiab and N. Afshordi, “Neutron Stars and the Cosmological Constant Problem,” *Phys.Rev.* **D84** (2011) 063011, [arXiv:1104.5704 \[astro-ph.CO\]](#).
- [42] J. Martin, “Everything You Always Wanted To Know About The Cosmological Constant Problem (But Were Afraid To Ask),” *Comptes Rendus Physique* **13** (2012) 566–665, [arXiv:1205.3365 \[astro-ph.CO\]](#).
- [43] D. Kirzhnits and A. D. Linde, “Macroscopic Consequences of the Weinberg Model,” *Phys.Lett.* **B42** (1972) 471–474.
- [44] S. Weinberg, “Gauge and Global Symmetries at High Temperature,” *Phys.Rev.* **D9** (1974) 3357–3378.
- [45] D. Kirzhnits, “Weinberg model in the hot universe,” *JETP Lett.* **15** (1972) 529–531.
- [46] L. Dolan and R. Jackiw, “Symmetry Behavior at Finite Temperature,” *Phys.Rev.* **D9** (1974) 3320–3341.
- [47] D. Kirzhnits and A. D. Linde, “A Relativistic phase transition,” *Sov.Phys.JETP* **40** (1975) 628.
- [48] D. Kirzhnits and A. D. Linde, “Symmetry Behavior in Gauge Theories,” *Annals Phys.* **101** (1976) 195–238.
- [49] M. Dine, R. G. Leigh, P. Y. Huet, A. D. Linde, and D. A. Linde, “Towards the theory of the electroweak phase transition,” *Phys.Rev.* **D46** (1992) 550–571, [arXiv:hep-ph/9203203 \[hep-ph\]](#).
- [50] A. Sakharov, “Violation of CP Invariance, c Asymmetry, and Baryon Asymmetry of the Universe,” *Pisma Zh.Eksp.Teor.Fiz.* **5** (1967) 32–35.
- [51] G. W. Anderson and L. J. Hall, “The Electroweak phase transition and baryogenesis,” *Phys.Rev.* **D45** (1992) 2685–2698.
- [52] G. R. Farrar and M. Shaposhnikov, “Baryon asymmetry of the universe in the standard electroweak theory,” *Phys.Rev.* **D50** (1994) 774, [arXiv:hep-ph/9305275 \[hep-ph\]](#).
- [53] A. G. Cohen, D. Kaplan, and A. Nelson, “Progress in electroweak baryogenesis,”

- Ann.Rev.Nucl.Part.Sci.* **43** (1993) 27–70, [arXiv:hep-ph/9302210](#) [hep-ph].
- [54] A. Riotto and M. Trodden, “Recent progress in baryogenesis,” *Ann.Rev.Nucl.Part.Sci.* **49** (1999) 35–75, [arXiv:hep-ph/9901362](#) [hep-ph].
- [55] K. A. Olive, “The Thermodynamics of the Quark - Hadron Phase Transition in the Early Universe,” *Nucl.Phys.* **B190** (1981) 483.
- [56] E. Suhonen, “The Quark - Hadron Phase Transition in the Early Universe,” *Phys.Lett.* **B119** (1982) 81.
- [57] M. Crawford and D. N. Schramm, “Spontaneous Generation of Density Perturbations in the Early Universe,” *Nature* **298** (1982) 538–540.
- [58] J. Applegate and C. Hogan, “Relics of Cosmic Quark Condensation,” *Phys.Rev.* **D31** (1985) 3037–3045.
- [59] H. Satz, “The Transition From Hadron Matter to Quark - Gluon Plasma,” *Ann.Rev.Nucl.Part.Sci.* **35** (1985) 245–270.
- [60] G. Fuller, G. Mathews, and C. Alcock, “The Quark - Hadron Phase Transition in the Early Universe: Isothermal Baryon Number Fluctuations and Primordial Nucleosynthesis,” *Phys.Rev.* **D37** (1988) 1380.
- [61] B.-l. Cheng and A. V. Olinto, “Primordial magnetic fields generated in the quark - hadron transition,” *Phys.Rev.* **D50** (1994) 2421–2424.
- [62] C. Alcock, G. Fuller, and G. Mathews, “The Quark - hadron phase transition and primordial nucleosynthesis,” *Astrophys.J.* **320** (1987) 439–447.
- [63] **WMAP** Collaboration, G. Hinshaw *et al.*, “Nine-Year Wilkinson Microwave Anisotropy Probe (WMAP) Observations: Cosmological Parameter Results,” *Astrophys.J.Suppl.* **208** (2013) 19, [arXiv:1212.5226](#) [astro-ph.CO].
- [64] R. Alpher, H. Bethe, and G. Gamow, “The origin of chemical elements,” *Phys.Rev.* **73** (1948) 803–804.
- [65] R. V. Wagoner, W. A. Fowler, and F. Hoyle, “On the Synthesis of elements at very high temperatures,” *Astrophys.J.* **148** (1967) 3–49.
- [66] S. Sarkar, “Big bang nucleosynthesis and physics beyond the standard model,” *Rept.Prog.Phys.* **59** (1996) 1493–1610, [arXiv:hep-ph/9602260](#) [hep-ph].
- [67] D. N. Schramm and M. S. Turner, “Big bang nucleosynthesis enters the precision era,” *Rev.Mod.Phys.* **70** (1998) 303–318, [arXiv:astro-ph/9706069](#) [astro-ph].
- [68] A. Coc, E. Vangioni-Flam, P. Descouvemont, A. Adahchour, and C. Angulo, “Updated Big Bang nucleosynthesis confronted to WMAP observations and to the abundance of light elements,” *Astrophys.J.* **600** (2004) 544–552, [arXiv:astro-ph/0309480](#) [astro-ph].
- [69] G. Steigman, “Big bang nucleosynthesis: Probing the first 20 minutes,” [arXiv:astro-ph/0307244](#) [astro-ph].

- 
- [70] G. Steigman, “Primordial Nucleosynthesis in the Precision Cosmology Era,” *Ann.Rev.Nucl.Part.Sci.* **57** (2007) 463–491, [arXiv:0712.1100](#) [astro-ph].
- [71] F. Iocco, G. Mangano, G. Miele, O. Pisanti, and P. D. Serpico, “Primordial Nucleosynthesis: from precision cosmology to fundamental physics,” *Phys.Rept.* **472** (2009) 1–76, [arXiv:0809.0631](#) [astro-ph].
- [72] K. Jedamzik and M. Pospelov, “Big Bang Nucleosynthesis and Particle Dark Matter,” *New J.Phys.* **11** (2009) 105028, [arXiv:0906.2087](#) [hep-ph].
- [73] M. Pospelov and J. Pradler, “Big Bang Nucleosynthesis as a Probe of New Physics,” *Ann.Rev.Nucl.Part.Sci.* **60** (2010) 539–568, [arXiv:1011.1054](#) [hep-ph].
- [74] B. D. Fields, “The primordial lithium problem,” *Ann.Rev.Nucl.Part.Sci.* **61** (2011) 47–68, [arXiv:1203.3551](#) [astro-ph.CO].
- [75] A. Coc, J.-P. Uzan, and E. Vangioni, “Standard Big-Bang Nucleosynthesis after Planck,” [arXiv:1307.6955](#) [astro-ph.CO].
- [76] **Planck Collaboration** Collaboration, P. Ade *et al.*, “Planck 2013 results. I. Overview of products and scientific results,” [arXiv:1303.5062](#) [astro-ph.CO].
- [77] A. A. Penzias and R. W. Wilson, “A Measurement of excess antenna temperature at 4080-Mc/s,” *Astrophys.J.* **142** (1965) 419–421.
- [78] J. E. Gunn and B. A. Peterson, “On the Density of Neutral Hydrogen in Intergalactic Space,” *Astrophys.J.* **142** (1965) 1633.
- [79] **SDSS Collaboration** Collaboration, R. H. Becker *et al.*, “Evidence for reionization at  $Z \approx 6$ : Detection of a Gunn-Peterson trough in a  $Z = 6.28$  quasar,” *Astron.J.* **122** (2001) 2850, [arXiv:astro-ph/0108097](#) [astro-ph].
- [80] R. Barkana and A. Loeb, “In the beginning: The First sources of light and the reionization of the Universe,” *Phys.Rept.* **349** (2001) 125–238, [arXiv:astro-ph/0010468](#) [astro-ph].
- [81] E. T. Vishniac, “Reionization and small-scale fluctuations in the microwave background,” *Astrophys.J.* **322** (1987) 597–604.
- [82] K. Heitmann, P. M. Ricker, M. S. Warren, and S. Habib, “Robustness of cosmological simulations. 1. Large scale structure,” *Astrophys.J.Suppl.* **160** (2005) 28–58, [arXiv:astro-ph/0411795](#) [astro-ph].
- [83] K. Heitmann. Personal communication.
- [84] **Supernova Search Team** Collaboration, A. G. Riess *et al.*, “Observational evidence from supernovae for an accelerating universe and a cosmological constant,” *Astron.J.* **116** (1998) 1009–1038, [arXiv:astro-ph/9805201](#) [astro-ph].
- [85] **Supernova Cosmology Project** Collaboration, S. Perlmutter *et al.*, “Measurements of Omega and Lambda from 42 high redshift supernovae,” *Astrophys.J.* **517** (1999) 565–586, [arXiv:astro-ph/9812133](#) [astro-ph].

- [86] G. Ellis and S. Stoeger, William R., “Horizons in Inflationary Universes,” *Class.Quant.Grav.* **5** (1988) 207–220.
- [87] J. Martin, “Inflation and precision cosmology,” *Braz.J.Phys.* **34** (2004) 1307–1321, [arXiv:astro-ph/0312492](#) [astro-ph].
- [88] W. Rindler, “Visual horizons in world-models,” *Mon.Not.Roy.Astron.Soc.* **116** (1956) 662–677.
- [89] C. W. Misner, “The Isotropy of the Universe,” *The Astrophysical Journal* **151** (1967) 431.
- [90] A. H. Guth, “The Inflationary Universe: A Possible Solution to the Horizon and Flatness Problems,” *Phys.Rev.* **D23** (1981) 347–356.
- [91] A. A. Starobinsky, “A New Type of Isotropic Cosmological Models Without Singularity,” *Phys.Lett.* **B91** (1980) 99–102.
- [92] R. Dicke, “Gravitation and the Universe: The Jayne Lectures for 1969,” *Philadelphia: American Philosophical Institute* (1970) 61–62.
- [93] R. Dicke and P. Peebles, “General Relativity: An Einstein Centenary Survey,” *Cambridge University Press, edited by S. W. Hawking and W. Israel* (1979) .
- [94] H. Georgi and S. Glashow, “Unity of All Elementary Particle Forces,” *Phys.Rev.Lett.* **32** (1974) 438–441.
- [95] J. C. Pati and A. Salam, “Lepton Number as the Fourth Color,” *Phys.Rev.* **D10** (1974) 275–289.
- [96] A. Buras, J. R. Ellis, M. Gaillard, and D. V. Nanopoulos, “Aspects of the Grand Unification of Strong, Weak and Electromagnetic Interactions,” *Nucl.Phys.* **B135** (1978) 66–92.
- [97] G. ’t Hooft, “Magnetic Monopoles in Unified Gauge Theories,” *Nucl.Phys.* **B79** (1974) 276–284.
- [98] A. M. Polyakov, “Particle Spectrum in the Quantum Field Theory,” *JETP Lett.* **20** (1974) 194–195.
- [99] A. H. Guth and S. Tye, “Phase Transitions and Magnetic Monopole Production in the Very Early Universe,” *Phys.Rev.Lett.* **44** (1980) 631.
- [100] M. B. Einhorn, D. Stein, and D. Toussaint, “Are Grand Unified Theories Compatible with Standard Cosmology?,” *Phys.Rev.* **D21** (1980) 3295.
- [101] Y. Zeldovich and M. Y. Khlopov, “On the Concentration of Relic Magnetic Monopoles in the Universe,” *Phys.Lett.* **B79** (1978) 239–241.
- [102] J. Preskill, “Cosmological Production of Superheavy Magnetic Monopoles,” *Phys.Rev.Lett.* **43** (1979) 1365.
- [103] L. W. Alvarez, “Analysis of a Reported Magnetic Monopole,” .

- 
- [104] P. Price, E. Shirk, W. Osborne, and L. S. Pinsky, “Evidence for Detection of a Moving Magnetic Monopole,” *Phys.Rev.Lett.* **35** (1975) 487–490.
- [105] B. Cabrera, “First Results from a Superconductive Detector for Moving Magnetic Monopoles,” *Phys.Rev.Lett.* **48** (1982) 1378–1380.
- [106] P. Price, S.-l. Guo, S. Ahlen, and R. Fleischer, “Search for GUT Magnetic Monopoles at a Flux Level Below the Parker Limit,” *Phys.Rev.Lett.* **52** (1984) 1265.
- [107] **MACRO Collaboration** Collaboration, M. Ambrosio *et al.*, “Search for nucleon decays induced by GUT magnetic monopoles with the MACRO experiment,” *Eur.Phys.J.* **C26** (2002) 163–172, [arXiv:hep-ex/0207024](#) [hep-ex].
- [108] **MOEDAL Collaboration** Collaboration, J. Pinfold, “MoEDAL becomes the LHC’s magnificent seventh,” *CERN Cour.* **50N4** (2010) 19–20.
- [109] A. D. Linde and R. Brandenberger, *Inflation and quantum cosmology*. Boston, USA: Academic, 1990.
- [110] A. D. Linde, *Particle physics and inflationary cosmology*, vol. 5. Contemp.Concepts Phys., 1990. [arXiv:hep-th/0503203](#) [hep-th].
- [111] A. H. Guth, *The inflationary universe: The quest for a new theory of cosmic origins*. Reading, USA: Addison-Wesley, 1997.
- [112] S. Winitzki, *Eternal inflation*. Hackensack, USA: World Scientific, 2008.
- [113] M. Lemoine, J. Martin, and P. Peter, *Inflationary cosmology*. Lemoine, Martin, 2008.
- [114] A. H. Guth, “The Inflationary Universe: A Possible Solution to the Horizon and Flatness Problems,” *Phys.Rev.* **D23** (1981) 347–356.
- [115] D. Kazanas, “Dynamics of the Universe and Spontaneous Symmetry Breaking,” *Astrophys.J.* **241** (1980) L59–L63.
- [116] A. D. Linde, “A New Inflationary Universe Scenario: A Possible Solution of the Horizon, Flatness, Homogeneity, Isotropy and Primordial Monopole Problems,” *Phys.Lett.* **B108** (1982) 389–393.
- [117] K. Sato, “Cosmological Baryon Number Domain Structure and the First Order Phase Transition of a Vacuum,” *Phys.Lett.* **B99** (1981) 66–70.
- [118] A. Albrecht and P. J. Steinhardt, “Cosmology for Grand Unified Theories with Radiatively Induced Symmetry Breaking,” *Phys.Rev.Lett.* **48** (1982) 1220–1223.
- [119] A. D. Linde, “Chaotic Inflation,” *Phys.Lett.* **B129** (1983) 177–181.
- [120] J. Martin and C. Ringeval, “Inflation after WMAP3: Confronting the Slow-Roll and Exact Power Spectra to CMB Data,” *JCAP* **0608** (2006) 009, [arXiv:astro-ph/0605367](#) [astro-ph].
- [121] A. A. Starobinsky, “Relict Gravitation Radiation Spectrum and Initial State of the Universe. (In Russian),” *JETP Lett.* **30** (1979) 682–685.

- [122] V. F. Mukhanov and G. Chibisov, “Quantum Fluctuation and Nonsingular Universe. (In Russian),” *JETP Lett.* **33** (1981) 532–535.
- [123] V. F. Mukhanov and G. Chibisov, “The Vacuum energy and large scale structure of the universe,” *Sov.Phys.JETP* **56** (1982) 258–265.
- [124] S. Hawking, “The Development of Irregularities in a Single Bubble Inflationary Universe,” *Phys.Lett.* **B115** (1982) 295.
- [125] A. A. Starobinsky, “Dynamics of Phase Transition in the New Inflationary Universe Scenario and Generation of Perturbations,” *Phys.Lett.* **B117** (1982) 175–178.
- [126] A. H. Guth and S. Pi, “Fluctuations in the New Inflationary Universe,” *Phys.Rev.Lett.* **49** (1982) 1110–1113.
- [127] J. M. Bardeen, P. J. Steinhardt, and M. S. Turner, “Spontaneous Creation of Almost Scale - Free Density Perturbations in an Inflationary Universe,” *Phys.Rev.* **D28** (1983) 679.
- [128] E. D. Stewart and D. H. Lyth, “A More accurate analytic calculation of the spectrum of cosmological perturbations produced during inflation,” *Phys.Lett.* **B302** (1993) 171–175, [arXiv:gr-qc/9302019 \[gr-qc\]](#).
- [129] V. F. Mukhanov, H. Feldman, and R. H. Brandenberger, “Theory of cosmological perturbations. Part 1. Classical perturbations. Part 2. Quantum theory of perturbations. Part 3. Extensions,” *Phys.Rept.* **215** (1992) 203–333.
- [130] A. R. Liddle, P. Parsons, and J. D. Barrow, “Formalizing the slow roll approximation in inflation,” *Phys. Rev.* **D50** (1994) 7222–7232, [arXiv:astro-ph/9408015](#).
- [131] L. Grishchuk and Y. Sidorov, “Squeezed quantum states of relic gravitons and primordial density fluctuations,” *Phys.Rev.* **D42** (1990) 3413–3421.
- [132] D. Polarski and A. A. Starobinsky, “Semiclassicality and decoherence of cosmological perturbations,” *Class.Quant.Grav.* **13** (1996) 377–392, [arXiv:gr-qc/9504030 \[gr-qc\]](#).
- [133] C. Kiefer, D. Polarski, and A. A. Starobinsky, “Quantum to classical transition for fluctuations in the early universe,” *Int.J.Mod.Phys.* **D7** (1998) 455–462, [arXiv:gr-qc/9802003 \[gr-qc\]](#).
- [134] J. Martin, “Inflationary cosmological perturbations of quantum- mechanical origin,” *Lect. Notes Phys.* **669** (2005) 199–244, [arXiv:hep-th/0406011](#).
- [135] J. Martin, “Inflationary perturbations: The Cosmological Schwinger effect,” *Lect.Notes Phys.* **738** (2008) 193–241, [arXiv:0704.3540 \[hep-th\]](#).
- [136] C. Kiefer and D. Polarski, “Why do cosmological perturbations look classical to us?,” *Adv.Sci.Lett.* **2** (2009) 164–173, [arXiv:0810.0087 \[astro-ph\]](#).
- [137] D. Sudarsky, “Shortcomings in the Understanding of Why Cosmological Perturbations Look Classical,” *Int.J.Mod.Phys.* **D20** (2011) 509–552, [arXiv:0906.0315 \[gr-qc\]](#).
- [138] J. Martin, V. Vennin, and P. Peter, “Cosmological Inflation and the Quantum

- Measurement Problem,” *Phys.Rev.* **D86** (2012) 103524, [arXiv:1207.2086 \[hep-th\]](#).
- [139] J. Martin, “The Quantum State of Inflationary Perturbations,” *J.Phys.Conf.Ser.* **405** (2012) 012004, [arXiv:1209.3092 \[hep-th\]](#).
- [140] S. Alexander, R. H. Brandenberger, and D. Easson, “Brane gases in the early universe,” *Phys.Rev.* **D62** (2000) 103509, [arXiv:hep-th/0005212 \[hep-th\]](#).
- [141] J. Khoury, B. A. Ovrut, N. Seiberg, P. J. Steinhardt, and N. Turok, “From big crunch to big bang,” *Phys.Rev.* **D65** (2002) 086007, [arXiv:hep-th/0108187 \[hep-th\]](#).
- [142] J. Martin, P. Peter, N. Pinto Neto, and D. J. Schwarz, “Passing through the bounce in the ekpyrotic models,” *Phys.Rev.* **D65** (2002) 123513, [arXiv:hep-th/0112128 \[hep-th\]](#).
- [143] P. Steinhardt and N. Turok, “A cyclic model of the universe,” *Science* **296** (2002) 1436–1439.
- [144] F. Finelli and R. Brandenberger, “On the generation of a scale invariant spectrum of adiabatic fluctuations in cosmological models with a contracting phase,” *Phys.Rev.* **D65** (2002) 103522, [arXiv:hep-th/0112249 \[hep-th\]](#).
- [145] R. Brandenberger, D. A. Easson, and D. Kimberly, “Loitering phase in brane gas cosmology,” *Nucl.Phys.* **B623** (2002) 421–436, [arXiv:hep-th/0109165 \[hep-th\]](#).
- [146] R. Kallosh, L. Kofman, and A. D. Linde, “Pyrotechnic universe,” *Phys.Rev.* **D64** (2001) 123523, [arXiv:hep-th/0104073 \[hep-th\]](#).
- [147] P. Peter and N. Pinto-Neto, “Primordial perturbations in a non singular bouncing universe model,” *Phys.Rev.* **D66** (2002) 063509, [arXiv:hep-th/0203013 \[hep-th\]](#).
- [148] S. Tsujikawa, R. Brandenberger, and F. Finelli, “On the construction of nonsingular pre - big bang and ekpyrotic cosmologies and the resulting density perturbations,” *Phys.Rev.* **D66** (2002) 083513, [arXiv:hep-th/0207228 \[hep-th\]](#).
- [149] L. Kofman, A. D. Linde, and V. F. Mukhanov, “Inflationary theory and alternative cosmology,” *JHEP* **0210** (2002) 057, [arXiv:hep-th/0206088 \[hep-th\]](#).
- [150] J. Khoury, P. J. Steinhardt, and N. Turok, “Designing cyclic universe models,” *Phys.Rev.Lett.* **92** (2004) 031302, [arXiv:hep-th/0307132 \[hep-th\]](#).
- [151] J. Martin and P. Peter, “On the properties of the transition matrix in bouncing cosmologies,” *Phys.Rev.* **D69** (2004) 107301, [arXiv:hep-th/0403173 \[hep-th\]](#).
- [152] A. Nayeri, R. H. Brandenberger, and C. Vafa, “Producing a scale-invariant spectrum of perturbations in a Hagedorn phase of string cosmology,” *Phys.Rev.Lett.* **97** (2006) 021302, [arXiv:hep-th/0511140 \[hep-th\]](#).
- [153] P. Peter, E. J. Pinho, and N. Pinto-Neto, “A Non inflationary model with scale invariant cosmological perturbations,” *Phys.Rev.* **D75** (2007) 023516, [arXiv:hep-th/0610205 \[hep-th\]](#).
- [154] F. Finelli, P. Peter, and N. Pinto-Neto, “Spectra of primordial fluctuations in

- two-perfect-fluid regular bounces,” *Phys.Rev.* **D77** (2008) 103508, [arXiv:0709.3074 \[gr-qc\]](#).
- [155] F. T. Falciano, M. Lilley, and P. Peter, “A Classical bounce: Constraints and consequences,” *Phys.Rev.* **D77** (2008) 083513, [arXiv:0802.1196 \[gr-qc\]](#).
- [156] A. Linde, V. Mukhanov, and A. Vikman, “On adiabatic perturbations in the ekpyrotic scenario,” *JCAP* **1002** (2010) 006, [arXiv:0912.0944 \[hep-th\]](#).
- [157] L. R. Abramo, I. Yasuda, and P. Peter, “Non singular bounce in modified gravity,” *Phys.Rev.* **D81** (2010) 023511, [arXiv:0910.3422 \[hep-th\]](#).
- [158] R. Brandenberger, “Matter Bounce in Horava-Lifshitz Cosmology,” *Phys.Rev.* **D80** (2009) 043516, [arXiv:0904.2835 \[hep-th\]](#).
- [159] R. H. Brandenberger, “String Gas Cosmology: Progress and Problems,” *Class.Quant.Grav.* **28** (2011) 204005, [arXiv:1105.3247 \[hep-th\]](#).
- [160] R. H. Brandenberger, “The Matter Bounce Alternative to Inflationary Cosmology,” [arXiv:1206.4196 \[astro-ph.CO\]](#).
- [161] Y.-F. Cai, D. A. Easson, and R. Brandenberger, “Towards a Nonsingular Bouncing Cosmology,” *JCAP* **1208** (2012) 020, [arXiv:1206.2382 \[hep-th\]](#).
- [162] Y.-F. Cai, R. Brandenberger, and P. Peter, “Anisotropy in a Nonsingular Bounce,” [arXiv:1301.4703 \[gr-qc\]](#).
- [163] **Planck Collaboration** Collaboration, P. Ade *et al.*, “Planck 2013 results. XV. CMB power spectra and likelihood,” [arXiv:1303.5075 \[astro-ph.CO\]](#).
- [164] **BICEP2 Collaboration** Collaboration, P. Ade *et al.*, “BICEP2 I: Detection Of B-mode Polarization at Degree Angular Scales,” [arXiv:1403.3985 \[astro-ph.CO\]](#).
- [165] C. Bennett, D. Larson, J. Weiland, N. Jarosik, G. Hinshaw, *et al.*, “Nine-Year Wilkinson Microwave Anisotropy Probe (WMAP) Observations: Final Maps and Results,” [arXiv:1212.5225 \[astro-ph.CO\]](#).
- [166] G. Hinshaw, D. Larson, E. Komatsu, D. Spergel, C. Bennett, *et al.*, “Nine-Year Wilkinson Microwave Anisotropy Probe (WMAP) Observations: Cosmological Parameter Results,” [arXiv:1212.5226 \[astro-ph.CO\]](#).
- [167] **Planck Collaboration** Collaboration, P. Ade *et al.*, “Planck 2013 results. XXII. Constraints on inflation,” [arXiv:1303.5082 \[astro-ph.CO\]](#).
- [168] **Planck Collaboration** Collaboration, P. Ade *et al.*, “Planck 2013 Results. XXIV. Constraints on primordial non-Gaussianity,” [arXiv:1303.5084 \[astro-ph.CO\]](#).
- [169] J. Dunkley, E. Calabrese, J. Sievers, G. Addison, N. Battaglia, *et al.*, “The Atacama Cosmology Telescope: likelihood for small-scale CMB data,” [arXiv:1301.0776 \[astro-ph.CO\]](#).
- [170] J. L. Sievers, R. A. Hlozek, M. R. Nolta, V. Acquaviva, G. E. Addison, *et al.*, “The Atacama Cosmology Telescope: Cosmological parameters from three seasons of data,”

- [arXiv:1301.0824](#) [[astro-ph.CO](#)].
- [171] Z. Hou, C. Reichardt, K. Story, B. Follin, R. Keisler, *et al.*, “Constraints on Cosmology from the Cosmic Microwave Background Power Spectrum of the 2500-square degree SPT-SZ Survey,” [arXiv:1212.6267](#) [[astro-ph.CO](#)].
- [172] K. Story, C. Reichardt, Z. Hou, R. Keisler, K. Aird, *et al.*, “A Measurement of the Cosmic Microwave Background Damping Tail from the 2500-square-degree SPT-SZ survey,” [arXiv:1210.7231](#) [[astro-ph.CO](#)].
- [173] **CMBPol Study Team** Collaboration, D. Baumann *et al.*, “CMBPol Mission Concept Study: Probing Inflation with CMB Polarization,” *AIP Conf.Proc.* **1141** (2009) 10–120, [arXiv:0811.3919](#) [[astro-ph](#)].
- [174] J. Bock, A. Cooray, S. Hanany, B. Keating, A. Lee, *et al.*, “The Experimental Probe of Inflationary Cosmology (EPIC): A Mission Concept Study for NASA’s Einstein Inflation Probe,” [arXiv:0805.4207](#) [[astro-ph](#)].
- [175] B. Crill, P. Ade, E. Battistelli, S. Benton, R. Bihary, *et al.*, “SPIDER: A Balloon-borne Large-scale CMB Polarimeter,” [arXiv:0807.1548](#) [[astro-ph](#)].
- [176] A. Kogut, D. Fixsen, D. Chuss, J. Dotson, E. Dwek, *et al.*, “The Primordial Inflation Explorer (PIXIE): A Nulling Polarimeter for Cosmic Microwave Background Observations,” *JCAP* **1107** (2011) 025, [arXiv:1105.2044](#) [[astro-ph.CO](#)].
- [177] T. Matsumura, Y. Akiba, J. Borrill, Y. Chinone, M. Dobbs, *et al.*, “Mission design of LiteBIRD,” [arXiv:1311.2847](#) [[astro-ph.IM](#)].
- [178] **PRISM Collaboration** Collaboration, P. Andre *et al.*, “PRISM (Polarized Radiation Imaging and Spectroscopy Mission): A White Paper on the Ultimate Polarimetric Spectro-Imaging of the Microwave and Far-Infrared Sky,” [arXiv:1306.2259](#) [[astro-ph.CO](#)].
- [179] **Supernova Search Team** Collaboration, J. L. Tonry *et al.*, “Cosmological results from high- $z$  supernovae,” *Astrophys.J.* **594** (2003) 1–24, [arXiv:astro-ph/0305008](#) [[astro-ph](#)].
- [180] **Supernova Search Team** Collaboration, A. G. Riess *et al.*, “Type Ia supernova discoveries at  $z \lesssim 1$  from the Hubble Space Telescope: Evidence for past deceleration and constraints on dark energy evolution,” *Astrophys.J.* **607** (2004) 665–687, [arXiv:astro-ph/0402512](#) [[astro-ph](#)].
- [181] A. G. Riess, L.-G. Strolger, S. Casertano, H. C. Ferguson, B. Mobasher, *et al.*, “New Hubble Space Telescope Discoveries of Type Ia Supernovae at  $z \lesssim 1$ : Narrowing Constraints on the Early Behavior of Dark Energy,” *Astrophys.J.* **659** (2007) 98–121, [arXiv:astro-ph/0611572](#) [[astro-ph](#)].
- [182] A. G. Riess, L. Macri, S. Casertano, H. Lampeitl, H. C. Ferguson, *et al.*, “A 3Telescope and Wide Field Camera 3,” *Astrophys.J.* **730** (2011) 119, [arXiv:1103.2976](#) [[astro-ph.CO](#)].
- [183] **SDSS Collaboration** Collaboration, J. K. Adelman-McCarthy *et al.*, “The Sixth Data

- Release of the Sloan Digital Sky Survey,” *Astrophys.J.Suppl.* **175** (2008) 297–313, [arXiv:0707.3413 \[astro-ph\]](#).
- [184] **SDSS Collaboration** Collaboration, K. N. Abazajian *et al.*, “The Seventh Data Release of the Sloan Digital Sky Survey,” *Astrophys.J.Suppl.* **182** (2009) 543–558, [arXiv:0812.0649 \[astro-ph\]](#).
- [185] **Euclid collaboration** Collaboration, J. Amiaux *et al.*, “Euclid Mission: building of a Reference Survey,” [arXiv:1209.2228 \[astro-ph.IM\]](#).
- [186] M. S. Turner, M. J. White, and J. E. Lidsey, “Tensor perturbations in inflationary models as a probe of cosmology,” *Phys.Rev.* **D48** (1993) 4613–4622, [arXiv:astro-ph/9306029 \[astro-ph\]](#).
- [187] M. Maggiore, “Gravitational wave experiments and early universe cosmology,” *Phys.Rept.* **331** (2000) 283–367, [arXiv:gr-qc/9909001 \[gr-qc\]](#).
- [188] H. Kudoh, A. Taruya, T. Hiramatsu, and Y. Himemoto, “Detecting a gravitational-wave background with next-generation space interferometers,” *Phys.Rev.* **D73** (2006) 064006, [arXiv:gr-qc/0511145 \[gr-qc\]](#).
- [189] K. Nakayama, S. Saito, Y. Suwa, and J. Yokoyama, “Probing reheating temperature of the universe with gravitational wave background,” *JCAP* **0806** (2008) 020, [arXiv:0804.1827 \[astro-ph\]](#).
- [190] S. Kuroyanagi, C. Gordon, J. Silk, and N. Sugiyama, “Forecast Constraints on Inflation from Combined CMB and Gravitational Wave Direct Detection Experiments,” *Phys.Rev.* **D81** (2010) 083524, [arXiv:0912.3683 \[astro-ph.CO\]](#).
- [191] J. Crowder and N. J. Cornish, “Beyond LISA: Exploring future gravitational wave missions,” *Phys.Rev.* **D72** (2005) 083005, [arXiv:gr-qc/0506015 \[gr-qc\]](#).
- [192] M. Ando, S. Kawamura, N. Seto, S. Sato, T. Nakamura, *et al.*, “DECIGO and DECIGO pathfinder,” *Class.Quant.Grav.* **27** (2010) 084010.
- [193] S. Kawamura, M. Ando, N. Seto, S. Sato, T. Nakamura, *et al.*, “The Japanese space gravitational wave antenna: DECIGO,” *Class.Quant.Grav.* **28** (2011) 094011.
- [194] P. Amaro-Seoane, S. Aoudia, S. Babak, P. Binetruy, E. Berti, *et al.*, “eLISA: Astrophysics and cosmology in the millihertz regime,” [arXiv:1201.3621 \[astro-ph.CO\]](#).
- [195] S. Kuroyanagi, C. Ringeval, and T. Takahashi, “Early Universe Tomography with CMB and Gravitational Waves,” *Phys. Rev. D* **87** (2013) 083502, [arXiv:1301.1778 \[astro-ph.CO\]](#).
- [196] K. Jedamzik, M. Lemoine, and J. Martin, “Generation of gravitational waves during early structure formation between cosmic inflation and reheating,” *JCAP* **1004** (2010) 021, [arXiv:1002.3278 \[astro-ph.CO\]](#).
- [197] D. Gorbunov and A. Tokareva, “ $R^2$ -inflation with conformal SM Higgs field,” *JCAP* **1312** (2013) 021, [arXiv:1212.4466 \[astro-ph.CO\]](#).

- 
- [198] M. Zaldarriaga, S. R. Furlanetto, and L. Hernquist, “21 Centimeter fluctuations from cosmic gas at high redshifts,” *Astrophys.J.* **608** (2004) 622–635, [arXiv:astro-ph/0311514](#) [astro-ph].
- [199] A. Lewis and A. Challinor, “The 21cm angular-power spectrum from the dark ages,” *Phys. Rev.* **D76** (2007) 083005, [arXiv:astro-ph/0702600](#).
- [200] M. Tegmark and M. Zaldarriaga, “The Fast Fourier Transform Telescope,” *Phys. Rev.* **D79** (2009) 083530, [arXiv:0805.4414](#) [astro-ph].
- [201] V. Barger, Y. Gao, Y. Mao, and D. Marfatia, “Inflationary Potential from 21 cm Tomography and Planck,” *Phys. Lett.* **B673** (2009) 173–178, [arXiv:0810.3337](#) [astro-ph].
- [202] Y. Mao, M. Tegmark, M. McQuinn, M. Zaldarriaga, and O. Zahn, “How accurately can 21 cm tomography constrain cosmology?,” *Phys. Rev.* **D78** (2008) 023529, [arXiv:0802.1710](#) [astro-ph].
- [203] P. Adshead, R. Easther, J. Pritchard, and A. Loeb, “Inflation and the Scale Dependent Spectral Index: Prospects and Strategies,” *JCAP* **1102** (2011) 021, [arXiv:1007.3748](#) [astro-ph.CO].
- [204] S. Clesse, L. Lopez-Honorez, C. Ringeval, H. Tashiro, and M. H. Tytgat, “Background reionization history from omniscopes,” *Phys.Rev.* **D86** (2012) 123506, [arXiv:1208.4277](#) [astro-ph.CO].
- [205] J. Martin, C. Ringeval, and V. Vennin, “Encyclopædia Inflationaris,” *Phys.Dark Univ.* (2014) , [arXiv:1303.3787](#) [astro-ph.CO].
- [206] J. Martin, C. Ringeval, R. Trotta, and V. Vennin, “The Best Inflationary Models After Planck,” *JCAP* **1403** (2014) 039, [arXiv:1312.3529](#) [astro-ph.CO].
- [207] J. Martin, C. Ringeval, R. Trotta, and V. Vennin, “Compatibility of Planck and BICEP2 in the Light of Inflation,” [arXiv:1405.7272](#) [astro-ph.CO].
- [208] V. Vennin, “Horizon-Flow off-track for Inflation,” *Phys. Rev. D89*, **083526** (2014) 083526, [arXiv:1401.2926](#) [astro-ph.CO].
- [209] J. Martin, C. Ringeval, and V. Vennin, “K-inflationary Power Spectra at Second Order,” *JCAP* **1306** (2013) 021, [arXiv:1303.2120](#) [astro-ph.CO].
- [210] J. Martin and V. Vennin, “Stochastic Effects in Hybrid Inflation,” *Phys.Rev.* **D85** (2012) 043525, [arXiv:1110.2070](#) [astro-ph.CO].
- [211] L. Perreault Levasseur, V. Vennin, and R. Brandenberger, “Recursive Stochastic Effects in Valley Hybrid Inflation,” *Phys. Rev. D88*, **083538** (2013) 083538, [arXiv:1307.2575](#).
- [212] D. H. Lyth and A. Riotto, “Particle physics models of inflation and the cosmological density perturbation,” *Phys. Rept.* **314** (1999) 1–146, [arXiv:hep-ph/9807278](#).
- [213] M. S. Turner, “Coherent Scalar Field Oscillations in an Expanding Universe,” *Phys. Rev.* **D28** (1983) 1243.

- [214] L. Kofman, A. D. Linde, and A. A. Starobinsky, “Towards the theory of reheating after inflation,” *Phys.Rev.* **D56** (1997) 3258–3295, [arXiv:hep-ph/9704452 \[hep-ph\]](#).
- [215] B. A. Bassett, D. I. Kaiser, and R. Maartens, “General relativistic preheating after inflation,” *Phys.Lett.* **B455** (1999) 84–89, [arXiv:hep-ph/9808404 \[hep-ph\]](#).
- [216] F. Finelli and R. H. Brandenberger, “Parametric amplification of metric fluctuations during reheating in two field models,” *Phys. Rev.* **D62** (2000) 083502, [arXiv:hep-ph/0003172 \[hep-ph\]](#).
- [217] B. A. Bassett, S. Tsujikawa, and D. Wands, “Inflation dynamics and reheating,” *Rev. Mod. Phys.* **78** (2006) 537–589, [arXiv:astro-ph/0507632](#).
- [218] A. Mazumdar and J. Rocher, “Particle physics models of inflation and curvaton scenarios,” *Phys. Rept.* **497** (2011) 85–215, [arXiv:1001.0993 \[hep-ph\]](#).
- [219] K. Jedamzik, M. Lemoine, and J. Martin, “Collapse of Small-Scale Density Perturbations during Preheating in Single Field Inflation,” *JCAP* **1009** (2010) 034, [arXiv:1002.3039 \[astro-ph.CO\]](#).
- [220] R. Easther, R. Flauger, and J. B. Gilmore, “Delayed Reheating and the Breakdown of Coherent Oscillations,” *JCAP* **1104** (2011) 027, [arXiv:1003.3011 \[astro-ph.CO\]](#).
- [221] A. Albrecht, P. J. Steinhardt, M. S. Turner, and F. Wilczek, “Reheating an Inflationary Universe,” *Phys.Rev.Lett.* **48** (1982) 1437.
- [222] L. Kofman, A. D. Linde, and A. A. Starobinsky, “Reheating after inflation,” *Phys.Rev.Lett.* **73** (1994) 3195–3198, [arXiv:hep-th/9405187 \[hep-th\]](#).
- [223] Y. Shtanov, J. H. Traschen, and R. H. Brandenberger, “Universe reheating after inflation,” *Phys.Rev.* **D51** (1995) 5438–5455, [arXiv:hep-ph/9407247 \[hep-ph\]](#).
- [224] V. Kuzmin and V. Rubakov, “Ultrahigh-energy cosmic rays: A Window to postinflationary reheating epoch of the universe?,” *Phys.Atom.Nucl.* **61** (1998) 1028–1030, [arXiv:astro-ph/9709187 \[astro-ph\]](#).
- [225] F. Finelli and R. H. Brandenberger, “Parametric amplification of gravitational fluctuations during reheating,” *Phys.Rev.Lett.* **82** (1999) 1362–1365, [arXiv:hep-ph/9809490 \[hep-ph\]](#).
- [226] D. J. Schwarz, C. A. Terrero-Escalante, and A. A. Garcia, “Higher order corrections to primordial spectra from cosmological inflation,” *Phys.Lett.* **B517** (2001) 243–249, [arXiv:astro-ph/0106020 \[astro-ph\]](#).
- [227] D. J. Schwarz and C. A. Terrero-Escalante, “Primordial fluctuations and cosmological inflation after WMAP 1.0,” *JCAP* **0408** (2004) 003, [arXiv:hep-ph/0403129 \[hep-ph\]](#).
- [228] G. N. Remmen and S. M. Carroll, “Attractor Solutions in Scalar-Field Cosmology,” *Phys.Rev.* **D88** (2013) 083518, [arXiv:1309.2611 \[gr-qc\]](#).
- [229] D. Larson, J. Dunkley, G. Hinshaw, E. Komatsu, M. Nolta, *et al.*, “Seven-Year Wilkinson Microwave Anisotropy Probe (WMAP) Observations: Power Spectra and WMAP-Derived Parameters,” *Astrophys.J.Suppl.* **192** (2011) 16, [arXiv:1001.4635](#)

- [astro-ph.CO].
- [230] **WMAP Collaboration** Collaboration, E. Komatsu *et al.*, “Seven-Year Wilkinson Microwave Anisotropy Probe (WMAP) Observations: Cosmological Interpretation,” *Astrophys.J.Suppl.* **192** (2011) 18, [arXiv:1001.4538](#) [astro-ph.CO].
- [231] L. Lorenz, J. Martin, and C. Ringeval, “Constraints on Kinetically Modified Inflation from WMAP5,” *Phys.Rev.* **D78** (2008) 063543, [arXiv:0807.2414](#) [astro-ph].
- [232] J. Martin and C. Ringeval, “First CMB Constraints on the Inflationary Reheating Temperature,” *Phys.Rev.* **D82** (2010) 023511, [arXiv:1004.5525](#) [astro-ph.CO].
- [233] R. Easther and W. H. Kinney, “Monte Carlo reconstruction of the inflationary potential,” *Phys.Rev.* **D67** (2003) 043511, [arXiv:astro-ph/0210345](#) [astro-ph].
- [234] W. H. Kinney, E. W. Kolb, A. Melchiorri, and A. Riotto, “WMAPping inflationary physics,” *Phys.Rev.* **D69** (2004) 103516, [arXiv:hep-ph/0305130](#) [hep-ph].
- [235] C.-Y. Chen, B. Feng, X.-L. Wang, and Z.-Y. Yang, “Reconstructing large running-index inflaton potentials,” *Class.Quant.Grav.* **21** (2004) 3223–3236, [arXiv:astro-ph/0404419](#) [astro-ph].
- [236] B. A. Powell, K. Tzirakis, and W. H. Kinney, “Tensors, non-Gaussianities, and the future of potential reconstruction,” *JCAP* **0904** (2009) 019, [arXiv:0812.1797](#) [astro-ph].
- [237] J. Martin, C. Ringeval, and R. Trotta, “Hunting Down the Best Model of Inflation with Bayesian Evidence,” *Phys.Rev.* **D83** (2011) 063524, [arXiv:1009.4157](#) [astro-ph.CO].
- [238] J. Bardeen, “Gauge invariant cosmological perturbations,” *Phys.Rev.* **D22** (1981) 1882.
- [239] J. M. Bardeen, “Gauge Invariant Cosmological Perturbations,” *Phys.Rev.* **D22** (1980) 1882–1905.
- [240] J. Martin and D. J. Schwarz, “The Influence of cosmological transitions on the evolution of density perturbations,” *Phys.Rev.* **D57** (1998) 3302–3316, [arXiv:gr-qc/9704049](#) [gr-qc].
- [241] H. Kodama and M. Sasaki, “Cosmological Perturbation Theory,” *Prog.Theor.Phys.Suppl.* **78** (1984) 1–166.
- [242] V. F. Mukhanov, “Quantum Theory of Gauge Invariant Cosmological Perturbations,” *Sov.Phys.JETP* **67** (1988) 1297–1302.
- [243] F. L. Claude Cohen-Tannoudji, Bernard Diu, *Quantum Mechanics*. Hermann, 1973.
- [244] T. Bunch and P. Davies, “Quantum Field Theory in de Sitter Space: Renormalization by Point Splitting,” *Proc.Roy.Soc.Lond.* **A360** (1978) 117–134.
- [245] N. Birrell and P. Davies, “Quantum Fields in Curved Space,” *Cambridge Monogr.Math.Phys.* (1982) .
- [246] J. Martin and R. H. Brandenberger, “The TransPlanckian problem of inflationary cosmology,” *Phys.Rev.* **D63** (2001) 123501, [arXiv:hep-th/0005209](#) [hep-th].

- [247] J. Martin and R. H. Brandenberger, “The Corley-Jacobson dispersion relation and transPlanckian inflation,” *Phys.Rev.* **D65** (2002) 103514, [arXiv:hep-th/0201189 \[hep-th\]](#).
- [248] J. Martin and R. Brandenberger, “On the dependence of the spectra of fluctuations in inflationary cosmology on transPlanckian physics,” *Phys.Rev.* **D68** (2003) 063513, [arXiv:hep-th/0305161 \[hep-th\]](#).
- [249] R. H. Brandenberger and J. Martin, “Back-reaction and the trans-Planckian problem of inflation revisited,” *Phys.Rev.* **D71** (2005) 023504, [arXiv:hep-th/0410223 \[hep-th\]](#).
- [250] N. Kaloper, M. Kleban, A. Lawrence, S. Shenker, and L. Susskind, “Initial conditions for inflation,” *JHEP* **0211** (2002) 037, [arXiv:hep-th/0209231 \[hep-th\]](#).
- [251] U. H. Danielsson, “A Note on inflation and transPlanckian physics,” *Phys.Rev.* **D66** (2002) 023511, [arXiv:hep-th/0203198 \[hep-th\]](#).
- [252] K. Goldstein and D. A. Lowe, “A Note on alpha vacua and interacting field theory in de Sitter space,” *Nucl.Phys.* **B669** (2003) 325–340, [arXiv:hep-th/0302050 \[hep-th\]](#).
- [253] H. Collins and R. Holman, “Taming the alpha vacuum,” *Phys.Rev.* **D70** (2004) 084019, [arXiv:hep-th/0312143 \[hep-th\]](#).
- [254] H. Collins, R. Holman, and M. R. Martin, “The Fate of the alpha vacuum,” *Phys.Rev.* **D68** (2003) 124012, [arXiv:hep-th/0306028 \[hep-th\]](#).
- [255] R. Brunetti, K. Fredenhagen, and S. Hollands, “A Remark on alpha vacua for quantum field theories on de Sitter space,” *JHEP* **0505** (2005) 063, [arXiv:hep-th/0503022 \[hep-th\]](#).
- [256] U. H. Danielsson, “Transplanckian energy production and slow roll inflation,” *Phys.Rev.* **D71** (2005) 023516, [arXiv:hep-th/0411172 \[hep-th\]](#).
- [257] B. Greene, K. Schalm, J. P. van der Schaar, and G. Shiu, “Extracting new physics from the CMB,” *eConf* **C041213** (2004) 0001, [arXiv:astro-ph/0503458 \[astro-ph\]](#).
- [258] K. Bhattacharya, S. Mohanty, and R. Rangarajan, “Temperature of the inflaton and duration of inflation from WMAP data,” *Phys.Rev.Lett.* **96** (2006) 121302, [arXiv:hep-ph/0508070 \[hep-ph\]](#).
- [259] R. Easther, W. H. Kinney, and H. Peiris, “Boundary effective field theory and trans-Planckian perturbations: Astrophysical implications,” *JCAP* **0508** (2005) 001, [arXiv:astro-ph/0505426 \[astro-ph\]](#).
- [260] M. Giovannini, “Hanbury Brown-Twiss interferometry and second-order correlations of inflaton quanta,” *Phys.Rev.* **D83** (2011) 023515, [arXiv:1011.1673 \[astro-ph.CO\]](#).
- [261] A. Ashoorioon and G. Shiu, “A Note on Calm Excited States of Inflation,” *JCAP* **1103** (2011) 025, [arXiv:1012.3392 \[astro-ph.CO\]](#).
- [262] I. Agullo and L. Parker, “Non-gaussianities and the Stimulated creation of quanta in the inflationary universe,” *Phys.Rev.* **D83** (2011) 063526, [arXiv:1010.5766 \[astro-ph.CO\]](#).

- 
- [263] D. Carney, W. Fischler, S. Paban, and N. Sivanandam, “The Inflationary Wavefunction and its Initial Conditions,” *JCAP* **1212** (2012) 012, [arXiv:1109.6566 \[hep-th\]](#).
- [264] A. Dey and S. Paban, “Non-Gaussianities in the Cosmological Perturbation Spectrum due to Primordial Anisotropy,” *JCAP* **1204** (2012) 039, [arXiv:1106.5840 \[hep-th\]](#).
- [265] A. Dey, E. Kovetz, and S. Paban, “Non-Gaussianities in the Cosmological Perturbation Spectrum due to Primordial Anisotropy II,” *JCAP* **1210** (2012) 055, [arXiv:1205.2758 \[astro-ph.CO\]](#).
- [266] S. Kundu, “Inflation with General Initial Conditions for Scalar Perturbations,” *JCAP* **1202** (2012) 005, [arXiv:1110.4688 \[astro-ph.CO\]](#).
- [267] D. Lyth, “Large Scale Energy Density Perturbations and Inflation,” *Phys.Rev.* **D31** (1985) 1792–1798.
- [268] J. H. Traschen and R. H. Brandenberger, “Particle Production During Out-of-equilibrium Phase Transitions,” *Phys.Rev.* **D42** (1990) 2491–2504.
- [269] M. Abramowitz and I. Stegun, *Handbook of Mathematical Functions*. Dover, New York, fifth ed., 1964.
- [270] V. F. Mukhanov, “Gravitational Instability of the Universe Filled with a Scalar Field,” *JETP Lett.* **41** (1985) 493–496.
- [271] F. Lucchin and S. Matarrese, “Power Law Inflation,” *Phys.Rev.* **D32** (1985) 1316.
- [272] J.-O. Gong and E. D. Stewart, “The Density perturbation power spectrum to second order corrections in the slow roll expansion,” *Phys.Lett.* **B510** (2001) 1–9, [arXiv:astro-ph/0101225 \[astro-ph\]](#).
- [273] J. Martin and D. J. Schwarz, “WKB approximation for inflationary cosmological perturbations,” *Phys.Rev.* **D67** (2003) 083512, [arXiv:astro-ph/0210090 \[astro-ph\]](#).
- [274] S. Habib, K. Heitmann, G. Jungman, and C. Molina-Paris, “The Inflationary perturbation spectrum,” *Phys.Rev.Lett.* **89** (2002) 281301, [arXiv:astro-ph/0208443 \[astro-ph\]](#).
- [275] S. Habib, A. Heinen, K. Heitmann, G. Jungman, and C. Molina-Paris, “Characterizing inflationary perturbations: The Uniform approximation,” *Phys.Rev.* **D70** (2004) 083507, [arXiv:astro-ph/0406134 \[astro-ph\]](#).
- [276] R. Casadio, F. Finelli, M. Luzzi, and G. Venturi, “Improved WKB analysis of cosmological perturbations,” *Phys.Rev.* **D71** (2005) 043517, [arXiv:gr-qc/0410092 \[gr-qc\]](#).
- [277] R. Casadio, F. Finelli, M. Luzzi, and G. Venturi, “Higher order slow-roll predictions for inflation,” *Phys.Lett.* **B625** (2005) 1–6, [arXiv:gr-qc/0506043 \[gr-qc\]](#).
- [278] S. M. Leach, A. R. Liddle, J. Martin, and D. J. Schwarz, “Cosmological parameter estimation and the inflationary cosmology,” *Phys.Rev.* **D66** (2002) 023515, [arXiv:astro-ph/0202094 \[astro-ph\]](#).

- [279] V. Mukhanov, “Quantum Cosmological Perturbations: Predictions and Observations,” *Eur.Phys.J.* **C73** (2013) 2486, [arXiv:1303.3925 \[astro-ph.CO\]](#).
- [280] R. H. Brandenberger, A. Nayeri, and S. P. Patil, “Closed String Thermodynamics and a Blue Tensor Spectrum,” [arXiv:1403.4927 \[astro-ph.CO\]](#).
- [281] D. H. Lyth, “What would we learn by detecting a gravitational wave signal in the cosmic microwave background anisotropy?,” *Phys.Rev.Lett.* **78** (1997) 1861–1863, [arXiv:hep-ph/9606387 \[hep-ph\]](#).
- [282] S. Antusch and D. Nolde, “BICEP2 implications for single-field slow-roll inflation revisited,” *JCAP* **1405** (2014) 035, [arXiv:1404.1821 \[hep-ph\]](#).
- [283] D. Baumann and L. McAllister, “Inflation and String Theory,” [arXiv:1404.2601 \[hep-th\]](#).
- [284] A. Vilenkin, “Quantum Fluctuations in the New Inflationary Universe,” *Nucl.Phys.* **B226** (1983) 527.
- [285] A. Vilenkin, “The Birth of Inflationary Universes,” *Phys.Rev.* **D27** (1983) 2848.
- [286] M. Sasaki, Y. Nambu, and K.-i. Nakao, “Classical Behavior of a Scalar Field in the Inflationary Universe,” *Nucl.Phys.* **B308** (1988) 868.
- [287] A. Goncharov, A. D. Linde, and V. F. Mukhanov, “The Global Structure of the Inflationary Universe,” *Int.J.Mod.Phys.* **A2** (1987) 561–591.
- [288] D. Salopek and J. Bond, “Nonlinear evolution of long wavelength metric fluctuations in inflationary models,” *Phys.Rev.* **D42** (1990) 3936–3962.
- [289] A. D. Linde, D. A. Linde, and A. Mezhlumian, “From the Big Bang theory to the theory of a stationary universe,” *Phys.Rev.* **D49** (1994) 1783–1826, [arXiv:gr-qc/9306035 \[gr-qc\]](#).
- [290] A. A. Starobinsky, “STOCHASTIC DE SITTER (INFLATIONARY) STAGE IN THE EARLY UNIVERSE,” *Lect.Notes Phys.* **246** (1986) 107–126.
- [291] Y. Nambu and M. Sasaki, “Stochastic Stage of an Inflationary Universe Model,” *Phys.Lett.* **B205** (1988) 441.
- [292] Y. Nambu and M. Sasaki, “Stochastic Approach to Chaotic Inflation and the Distribution of Universes,” *Phys.Lett.* **B219** (1989) 240.
- [293] H. E. Kandrup, “Stochastic inflation as a time dependent random walk,” *Phys.Rev.* **D39** (1989) 2245.
- [294] K.-i. Nakao, Y. Nambu, and M. Sasaki, “Stochastic Dynamics of New Inflation,” *Prog.Theor.Phys.* **80** (1988) 1041.
- [295] Y. Nambu, “Stochastic Dynamics of an Inflationary Model and Initial Distribution of Universes,” *Prog.Theor.Phys.* **81** (1989) 1037.
- [296] D. Salopek and J. Bond, “Stochastic inflation and nonlinear gravity,” *Phys.Rev.* **D43**

- (1991) 1005–1031.
- [297] S. Mollerach, S. Matarrese, A. Ortolan, and F. Lucchin, “Stochastic inflation in a simple two field model,” *Phys.Rev.* **D44** (1991) 1670–1679.
- [298] A. A. Starobinsky and J. Yokoyama, “Equilibrium state of a selfinteracting scalar field in the De Sitter background,” *Phys.Rev.* **D50** (1994) 6357–6368, [arXiv:astro-ph/9407016 \[astro-ph\]](#).
- [299] F. Finelli, G. Marozzi, A. Starobinsky, G. Vacca, and G. Venturi, “Generation of fluctuations during inflation: Comparison of stochastic and field-theoretic approaches,” *Phys.Rev.* **D79** (2009) 044007, [arXiv:0808.1786 \[hep-th\]](#).
- [300] F. Finelli, G. Marozzi, A. Starobinsky, G. Vacca, and G. Venturi, “Stochastic growth of quantum fluctuations during slow-roll inflation,” *Phys.Rev.* **D82** (2010) 064020, [arXiv:1003.1327 \[hep-th\]](#).
- [301] B. Garbrecht, G. Rigopoulos, and Y. Zhu, “Infrared Correlations in de Sitter Space: Field Theoretic vs. Stochastic Approach,” *Phys.Rev.* **D89** (2014) 063506, [arXiv:1310.0367 \[hep-th\]](#).
- [302] N. Tsamis and R. Woodard, “Stochastic quantum gravitational inflation,” *Nucl.Phys.* **B724** (2005) 295–328, [arXiv:gr-qc/0505115 \[gr-qc\]](#).
- [303] T. Prokopec, N. Tsamis, and R. Woodard, “Stochastic Inflationary Scalar Electrodynamics,” *Annals Phys.* **323** (2008) 1324–1360, [arXiv:0707.0847 \[gr-qc\]](#).
- [304] T. Prokopec, N. C. Tsamis, and R. P. Woodard, “Two loop stress-energy tensor for inflationary scalar electrodynamics,” *Phys.Rev.* **D78** (2008) 043523, [arXiv:0802.3673 \[gr-qc\]](#).
- [305] M. Morikawa, “Dissipation and Fluctuation of Quantum Fields in Expanding Universes,” *Phys.Rev.* **D42** (1990) 1027–1034.
- [306] B. Hu and S. Sinha, “A Fluctuation - dissipation relation for semiclassical cosmology,” *Phys.Rev.* **D51** (1995) 1587–1606, [arXiv:gr-qc/9403054 \[gr-qc\]](#).
- [307] L. Grishchuk, H. Haus, and K. Bergman, “Generation of squeezed radiation from vacuum in the cosmos and the laboratory,” *Phys.Rev.* **D46** (1992) 1440–1449.
- [308] A. H. Guth and S.-Y. Pi, “The Quantum Mechanics of the Scalar Field in the New Inflationary Universe,” *Phys.Rev.* **D32** (1985) 1899–1920.
- [309] J. Lesgourgues, D. Polarski, and A. A. Starobinsky, “Quantum to classical transition of cosmological perturbations for nonvacuum initial states,” *Nucl.Phys.* **B497** (1997) 479–510, [arXiv:gr-qc/9611019 \[gr-qc\]](#).
- [310] M. Mijic, “Quantum squeezing and late time classical behavior of massive fields in expanding Robertson-Walker universe,” *Int.J.Mod.Phys.* **D6** (1997) 505–514, [arXiv:gr-qc/9706016 \[gr-qc\]](#).
- [311] W. Zurek, “Pointer Basis of Quantum Apparatus: Into What Mixture Does the Wave Packet Collapse?,” *Phys.Rev.* **D24** (1981) 1516–1525.

- [312] W. Zurek, “Environment induced superselection rules,” *Phys.Rev.* **D26** (1982) 1862–1880.
- [313] E. Joos and H. Zeh, “The Emergence of classical properties through interaction with the environment,” *Z.Phys.* **B59** (1985) 223–243.
- [314] E. Calzetta and B. Hu, “Quantum fluctuations, decoherence of the mean field, and structure formation in the early universe,” *Phys.Rev.* **D52** (1995) 6770–6788, [arXiv:gr-qc/9505046](#) [gr-qc].
- [315] C. Kiefer, I. Lohmar, D. Polarski, and A. A. Starobinsky, “Pointer states for primordial fluctuations in inflationary cosmology,” *Class.Quant.Grav.* **24** (2007) 1699–1718, [arXiv:astro-ph/0610700](#) [astro-ph].
- [316] I. Egusquiza, A. Feinstein, M. Perez Sebastian, and M. Valle Basagoiti, “On the entropy and the density matrix of cosmological perturbations,” *Class.Quant.Grav.* **15** (1998) 1927–1936, [arXiv:gr-qc/9709061](#) [gr-qc].
- [317] P. R. Anderson, C. Molina-Paris, and E. Mottola, “Short distance and initial state effects in inflation: Stress tensor and decoherence,” *Phys.Rev.* **D72** (2005) 043515, [arXiv:hep-th/0504134](#) [hep-th].
- [318] C. P. Burgess, R. Holman, and D. Hoover, “Decoherence of inflationary primordial fluctuations,” *Phys.Rev.* **D77** (2008) 063534, [arXiv:astro-ph/0601646](#) [astro-ph].
- [319] P. Martineau, “On the decoherence of primordial fluctuations during inflation,” *Class.Quant.Grav.* **24** (2007) 5817–5834, [arXiv:astro-ph/0601134](#) [astro-ph].
- [320] H. Casini, R. Montemayor, and P. Sisterna, “Stochastic approach to inflation. 2. Classicality, coarse graining and noises,” *Phys.Rev.* **D59** (1999) 063512, [arXiv:gr-qc/9811083](#) [gr-qc].
- [321] S. Matarrese, M. A. Musso, and A. Riotto, “Influence of superhorizon scales on cosmological observables generated during inflation,” *JCAP* **0405** (2004) 008, [arXiv:hep-th/0311059](#) [hep-th].
- [322] M. Liguori, S. Matarrese, M. Musso, and A. Riotto, “Stochastic inflation and the lower multipoles in the CMB anisotropies,” *JCAP* **0408** (2004) 011, [arXiv:astro-ph/0405544](#) [astro-ph].
- [323] B. Hu, J. P. Paz, and Y. Zhang, “Quantum origin of noise and fluctuations in cosmology,” [arXiv:gr-qc/9512049](#) [gr-qc].
- [324] S. Winitzki and A. Vilenkin, “Effective noise in stochastic description of inflation,” *Phys.Rev.* **D61** (2000) 084008, [arXiv:gr-qc/9911029](#) [gr-qc].
- [325] H. M. Hodges, “Analytic Solution of a Chaotic Inflaton,” *Phys.Rev.* **D39** (1989) 3568–3570.
- [326] H. M. Hodges, “Is double inflation likely?,” *Phys.Rev.Lett.* **64** (1990) 1080.
- [327] A. Matacz, “Inflation and the fine tuning problem,” *Phys.Rev.* **D56** (1997) 1836–1840, [arXiv:gr-qc/9611063](#) [gr-qc].

- 
- [328] J. Martin and M. Musso, “Solving stochastic inflation for arbitrary potentials,” *Phys.Rev.* **D73** (2006) 043516, [arXiv:hep-th/0511214](#) [hep-th].
- [329] J. Martin and M. Musso, “On the reliability of the Langevin perturbative solution in stochastic inflation,” *Phys.Rev.* **D73** (2006) 043517, [arXiv:hep-th/0511292](#) [hep-th].
- [330] S. Gratton and N. Turok, “Langevin analysis of eternal inflation,” *Phys.Rev.* **D72** (2005) 043507, [arXiv:hep-th/0503063](#) [hep-th].
- [331] K. E. Kunze, “Perturbations in stochastic inflation,” *JCAP* **0607** (2006) 014, [arXiv:astro-ph/0603575](#) [astro-ph].
- [332] J. Garcia-Bellido and A. D. Linde, “Stationarity of inflation and predictions of quantum cosmology,” *Phys.Rev.* **D51** (1995) 429–443, [arXiv:hep-th/9408023](#) [hep-th].
- [333] A. Vilenkin, “Making predictions in eternally inflating universe,” *Phys.Rev.* **D52** (1995) 3365–3374, [arXiv:gr-qc/9505031](#) [gr-qc].
- [334] H. Risken, *The Fokker-Planck Equation*, vol. 18. Springer Series in Synergetics, 1984.
- [335] F. Finelli, G. Marozzi, A. Starobinsky, G. Vacca, and G. Venturi, “Stochastic growth of quantum fluctuations during inflation,” *AIP Conf.Proc.* **1446** (2010) 320–332, [arXiv:1102.0216](#) [hep-th].
- [336] K. A. Malik, “Gauge-invariant perturbations at second order: Multiple scalar fields on large scales,” *JCAP* **0511** (2005) 005, [arXiv:astro-ph/0506532](#) [astro-ph].
- [337] K. A. Malik and D. Wands, “Evolution of second-order cosmological perturbations,” *Class.Quant.Grav.* **21** (2004) L65–L72, [arXiv:astro-ph/0307055](#) [astro-ph].
- [338] H. Noh and J.-c. Hwang, “Second-order perturbations of the friedmann world model,” [arXiv:astro-ph/0305123](#) [astro-ph].
- [339] D. Wands, K. A. Malik, D. H. Lyth, and A. R. Liddle, “A New approach to the evolution of cosmological perturbations on large scales,” *Phys.Rev.* **D62** (2000) 043527, [arXiv:astro-ph/0003278](#) [astro-ph].
- [340] F. Finelli, G. Marozzi, G. Vacca, and G. Venturi, “Energy momentum tensor of cosmological fluctuations during inflation,” *Phys.Rev.* **D69** (2004) 123508, [arXiv:gr-qc/0310086](#) [gr-qc].
- [341] G. Marozzi, “Back-reaction of Cosmological Fluctuations during Power-Law Inflation,” *Phys.Rev.* **D76** (2007) 043504, [arXiv:gr-qc/0612148](#) [gr-qc].
- [342] K. A. Malik, “A not so short note on the Klein-Gordon equation at second order,” *JCAP* **0703** (2007) 004, [arXiv:astro-ph/0610864](#) [astro-ph].
- [343] K. A. Malik and D. Wands, “Cosmological perturbations,” *Phys.Rept.* **475** (2009) 1–51, [arXiv:0809.4944](#) [astro-ph].
- [344] K. A. Malik and D. R. Matravers, “A Concise Introduction to Perturbation Theory in Cosmology,” *Class.Quant.Grav.* **25** (2008) 193001, [arXiv:0804.3276](#) [astro-ph].

- [345] I. Huston and K. A. Malik, “Numerical calculation of second order perturbations,” *JCAP* **0909** (2009) 019, [arXiv:0907.2917 \[astro-ph.CO\]](#).
- [346] I. Huston and K. A. Malik, “Second Order Perturbations During Inflation Beyond Slow-roll,” *JCAP* **1110** (2011) 029, [arXiv:1103.0912 \[astro-ph.CO\]](#).
- [347] F. Kuhnel and D. J. Schwarz, “Stochastic Inflation and Dimensional Reduction,” *Phys.Rev.* **D78** (2008) 103501, [arXiv:0805.1998 \[gr-qc\]](#).
- [348] F. Kuhnel and D. J. Schwarz, “Stochastic Inflation and Replica Field Theory,” *Phys.Rev.* **D79** (2009) 044009, [arXiv:0810.5686 \[gr-qc\]](#).
- [349] F. Kuhnel and D. J. Schwarz, “Large-Scale Suppression from Stochastic Inflation,” *Phys.Rev.Lett.* **105** (2010) 211302, [arXiv:1003.3014 \[hep-ph\]](#).
- [350] T. Fujita, M. Kawasaki, Y. Tada, and T. Takesako, “A new algorithm for calculating the curvature perturbations in stochastic inflation,” *JCAP* **1312** (2013) 036, [arXiv:1308.4754 \[astro-ph.CO\]](#).
- [351] T. Fujita, M. Kawasaki, and Y. Tada, “Non-perturbative approach for curvature perturbations in stochastic- $\delta N$  formalism,” [arXiv:1405.2187 \[astro-ph.CO\]](#).
- [352] A. A. Starobinsky, “Multicomponent de Sitter (Inflationary) Stages and the Generation of Perturbations,” *JETP Lett.* **42** (1985) 152–155.
- [353] M. Sasaki and E. D. Stewart, “A General analytic formula for the spectral index of the density perturbations produced during inflation,” *Prog.Theor.Phys.* **95** (1996) 71–78, [arXiv:astro-ph/9507001 \[astro-ph\]](#).
- [354] M. Sasaki and T. Tanaka, “Superhorizon scale dynamics of multiscalar inflation,” *Prog.Theor.Phys.* **99** (1998) 763–782, [arXiv:gr-qc/9801017 \[gr-qc\]](#).
- [355] D. H. Lyth, K. A. Malik, and M. Sasaki, “A General proof of the conservation of the curvature perturbation,” *JCAP* **0505** (2005) 004, [arXiv:astro-ph/0411220 \[astro-ph\]](#).
- [356] D. H. Lyth and Y. Rodriguez, “The Inflationary prediction for primordial non-Gaussianity,” *Phys.Rev.Lett.* **95** (2005) 121302, [arXiv:astro-ph/0504045 \[astro-ph\]](#).
- [357] P. Creminelli and M. Zaldarriaga, “Single field consistency relation for the 3-point function,” *JCAP* **0410** (2004) 006, [arXiv:astro-ph/0407059 \[astro-ph\]](#).
- [358] D. H. Lyth and D. Wands, “Conserved cosmological perturbations,” *Phys.Rev.* **D68** (2003) 103515, [arXiv:astro-ph/0306498 \[astro-ph\]](#).
- [359] J. Garcia-Bellido, “Flat direction MSSM (A-term) inflation,” *AIP Conf.Proc.* **878** (2006) 277–283, [arXiv:hep-ph/0610152 \[hep-ph\]](#).
- [360] R. Allahverdi, “MSSM flat direction inflation,” *eConf* **C0605151** (2006) 0020, [arXiv:hep-ph/0610180 \[hep-ph\]](#).
- [361] D. H. Lyth, “MSSM inflation,” *JCAP* **0704** (2007) 006, [arXiv:hep-ph/0605283](#)

- [hep-ph].
- [362] R. Allahverdi and A. Mazumdar, “Spectral tilt in A-term inflation,” [arXiv:hep-ph/0610069](#) [hep-ph].
- [363] R. Allahverdi, B. Dutta, and A. Mazumdar, “Probing the parameter space for an MSSM inflation and the neutralino dark matter,” *Phys.Rev.* **D75** (2007) 075018, [arXiv:hep-ph/0702112](#) [HEP-PH].
- [364] K. Enqvist, L. Mether, and S. Nurmi, “Supergravity origin of the MSSM inflation,” *JCAP* **0711** (2007) 014, [arXiv:0706.2355](#) [hep-th].
- [365] R. Allahverdi, B. Dutta, and A. Mazumdar, “Attraction towards an inflection point inflation,” *Phys.Rev.* **D78** (2008) 063507, [arXiv:0806.4557](#) [hep-ph].
- [366] K. Kamada and J. Yokoyama, “On the realization of the MSSM inflation,” *Prog.Theor.Phys.* **122** (2010) 969–986, [arXiv:0906.3402](#) [hep-ph].
- [367] R. Allahverdi, B. Dutta, and Y. Santoso, “MSSM inflation, dark matter, and the LHC,” *Phys.Rev.* **D82** (2010) 035012, [arXiv:1004.2741](#) [hep-ph].
- [368] K. Enqvist, A. Mazumdar, and P. Stephens, “Inflection point inflation within supersymmetry,” *JCAP* **1006** (2010) 020, [arXiv:1004.3724](#) [hep-ph].
- [369] K. Kohri and C.-M. Lin, “Hilltop Supernatural Inflation and Gravitino Problem,” *JCAP* **1011** (2010) 010, [arXiv:1008.3200](#) [hep-ph].
- [370] S. Choudhury and A. Mazumdar, “An accurate bound on tensor-to-scalar ratio and the scale of inflation,” *Nucl.Phys.* **B882** (2014) 386–396, [arXiv:1306.4496](#) [hep-ph].
- [371] R. K. Jain, P. Chingangbam, J.-O. Gong, L. Sriramkumar, and T. Souradeep, “Punctuated inflation and the low CMB multipoles,” *JCAP* **0901** (2009) 009, [arXiv:0809.3915](#) [astro-ph].
- [372] R. K. Jain, P. Chingangbam, L. Sriramkumar, and T. Souradeep, “The tensor-to-scalar ratio in punctuated inflation,” *Phys.Rev.* **D82** (2010) 023509, [arXiv:0904.2518](#) [astro-ph.CO].
- [373] D. A. Lowe and S. Roy, “Punctuated eternal inflation via AdS/CFT,” *Phys.Rev.* **D82** (2010) 063508, [arXiv:1004.1402](#) [hep-th].
- [374] A. D. Linde, “Hybrid inflation,” *Phys.Rev.* **D49** (1994) 748–754, [arXiv:astro-ph/9307002](#) [astro-ph].
- [375] L. Covi, “Models of inflation, supersymmetry breaking and observational constraints,” [arXiv:hep-ph/0012245](#) [hep-ph].
- [376] A. D. Linde, “Axions in inflationary cosmology,” *Phys. Lett.* **B259** (1991) 38–47.
- [377] C. Panagiotakopoulos, “Hybrid inflation and supergravity,” [arXiv:hep-ph/0011261](#) [hep-ph].
- [378] G. Lazarides, “Supersymmetric hybrid inflation,” [arXiv:hep-ph/0011130](#) [hep-ph].

- [379] G. Dvali and S. H. Tye, “Brane inflation,” *Phys.Lett.* **B450** (1999) 72–82, [arXiv:hep-ph/9812483](#) [hep-ph].
- [380] R. Maartens, D. Wands, B. A. Bassett, and I. Heard, “Chaotic inflation on the brane,” *Phys.Rev.* **D62** (2000) 041301, [arXiv:hep-ph/9912464](#) [hep-ph].
- [381] S. H. Alexander, “Inflation from D - anti-D-brane annihilation,” *Phys.Rev.* **D65** (2002) 023507, [arXiv:hep-th/0105032](#) [hep-th].
- [382] N. T. Jones, H. Stoica, and S. H. Tye, “Brane interaction as the origin of inflation,” *JHEP* **0207** (2002) 051, [arXiv:hep-th/0203163](#) [hep-th].
- [383] C. Armendariz-Picon, T. Damour, and V. F. Mukhanov, “k - inflation,” *Phys.Lett.* **B458** (1999) 209–218, [arXiv:hep-th/9904075](#) [hep-th].
- [384] J. Garriga and V. F. Mukhanov, “Perturbations in k-inflation,” *Phys.Lett.* **B458** (1999) 219–225, [arXiv:hep-th/9904176](#) [hep-th].
- [385] I. Gihman and A. Skorohod, *Stochastic Differential Equations*. p.108, Springer Verlag, Berlin Heidelberg New York, 1972.
- [386] K. Itô, “Stochastic integral,” *Proceedings of the Imperial Academy* **20** (1944) no. 8, 519–524. <http://dx.doi.org/10.3792/pia/1195572786>.
- [387] R. W. Butler, *Saddlepoint approximations and applications*. Cambridge University Press, 2007.
- [388] L. Smolin, “Gravitational Radiative Corrections as the Origin of Spontaneous Symmetry Breaking!,” *Phys.Lett.* **B93** (1980) 95.
- [389] A. D. Linde, “Chaotic Inflation With Constrained Fields,” *Phys.Lett.* **B202** (1988) 194.
- [390] Y. Watanabe, “ $\delta N$  versus covariant perturbative approach to non-Gaussianity outside the horizon in multifield inflation,” *Phys.Rev.* **D85** (2012) 103505, [arXiv:1110.2462](#) [astro-ph.CO].
- [391] T. Tanaka, T. Suyama, and S. Yokoyama, “Use of delta N formalism - Difficulties in generating large local-type non-Gaussianity during inflation -,” *Class.Quant.Grav.* **27** (2010) 124003, [arXiv:1003.5057](#) [astro-ph.CO].
- [392] C. Burgess, M. Majumdar, D. Nolte, F. Quevedo, G. Rajesh, *et al.*, “The Inflationary brane anti-brane universe,” *JHEP* **0107** (2001) 047, [arXiv:hep-th/0105204](#) [hep-th].
- [393] S. Kachru, R. Kallosh, A. D. Linde, J. M. Maldacena, L. P. McAllister, *et al.*, “Towards inflation in string theory,” *JCAP* **0310** (2003) 013, [arXiv:hep-th/0308055](#) [hep-th].
- [394] E. Silverstein and D. Tong, “Scalar speed limits and cosmology: Acceleration from D-celeration,” *Phys.Rev.* **D70** (2004) 103505, [arXiv:hep-th/0310221](#) [hep-th].
- [395] M. Alishahiha, E. Silverstein, and D. Tong, “DBI in the sky,” *Phys.Rev.* **D70** (2004) 123505, [arXiv:hep-th/0404084](#) [hep-th].
- [396] D. Baumann, A. Dymarsky, I. R. Klebanov, J. M. Maldacena, L. P. McAllister, *et al.*,

- “On D3-brane Potentials in Compactifications with Fluxes and Wrapped D-branes,” *JHEP* **0611** (2006) 031, [arXiv:hep-th/0607050](#) [[hep-th](#)].
- [397] D. Baumann, A. Dymarsky, I. R. Klebanov, L. McAllister, and P. J. Steinhardt, “A Delicate universe,” *Phys.Rev.Lett.* **99** (2007) 141601, [arXiv:0705.3837](#) [[hep-th](#)].
- [398] D. Baumann, A. Dymarsky, I. R. Klebanov, and L. McAllister, “Towards an Explicit Model of D-brane Inflation,” *JCAP* **0801** (2008) 024, [arXiv:0706.0360](#) [[hep-th](#)].
- [399] A. Krause and E. Pajer, “Chasing brane inflation in string-theory,” *JCAP* **0807** (2008) 023, [arXiv:0705.4682](#) [[hep-th](#)].
- [400] E. Pajer, “Inflation at the Tip,” *JCAP* **0804** (2008) 031, [arXiv:0802.2916](#) [[hep-th](#)].
- [401] D. Baumann, A. Dymarsky, S. Kachru, I. R. Klebanov, and L. McAllister, “Holographic Systematics of D-brane Inflation,” *JHEP* **0903** (2009) 093, [arXiv:0808.2811](#) [[hep-th](#)].
- [402] X. Chen, S. Sarangi, S.-H. Henry Tye, and J. Xu, “Is brane inflation eternal?,” *JCAP* **0611** (2006) 015, [arXiv:hep-th/0608082](#) [[hep-th](#)].
- [403] F. Helmer and S. Winitzki, “Self-reproduction in k-inflation,” *Phys.Rev.* **D74** (2006) 063528, [arXiv:gr-qc/0608019](#) [[gr-qc](#)].
- [404] A. J. Tolley and M. Wyman, “Stochastic Inflation Revisited: Non-Slow Roll Statistics and DBI Inflation,” *JCAP* **0804** (2008) 028, [arXiv:0801.1854](#) [[hep-th](#)].
- [405] L. Lorenz, J. Martin, and J. Yokoyama, “Geometrically Consistent Approach to Stochastic DBI Inflation,” *Phys.Rev.* **D82** (2010) 023515, [arXiv:1004.3734](#) [[hep-th](#)].
- [406] C. Cheung, P. Creminelli, A. L. Fitzpatrick, J. Kaplan, and L. Senatore, “The Effective Field Theory of Inflation,” *JHEP* **0803** (2008) 014, [arXiv:0709.0293](#) [[hep-th](#)].
- [407] A. Nicolis, R. Rattazzi, and E. Trincherini, “The Galileon as a local modification of gravity,” *Phys.Rev.* **D79** (2009) 064036, [arXiv:0811.2197](#) [[hep-th](#)].
- [408] S. Das, K. Lochan, S. Sahu, and T. Singh, “Quantum to Classical Transition of Inflationary Perturbations - Continuous Spontaneous Localization as a Possible Mechanism -,” *Phys.Rev.* **D88** (2013) 085020, [arXiv:1304.5094](#) [[astro-ph.CO](#)].
- [409] S. Dodelson, “How much can we learn about the physics of inflation?,” *Phys.Rev.Lett.* **112** (2014) 191301, [arXiv:1403.6310](#) [[astro-ph.CO](#)].
- [410] G. W. Pettinari, C. Fidler, R. Crittenden, K. Koyama, A. Lewis, *et al.*, “Impact of polarisation on the intrinsic CMB bispectrum,” [arXiv:1406.2981](#) [[astro-ph.CO](#)].
- [411] I. Ogburn, R.W., P. Ade, R. Aikin, M. Amiri, S. Benton, *et al.*, “BICEP2 and Keck Array operational overview and status of observations,” [arXiv:1208.0638](#) [[astro-ph.IM](#)].
- [412] C. Kiefer, “Origin of classical structure from inflation,” *Nucl.Phys.Proc.Suppl.* **88** (2000) 255–258, [arXiv:astro-ph/0006252](#) [[astro-ph](#)].
- [413] C. Kiefer and D. Polarski, “Emergence of classicality for primordial fluctuations:

- Concepts and analogies,” *Annalen Phys.* **7** (1998) 137–158, [arXiv:gr-qc/9805014](#) [[gr-qc](#)].
- [414] S. L. Adler, “Why decoherence has not solved the measurement problem: A Response to P. W. Anderson,” *Stud.Hist.Philos.Mod.Phys.* **34** (2003) 135–142, [arXiv:quant-ph/0112095](#) [[quant-ph](#)].
- [415] M. Schlosshauer, “Decoherence, the measurement problem, and interpretations of quantum mechanics,” *Rev.Mod.Phys.* **76** (2004) 1267–1305, [arXiv:quant-ph/0312059](#) [[quant-ph](#)].
- [416] Y. Nomura, “Physical Theories, Eternal Inflation, and Quantum Universe,” *JHEP* **1111** (2011) 063, [arXiv:1104.2324](#) [[hep-th](#)].
- [417] Y. Nomura, “Quantum Mechanics, Spacetime Locality, and Gravity,” *Found.Phys.* **43** (2013) 978–1007, [arXiv:1110.4630](#) [[hep-th](#)].
- [418] R. Bousso and L. Susskind, “The Multiverse Interpretation of Quantum Mechanics,” *Phys.Rev.* **D85** (2012) 045007, [arXiv:1105.3796](#) [[hep-th](#)].
- [419] C. A. Fuchs, “Quantum Mechanics as Quantum Information (and only a little more),” [arXiv:quant-ph/0205039](#).
- [420] P. Holland, “The de Broglie-Bohm theory of motion and quantum field theory,” *Phys.Rept.* **224** (1993) 95–150.
- [421] P. Peter, E. Pinho, and N. Pinto-Neto, “Tensor perturbations in quantum cosmological backgrounds,” *JCAP* **0507** (2005) 014, [arXiv:hep-th/0509232](#) [[hep-th](#)].
- [422] P. Peter, E. J. Pinho, and N. Pinto-Neto, “Gravitational wave background in perfect fluid quantum cosmologies,” *Phys. Rev.* **D73** (2006) 104017, [arXiv:gr-qc/0605060](#) [[gr-qc](#)].
- [423] N. Pinto-Neto, G. Santos, and W. Struyve, “Quantum-to-classical transition of primordial cosmological perturbations in de Broglie–Bohm quantum theory,” *Phys.Rev.* **D85** (2012) 083506, [arXiv:1110.1339](#) [[gr-qc](#)].
- [424] P. M. Pearle, “Reduction of the State Vector by a Nonlinear Schrodinger Equation,” *Phys.Rev.* **D13** (1976) 857–868.
- [425] G. Ghirardi, A. Rimini, and T. Weber, “A Unified Dynamics for Micro and MACRO Systems,” *Phys.Rev.* **D34** (1986) 470.
- [426] P. M. Pearle, “Combining Stochastic Dynamical State Vector Reduction With Spontaneous Localization,” *Phys.Rev.* **A39** (1989) 2277–2289.
- [427] L. Diosi, “LOCALIZED SOLUTION OF SIMPLE NONLINEAR QUANTUM LANGEVIN EQUATION,”.
- [428] G. C. Ghirardi, P. M. Pearle, and A. Rimini, “MARKOV PROCESSES IN HILBERT SPACE AND CONTINUOUS SPONTANEOUS LOCALIZATION OF SYSTEMS OF IDENTICAL PARTICLES,” *Phys.Rev.* **A42** (1990) 78–79.
- [429] A. Bassi and G. C. Ghirardi, “Dynamical reduction models,” *Phys.Rept.* **379** (2003) 257,

- [arXiv:quant-ph/0302164](#) [quant-ph].
- [430] S. Weinberg, “Collapse of the State Vector,” [arXiv:1109.6462](#) [quant-ph].
- [431] A. Bassi, K. Lochan, S. Satin, T. P. Singh, and H. Ulbricht, “Models of Wave-function Collapse, Underlying Theories, and Experimental Tests,” [arXiv:1204.4325](#) [quant-ph].



# Compte Rendu Français

*Ce court compte rendu contient une description en langue française des résultats importants obtenus lors de la thèse et présentés dans ce document.*

## 5.1. L'inflation et le Modèle Standard de la Cosmologie

Nous commençons par rappeler les aspects essentiels du modèle standard de la cosmologie. Le modèle du Big Bang chaud décrit avec succès une série d'événements se déroulant dans un univers en expansion, dont la densité d'énergie et la température décroissent au cours du temps depuis une singularité initiale il y a 13.7 milliards d'année. Un certain nombre de questions sont néanmoins laissées en suspens, et nous expliquons comment une phase d'inflation, c'est à dire d'expansion accélérée, permet d'y répondre.

### 5.1.1. L'Univers Homogène

Les observations faites à grandes échelles de la distribution de matière dans l'Univers laissent apparaître que notre Univers est isotrope sur des distances supérieures à  $\sim 100$  Mpc. Ce constat, combiné au principe Copernicien qui suppose que nous n'occupons pas une place spécifique ou "centrale" dans l'Univers, nous amène à considérer un Univers homogène aux grandes échelles. Sous l'hypothèse de cette symétrie, la métrique de l'espace-temps  $ds^2 = g_{\mu\nu}dx^\mu dx^\nu$  est entièrement déterminée par une fonction du temps  $a(t)$  appelée facteur d'échelle, et un paramètre discret  $\mathcal{K} = -1, 0, 1$  qui caractérise la courbure spatiale de l'Univers (ouvert, plat ou fermé). Cette métrique est celle des espaces-temps de Friedmann-Lemaître-Robertson-Walker (FLRW), et elle peut s'écrire [9, 10, 11, 12]

$$ds^2 = -dt^2 + a^2(t) \left[ \frac{dr^2}{1 - \mathcal{K}r^2} + r^2 (d\theta^2 + \sin^2 \theta d\phi^2) \right]. \quad (5.1)$$

Dans cette paramétrisation,  $t$  est le temps cosmique,  $r$  est la coordonnée radiale comobile, et  $\theta$  et  $\phi$  sont des coordonnées angulaires comobiles. A l'intérieur de ces espaces-temps, la distance physique  $L_{\text{phys}}$  séparant deux points, mesurée sur une hypersurface à  $t$  constant, est proportionnelle au facteur d'échelle  $a$ . En pratique, nous avons donc  $L_{\text{phys}} = a(t)L_{\text{com}}$ , où  $L_{\text{com}}$  est la distance comobile, constante pour deux objets au repos dans les coordonnées FLRW. Ainsi, le facteur d'échelle  $a$  définit le niveau global d'expansion (ou de contraction) des hypersurfaces de type espace. Une autre conséquence de la forme de la métrique (5.1) est l'existence d'une relation linéaire entre vitesse et distance, appelée loi de Hubble [13]. En effet, lorsque l'on dérive la relation  $L_{\text{phys}} = a(t)L_{\text{com}}$  par rapport au temps, on obtient

$$v = \frac{dL_{\text{phys}}}{dt} = \frac{\dot{a}}{a} L_{\text{phys}} = H L_{\text{phys}}, \quad (5.2)$$

où nous avons défini le paramètre de Hubble  $H = \dot{a}/a$ . La valeur actuelle de  $H$ , souvent dénotée  $H_0$ , a été mesurée [15] autour de 67 km/sec/Mpc.

Dans le cadre de la relativité générale, la dynamique des espaces-temps est décrite par l'action de Einstein-Hilbert [22, 23, 24],

$$\mathcal{S} = \mathcal{S}_{\text{grav}} + \mathcal{S}_{\text{mat}} = \frac{1}{2\kappa} \int d^4x \sqrt{-g} (R - 2\Lambda) + \mathcal{S}_{\text{mat}}. \quad (5.3)$$

Dans cette expression,  $\kappa \equiv 8\pi G = 1/M_{\text{Pl}}^2$  où  $G$  est la constante de Newton et  $M_{\text{Pl}}$  est la masse de Planck réduite  $M_{\text{Pl}} \simeq 2.4 \times 10^{18}$  GeV. La partie gravitationnelle de l'action  $\mathcal{S}_{\text{grav}}$  fait intervenir une constante cosmologique éventuelle  $\Lambda$ , le déterminant  $g$  de la métrique  $g_{\mu\nu}$  et la courbure de Ricci  $R$  associée à la métrique. La partie de matière  $\mathcal{S}_{\text{mat}}$  contient tous les champs du modèle standard de la physique des particules et de ses extensions éventuelles. Sa forme exacte est donc en général relativement complexe. Néanmoins, dans la limite où le constituant dominant (en terme de densité d'énergie) est un fluide parfait homogène, son expression peut être largement simplifiée et la variation de l'action (5.3) par rapport aux composantes de la métrique  $g_{\mu\nu}$  donne lieu à deux équations dynamiques,

$$H^2 = \frac{\kappa}{3}\rho - \frac{\mathcal{K}}{a^2} + \frac{\Lambda}{3}, \quad (5.4)$$

$$\frac{\ddot{a}}{a} = -\frac{\kappa}{6}(\rho + 3p) + \frac{\Lambda}{3}, \quad (5.5)$$

où  $\rho$  et  $p$  sont respectivement la densité d'énergie et la pression du fluide parfait. La première de ces équations s'appelle équation de Friedmann [25] et relie le taux d'expansion de l'Univers à sa densité d'énergie, sa courbure spatiale et la valeur de la constante cosmologique. La deuxième équation s'appelle équation de Raychaudhuri [26] et relie son accélération à une combinaison de la densité d'énergie et de la pression, ainsi qu'à la valeur de la constante cosmologique. Lorsque l'on combine ces deux relations, on obtient l'équation de continuité<sup>1</sup>

$$\dot{\rho} + 3H(\rho + p) = 0. \quad (5.6)$$

De façon heuristique, cette équation peut être comprise comme étant une traduction de la première loi de la thermodynamique,  $dU = -pdV$ , avec  $U = \rho V$  and  $V = a^3$ .

### 5.1.2. Le Modèle du Big Bang Chaud et ses Problèmes

Nous venons d'établir que pour un Univers homogène et isotrope, la Relativité Générale décrit un espace-temps en expansion, le taux d'expansion et son accélération étant reliés au contenu en matière de l'Univers, à sa courbure et à une éventuelle constante cosmologique. Cela implique qu'en remontant le temps et en regardant dans le passé, l'Univers est de plus en plus contracté, les densités d'énergie sont de plus en plus importantes, jusqu'à une singularité initiale où  $a = 0$ . Pour un univers principalement constitué de matière froide et de rayonnement, ces considérations donnent lieu au modèle dit du Big Bang chaud, dans lequel les éléments constitutifs de la matière baryonique aujourd'hui s'assemblent peu à peu, au fur et à mesure que les énergies en jeu diminuent et permettent leur existence stable, et les grandes structures de l'Univers (galaxies, amas, filaments, ...) se forment et croissent par instabilité gravitationnelle.

<sup>1</sup>L'équation de continuité s'obtient également à partir de la relation de conservation  $\nabla_\mu T^{\mu\nu} = 0$ , ce qui une conséquence des identités de Bianchi.

Néanmoins, ce scénario pose un certain nombre de questions appelés “problèmes” du modèle du Big Bang chaud. Ce ne sont pas des problèmes d'impossibilité pure à proprement parler, mais ils montrent que le modèle du Big Bang chaud repose en fait sur des hypothèses très fortes concernant ses conditions initiales, qui doivent être finement réglées autour de configurations peu “naturelles” pour pouvoir expliquer les propriétés de l'Univers telles que nous les observons aujourd'hui.

Le premier de ces problèmes est celui dit de l'horizon [88, 89]. Une des propriétés fondamentales des espaces-temps décrits plus haut est le fait qu'ils sont dotés d'horizon causaux, c'est à dire de frontières séparant les événements observables des événements non observables, définis relativement à un observateur. Par causalité, aucun processus physique ne peut agir sur des distances plus grandes que l'horizon, et l'on s'attend donc à ce que l'Univers soit relativement inhomogène sur ces échelles. Cette hypothèse naturelle est en contradiction avec les observations, qui mettent en évidence un Univers redoutablement homogène sur des échelles qui, sous l'hypothèse du modèle standard du Big Bang chaud, devraient être bien plus étendues que l'horizon. Le modèle du Big Bang chaud suppose donc pour commencer que l'Univers ait été initialement parfaitement homogène, y compris au delà de son horizon causal.

Le deuxième problème est celui de la platitude [92, 93], qui se pose à partir des mesures actuelles de la courbure spatiale de l'Univers. Ces observations sont compatibles avec l'hypothèse d'un univers parfaitement plat, et contraignent en tout état de cause la courbure spatiale à des niveaux extrêmement faibles. Or, dans un Univers dominé par de la matière froide ou du rayonnement, la déviation à un Univers plat ne peut qu'augmenter avec le temps. Par conséquent, si l'Univers actuel est redoutablement plat, cela implique qu'il l'était encore bien davantage dans le passé. Malheureusement, il n'y a aucune raison qui explique a priori que la courbure ait été initialement si faible. Là aussi, le modèle du Big Bang chaud suppose le réglage ultra-fin d'un paramètre (la courbure) à une valeur initiale minuscule.

Finalement, le troisième problème, plus spéculatif, est celui des monopôles [101, 102, 99, 100], qui sont des défauts topologiques pouvant apparaître notamment lors de la transition de phase entre une théorie de grande unification et la symétrie de jauge du modèle standard  $SU(3) \times SU(2) \times U(1)$ . Ces transitions se produisent à une échelle d'énergie de l'ordre de  $M_{\text{GUT}} \simeq 10^{16}$  GeV, et donnent lieu à la production de monopôles magnétiques qui devraient perdurer jusqu'à l'heure actuelle. Lorsqu'on la calcule dans le cadre du modèle standard du Big Bang chaud, la densité de ces monopôles aujourd'hui devrait être colossale, en fait, ils devraient même dominer le contenu énergétique de l'Univers actuel. Ce n'est clairement pas le cas. Des recherches pour leur détection ont même été menées et des contraintes très importantes [103, 104, 105, 106, 107, 108] sur leur densité ont pu être dérivées (typiquement, moins de 1 monopôle par  $\sim 10^{30}$  nucléon). Ce troisième problème est bien entendu plus délicat à cerner, car il met en jeu de la physique au delà du modèle standard.

### 5.1.3. L'Inflation Cosmologique

Dans la section précédente, nous avons vu que le modèle standard du Big Bang chaud, dans lequel l'Univers est principalement constitué de matière froide et de rayonnement, souffre d'hypothèses très fortes et peu naturelles concernant ses conditions initiales et sur lesquelles il repose. Un remède possible est de supposer qu'une phase initiale d'accélération de l'expansion (c'est à dire lors de laquelle  $\ddot{a} > 0$ ), a eu lieu dans l'Univers primordial [90, 91]. C'est ce que l'on appelle l'inflation cosmologique [114, 116, 118, 119].

L'équation de Raychaudhuri (5.5) nous indique que pour avoir  $\ddot{a} > 0$ , en l'absence de constante cosmologique, la quantité  $\rho + 3p$  doit être négative. Puisque la densité d'énergie  $\rho$  est toujours positive, la pression doit donc être, a fortiori, négative. Bien entendu, la question est de savoir quel système physique est susceptible de générer une telle pression négative. Ce qui rend l'idée inflationnaire relativement attractive est le fait que le système physique le plus simple compatible avec les symétries du problème, à savoir un champ scalaire homogène  $\phi$  minimalement couplé à la gravité, permet de réaliser cette condition. La partie de matière  $\mathcal{S}_{\text{mat}}$  de l'action pour un tel champ est donnée par

$$S_\phi = - \int d^4x \sqrt{-g} \left[ \frac{1}{2} g^{\mu\nu} \partial_\mu \phi \partial_\nu \phi + V(\phi) \right], \quad (5.7)$$

où  $V(\phi)$  est un terme potentiel que nous ne spécifions pas pour le moment. En effet, la nature physique du champ  $\phi$ , dénommé inflaton, et ses relations avec les autres champs du modèle standard de la physique des particules n'a toujours pas été établi et bon nombre de candidats ont été proposés et sont étudiés à l'heure actuelle. Il est intéressant de noter que l'action écrite plus haut peut être vue comme celle d'un fluide parfait, dont la densité d'énergie et la pression sont respectivement données par

$$\rho = \frac{\dot{\phi}^2}{2} + V, \quad (5.8)$$

$$p = \frac{\dot{\phi}^2}{2} - V. \quad (5.9)$$

Une conséquence directe de ce résultat est le fait que la condition d'accélération de l'expansion,  $\rho + 3p < 0$ , est remplie dès lors que  $V > \dot{\phi}^2$ . Cela implique qu'une phase d'inflation peut être obtenue lorsque l'inflaton descend lentement le long de son potentiel, suffisamment lentement pour que son énergie potentielle dépasse le double de son énergie cinétique. Son potentiel doit donc être suffisamment plat, ce qui n'est pas toujours facile à réaliser en pratique.

## 5.2. Prédiction Inflationnaires et Observations en Données Massives

Nous entrons à présent dans la description résumée des principaux résultats obtenus lors de cette thèse. La cosmologie moderne est entrée dans une "ère de précision" avec l'arrivée de données astrophysiques massives, en particulier celles concernant le fond diffus cosmologique (FDC). Notamment, au cours de cette thèse, le satellite Planck a publié des mesures sans précédent des fluctuations primordiales de température du FDC. D'un autre côté, comme nous venons de le mentionner, de nombreux candidats à l'inflation ont été proposés jusqu'à aujourd'hui et il reste a priori difficile de déterminer lesquels sont favorisés par les observations. Un des objectifs de cette thèse a donc été de développer les méthodes et les outils permettant une approche systématique de ce problème, et menant à un changement d'échelle à la fois dans la prise en compte des données et dans le nombre de modèles traités.

### 5.2.1. Roulement Lent et Flot de Hubble

Une des manières d'aborder la question est d'utiliser des approches indépendantes du modèle inflationnaire. Dans la Ref. [208] (section 3.1), nous nous sommes intéressés à l'une d'entre elles, le "flot de Hubble". Dans cette paramétrisation, la hiérarchie des paramètres de roulement lent

est tronquée à un certain ordre  $M$ , c'est à dire que l'ensemble des paramètres d'ordre supérieur à  $M$  sont pris comme identiquement nuls. L'évolution des paramètres restants est intégrée numériquement à partir de conditions initiales tirées au hasard dans des intervalles prédéfinis, et en utilisant l'inflaton  $\phi$  lui-même comme variable temporelle. Le même processus est réitéré pour différentes conditions initiales, et ce un grand nombre de fois. De cette manière, on cherche à dériver des prédictions typiques pour l'inflation, ne reposant pas sur une forme explicite du potentiel mais ayant une portée "générique".

Nous avons montré qu'une telle approche comporte en réalité un certain nombre de biais. Premièrement, puisque les paramètres de roulement lent sont reliés à une fonction de Hubble  $H(\phi)$  et à ses dérivées successives, tronquer leur hiérarchie à un ordre  $M$  revient à imposer une forme polynomiale pour  $H(\phi)$ , d'ordre  $M + 1$ . Dans la mesure où  $V$  et  $H$  sont explicitement reliés via la relation  $V = 3M_{\text{Pl}}^2 H^2 - 2M_{\text{Pl}}^4 H'^2$  (où un prime signifie une dérivation par rapport à l'inflaton  $\phi$ ), une famille spécifique de potentiels est en fait implicitement étudiée par l'approche du flot de Hubble. Ces potentiels sont des polynômes d'ordre  $2M + 2$  dans le champ scalaire  $\phi$ , avec certaines relations imposées entre les coefficients. Nous avons étudié cette famille de potentiels et nous avons montré qu'elle est directement responsable des prédictions soit-disant "génériques" qui semblaient avoir été dérivées dans la littérature. Cette méthode n'est donc pas indépendante du modèle dans la mesure où elle ne permet d'étudier qu'une famille restreinte de potentiels, qui n'ont par ailleurs pas de justification physique et sont purement phénoménologiques.

Ensuite, nous avons établi qu'une fois le potentiel fixé, le flot de Hubble résout la dynamique inflationnaire le long d'une seule trajectoire dans l'espace des phases uniquement. En effet, puisqu'en toute généralité,  $\dot{\phi} = -2M_{\text{Pl}}^2 H'$ , partir d'une fonction  $H(\phi)$  revient à fixer à l'avance la trajectoire inflationnaire. Ceci pose deux types de problèmes. Tout d'abord, cette trajectoire est en général différente de la trajectoire de roulement lent, qui est pourtant un attracteur du système dynamique. Par conséquent, autant cela fait du sens d'étudier l'inflation le long de la trajectoire de roulement lent puisqu'elle est asymptotiquement approchée depuis un large bassin de conditions initiales, autant la trajectoire reliée au flot de Hubble ne jouit pas d'une telle justification physique.<sup>2</sup> Ensuite, à l'intérieur d'un potentiel, il arrive souvent que l'inflation puisse se produire le long de différentes branches, notamment lorsque le potentiel n'est pas une fonction monotone du champ scalaire  $\phi$  (ce qui est courant pour les potentiels décrits par le flot de Hubble et mentionnés plus haut). La trajectoire "imposée" par la fonction  $H(\phi)$  ne permet d'étudier l'inflation que sur l'une de ces branches, ce qui représente un biais supplémentaire dans l'étude de ces potentiels.

Pour l'ensemble de ces raisons, nous avons conclu que le flot de Hubble conduit à une analyse biaisée des dynamiques inflationnaires et de leurs prédictions physiques, et avons donc opté pour une étude systématique de l'ensemble des potentiels inflationnaires proposés dans la littérature, le long des trajectoires de roulement lent.

### 5.2.2. Modèles à un Champ et *Encyclopædia Inflationaris*

Dans la mesure où plusieurs centaines de scénarios inflationnaires ont été proposés dans la littérature, il semble naturel de commencer par étudier les plus simples, à savoir les modèles à un champ scalaire, avec terme cinétique standard, et dont la dynamique satisfait à l'approximation

<sup>2</sup>Dans certains cas, nous avons même montré que les trajectoire reliées au flot de Hubble sont instables dans l'espace des phases.

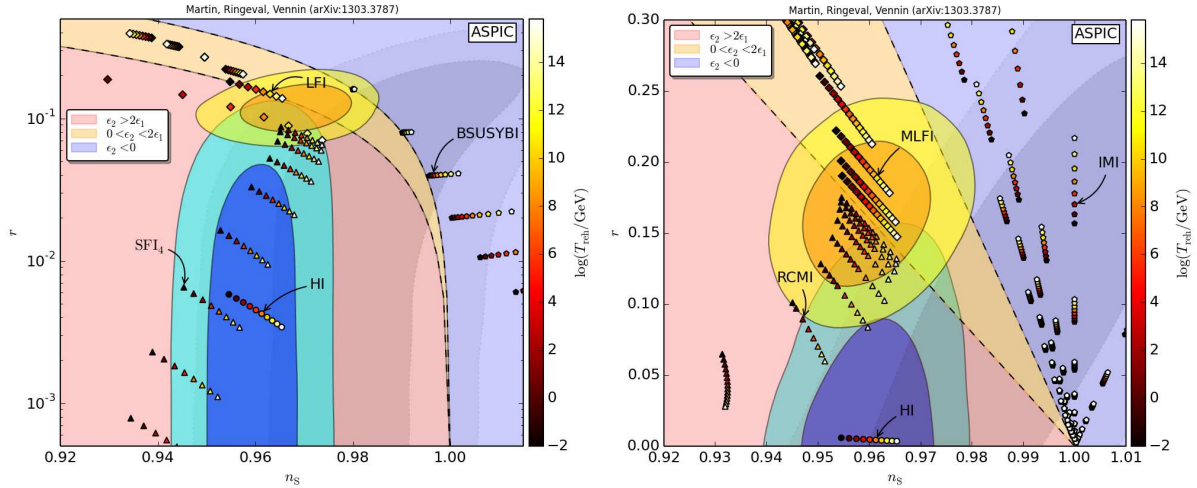


Figure 5.1.: Prédictions de quelques modèles implémentés dans la bibliothèque ASPIC, calculées dans l’approximation du roulement lent et en intégrant de façon cohérente la phase de réchauffement. Ces prédictions sont tracées dans le plan  $(n_s, r)$ , et sont superposées aux contours à un et deux sigma de WMAP9 (en gris), PLANCK (en bleu) et PLANCK+BICEP2 (en jaune). Une loi a priori de Jeffreys a été utilisée pour le premier paramètre de roulement lent dans la figure de gauche, tandis qu’une loi a priori plate a été utilisée dans la figure de droite. Les valeurs annotées représentent le logarithme de l’échelle d’énergie,  $\log(T_{\text{reh}}/\text{GeV})$ , à laquelle une phase de réchauffement dominée par de la matière se termine. La zone rose délimite les modèles pour lesquels l’énergie cinétique et son rapport avec l’énergie totale augmentent, la zone jaune indique les modèles pour lesquels l’énergie cinétique diminue mais son rapport avec l’énergie totale augmente, et la zone violette recouvre les modèles pour lesquels l’énergie cinétique et son rapport avec l’énergie totale diminuent, au moment où les prédictions sont calculées.

du roulement lent. En effet, les extensions à ce cadre minimal (terme cinétique non-standard, présence de champs multiples, sortie transitoire du régime de roulement lent, *etc.*) prédisent souvent la présence de signaux (non-Gaussianités, perturbations entropiques, running, *etc.*) qui n’ont pour l’instant jamais été détectés. C’est pourquoi à ce stade, et tant que les données ne les excluent pas, il semble raisonnable de commencer en abordant les scénarios les moins complexes.

Nous avons recensé environ 75 potentiels appartenant à cette catégorie, pour lesquelles nous avons dérivé les prédictions dans l’approximation du roulement lent, que nous avons présentées dans la Ref. [205], *Encyclopædia Inflationaris* (section 3.2). Nous avons également conçu une bibliothèque numérique publique dénommée ASPIC<sup>3</sup> (pour “Accurate Slow-roll Predictions for Inflationary Cosmology”) qui contient l’ensemble des programmes permettant le calcul numérique des prédictions inflationnaires de ces modèles et leur comparaison aux observations. Ce code libre d’accès est un projet évolutif, et est amené à être complété au fur et à mesure que de nouveaux modèles sont considérés.

Il est important de noter qu’aucune autre approximation que celle du roulement n’a été effectuée dans cette analyse, là où des approximations supplémentaires ont souvent été utilisées dans la littérature. En effet, nous avons montré que la précision actuelle des données est telle que le calcul

<sup>3</sup><http://theory.physics.unige.ch/~ringeval/aspic.html>

des prédictions se doit d’être le plus précis possible, et que ces approximations supplémentaires conduisent souvent à des résultats erronés. La phase de réchauffement a également été prise en compte de façon cohérente, là où la plupart des travaux se contentent de tirer le paramètre  $\Delta N_*$  (représentant le nombre d’ $e$ -folds entre le croisement de l’échelle de pivot des spectres de puissance avec le rayon de Hubble et la fin de l’inflation) dans un intervalle prédéfini. Cette procédure peut conduire à des situations non-physiques où l’énergie à la fin de l’ère de réchauffement est plus élevée que l’énergie à la fin de l’inflation, ou plus faible que l’énergie au moment de la nucléation.

Le détail des prédictions dérivées potentiel par potentiel est présenté dans la section 3.2 et nous ne donnons ici que quelques éléments conclusifs. Une manière de résumer les résultats obtenus est d’utiliser une classification des modèles d’inflation basée sur la variation temporelle des énergies qui leur sont associées et permettant de découper le plan  $(n_s, r)$  (où  $n_s$  est l’indice spectral des perturbations scalaires et  $r$  est l’amplitude du spectre des ondes gravitationnelles normalisé au spectre des perturbations scalaires) en trois zones, représentées sur la figure 5.1. La première zone, en rose, contient les modèles pour lesquels l’énergie cinétique  $\dot{\phi}^2/2$  et le rapport de l’énergie cinétique avec l’énergie totale  $\dot{\phi}^2/2/(V + \dot{\phi}^2/2)$  augmentent au moment où les prédictions sont calculées, c’est à dire lorsque l’échelle pivot des spectres de puissance croise le rayon de Hubble. La deuxième zone, en jaune pâle, recouvre les modèles pour lesquels l’énergie cinétique diminue mais son rapport avec l’énergie totale augmente, tandis que la troisième zone, en bleu, indique les modèles pour lesquels l’énergie cinétique et son rapport avec l’énergie totale diminuent. S’il est clair que les données du satellite WMAP ne sont pas discriminantes vis à vis de cette classification, dans la mesure où des modèles compatibles avec ses mesures existent dans chacune des trois zones, l’apport du satellite PLANCK apparaît clairement dans le fait que ses observations indiquent une nette préférence pour les modèles de la première catégorie. Ces modèles ont des potentiels concaves, soit en forme de “sommet de colline”, soit en forme de “plateau”. Parmi les 75 familles de potentiels que nous avons étudiées, ce sont donc ces potentiels qui semblent être “préférés” par les données (le fait que BICEP2 nous amène à reconsidérer ou non cette affirmation sera discutée plus bas).

Pour aller plus loin que ce simple constat “à l’œil”, pour quantifier précisément cette préférence et pour dégager les tout meilleurs modèles, nous avons ensuite appliqué les méthodes de l’inférence Bayésienne au problème étudié.

### 5.2.3. Inférence Bayésienne et Meilleurs Modèles Inflationnaires selon Planck

Étant donné le nombre important de modèles à traiter (75 familles de potentiels, et près de 200 modèles), il nous faut disposer d’un moyen de quantifier rigoureusement une affirmation du type “le modèle A est meilleur que le modèle B”. Le programme Bayésien de comparaison de modèles répond à ce besoin, et nécessite de calculer l’évidence Bayésienne, c’est à dire l’intégrale de la fonction de vraisemblance sur l’espace des lois a priori, pour chaque modèle. Le rapport entre ces évidences donne le facteur de Bayes, qui représente le degré avec lequel les données ont modifié notre niveau de confiance relative entre les différents modèles. De cette manière, nous pouvons identifier les “meilleurs” (au sens Bayésien du terme) modèles d’inflation.

Dans la Ref. [206] (section 3.3), nous avons donc calculé l’évidence Bayésienne de l’ensemble des modèles implémentés dans la bibliothèque ASPIC. Pour ce faire, nous avons mis au point un bloc de traitement numérique qui réalise l’interface entre une fonction de vraisemblance inflationnaire effective, la bibliothèque ASPIC, et un algorithme d’échantillonnage adaptatif. De

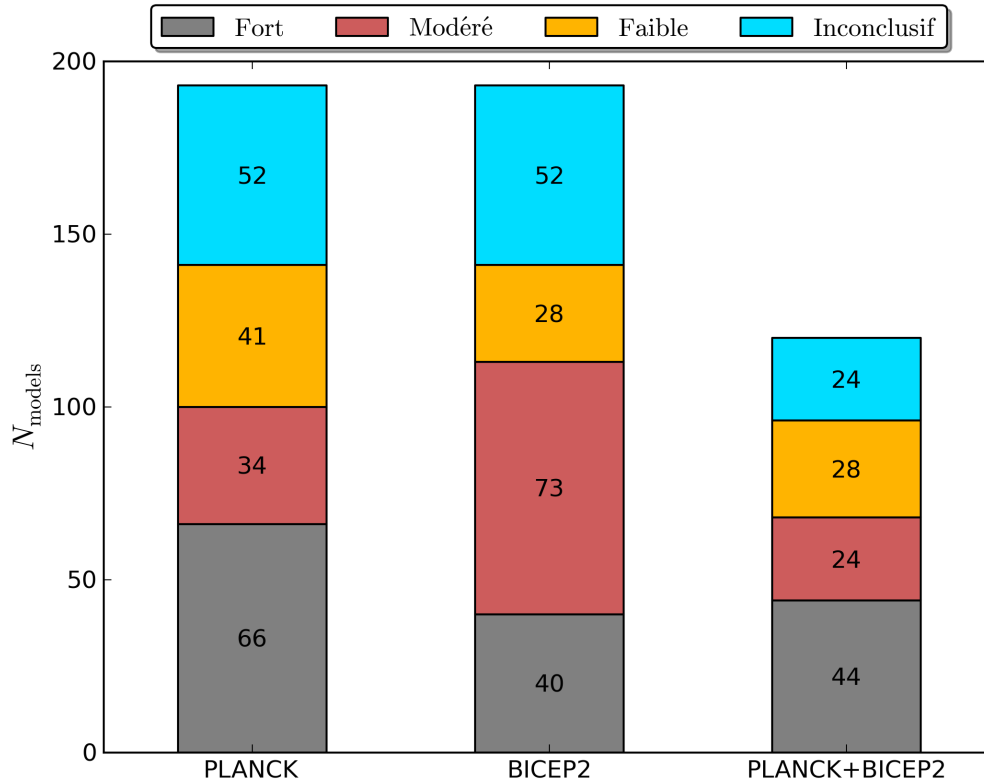


Figure 5.2.: Nombre de modèles inflationnaires dans chaque catégorie de Jeffreys (définies par rapport au meilleur modèle pour chaque expérience) pour les jeux de données PLANCK, BICEP2 et PLANCK+BICEP2. Pour les données de PLANCK et BICEP2 combinées, seuls les modèles n’indiquant pas d’incompatibilité entre PLANCK et BICEP2 sont comptabilisés.

cette manière, nous avons identifié les 26% des modèles qui sont favorisés<sup>4</sup> par les données de PLANCK, ce qui correspond à 15 familles de potentiels. Le détail des effectifs au sein de chaque catégorie de Jeffreys est présenté dans la figure 5.2. En incluant la complexité Bayésienne dans l’analyse, qui permet d’identifier le nombre de paramètres non contraints par les observations et d’estimer ainsi le niveau de complexité superflue, seulement 9% des modèles arrivent en tête, qui correspondent tous à des potentiels ayant une forme de “plateau”. Le détail des résultats est donné dans la section 3.3.

#### 5.2.4. Inflation et Tension entre Planck et BICEP2

Si l’on regarde attentivement la figure 5.1, l’on est en droit de se demander si les mesures de l’expérience BICEP2 ne remettent pas en cause ces conclusions, dans la mesure où la zone

<sup>4</sup>Le terme “favorisé” doit être entendu ici comme appartenant à la zone inconclusive de la classification de Jeffreys, définie relativement au meilleur modèle. L’échelle de Jeffreys permet de qualifier conventionnellement le rapport entre les évidences  $\mathcal{E}_A$  et  $\mathcal{E}_B$  de deux modèles  $A$  et  $B$  selon quatre catégories. Lorsque  $\ln(\mathcal{E}_A/\mathcal{E}_B) < 1$ , la situation est dite “inconclusive”, lorsque  $1 < \ln(\mathcal{E}_A/\mathcal{E}_B) < 2.5$ , la conclusion que le modèle  $A$  est meilleur que le modèle  $B$  est dite “faible”, lorsque  $2.5 < \ln(\mathcal{E}_A/\mathcal{E}_B) < 5$  elle est dite “modérée”, et lorsque  $\ln(\mathcal{E}_A/\mathcal{E}_B) > 5$  elle est dite “forte”.

préférée par la combinaison PLANCK+BICEP2 recouvre à présent certains modèles de la deuxième zone, celle en jaune pâle. Ces modèles correspondent typiquement à des potentiels convexes, s'annulant à leur minimum. D'un autre côté, l'existence d'une possible tension entre PLANCK et BICEP2 a été discutée dans la littérature, ainsi que la question de la correcte prise en compte des avant plans de poussière par BICEP2. En attendant une clarification de cette situation, il s'agit donc d'être prudent lorsque l'on combine ces deux jeux de données.

Dans la Ref. [207] (section 3.4), nous avons donc discuté les conséquences de la détection du mode  $B$  de polarisation dans le FDC par l'expérience BICEP2, si cette détection est confirmée. En particulier, nous avons mené une étude complète dans l'espace des paramètres cosmologiques et des paramètres inflationnaires de roulement lent, en utilisant les données de polarisation de BICEP2 seules. Nous avons ensuite extrait les évidences Bayésiennes et les complexités des  $\sim 200$  modèles que nous avons traités avec PLANCK. De cette manière, nous avons là aussi identifié les meilleurs modèles d'après BICEP2. Cela nous a permis de constater que la liste des modèles préférés par PLANCK et la liste des modèles préférés par BICEP2 sont presque disjointes, ce qui confirme l'existence d'une possible tension entre les deux jeux de données.

Pour aller plus loin, nous avons donc cherché à quantifier cette tension à l'aide d'une mesure Bayésienne de la compatibilité entre PLANCK et BICEP2, définie relativement à chaque modèle. Nous avons ainsi établi que pour les modèles préférés par PLANCK, les deux jeux de données montrent une tendance à l'incompatibilité, alors qu'il y a une indication modérée de compatibilité pour certains des modèles préférés par BICEP2. C'est pourquoi il est en particulier prématuré de tirer des conclusions trop hâtives et définitives concernant les modèles favorisés par PLANCK tels que le modèle de Starobinsky. Pour le sous-ensemble constitué des modèles n'indiquant pas d'incompatibilité, nous avons finalement mis à jour nos calculs d'évidence et de complexité en utilisant la combinaison des deux jeux de données PLANCK+BICEP2. La distribution des modèles au sein des différentes catégories de Jeffreys est présentée dans la figure 5.2 pour BICEP2 seul, et pour la combinaison des données de PLANCK et de BICEP2 où seuls les modèles n'indiquant pas d'incompatibilité entre les deux jeux de données sont dénombrés.

Ce travail ouvre de nombreuses perspectives. Tout d'abord, le projet ASPIC est évolutif, dans le sens qu'il a vocation à être complété par de nouveaux modèles au gré de leur apparition, qu'il peut être étendu à d'autres classes de modèles que celle considérée ici (modèles à un champ scalaire avec terme cinétique standard et dans l'approximation du roulement lent), et qu'il se doit enfin d'intégrer de nouveaux jeux de données au fur et à mesure que ceux-ci sont publiés. Ainsi, dès l'automne 2014, les mesures de polarisation réalisées par le satellite Planck devraient être disponibles, et d'autres expériences viendront bientôt les compléter [174, 411, 178, 177].

L'exploitation des résultats de notre analyse Bayésienne peut également se poursuivre concernant la phase de réchauffement. En effet, comme nous l'avons mentionné, les prédictions inflationnaires sont sensibles à la phase de réchauffement à travers deux quantités, le paramètre d'équation d'état moyen (c'est à dire moyenné sur le nombre d' $e$ -folds)  $\bar{w}_{\text{reh}}$  pendant la phase de réchauffement, et la densité d'énergie  $\rho_{\text{reh}}$  au moment où  $w = 1/3$  et où la phase de radiation commence. Ces deux paramètres décrivent l'expansion réalisée entre la fin de l'inflation et le début de la phase de radiation, et sont contraints par l'analyse Bayésienne que nous avons menée. Nous travaillons actuellement à caractériser précisément ces contraintes pour l'ensemble des modèles implémentés.

Enfin, un problème largement discuté par la communauté à l'heure actuelle est celle des caractéristiques techniques requises pour les prochaines expériences. La question générale est de savoir quel niveau de précision doit être atteint dans les mesures pour permettre une progres-

sion notable de notre niveau de connaissance de l'Univers primordial. En particulier, le niveau de sensibilité en  $r$ , l'amplitude du spectre de puissance des ondes gravitationnelles normalisé au spectre des perturbations scalaires, semble crucial. Notre approche permet de répondre très explicitement à cette question. En effet, en dérivant la vraisemblance effective que nous observons pour un niveau de bruit fixé dans les détecteurs et pour un modèle fiduciel donné, nous pouvons calculer les évidences de chaque modèle de la bibliothèque ASPIC sous ces hypothèses et caractériser ainsi le gain d'information associé sur les modèles d'inflation. Nous menons actuellement cette étude prospective, qui va permettre de quantifier exactement l'apport des futures expériences.

Finalement, on est en droit de se demander si le niveau de précision théorique des approches calculatoires utilisées sera suffisant. En particulier, les résultats présentés ici sont dérivés à partir d'un calcul au premier ou au deuxième ordre dans l'approximation du roulement lent, et il faut établir à quel ordre il sera nécessaire de travailler avec les données des futures expériences. L'étude prospective que nous venons d'évoquer permettra aussi d'étudier cette question en détail.

### 5.2.5. Spectres de Puissance au Deuxième Ordre en Inflation-k

Comme nous venons de l'expliquer, un prolongement possible à ce travail est l'intégration de nouveaux modèles d'inflation, et de nouvelles catégories de modèles. Par exemple, l'inflation-k [383, 384] représente un cadre général décrivant les modèles avec une action effective quadratique pour les perturbations de courbure et une vitesse du son  $c_s$  variable (voir aussi Refs. [406, 407]). Si ces modèles prédisent souvent la production de non-Gaussianités à un niveau exclu par les observations, il reste intéressant de pouvoir les contraindre précisément. C'est pourquoi dans la Ref. [209] (section 3.5), nous avons calculé pour la première fois les spectres de puissance scalaire et tensorielle au deuxième ordre pour l'inflation-k. Techniquement, nous avons utilisé l'approximation uniforme assortie d'un développement au deuxième ordre dans les paramètres de roulement lent et dans les paramètres de flot de la vitesse du son. A titre illustratif, le résultat obtenu pour le spectre de puissance des perturbations de courbure s'écrit

$$\begin{aligned}
 \mathcal{P}_\zeta = & \frac{H_\diamond^2 (18 e^{-3})}{8\pi^2 M_{\text{Pl}}^2 \epsilon_{1\diamond} c_{s\diamond}} \left\{ 1 - 2(1 + D)\epsilon_{1\diamond} - D\epsilon_{2\diamond} + (2 + D)\delta_{1\diamond} + \left(\frac{2}{9} + D + \frac{D^2}{2}\right) \delta_{1\diamond}^2 \right. \\
 & + \left(\frac{37}{18} + 2D + \frac{D^2}{2} - \frac{\pi^2}{24}\right) \delta_{1\diamond}\delta_{2\diamond} + \left(-\frac{8}{9} - 3D - 2D^2\right) \epsilon_{1\diamond}\delta_{1\diamond} + \left(\frac{17}{9} + 2D + 2D^2\right) \epsilon_{1\diamond}^2 \\
 & + \left(\frac{5}{9} - D - D^2\right) \epsilon_{2\diamond}\delta_{1\diamond} + \left(-\frac{11}{9} - D + D^2 + \frac{\pi^2}{12}\right) \epsilon_{1\diamond}\epsilon_{2\diamond} + \left(\frac{2}{9} + \frac{D^2}{2}\right) \epsilon_{2\diamond}^2 \\
 & + \left(\frac{\pi^2}{24} - \frac{1}{18} - \frac{D^2}{2}\right) \epsilon_{2\diamond}\epsilon_{3\diamond} + [-2\epsilon_{1\diamond} - \epsilon_{2\diamond} + \delta_{1\diamond} + (1 + D)\delta_{1\diamond}^2 \\
 & + (2 + D)\delta_{1\diamond}\delta_{2\diamond} - (3 + 4D)\epsilon_{1\diamond}\delta_{1\diamond} + 2(1 + 2D)\epsilon_{1\diamond}^2 - (1 + 2D)\epsilon_{2\diamond}\delta_{1\diamond} - (1 - 2D)\epsilon_{1\diamond}\epsilon_{2\diamond} \\
 & + D\epsilon_{2\diamond}^2 - D\epsilon_{2\diamond}\epsilon_{3\diamond}] \ln \frac{k}{k_\diamond} + \left(2\epsilon_{1\diamond}^2 + \epsilon_{1\diamond}\epsilon_{2\diamond} + \frac{1}{2}\epsilon_{2\diamond}^2 - \frac{1}{2}\epsilon_{2\diamond}\epsilon_{3\diamond} + \frac{1}{2}\delta_{1\diamond}^2 + \frac{1}{2}\delta_{1\diamond}\delta_{2\diamond} \right. \\
 & \left. - 2\epsilon_{1\diamond}\delta_{1\diamond} - \epsilon_{2\diamond}\delta_{1\diamond}\right) \ln^2 \frac{k}{k_\diamond} \left. \right\}, \tag{5.10}
 \end{aligned}$$

où nous avons introduit la quantité  $D$  définie par  $D \equiv 1/3 - \ln 3$ . Les paramètres  $\epsilon_i$  sont les paramètres de roulement lent et les paramètres  $\delta_i$  sont les paramètres de flot de la vitesse du son. La présence du  $\diamond$  en indice indique que les quantités sont calculées au moment où l'échelle

de pivot  $k_\diamond$  croise le rayon de Hubble. Avec les mêmes notations, le spectre de puissance des ondes gravitationnelles est donné par

$$\begin{aligned} \mathcal{P}_h = & \frac{2(18e^{-3})H_\diamond^2}{\pi^2 M_{\text{Pl}}^2} \left\{ 1 - 2(1 + D - \ln c_{\text{so}})\epsilon_{1_\diamond} + \left[ \frac{17}{9} + 2D + 2D^2 + 2\ln^2 c_{\text{so}} \right. \right. \\ & - 2(1 + 2D)\ln c_{\text{so}} \left. \right] \epsilon_{1_\diamond}^2 + \left[ -\frac{19}{9} + \frac{\pi^2}{12} - 2D - D^2 + 2(1 + D)\ln c_{\text{so}} - \ln^2 c_{\text{so}} \right] \epsilon_{1_\diamond}\epsilon_{2_\diamond} \\ & + \left[ -2\epsilon_{1_\diamond} + (2 + 4D - 4\ln c_{\text{so}})\epsilon_{1_\diamond}^2 + (-2 - 2D + 2\ln c_{\text{so}})\epsilon_{1_\diamond}\epsilon_{2_\diamond} \right] \ln \frac{k}{k_\diamond} \\ & \left. + (2\epsilon_{1_\diamond}^2 - \epsilon_{1_\diamond}\epsilon_{2_\diamond}) \ln^2 \frac{k}{k_\diamond} \right\}. \end{aligned} \quad (5.11)$$

Ces deux résultats mettent en évidence qu'à l'ordre dominant dans l'approximation du roulement lent et lorsque  $c_s = 1$ , les spectres de puissances sont invariants d'échelle, c'est à dire qu'ils ne dépendent pas de  $k$ . La dépendance en  $k$  apparaît de façon logarithmique uniquement, et son amplitude dépend des paramètres de roulement lent et des paramètres de flot de la vitesse du son. Les termes correspondants sont en rouge dans les équations (5.10) et (5.11). Dans ce contexte, une expression au "deuxième" ordre en  $\{\epsilon_i, \delta_i\}$  des spectres implique que l'on étende le résultat jusqu'à l'ordre  $\ln^2(k/k_\diamond)$ .

### 5.3. Aspects Quantiques de l'Inflation et Formalisme Stochastique

Sur le plan théorique, un des aspects intéressants de l'inflation est qu'elle permet d'expliquer l'existence de fluctuations cosmologiques et de caractériser leurs propriétés statistiques à partir de considérations quantiques. D'une certaine manière, un tel mécanisme repose à la fois sur la Relativité Générale et sur la Mécanique Quantique, deux théories que l'on sait difficile à combiner, et conduit à des prédictions que l'on peut tester expérimentalement. C'est pourquoi la physique inflationnaire représente un objet d'étude intéressant pour aborder un certain nombre de questions fondamentales.

Dans la description standard des champs en inflation, on considère la plupart du temps que la partie homogène des champs se comporte de façon classique, tandis que les petites déviations à l'homogénéité sont traitées comme des fluctuations quantiques, évoluant sur ce fonds classique. Dans le sens où seule une partie du système est ainsi quantifiée, l'approche standard peut donc être qualifiée de semi-classique.

Le formalisme de l'inflation stochastique [290, 291, 292, 293, 294, 295, 296, 297, 289, 298] permet d'aller au delà et d'incorporer les corrections quantiques à la trajectoire classique. L'idée est de dériver une théorie effective pour les modes scalaires de grandes longueurs d'onde uniquement, en intégrant les modes de petites longueurs d'onde dans l'action du champ scalaire. Les modes de grandes longueurs d'onde sont rassemblés dans un champ filtré  $\varphi$ , que l'on peut définir à partir du champ total  $\phi$  de la manière suivante:

$$\varphi(\mathbf{x}, N) = \int \frac{d^3\mathbf{k}}{(2\pi)^{3/2}} W\left(\frac{k}{\sigma a H}\right) \left[ \phi_{\mathbf{k}}(N) \hat{a}_{\mathbf{k}} e^{i\mathbf{k}\cdot\mathbf{x}} + \phi_{\mathbf{k}}^*(N) \hat{a}_{\mathbf{k}}^\dagger e^{-i\mathbf{k}\cdot\mathbf{x}} \right]. \quad (5.12)$$

Dans cette expression,  $W$  est une fonction de filtrage qui sélectionne les modes de grandes longueurs d'onde, c'est à dire que  $W \simeq 0$  lorsque  $k \gg \sigma a H$  et  $W \simeq 1$  lorsque  $k \ll \sigma a H$ . Le paramètre  $\sigma \ll 1$  est une constante fixant l'échelle à laquelle le lissage a lieu. En écrivant le

champ total comme  $\phi = \varphi + \delta\phi$ , l'idée est donc de dériver une théorie effective pour  $\varphi$  uniquement en intégrant  $\delta\phi$ . On peut alors montrer que les fluctuations quantiques présentes dans le secteur  $\delta\phi$  affectent la dynamique de  $\varphi$  par l'introduction d'un terme de bruit stochastique dans son équation du mouvement. A l'ordre dominant dans l'approximation du roulement lent, celle-ci s'écrit

$$\frac{d\varphi}{dN} = -\frac{V'}{3H^2} + \frac{H}{2\pi}\xi(N). \quad (5.13)$$

Dans cette équation, le premier terme  $-V'/(3H^2)$  est le terme classique standard de l'équation de Klein-Gordon et  $\xi$  est un bruit blanc Gaussien (pour une fonction filtre de Heaviside), telle que  $\langle \xi(N) \rangle = 0$  et  $\langle \xi(N_1)\xi(N_2) \rangle = \delta(N_1 - N_2)$ . L'équation du mouvement pour le champ scalaire devient donc une équation stochastique appelée équation de Langevin. Sa résolution permet de calculer efficacement des effets de pure théorie quantique des champs, comme cela est montré pour différents systèmes dans les Refs. [298, 302, 303, 304, 299, 300, 301]. Dans la section 2.4.3, nous avons notamment montré que l'équation de Langevin permet de calculer la statistique des fluctuations du champ, c'est à dire le spectre de puissance des perturbations scalaires. Plus précisément, nous avons établi que l'intégration exacte de l'équation (5.13) conduit au spectre de puissance des perturbations de courbure

$$\mathcal{P}_\zeta(\phi) = 2 \int_{\phi}^{\hat{\phi}} d\psi \frac{f'^2(\psi)}{f(\phi)} \exp \left[ \frac{24\pi^2 M_{\text{Pl}}^4}{V(\psi)} - \frac{24\pi^2 M_{\text{Pl}}^4}{V(\phi)} \right], \quad (5.14)$$

où  $\mathcal{P}_\zeta(\phi)$  représente le spectre de puissance calculé au mode  $k$  pour lequel la valeur du champ scalaire lorsque  $k$  croise le rayon de Hubble vaut  $\phi$ , et où la fonction  $f(\phi)$  est définie par

$$f(\phi) = -24\pi^2 M_{\text{Pl}}^2 \int_{\phi_{\text{end}}}^{\phi} du \int_{\bar{\phi}}^u \frac{dv}{V(v)} \exp \left\{ 24\pi^2 M_{\text{Pl}}^4 \left[ \frac{1}{V(v)} - \frac{1}{V(u)} \right] \right\}. \quad (5.15)$$

Dans ces deux expressions,  $\hat{\phi}$  et  $\bar{\phi}$  sont des constantes d'intégration qui valent dans la plupart des cas  $\hat{\phi} = \bar{\phi} = \pm\infty$ . A l'ordre dominant dans l'approximation classique, c'est à dire lorsque  $V \ll M_{\text{Pl}}^4$  et que les corrections attendues en gravité quantiques sont faibles, l'expression standard du spectre de puissance est retrouvée comme cas limite de l'équation (5.14).

### 5.3.1. Effets Stochastiques en Inflation Hybride

Une situation d'intérêt pour l'inflation stochastique est celle des modèles à champs multiples, pour lesquels plusieurs équations de Langevin couplées régissent les trajectoires inflationnaires et donnent lieu à une dynamique non triviale. Dans la Ref. [210] (section 4.1) nous nous sommes intéressés à l'un d'entre eux, le modèle d'inflation hybride.

Ce modèle est celui d'un potentiel à deux champs, un inflaton  $\varphi$  et un champ auxiliaire  $\psi$  dont la masse est proportionnelle à  $\varphi^2 - \phi_c^2$ , où  $\phi_c$  est une constante fixant la valeur de l'inflaton à partir de laquelle le champ auxiliaire devient tachyonique. L'inflation a d'abord lieu dans la "vallée"  $\varphi > \phi_c$  où elle est conduite par l'inflaton et où le champ auxiliaire, lourd, est tel que  $\psi \simeq 0$ . Puis, lorsque  $\varphi$  passe la valeur critique  $\phi_c$ , la masse du champ auxiliaire devient négative ce qui déclenche son instabilité tachyonique et termine l'inflation. Au voisinage de ce point critique, les corrections stochastiques sont importantes et donnent lieu à des effets que nous avons étudiés numériquement. A titre illustratif, nous avons représenté dans la Fig. 5.3 la densité de probabilité de présence du système dans le plan  $(\varphi, \psi)$ , en partant d'une distribution de Dirac initialisée suffisamment haut dans la vallée. Dans un premier temps, le système descend le long de la vallée et la distribution reste relativement piquée. Puis, arrivée au point critique,

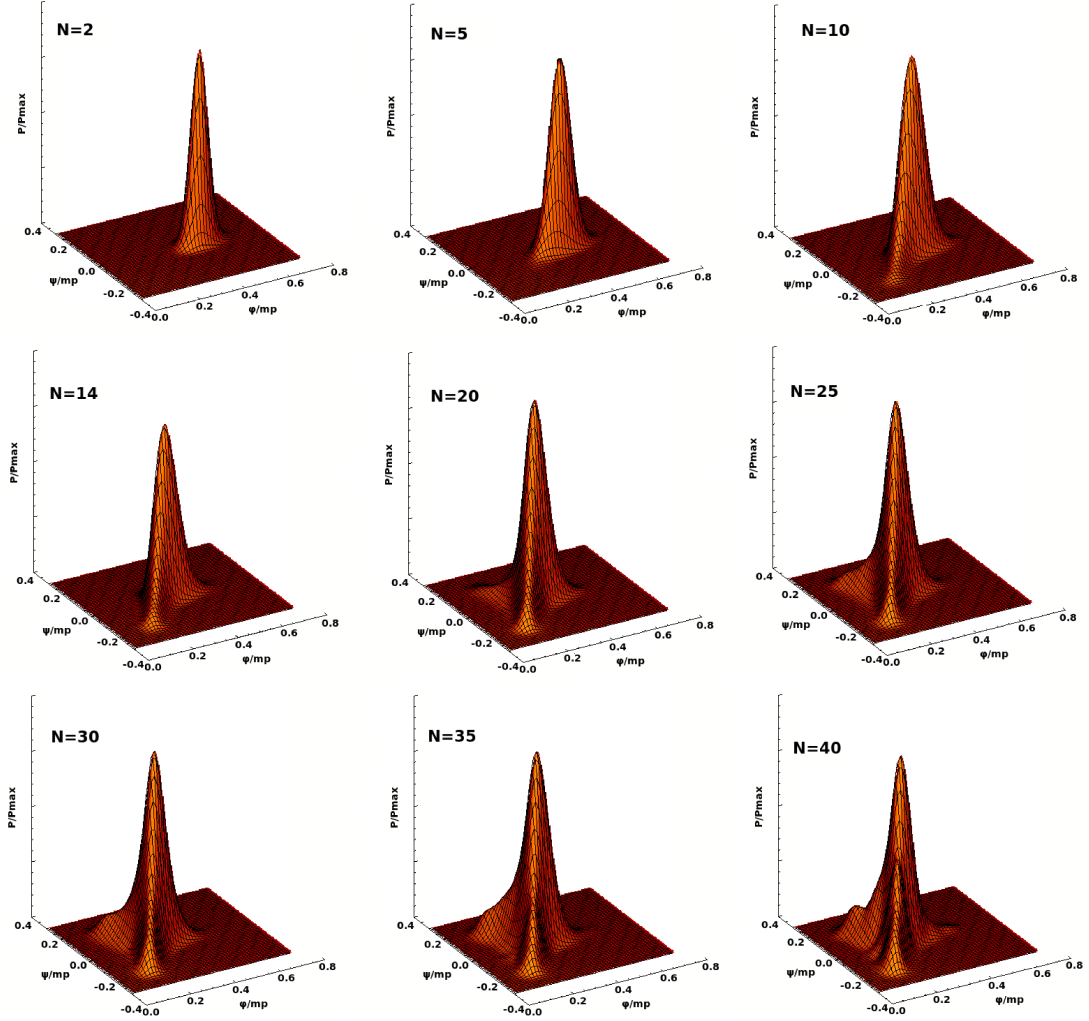


Figure 5.3.: Densité de probabilité de présence calculée à différents temps  $N$  pour le modèle d'inflation hybride, et représentée dans le plan  $(\varphi, \psi)$ . La distribution initiale est celle d'une fonction de Dirac prise suffisamment haute dans la vallée. Le potentiel hybride est donné par  $V = \Lambda^4 \left[ (1 - \psi^2/M^2)^2 + \varphi^2/\mu^2 + 2\varphi^2\psi^2/(\phi_c^2 M^2) \right]$ , et les paramètres utilisés sont  $\Lambda = 1.06347M_{\text{Pl}}$ ,  $\phi_c = M = 1.50398M_{\text{Pl}}$  et  $\mu = 7.74597M_{\text{Pl}}$ .

elle s'étend rapidement, notamment dans la direction des deux vallées secondaires menant le système aux minimas ( $\varphi = 0, \psi = \pm M$ ).

Une question importante relative à ce modèle est la durée de la période d'instabilité tachyonique lors de laquelle  $\varphi < \phi_c$ . En effet, si la fenêtre observationnelle du FDC se trouve à l'extérieur de cette phase, l'indice spectral des perturbations scalaires est bleu, ce qui est en désaccord avec les observations. Typiquement, le modèle est donc viable uniquement si la période d'instabilité tachyonique s'étend sur plus de 40 ou 50  $e$ -folds. Cette durée étant essentiellement dépendante des effets stochastiques et de la dispersion moyenne des champs au point critique qui en découle, nous avons étudié cette quantité avec attention. En particulier, nous avons caractérisé, en fonction des paramètres du potentiel, la dispersion stochastique dans le champ  $\psi$  au point critique et la distribution du nombre d' $e$ -folds réalisé dans la période d'instabilité tachyonique.

Une autre quantité à laquelle nous nous sommes intéressés est le point de sortie de l'inflation.

Lorsque l'inflation est réalisée par un seul champ  $\varphi$ , le point de sortie de l'inflation  $\varphi_{\text{end}}$  est unique (du moins dans l'approximation du roulement lent) et ne dépend pas des conditions initiales ou de la réalisation stochastique. Dans le modèle d'inflation hybride en revanche, la ligne de niveau  $\epsilon_1 = 1$  définit une infinité de points de sortie possibles  $(\varphi_{\text{end}}, \psi_{\text{end}})$ , qui dépendent a priori de la réalisation stochastique. Or, nous avons montré qu'en pratique, les trajectoires stochastiques terminent toutes l'inflation très près du point de sortie classique (c'est à dire là où sort la solution des équations du mouvement sans le terme stochastique). En effet, lors des derniers  $e$ -folds avant la fin de l'inflation, les termes de bruit dans les équations de Langevin sont fortement sous-dominants. Puisque la trajectoire de roulement lent est un attracteur dynamique, le système se rapproche alors rapidement de cette trajectoire classique, peu importe l'endroit par lequel les effets stochastiques lui ont fait quitter la zone du potentiel dominée par le bruit. Cela explique que la distribution finale soit très piquée autour de la valeur classique.

### 5.3.2. Formalisme Stochastique Récursif

Dans l'approche standard de l'inflation stochastique, les corrélations des termes de bruit dans l'équation de Langevin sont calculées à partir de l'amplitude des perturbations en champs scalaires, lorsqu'elles croisent l'échelle de lissage  $\sigma aH$ . Ces perturbations sont elles-mêmes obtenues à partir de leur équation d'évolution sur un fonds classique. Ce schéma est valable dans la limite où les effets stochastiques ne représentent qu'une petite perturbation à la trajectoire classique, mais en principe, si l'on évolue les perturbations sur un fonds corrigé par les effets stochastiques, leur amplitude devrait en être légèrement affectée. Ainsi, les corrélations du bruit devraient être corrigées par cet effet, et donc la dynamique du fonds, et donc l'amplitude du bruit, et ainsi de suite.

Pour étudier plus en détails cet effet, dans la Ref. [211] (section 4.2), nous avons mis au point un formalisme récursif intégrant la correction des corrélations du bruit par les effets stochastiques eux-mêmes. Nous avons ensuite appliqué ce formalisme au modèle d'inflation hybride, pour l'illustrer concrètement. Nous avons également pris soin d'incorporer les effets de la masse du champs auxiliaire  $\psi$  dans le calcul des corrélations du bruit agissant sur  $\psi$ , puisque dans la vallée cette masse n'est plus négligeable devant le paramètre de Hubble  $H$  et a tendance à diminuer l'amplitude des perturbations. De cette manière, la dispersion stochastique dans le champs auxiliaire est réduite au point critique, ce qui augmente la durée de la phase d'instabilité tachyonique.

Une bonne prise en compte des effets stochastiques dans la vallée montre également que le problème de l'indice spectral bleu est plus grave encore lorsque les corrections quantiques à la trajectoire sont implémentées. Cela renforce l'hypothèse d'une instabilité tachyonique longue. D'un autre côté, nous avons établi que le formalisme récursif présente de bonnes propriétés de convergence dans la vallée mais diverge dans la phase d'instabilité tachyonique. Cette période peut donc difficilement être décrite par une approche perturbative, ce qui rend son traitement délicat en général. Pourtant, outre le problème de l'indice spectral, le scénario d'une instabilité courte pose le problème de l'évolution de la distribution du champ auxiliaire qui n'est plus quasi-statique dans la vallée. Cela induit des valeurs de sa dispersion encore plus faibles au point critique que ce que le calcul usuel suggère, et qui sont incompatibles avec l'hypothèse d'une instabilité courte. Enfin, dans le cas d'une instabilité courte, les grandes longueurs d'onde du champs auxiliaire ne sont plus dans un état quantique comprimé. Cette caractéristique de la fonction d'onde des perturbations est pourtant un ingrédient important de la transition quantique-classique que nous décrivons dans la section suivante.

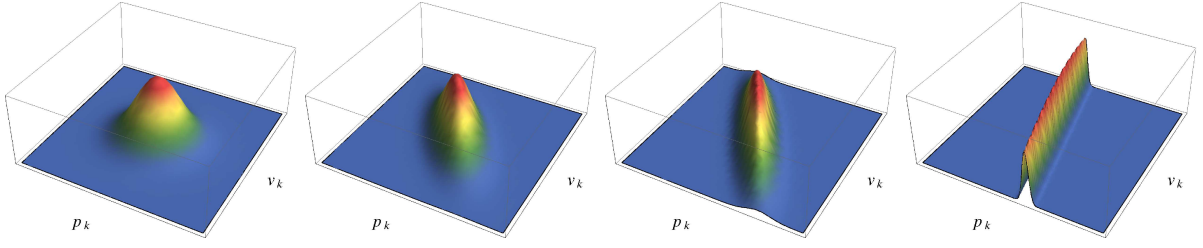


Figure 5.4.: Fonction de Wigner de l'état quantique comprimé d'un mode  $k$  de perturbation scalaire à différents instants durant l'inflation, correspondants successivement à  $r_{\mathbf{k}} = 0.0005$ ,  $r_{\mathbf{k}} = 0.48$ ,  $r_{\mathbf{k}} = 0.88$  et  $r_{\mathbf{k}} = 2.31$ .

### 5.3.3. Le Problème de la Mesure Quantique en Cosmologie

Une des questions largement discutées dans le contexte de l'inflation est la transition quantique-classique des perturbations cosmologiques. En effet, si les fluctuations des champs inflationnaires sont traitées quantiquement, il est d'usage de considérer que les coefficients  $a_{lm}$  mesurés sur le FDC par exemple se comportent comme des réalisations stochastiques de ces variables quantiques. Ils sont alors interprétés comme des graines de perturbations classiques donnant lieu à la croissance de structures cosmologiques par instabilité gravitationnelle telles que les galaxies, les amas de galaxies, *etc.* Il s'agit donc de savoir comment cette projection sur des états classiques s'effectue en pratique.

Une première réponse souvent avancée est la compression des états quantiques [131, 307, 132, 309, 133, 412]. En effet, lorsqu'elles évoluent sur des échelles plus grandes que le rayon de Hubble durant l'inflation, les perturbations cosmologiques subissent une compression de leur état quantique. Cette compression peut être décrite via la fonction de Wigner  $W$ , qui est une distribution de quasi-probabilité définie dans l'espace des phases  $(v_{\mathbf{k}}, p_{\mathbf{k}})$  pour chaque mode  $k$ , où  $v$  est la variable de Mukhanov et  $p$  est son moment canoniquement conjugué. Pour un état quantique  $|\Psi_{\mathbf{k}}(v_{\mathbf{k}})\rangle$  Gaussien, cette fonction est de la forme

$$W(v_{\mathbf{k}}, p_{\mathbf{k}}) \propto \exp \left[ -\frac{k}{\cosh(2r_{\mathbf{k}}) + \cos(2\phi_{\mathbf{k}}) \sinh(2r_{\mathbf{k}})} v_{\mathbf{k}}^2 \right] \times \exp \left\{ -k [\cosh(2r_{\mathbf{k}}) + \cos(2\phi_{\mathbf{k}}) \sinh(2r_{\mathbf{k}})] \left[ \frac{p_{\mathbf{k}}}{k} + v_{\mathbf{k}} \frac{\sin(2\phi_{\mathbf{k}}) \sinh(2r_{\mathbf{k}})}{\cosh(2r_{\mathbf{k}}) + \cos(2\phi_{\mathbf{k}}) \sinh(2r_{\mathbf{k}})} \right]^2 \right\}. \quad (5.16)$$

Dans cette expression,  $r_{\mathbf{k}}$  et  $\phi_{\mathbf{k}}$  sont deux fonctions du temps appelées respectivement paramètre de compression et angle de compression. Dans un espace-temps de de Sitter (c'est à dire dans lequel le paramètre de Hubble  $H$  est constant), elles sont données par

$$r_{\mathbf{k}} = \operatorname{argsinh} \left( \frac{aH}{2k} \right), \quad (5.17)$$

$$\phi_{\mathbf{k}} = \frac{\pi}{4} - \frac{1}{2} \arctan \left( \frac{aH}{2k} \right). \quad (5.18)$$

La fonction de Wigner décrite par ces relations est représentée sur la figure 5.4 à différents temps, ou de façon équivalente, à différentes valeurs de  $r_{\mathbf{k}}$  ( $r_{\mathbf{k}} = 0.0005$ ,  $r_{\mathbf{k}} = 0.48$ ,  $r_{\mathbf{k}} = 0.88$  et  $r_{\mathbf{k}} = 2.31$ ). Initialement, dans le régime où le mode considéré correspond à une échelle de longueur plus petite que le rayon de Hubble,  $k \gg aH$ , on a  $r_{\mathbf{k}} \simeq 0$  et  $\phi_{\mathbf{k}} \simeq \pi/4$ . Dans cette

limite, la fonction de Wigner (5.16) est de la forme  $W \propto \exp(-kv_{\mathbf{k}}^2 - p_{\mathbf{k}}^2/k)$ , ce qui correspond à un état cohérent pour lequel l’extension de la fonction de Wigner est la même dans toutes les directions et sature l’inégalité de Heisenberg. En revanche, à la fin de l’inflation lorsque le mode considéré est largement au delà du rayon de Hubble,  $k \ll aH$ , on a<sup>5</sup>  $r_{\mathbf{k}} \gg 1$  et  $\phi_{\mathbf{k}} \simeq 0$ . La fonction de Wigner est alors de la forme  $W \propto \delta[p_{\mathbf{k}} + k \tan(\phi_{\mathbf{k}})v_{\mathbf{k}}]$ , ce qui correspond à un état comprimé dans la direction donnée par l’angle  $\phi_{\mathbf{k}}$ .

Les états comprimés sont bien connus en mécanique quantique (en particulier dans le domaine de l’optique quantique) car ils présentent des propriétés statistiques intéressantes. Notamment, leur évolution temporelle peut être décrite en terme d’une collection stochastique de processus classiques [136, 133, 413]. En d’autres termes, la fonction de Wigner peut être vue dans cette limite comme une véritable distribution de probabilité, répartissant un ensemble de processus dans l’espace des phases qui suivent tous les équations classiques du mouvement. La valeur moyenne de n’importe quelle observable définie dans l’espace des phases et calculée à l’aide de cette distribution coïncide alors avec les moyennes d’opérateurs quantiques. C’est pour cette raison qu’à partir de la fin de l’inflation, les perturbations cosmologiques aux grandes longueurs d’onde peuvent être traitées comme étant des fluctuations classiques, suivant une distribution initiale dont les propriétés statistiques coïncident avec les prédictions quantiques calculées pendant la phase inflationnaire. Dans ce sens, la compression des états quantiques joue un rôle clé pour l’ensemble du scénario cosmologique.

Un autre phénomène associé à la transition quantique-classique est celui de la décohérence. Les perturbations cosmologiques ne sont pas totalement isolées d’un environnement extérieur auquel elles sont nécessairement couplées [317, 318, 319]. Ce couplage a pour conséquence que leur matrice densité est dynamiquement diagonalisée avant la recombinaison [132, 309, 315, 133, 316], et le système peut alors être vu comme un mélange statistique d’état purs. Néanmoins, la décohérence des perturbations ne résout pas le problème de la mesure en mécanique quantique [414, 415], c’est à dire la production d’une réalisation unique. Ce problème apparaît de manière encore plus nette en cosmologie puisque nous disposons alors, par définition, d’une seule carte du FDC. L’interprétation standard de Copenhague de la mécanique quantique, qui stipule qu’une réalisation unique d’un processus quantique est produite par le biais d’une mesure réalisée par un expérimentateur extérieur qui projette la fonction d’onde du système sur un état propre de l’observable en question, pose problème dans le cas présent vue la difficulté à définir un observateur extérieur à l’Univers lui même. C’est pourquoi il est courant de postuler que le phénomène de décohérence est combiné avec une autre interprétation que celle de Copenhague, comme par exemple celle des mondes multiples [136, 416, 417, 418], de l’information quantique [419], ou en invoquant des variables cachées non locales [420, 421, 422, 153, 33, 423]. En fait, la seule alternative à la formulation standard de Copenhague qui propose une solution au problème de la mesure tout en étant falsifiable, est un modèle de réduction dynamique de la fonction d’onde [424, 425, 426, 427, 428, 429, 430, 431]. En effet, le problème de la mesure réside dans le fait que deux processus très différents par nature prennent place: l’évolution linéaire et unitaire de Schrödinger d’un côté et la réduction non linéaire et stochastique du paquet d’onde de l’autre.

Dans la Ref. [138] (section 4.3), nous nous sommes ainsi intéressés au modèle de CSL (pour “continuous spontaneous localization”) de Pearle, Ghirardi, Rimini et Weber [425, 426, 428,

<sup>5</sup>Plus précisément, on a  $a_{\text{end}}H/k = e^{\Delta N_*}$ , où  $\Delta N_*$  est le nombre d’e-folds réalisés entre le moment où le mode  $k$  croise le rayon de Hubble et la fin de l’inflation. Si  $k$  est à l’intérieur de la fenêtre observationnelle, on a typiquement  $\Delta N_* \simeq 50$ , et d’après l’équation (5.17),  $r_{\mathbf{k}}$  à la fin de l’inflation est de l’ordre de  $r_{\mathbf{k}} \simeq \Delta N_* \simeq 50$ . Il est intéressant de noter que le niveau de compression associé à de tels paramètres est colossal, et typiquement bien plus grand que ce qui peut être réalisé en laboratoire [307].

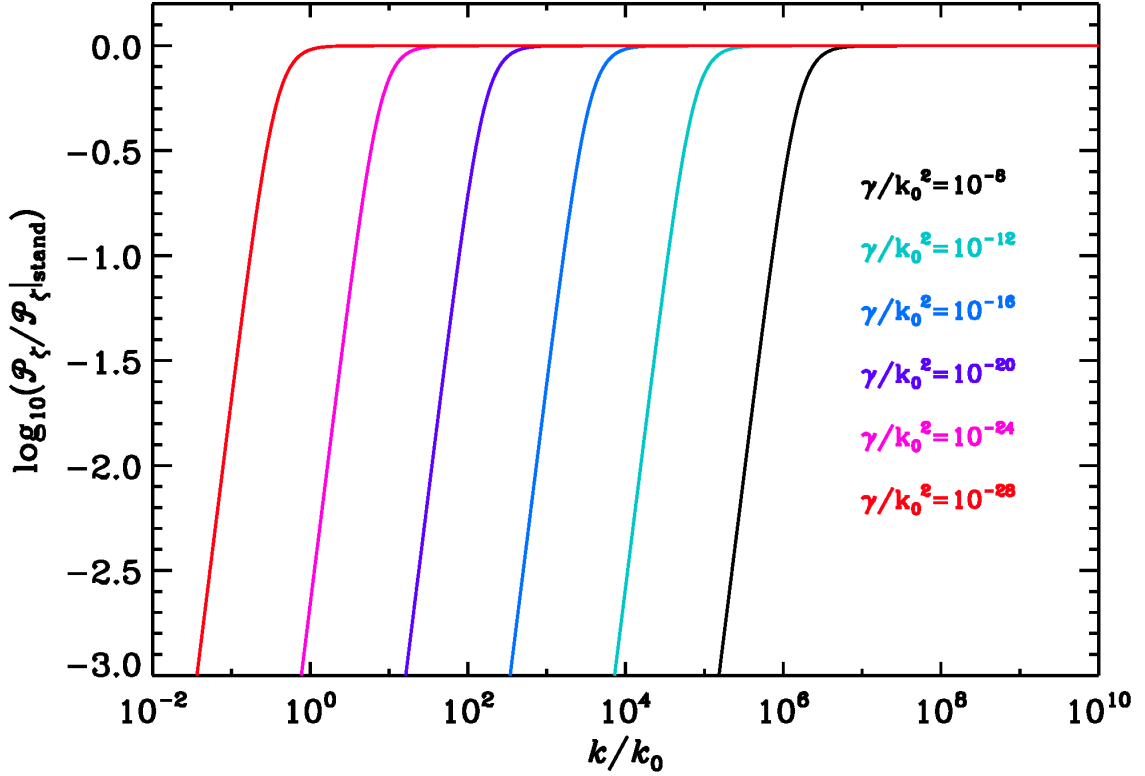


Figure 5.5.: Spectre de puissance des perturbations scalaires obtenu avec l'équation de Schrödinger modifiée (5.19), en prenant  $\hat{C} = \hat{v}_k$  pour chaque mode  $k$ , et pour différentes valeurs de  $\gamma$ . La quantité représentée est le spectre normalisé à sa valeur standard (c'est à dire lorsque  $\gamma = 0$ ). Le mode  $k_0$  correspond à une échelle pivot autour de laquelle le spectre est calculé.

429], dans lequel l'équation de Schrödinger est modifiée par l'ajout de termes non linéaires et stochastiques:

$$d|\psi\rangle = -i\hat{H}dt|\psi\rangle + \sqrt{\gamma}(\hat{C} - \langle\hat{C}\rangle)dW_t|\psi\rangle - \frac{\gamma}{2}(\hat{C} - \langle\hat{C}\rangle)^2 dt|\psi\rangle. \quad (5.19)$$

L'opérateur  $\hat{H}$  est le hamiltonien du système et le premier terme correspond donc à l'équation de Schrödinger standard. L'opérateur  $\hat{C}$  est l'opérateur de projection dont les états propres sont les directions le long desquelles on souhaite réaliser la réduction de la fonction d'onde. La non linéarité apparaît dans les termes  $\langle\hat{C}\rangle = \langle\psi|\hat{C}|\psi\rangle$ . La nature stochastique de cette équation de Schrödinger modifiée se traduit quant à elle par la présence d'un processus de Wiener  $W_t$ , et l'amplitude des termes non standards est définie par une constante de couplage  $\gamma$ . Cette théorie permet de projeter la fonction d'onde  $|\psi\rangle$  sur un des états propres de  $\hat{C}$  de façon dynamique, avec un temps caractéristique et à une précision près qui dépendent de  $\gamma$ , et selon des probabilités qui suivent la règle de Born.<sup>6</sup> De plus, ce modèle est doté d'un mécanisme d'amplification grâce auquel la constante de couplage  $\gamma$  effective d'un système constitué de  $N$  particules croît proportionnellement avec  $N$ . Cela permet d'expliquer que les objets macroscopiques soient bien

<sup>6</sup>De cette manière, les règles de Born n'ont pas besoin d'être postulées dans cette théorie, contrairement à ce qui est fait en mécanique quantique standard. Ici elles peuvent être démontrées à partir de l'équation d'évolution (5.19).

localisés, tout en laissant la dynamique des systèmes microscopiques, dont on sait qu'ils sont parfaitement décrits par la mécanique quantique standard, essentiellement inchangée.

Nous avons donc utilisé ce modèle pour décrire l'évolution des perturbations scalaires pendant l'inflation, afin d'établir quelles contraintes sur la théorie (c'est à dire principalement sur le paramètre  $\gamma$ ) la nécessité de réduire la fonction d'onde pendant l'inflation pouvait imposer. Nous avons choisi comme opérateur de projection la variable de Mukhanov-Sasaki  $v$  puisqu'elle est invariante de jauge. Un premier résultat a été obtenu en calculant le spectre de puissance produit par cette théorie, et représenté sur la figure 5.5 pour différentes valeurs de  $\gamma$ . Deux branches apparaissent nettement: une branche qui reste quasi invariante d'échelle et où les termes non standards jouent un rôle négligeable, et une branche très fortement dépendante de l'échelle où  $n_s = 4$  et où les termes non standards dominent. Afin que cette branche se situe au delà des échelles observables et pour préserver l'invariance d'échelle observée, la constante de couplage  $\gamma$  doit être suffisamment petite,

$$\frac{\gamma}{k_0^2} \ll e^{-\Delta N_*} \simeq 10^{-28}. \quad (5.20)$$

Dans cette expression,  $k_0$  est l'échelle pivot autour de laquelle le spectre de puissance est calculé. Néanmoins,  $\gamma$  ne peut pas être arbitrairement petit si l'on souhaite que la réduction du paquet d'onde se produise avant la fin de l'inflation. Pour des échelles situées à l'extérieur du rayon de Hubble, le nombre d' $e$ -folds requis pour que la réduction ait lieu est de l'ordre de  $\log(k^2/\gamma)$ , qui d'après la contrainte précédente doit être plus grand que  $\sim 28$ . Les  $\Delta N_* \sim 60$   $e$ -folds dont nous disposons sont donc suffisants. En revanche, dans la branche invariante d'échelle, l'efficacité de la réduction du paquet d'onde, mesurée par sa dispersion  $\sigma_{v_k}$  dans son état final, est donnée par

$$k\sigma_{v_k} \simeq \exp(2\Delta N_*) \gg 1. \quad (5.21)$$

En conclusion, l'invariance d'échelle contraint  $\gamma$  à prendre des valeurs si petites que la fonction d'onde est très mal localisée à la fin de l'inflation et que le modèle discuté ici ne peut pas expliquer correctement la production d'une réalisation bien définie au cours de l'inflation.

Notons néanmoins que les auteurs de la Ref. [408] ont généralisé notre calcul au cas où  $\gamma$  dépend de  $k$  par le biais d'une loi de puissance. Ils ont établi pour quel exposant dans cette loi l'indice spectral de la branche du spectre dominée par les termes non standards est invariante d'échelle. Dans ce cas, il n'y a plus de borne supérieure sur  $\gamma$  et quitte à prendre des grandes valeurs de  $\gamma$ , il est toujours possible de réaliser efficacement la réduction du paquet d'onde sans altérer l'invariance d'échelle du spectre.

## 5.4. Conclusion

Dans cette thèse, nous avons illustré la manière dont le paradigme inflationnaire permet de mieux cerner un certain nombre de questions fondamentales en physique, et d'appréhender leurs implications concrètes dans un cadre théorique pertinent. D'un autre côté, nous avons vu que de nombreuses mesures cosmologiques et astrophysiques permettent de contraindre explicitement les paramètres microphysiques décrivant cette phase d'expansion accélérée et de cette manière, d'en apprendre d'avantage sur les caractéristiques physiques de l'Univers primordial.

Pour conclure, il convient de discuter à présent les perspectives offertes par une telle démarche à moyen et long terme. Le paradigme inflationnaire est doté d'une solidité phénoménologique

qui peut rendre difficile l'identification de son origine microphysique, puisque ses prédictions dépendent d'un petit nombre d'observables génériques et que les échelles nous permettant de les sonder sont restreintes à quelques  $e$ -folds. Par conséquent, si la détection de  $r$  revendiquée par l'expérience BICEP2 se confirme, il est clair que tout doit être entrepris pour en mesurer précisément la valeur. Si l'ordre de grandeur annoncé  $r \sim 0.1$  est correct, cela signifie également que l'indice spectral des ondes gravitationnelles,  $n_T$ , peut aussi être mesuré [409] à moyen terme. De cette manière, le nombre de paramètres inflationnaires dont on aurait une mesure doublerait, passant de  $\{\mathcal{P}_{\zeta,*}, n_s\}$  à  $\{\mathcal{P}_{\zeta,*}, n_s, r, n_T\}$ . Si l'on ajoute à cela les corrélations  $EE$  et  $TE$  mesurées par Planck et qui devraient être publiées sous peu, il semble réaliste de vouloir réellement contraindre la forme du potentiel et son échelle d'énergie.

En revanche, si une détermination plus précise de la contribution des avant plans de poussière dans l'expérience BICEP2 fait disparaître le signal sur  $r$ , ce projet risque d'être fortement ralenti. En effet, pour bon nombre de modèles dont le potentiel a une forme de "plateau" (les modèles favorisés par Planck), tels que les modèles d'inflation branaire ou les modèles d'inflation avec module de Kähler, la valeur prédite pour  $r$  est minuscule, typiquement  $r < 10^{-6}$ . Pour l'instant, il semble totalement impossible d'atteindre de tels seuils de détection. De la même manière, pour les modèles d'inflation à un champ scalaire et avec terme cinétique standard (qui semblent pour le moment favorisés par les données), le niveau de non Gaussianités primordiales est très faible,  $f_{\text{NL}} \sim \epsilon$ , et ne semble pas être détectable pour le moment [410]. Le même constat s'applique pour les perturbations entropiques qui pourraient provenir de la présence d'autres champs massifs, ou pour le running du spectre de puissance  $\alpha_s \sim \epsilon^2$ . C'est pourquoi dans ce cas, il est fort possible que l'on assiste à un certain ralentissement de l'entreprise visant à contraindre l'inflation par les mesures du FDC.

Pour continuer à progresser dans notre compréhension de l'Univers primordial, deux chemins peuvent alors être empruntés. Le premier consiste à discriminer les modèles par des arguments théoriques, en continuant à examiner les possibilités offertes par les extensions du modèle standard de la physique des particules, en comprenant mieux le rôle des corrections radiatives, des couplages aux autres champs, des propriétés physiques de la phase de réchauffement qui en découlent, etc. Car indépendamment des observations, l'inflation soulève un certain nombre de problèmes fondamentaux qu'il reste à résoudre. Une autre possibilité est d'étudier plus en détails les connections existant entre les prédictions inflationnaires et d'autres sondes astrophysiques telles que les supernovae, la répartition des galaxies et des amas de galaxies, l'astrophysique à 21 cm, la reconstruction des conditions initiales par les simulations de grandes structures, etc. Le bras de levier entre les différentes échelles associées à ces objets est énorme et devrait nous permettre de mieux cerner l'Univers dans lequel ils évoluent.

La cosmologie est entrée dans une ère de données massives où des mesures d'observables fondamentalement différentes par nature doivent être intelligemment combinées dans le but de contraindre des processus physiques tout aussi différents. De cette manière, les avancées dans l'ensemble des champs de la cosmologie et même de l'astrophysique sont étroitement liées et dépendantes les unes des autres. Le décryptage de l'Univers primordial repose donc sur une compréhension de phénomènes physiques très variés, et sur la réalisation de mesures qui mettent au défi la technologie moderne. Seulement à ce prix pourrons nous avancer dans cette quête universelle qu'est la compréhension du monde dans lequel nous vivons.

